2018

DISCOVERY OF NEW ANTIMICROBIAL OPTIONS AND EVALUATION OF AMINOGLYCOSIDE RESISTANCE ENZYME-ASSOCIATED RESISTANCE EPIDEMIC

Selina Y. L. Holbrook
University of Kentucky, selinali.yijia@gmail.com
Digital Object Identifier: https://doi.org/10.13023/etd.2018.310

STUDENT AGREEMENT:

I represent that my thesis or dissertation and abstract are my original work. Proper attribution has been given to all outside sources. I understand that I am solely responsible for obtaining any needed copyright permissions. I have obtained needed written permission statement(s) from the owner(s) of each third-party copyrighted matter to be included in my work, allowing electronic distribution (if such use is not permitted by the fair use doctrine) which will be submitted to UKnowledge as Additional File.

I hereby grant to The University of Kentucky and its agents the irrevocable, non-exclusive, and royalty-free license to archive and make accessible my work in whole or in part in all forms of media, now or hereafter known. I agree that the document mentioned above may be made available immediately for worldwide access unless an embargo applies.

I retain all other ownership rights to the copyright of my work. I also retain the right to use in future works (such as articles or books) all or part of my work. I understand that I am free to register the copyright to my work.

REVIEW, APPROVAL AND ACCEPTANCE

The document mentioned above has been reviewed and accepted by the student's advisor, on behalf of the advisory committee, and by the Director of Graduate Studies (DGS), on behalf of the program; we verify that this is the final, approved version of the student's thesis including all changes required by the advisory committee. The undersigned agree to abide by the statements above.

Selina Y. L. Holbrook, Student

Dr. Sylvie Garneau-Tsodikova, Major Professor

Dr. David J. Feola, Director of Graduate Studies

DISCOVERY OF NEW ANTIMICROBIAL OPTIONS AND EVALUATION OF AMINOGLYCOSIDE RESISTANCE ENZYME-ASSOCIATED RESISTANCE EPIDEMIC

DISSERTATION

A dissertation submitted in partial fulfillment of the requirements for the degree of Doctor of Philosophy in the College of Pharmacy at the University of Kentucky

By
Selina Yijia Li Holbrook

Lexington, Kentucky

Director: Dr. Sylvie Garneau-Tsodikova, Associate Professor of Pharmaceutical Sciences

Lexington, Kentucky

2018

ABSTRACT OF DISSERTATION

DISCOVERY OF NEW ANTIMICROBIAL OPTIONS AND EVALUATION OF AMINOGLYCOSIDE RESISTANCE ENZYME-ASSOCIATED RESISTANCE EPIDEMIC

The extensive and sometimes incorrect and noncompliant use of various types of antimicrobial agents has accelerated the development of antimicrobial resistance (AMR). In fact, AMR has become one of the greatest global threat to human health in this era. The broad-spectrum antibiotics aminoglycosides (AGs) display excellent potency against most Gram-negative bacteria, mycobacteria, and some Gram-positive bacteria, such as *Staphylococcus aureus*. The AG antibiotics amikacin, gentamicin, kanamycin, and tobramycin are still commonly prescribed in the U.S.A. for the treatment of serious infections. Unfortunately, bacteria evolve to acquire resistance to AGs *via* four different mechanisms: i) changing in membrane permeability to resist drugs from entering, ii) upregulating efflux pumps for active removal of intracellular AGs, iii) modifying the antimicrobial target(s) to prevent drugs binding to their targets, and iv) acquiring resistance enzymes to chemically inactivate the compounds. Amongst all, the acquisition of resistance enzymes, AG-modifying enzymes (AMEs), is the most common resistance mechanism identified. Depending on the chemistry each enzyme catalyzes, AMEs can be further divided into AG *N*-acetyltransferases (AACs), AG *O*-phosphotransferases (APHs), and AG *O*-nucleotidyltransferases.

To overcome AME-related resistance, we need to better understand these resistance enzymes and further seek ways to either escape or inhibit their actions. In this dissertation, I summarized my efforts to characterize the AAC(6') domain and its mutant enzymes from a bifunctional AME, AAC(6')-Ie/APH(2")-Ia as well as another common AME, APH(3')-IIa. I also explained my attempt to inhibit the action of various AAC enzymes using metal salts. In an effort to explore the current resistance epidemic, I evaluated the resistance against carbapenem and AG antibiotics and the correlation between the resistance profiles and the AME genes in a collection of 122 *Pseudomonas aeruginosa* clinical isolates obtained from the University of Kentucky Hospital System. Besides tackling the resistance mechanisms in bacteria, I have also attempted to explore a new antifungal option by repurposing an existing antipsychotic drug, bromperidol, and a panel of its derivatives into

a combination therapy with the azole antifungals against a variety of pathogenic yeasts and filamentous fungi.

KEYWORDS: aminoglycoside-modifying enzyme (AME), enzyme engineering, substrate promiscuity, enzyme kinetics, minimum inhibitory concentrations (MICs), drug combination.

Selina Yijia Li Holbrook

June 27, 2018

Date

DISCOVERY OF NEW ANTIMICROBIAL OPTIONS AND EVALUATION OF AMINOGLYCOSIDE RESISTANCE ENZYME-ASSOCIATED RESISTANCE EPIDEMIC

By

Selina Yijia Li Holbrook

Dr. Sylvie Garneau-Tsodikova

Director of Dissertation

Dr. David J. Feola

Director of Graduate Studies

June 27, 2018

DEDICATION

In memory of my mother who brought me into this world, for throughout your entire life you demonstrated sacrificial and unconditional love for me.

For my husband and best friend who shares this life with me, for you love me, serve me, lead me, help me, and support me.

ACKNOWLEDGEMENTS

Throughout my journey as a graduate student I have been blessed with numerous people who helped and guided me to become a better scientist. Without the time, patience, and expertise they invested in me, I would not be able to accomplish my degree.

First of all, I would like to thank my Ph.D. advisor, Dr. Sylvie Garneau-Tsodikova, who has devoted enormous amount of time, funding, ideas, patience, and enthusiasm throughout my Ph.D. study and research. She teaches me to think with creativity, to execute with scientific accuracy, to observe with unbiased eyes, and to overcome difficulties with perseverance. She inspires me to challenge myself on a daily basis to achieve a better self and also sets an exceptional role model for an outstanding scientist and educator who serves both science and the people around her with a humble heart. With her guidance and funding, my Ph.D. study was made possible.

I would also like to give genuine gratitude to Dr. Matthew S. Gentry, Dr. Steve G. Van Lanen, Dr. Jürgan Rohr, and Dr. Chang-Guo Zhan for their selfless service on my Ph.D. committee. Their encouragement, inspiring comments, and thoughtful questions have helped guide me to be a better researcher. I would like to thank Dr. Gentry specially for his input into training me in cell culturing and immunohistochemistry techniques.

Furthermore, I would like to thank Dr. Oleg V. Tsodikov who, as a teacher and collaborator, provided his expertise in structural biology and enzyme dynamics in many of my projects.

His contribution broadened the scope and impact of my studies that without whom I would not be able to accomplish.

My gratitude also goes to all past and present S.G.-T. and O.V.T. lab members for all their support and encouragement throughout my study. I would like to thank Dr. Keith D. Green especially, for the time and energy he spent on training me lab techniques, teaching me scientific knowledge, and helping me in times of trouble shooting. I thank Taylor A. Lundy for her hugs. The support of all lab mates goes beyond friendship.

Last but not least, I would like to thank all parties that provided financial support throughout my graduate study, including the University of Kentucky College of Pharmacy Department of Pharmaceutical Sciences, the National Institutes of Health, the University of Kentucky Presidential fellowship, which provided funding from 2016 to 2017.

TABLE OF CONTENTS

ACKNOWLEDGEMENTS……..…….....iii

LIST OF TABLES…….…..xiii

LIST OF FIGURES……..xvi

LIST OF ABBREVIATIONS……....xxiii

Chapter 1. New trends in the use of aminoglycosides.……1

1.1. INTRODUCTION……..1

1.2. AMINOGLYCOSIDES MODE OF ACTION: BINDING TO THE RIBOSOME.7

1.2.1. Aminoglycosides binding to the A-site.…….……7

1.2.2. Aminoglycosides binding to h69.…….……10

1.3. AMPHIPHILIC AMINOGLYCOSIDES…….……12

1.4. AMINOGLYCOSIDES AS ANTIFUNGAL AGENTS……...…14

1.5. READING THROUGH THE FAULTY "STOPS" AT THE PREMATURE TERMINATION CODONS……...……16

1.5.1. Cystic fibrosis (CF)……..…17

1.5.2. Duchenne muscular dystrophy (DMD).……17

1.5.3. Rett syndrome (RTT).……...……20

1.5.4. Spinal muscular atrophy (SMA).……..……20

1.5.5. Other PTC diseases.……..……21

1.6. NEW WAYS TO ALLEVIATE AMINOGLYCOSIDE TOXICITY……...…22

1.6.1. Mechanisms of ototoxicity……...…23

1.6.2. Apramycin.……...……24

1.6.3. New AG: Plazomicin.……...……25

1.7. PERSPECTIVE AND CONCLUSIONS……..……27

1.8. ACKNOWLEDGEMENT……28

1.9. AUTHORS' CONTRIBUTIONS……...……...…29

Chapter 2. Expanding aminoglycoside resistance enzyme regiospecificity by mutation and truncation ……..…30

2.1. INTRODUCTION ……31

2.2. RESULTS AND DISCUSSION ……...……37

2.2.1. Molecular cloning and expression of AAC(6')/APH(2")-wt and its mutant enzymes ……..…37

2.2.2. Establishment of the substrate profiles of AAC(6')/APH(2")-wt and its three mutant enzymes by UV-Vis assays …….……39

2.2.3. Determination of kinetic paramenters for AAC(6')/APH(2")-wt and its three mutant enzymes ……..…41

2.2.4. Determination by MS and MS^2 of the position(s) acetylated on ABK and AMK by AAC(6')/APH(2")-wt and its three mutant enzymes ……46

2.3. CONCLUSIONS ……..……58

2.4. MATERIALS AND METHODS ……..……59

2.4.1. Materials and instrumentation …….……59

2.4.2. Cloning of $NHis_6$-tagged *aac(6')/aph(2")-1-240*, *aac(6')/aph(2")-D80G*, *aac(6')/aph(2")-D80G-1-240*, and *aac(6')/aph(2")-1-194* genes in pET28a 61

2.4.3. Overexpression and purification of AAC(6')/APH(2")-wt, AAC(6')/APH(2")-1-240, AAC(6')/APH(2")-D80G, AAC(6')/APH(2")-D80G-1-240, and AAC(6')/APH(2")-1-194 NHis$_6$-tagged proteins……....62

2.4.4. Establishment of the substrate profiles of AAC(6')/APH(2")-wt, AAC(6')/APH(2")-1-240, AAC(6')/APH(2")-D80G, and AAC(6')/APH(2")-D80G-1-240 by UV-Vis assays ……...……63

2.4.5. Determination of kinetic parameters for AAC(6')/APH(2")-wt, AAC(6')/APH(2")-1-240, AAC(6')/APH(2")-D80G, and AAC(6')/APH(2")-D80G-1-240 ……64

2.4.6. Mass spectrometry ……...…64

2.4.7. Disk diffusion assays ……...……65

2.5. ACKNOWLEDGEMENT ……66

2.6. AUTHORS' CONTRIBUTIONS ..……...……67

Chapter 3. Inhibition of aminoglycoside acetyltransferase resistance enzymes by metal salts ……....68

3.1. INTRODUCTION ……68

3.2. RESULTS ……...……..71

3.2.1. *In vitro* inhibition of AACs by metal salts …….……..71

3.2.2. Profiling of resistance enzymes in clinical isolates of various bacterial strains……..….79

3.2.3. Activity of AGs in combination with ZnPT in various bacterial strains …..80

3.3. DISCUSSION ……..82

3.4. CONCLUSIONS ……..87

3.5. MATERIALS AND METHODS ……..87

3.5.1. Materials and instrumentation ……..87

3.5.2. Cloning, overexpression, and purification of AAC(3)-Ia (NHis).……..…..88

3.5.3. Determination of inhibition of AAC enzymes by various metal salts.……..89

3.5.4. Determination of potential inhibition mechanism using EDTA.……...90

3.5.5. Inhibition of AACs by metal salts at near physiological salt concentration..91

3.5.6. Determination of IC_{50} values by UV-Vis assays ……91

3.5.7. Identification of AMEs in twelve bacterial strains ……...92

3.5.8. Determination of MIC values for combinations of metals and AGs ……..93

3.6. ACKNOWLEDGEMENT ……..…..94

3.7. AUTHORS' CONTRIBUTIONS …..…….……..94

Chapter 4. Nucleoside triphosphate cosubstrates control and substrate profile and efficiency of aminoglycoside 3'-*O*-phosphotransferase type IIa …….……...95

4.1. INTRODUCTION ……..…..95

4.2. RESULTS AND DISCUSSION ……...98

4.2.1. Determination of AG profiles of APH(3')-IIa with various NTPs …….….98

4.2.2. Thin-layer chromatography ……...…100

4.2.3. Determination of enzyme kinetics by UV-Vis assays ……104

4.2.4. Structural insights into the NTP effect of the AG profile ……..109

4.3. CONCLUSIONS ……113

4.4. MATERIALS AND METHODS ……114

4.4.1. Materials and instrumentation ……114

4.4.2. Cloning, expression and purification of APH(3')-IIa ……....114

4.4.3. Determination of AG profile of APH(3')-IIa with various NTPs ……..…115

4.4.4. Thin-layer chromatography ……...116

4.4.5. Determination of enzyme kinetics by UV-Vis assays ……116

4.4.6. Validation of PK efficiency in kinetics UV-Vis assays ……..117

4.5 ACKNOWLEDGEMENT ……...117

4.6. AUTHORS' CONTRIBUTIONS ..……118

Chapter 5. Evaluation of aminoglycoside and carbapenem resistance in a collection of drug-resistant *Pseudomonas aeruginosa* clinical isolates ……...…119

5.1. INTRODUCTION ……..…120

5.2. RESULTS AND DISCUSSION ……..…122

5.2.1. Susceptibility of various antibiotics against 122 *P. aeruginosa* clinical isolates ……..…122

5.2.2. Screen for AME genes by PCR ……..……132

5.3. CONCLUSIONS ……142

5.4. MATERIALS AND METHODS ……143

5.4.1. Materials and instrumentation ……143

5.4.2. Susceptibility for AGs and carbapenems ……...……144

5.4.3. Screen for AME genes by PCR ……..……145

5.4.4. Combination studies of AGs and carbapenem by checkerboard assays ….145

5.5. ACKNOWLEDGEMENT ……..146

5.6. AUTHORS' CONTRIBUTIONS ..……146

Chapter 6. Repurposing antipsychotic drugs into antifungal agents: synergistic combinations of azoles and bromperidol derivatives in the treatment of various fungal infections ……147

6.1. INTRODUCTION ……..…147

6.2. RESULTS AND DISCUSSION ……..…152

6.2.1. Chemical synthesis of bromperidol and its derivatives ……..……152

6.2.2. Antifungal synergy of the combinations of azole antifungals and bromperidol series compounds **1-5** by checkerboard assays ……..…153

6.2.3. Time-dependent antifungal activity of the combinations of azole antifungals and bromperidol series compounds ……...…162

6.2.4. Biofilm disruption with the combinations of representative azole antifungals and bromperidol series compounds ……...…164

6.2.5. Mammalian cytotoxicity of the combinations of representative azole antifungals and bromperidol series compounds ……165

6.3. CONCLUSIONS ……170

6.4. MATERIALS AND METHODS ……171

6.4.1. Chemistry methodology ……171

6.4.1.1. Materials and instrumentation for chemistry ……171

6.4.1.2. Synthesis and characterization of compounds used in this study ..…172

6.4.1.3. Compound characterization ……..…175

6.4.2. Biological testing methodology ……..…184

6.4.2.1. Biological reagents and instrumentation ……...…184

6.4.2.2. Determination of MIC values ……185

6.4.2.3. Combination studies of azoles and bromperidol series derivatives by checkerboard assays ……186
6.4.2.4. Time-kill assays ……187
6.4.2.5. Biofilm disruption assays ……188
6.4.2.6. Mammalian cytotoxicity assays ……189
6.5. ACKNOWLEDGEMENT ……190
6.6. AUTHORS' CONTRIBUTIONS ……191
Chapter 7. Conclusions and future directions ……192
7.1 CONCLUSIONS ……192
7.2 FUTURE DIRECTIONS ……194
7.2.1. Developing AGs as therapeutics for premature termination codon diseases ……194
7.2.2. Exploring PanD as a potential new target against *Mycobacterium tuberculosis* infections ……197
7.3. ACKNOWLEDGEMENT ……201
7.4. AUTHORS' CONTRIBUTIONS ……201
References ……202
Chapter 1 references ……202
Chapter 2 references ……228
Chapter 3 references ……235
Chapter 4 references ……239
Chapter 5 references ……244
Chapter 6 references ……252

Chapter 7 references ……..……...……259

Vita ……..……263

LIST OF TABLES

Table 2.1. Primers used for the PCR amplification of the *aac(6')/aph(2")* gene for various constructs…….39

Table 2.2. SOE PCR strategies to generate all new AAC(6')/APH(2") constructs used in this study…….39

Table 2.3. Purification yields of AAC(6')/APH(2") and mutant and/or truncated proteins……...…….39

Table 2.4. Substrate promiscuity for AAC(6')/APH(2")-wt and mutant constructs, including AAC(6')/APH(2")-1-240, AAC(6')/APH(2")-D80G, and AAC(6')/APH(2")-D80G-1-240…….……40

Table 2.5. Kinetic parameters determined for AAC(6')/APH(2")-wt and the mutant enzymes, including AAC(6')/APH(2")-1-240, AAC(6')/APH(2")-D80G, and AAC(6')/APH(2")-D80G-1-240, with various AGs……..…42

Table 2.6. Summary of mass spectrometry results obtained by using a single enzyme or sequentially using two enzymes……...……50

Table 3.1. Summary of inhibition of various AAC enzymes by metal salts in combination with different AGs. ……...……...75

Table 3.2. IC_{50} values for the various metal ions that have shown complete inhibition in UV-Vis assays against various AACs in combination with different AGs.…..78

Table 3.3. MIC values of AMK (μg/mL) in the presence of various concentrations of ZnPT against various Gram-negative bacterial strains……...80

Table 3.4. MIC values of TOB (μg/mL) in the presence of various concentrations of ZnPT against various Gram-negative bacterial strains……..80

Table 3.5. Resistance profiles of clinical isolates (isolate # into parenthesis) against the three AGs used for treatment of systemic infections in the U.S.A. as well as other clinically relevant antibiotics……..85

Table 4.1. AG substrate profile of APH(3')-IIa with various (d)NTPs…….....99

Table 4.2. Summary of TLC results based on whether each AG was phosphorylated by various (d)NTP with APH(3')-IIa enzyme……..100

Table 4.3. Kinetic parameters of APH(3')-IIa with respect to AGs……..……105

Table 5.1. MIC values (μg/mL) of various AGs and MEM against all clinical isolates studied……123

Table 5.2. Susceptibility of 122 *P. aeruginosa* clinical isolate strains to various antibiotics.....124

Table 5.3. Summary of the median MIC values, the range of MIC values, and the rate of resistance to each antibiotic based on the susceptibility to AMK, GEN, NET, SIS, TOB, and MEM. ……...….126

Table 5.4. Patterns of the four common AME genes in all clinical *P. aeruginosa* strains as detected by PCR. ……..…….133

Table 5.5. The median MIC values of each antibiotic based on the presence and absence of different AME gene patterns.…….……135

Table 5.6. MIC values of IPM (μg/mL) against selected *P. aeruginosa* clinical isolate..142

Table 6.1. The combinational effect of various azoles and compounds 1-5 against two representative *C. albicans* strains……..…..155

Table 6.2. FICI values of the combinations of 5 azoles and compounds 1-5 against two *C. albicans* strains…….…..158

Table 6.3. Combinational effect of POS or VOR with compounds 1-5 against a variety of fungal strains……....…161

Table 6.4. Inhibition of biofilm formation with azoles and compound 2 combinations...166

LIST OF FIGURES

Figure 1.1. Structures of parent AGs discussed in this chapter……2

Figure 1.2. A. Sites that are targeted by the different AMEs. B. Chemical modifications catalyzed by AMEs……..……..4

Figure 1.3. Structures of conformational constrained AGs……..…..…5

Figure 1.4. Representative TOB and NEA dimers with different linker attachments…...6

Figure 1.5. A. Representation of the internal loop structure of h44. B. Representation of h44 of the 16S rRNA showing residues destacking upon AG binding…….8

Figure 1.6. Modifications at the 3"-, 4"-, and 6"-positions of the antibacterial KANB result in the antifungal agent FG08…….…...16

Figure 1.7. Proposed mechanism of AG-induced PTC read-through……...18

Figure 1.8. Structures of synthetic AG derivatives used for PTC-associated diseases....19

Figure 2.1. Structures of the various AGs and CIP tested in this chapter…….32

Figure 2.2. A. Schematic diagram of all mutant enzyme constructs generated and used in this study. B and C. Crystal structures of the AAC(6') domain (PDB ID: 4QC6)[40] of the bifunctional enzyme AAC(6')/APH(2") in surface (B) and cartoon (C) representations……...36

Figure 2.3. Coomassie blue-stained 15% Tris-HCl SDS-PAGE gel showing purified $NHis_6$-tagged AAC(6')/APH(2") (59.0 kDa, lane 1), AAC(6')/APH(2")-D80G (59.0 kDa, lane 2), AAC(6')/APH(2")-1-240 (30.9 kDa, lane 3), and AAC(6')/APH(2")-D80G-1-240 (30.9 kDa, lane 4)……..38

Figure 2.4. Kinetic curves for AAC(6')/APH(2")-wt (NHis) with various AGs……..42

Figure 2.5. Kinetic curves for AAC(6')/APH(2")-1-240 (NHis) with various AGs…….43

Figure 2.6. Kinetic curves for AAC(6')/APH(2")-D80G (NHis) with various AGs……44

Figure 2.7. Kinetic curves for AAC(6')/APH(2")-D80G-1-240 (NHis) with various AG…….45

Figure 2.8. Structures of A. ABK and B. AMK with the potential acetylation sites of interest in this study (6'- and 4"'-amine positions) denoted with red arrows...47

Figure 2.9. Representative mass spectra of ABK control and ABK modified with various amount of AcCoA by various enzymes generated in this study either individually or sequentially…….……..48

Figure 2.10. Representative tandem mass spectra (MS^2) of A. AcABK and B. diAcABK with predicted fragmentation…….49

Figure 2.11. Representative mass spectra of AMK control and AMK modified with various amount of AcCoA by various enzymes generated in this study either individually or sequentially……..…….54

Figure 2.12. Representative tandem mass spectra (MS^2) of A. AcAMK and B. diAcAMK with predicted fragmentation……..…55

Figure 3.1. Structures of the AGs tested in this study……...……69

Figure 3.2. The inhibition of AAC enzymes by various metal salts with and without physiological concentration of NaCl. The clinical relevant AGs, AMK, GEN, and TOB, are presented here. Other AGs, KAN, NEO, NET, and SIS, are presented in Figure 3.3…….…73

Figure 3.3. The inhibition of AAC enzymes by various metal salts with and without physiological concentration of NaCl. The AGs that are not presented in Figure 3.2, KAN, NEO, NET, and SIS, are presented here…….……74

Figure 3.4. Representative IC_{50} plot……78

Figure 3.5. Representative graph demonstrating that addition of EDTA restored the ability of AACs to acetylate AGs as the metal ions were chelated……...79

Figure 3.6. Agarose gels of PCR reactions probing for AME genes in various ATCC strains and clinical isolates……81

Figure 3.7. SDS-PAGE gel of $NHis_6$-tagged AAC(3)-Ia (19.4 kDa) purified by Ni^{II}-NTA chromatography……89

Figure 4.1. Structures of A. AGs with their 2-DOS core highlighted in orange, and B. (d)NTPs used in this chapter……96

Figure 4.2. Schematic of the coupled UV-Vis assay used in this study for determination of substrate and cosubstrate profiles and kinetics……..99

Figure 4.3. Pictures of TLC plates of APH(3')-IIa reacting with ATP and various AGs as well as the corresponding R_f values for each lane……101

Figure 4.4A. Pictures of TLC plates of APH(3')-IIa reacting with various (d)NTPs and AGs……....102

Figure 4.4B. R_f values for each lane of TLC sample listed in Figure 4.4A presented on the previous page…….…….103

Figure 4.5. Michaelis-Menten graphs with the determined kinetics parameters of APH(3')-IIa with various AG substrates and NTP cosubstrates……..…107

Figure 4.6. Time course reaction for each NTP with APH(3')-IIa enzyme with either 1× or 2× PK-LDH concentration in the reaction…….…109

Figure 4.7. Computational superimposition of the protein structures of A. APH(3')-IIa (in beige) with KAN (in bright yellow) bound (PDB ID: 1ND4) and APH(3')-IIIa

(in pale blue) with KAN (in teal) bound (PDB ID:1L8T). B. APH(3')-IIa (in beige) with KAN (in bright yellow) bound (PDB ID: 1ND4) and APH(3')-IIIa (in pale green) with ADP (in dark green) and NEO (in bright green) bound (PDB ID:2B0Q……110

Figure 4.8. Superimposition of APH(3')-IIa (in pale yellow) with KAN (in bright yellow) bound (PDB ID: 1ND4) and two crystal structures of APH(2")-IVa with adenosine (APH(2")-IVa in light blue, adenosine in dark green, PDB ID: 4DT8) and guanosine (APH(2")-IVa in light purple, guanosine in purple, PDB ID: 4DT9) bound. Residues of APH(3')-IIa are colored in orange whereas the residues in APH(2")-IVa are colored in teal and dark purple. The specific interactions between each enzyme and nucleoside are shown in four separate panels in Figure 4.9……...112

Figure 4.9. Superimposition of crystal structures of APH(3')-IIa with KAN (PDB ID: 1ND4) and APH(2")-IVa with adenosine and guanosine (PDB IDs: 4DT8 and 4DT9, respectively). A. APH(2")-IVa (in light teal) and adenosine in dark green with the backbones of T96 and I98 colored in dark teal, B. APH(2")-IVa (in light purple) and guanosine in purple with the backbone of T96 and I98 colored in dark purple, C. APH(3')-IIa (in pale yellow) with KAN (in bright yellow) and the adenosine from APH(2")-IVa structure in dark green and the backbone of G95, V97, and G99 in orange, D. APH(3')-IIa (in pale yellow) with KAN (in bright yellow) and the guanosine from APH(2")-IVa structure in purple and the backbone of G95, V97, and G99 in orange…...113

Figure 5.1. Number of strains grouped by the number of antibiotics to which the *P. aeruginosa* strains are resistant……....125

Figure 5.2. Distribution of MIC values of each antibiotic based on the susceptibility to GEN……..…..127

Figure 5.3. Distribution of MIC values of each antibiotic based on the susceptibility to NET and SIS……..…..128

Figure 5.4. Distribution of MIC values of each antibiotic based on the susceptibility to TOB and MEM……....129

Figure 5.5. Sample agarose gel of representative PCR products for each AME gene probed…….132

Figure 5.6. Distribution of MIC values of each antibiotic grouped by the presence or absence of the *aac(6')-Ib* gene……...…..139

Figure 5.7. Distribution of MIC values of each antibiotic grouped by the presence and absence of *aph(3')-Ia*, and *aac(6')-Ib* + *aph(3')-Ia*……..……140

Figure 5.8. Number of *P. aeruginosa* clinical isolates harboring various AME gene patterns……....141

Figure 6.1. Structures of A. the common azole antifungals with the triazole pharmacophore highlighted in pink as well as B. the chemical synthesis of bromperidol series compounds (1-5) involved in this chapter……..150

Figure 6.2. Time- and dose-dependent antifungal synergy of the combinations of A. POS or B. VOR and compound 2 at various concentrations against *C. albicans* ATCC 64124 (strain *F*).……...163

Figure 6.3. Mammalian cytotoxicity evaluation of A. POS and VOR alone, B. compound 2 alone, C. and D. representative combinations of azoles (POS or VOR) at various concentrations along with compound 2 at 8 μg/mL (panel C) or 32 μg/mL (panel D) supplemented in the media against BEAS-2B, HEK-293, and J774A.1 cells……168

Figure 6.4. ^{1}H NMR spectrum for compound 1 in $CDCl_3$……..175

Figure 6.5. ^{13}C NMR spectrum for compound 1 in $CDCl_3$…….……176

Figure 6.6. HPLC trace for compound 1……..…..176

Figure 6.7. ^{1}H NMR spectrum for compound 2 in $CDCl_3$……..…177

Figure 6.8. ^{13}C NMR spectrum for compound 2 in $CDCl_3$…….177

Figure 6.9. HPLC trace for compound 2……178

Figure 6.10. ^{1}H NMR spectrum for compound 3 in $CDCl_3$……..178

Figure 6.11. ^{13}C NMR spectrum for compound 3 in $CDCl_3$……..…..179

Figure 6.12. HPLC trace for compound 3……179

Figure 6.13. ^{1}H NMR spectrum for compound 4 in $CDCl_3$……..180

Figure 6.14. ^{13}C NMR spectrum for compound 4 in $(CD_3)_2SO$…….……..181

Figure 6.15. HPLC trace for compound 4……182

Figure 6.16. ^{1}H NMR spectrum for compound 5 in $CDCl_3$…….182

Figure 6.17. ^{13}C NMR spectrum for compound 5 in CD_3OD……..……183

Figure 6.18. HPLC trace for compound 5……...….184

Figure 7.1. Western blot analysis of the PTC read-through induction in HEK293 cells transiently transfected with *laforin wt* (negative control), *laforin Y86X*, *laforin*

R241X, and *MeCP2 R294X* (positive control) by GEN at various concentrations.....196

Figure 7.2. SDS-PAGE of PanD wt and H21R-I49V proteins after Ni^{II} purification and after incubation at various temperatures……..199

Figure 7.3. DAB and BME quenching various concentrations of L-Asp and β-Ala….200

Figure 7.4. Enzymatic activity of PanD wt after Ni^{II} purification and incubation at 37 or 65 °C……...…200

Figure 7.5. Enzymatic activity of PanD wt and H21R-I49V double mutant in the presence of 5 or 50 μM of PZA or POA as an inhibitor……..…200

LIST OF ABBREVIATIONS

AAC	Aminoglycoside acetyltransferase
ABK	Arbekacin
AcCoA	Acetyl coenzyme A
ADD	Additive
ADP	Adenosine 5'-diphosphate
AG	Aminoglycoside
AHB	(*S*)-4-amino-2-hydroxybutyrate
AmB	Amphotericin B
AME	Aminoglycoside-modifying enzyme
AMK	Amikacin
ANT	Aminoglycoside nucleotidyltransferase
APH	Aminoglycoside phosphotransferase
APR	Apramycin
Arg or R	Arginine
Asp or D	Aspartate
A-T	Ataxia-telangiectasia
ATCC	American Type Culture Collection
ATG	Antagonistic
ATP	Adenosine 5'-triphosphate
AZA	Aztreonam
BME	β-mercaptoethanol
CDP	Cytidine 5'-diphosphate

CEFX	Ceftriaxone
CF	Cystic fibrosis
CFPM	Cefepime
CFTR	Cystic fibrosis transmembrane conductance regulator
CFU	Colony-forming unit
CFX	Cefoxitin
CFZ	Ceftazidime
CIP	Ciprofloxacin
CLSI	Clinical and Laboratory Standards Institute
CMD	Congenital muscular dystrophy
CTP	Cytidine 5'-triphosphate
DAB	*O*-diacetylbenzene
DMD	Duchenne muscular dystrophy
dATP	2'-deoxyadenosine 5'-triphosphate
dCTP	2'-deoxycytidine 5'-triphosphate
dGTP	2'-deoxyguanosine 5'-triphosphate
dNDP	2'-deoxynucleoside 5'-diphosphate
dNTP	2'-deoxyadenosine 5'-triphosphate
DTDP	4,4'-dithiodipyridine
DTNB	5,5'-dithiobis-(2-nitrobezoic acid)
dUTP	2'-deoxyuricine 5'-triphosphate
EDTA	Ethylenediaminetetraacetic acid
EFG	Elongation factor G

Eis	Enhanced intracellular survival
FDA	Food and Drug Administration
FHB	Fusarium Head Blight
FICI	Fractional inhibitory concentration index
FLC	Fluconazole
GDP	Guanosine 5'-diphosphate
GEN	Gentamicin
GTP	Guanosine 5'-triphosphate
G418	Geneticin
HAI	Healthcare-associated infection
His or H	Histidine
HRP	Horseradish peroxidase
HTS	High Throughput Screen
HYG	Hygromycin
Ile or I	Isoleucine
ITC	Itraconazole
IPM	Imipenem
IPTG	Isopropyl β-D-1-thiogalactopyranoside
ITP	Inosine 5'-triphosphate
KAN	Kanamycin
KANA	Kanamycin A
KANB	Kanamycin B
KPC	*Klebsiella pneumoniae* carbapenemase

KTC	Ketoconazole
LC_{50}	Half-maximum lethal concentration
LD	Lafora disease
LDH	Lactate dehydrogenase
LEV	Levofloxacin
MDR	Multidrug-resistant
MEM	Meropenem
MIC	Minimum inhibitory concentration
MRSA	Methicillin-resistant *Staphylococcus aureas*
MS	Mass spectrometry
MS^2	tandem mass spectrometry
NADH	Nicotinamide adenine dinucleotide
NDP	Nucleoside 5'-diphosphate
NEA	Neamine
NEO	Neomycin
NEO^R	Neomycin resistance
NET	Netilmicin
NMDA	*N*-methyl-D-aspartate
NMR	Nuclear magnetic resonance
NTF	Nitrofuratoin
NTP	Nucleoside 5'-triphosphate
PAR	Paromomycin
PCR	Polymerase chain reaction

PEP	Phosphoenolpyruvate
Phe or F	Phenylalanine
PK	Pyruvate kinase
PLZ	Plazomicin
POA	Pyrazinoic acid
POS	Posaconazole
pSYN	Partially synergistic
PTC	Premature termination codon
PZA	Pyrazinamide
RIB	Ribostamycin
RRF	Ribosome recycling factor
RTT	Rett syndrome
Ser or S	Serine
SIS	Sisomicin
SMA	Spinal muscular atrophy
smFRET	Single-molecule fluorescence resonance energy transfer
SMIC	Sessile minimum inhibitory concentration
SMN	Survival motor neuron
SOE	Single overlap extension
STR	Streptomycin
SYN	Synergistic
TDP	Thymidine 5'-diphosphate
TET	Tetracycline

Thr	Threonine
TLC	Thin layer chromatography
TOB	Tobramycin
TTP	Thymidine 5'-triphosphate
UTP	Uridine 5'-triphosphate
Val or V	Valine
VOR	Voriconazole
XTT	(2,3-bis(2-methoxy-4-nitro-5-sulfo-phenyl)-2H-tetrazolium-5-carboxanilide
YEPD	Yeast extract peptone dextrose
ZnPT	Zinc pyrithione
2-DOS	2-deoxystreptamine

Chapter 1. New trends in the use of aminoglycosides

Despite their inherent toxicity and the acquired bacterial resistance that continuously threatens their long-term clinical use, aminoglycosides (AGs) still remain valuable components of the antibiotic armamentarium. Recent literature showed that the AGs' role has been further expanded as multi-tasking players in different areas of study. This chapter aims at presenting some of the new trends observed in the use of AGs in the past decade that is related to this dissertation, along with the current understanding of their mechanisms of action in various bacterial and eukaryotic cellular processes.

1.1. INTRODUCTION

The 2-deoxystreptamine (2-DOS) aminoglycosides (AGs) are a group of naturally occurring and semi-synthetic aminocyclic sugars (Figure 1.1). AGs can be structurally classified as 4,5-disubstituted AGs (*e.g.*, neomycin B (NEO), paromomycin (PAR), and ribostamycin (RIB); *note*: although neamine (NEA) is a 4-monosubtituted AG, we included it in the 4,5-disubstituted AGs in Figure 1.1 as its structure is comprised in their scaffolds) as well as 4,6-disubstituted AGs (*e.g.*, amikacin (AMK), kanamycin A and B (KANA and KANB), tobramycin (TOB), gentamicin (GEN), geneticin (G418), netilmicin (NET), and sisomicin (SIS)). Other AG scaffolds include the monosubstituted AGs (*e.g.*, apramycin (APR) and hygromycin (HYG)), and streptomycin (STR).

AGs' broad-spectrum of activity against pathogenic bacteria has favored them as a valuable class of antibiotics for the past 70 years.[1] Studies of their antibacterial mode of action have revealed that AGs bind both to the aminoacyl site (A-site) of the 16S rRNA of bacteria,

where they perturb the "proof-reading" process that ensures protein translation fidelity,[2] and to the 50S ribosomal subunit, inhibiting translocation and ribosome recycling.[3-4]

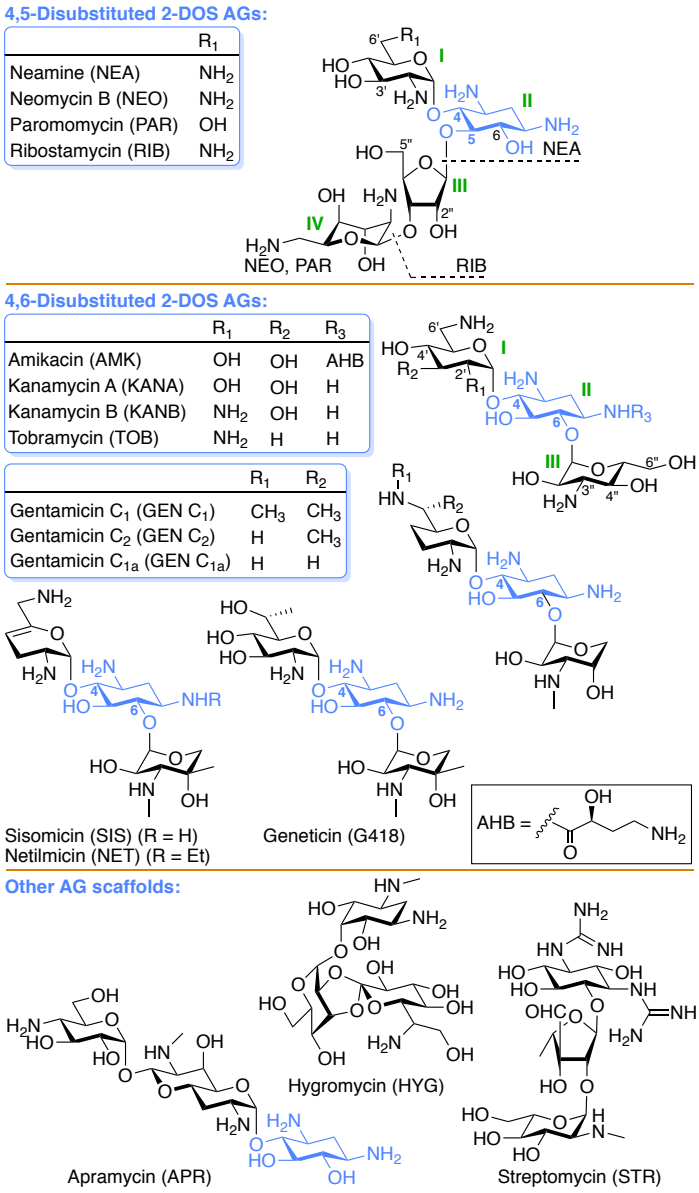

Figure 1.1. Structures of parent AGs discussed in this chapter. The 2-deoxystreptamine (2-DOS) ring is depicted in blue.

Naturally occurring AGs are produced by *Streptomyces* and *Micromonospora* soil bacteria,[5] which proactively methylate their ribosome to survive the bactericidal action of AGs' secondary metabolites.[6] This mechanism, along with the decrease in AG uptake and the emergence of aminoglycoside-modifying enzymes (AMEs), has significantly plagued the clinical efficacy of AGs.[7] AMEs, in particular, have been a serious threat to AGs' long term use and more than 100 of them have been identified.[8] These enzymes, which include AG *N*-acetyltransferases (AACs), AG *O*-phosphotransferases (APHs), and AG *O*-nucleotidyltransferases (ANTs) (Figure 1.2A) act through chemical modifications of the structures of AGs. Indeed, AACs catalyze the transfer of an acetyl group from acetyl coenzyme A (AcCoA) to the amine functionalities of AGs, while APHs and ANTs use ATP (and in some cases GTP)[9-12] to transfer a phosphate and an adenosine (guanidine) monophosphate moieties, respectively, to the hydroxyl groups of AGs (Figure 1.2B). Unlike other AACs, which are regiospecific, the newly discovered enhanced intracellular survival (Eis) is a versatile enzyme that can acetylate different amine positions of AGs.[13-22]

Soon after its introduction in the therapeutic regimen of tuberculosis, STR, the first AG ever discovered, displayed toxic side effects. Nephrotoxicity and ototoxicity, which are the most common adverse effects associated with AG antibiotics, have also hampered their clinical effectiveness. These serious shortages have sparked considerable interests in the scientific community. Our group has recently provided a comprehensive overview of AG antibiotics[1] and the recent approaches that have been developed to triumph over AMEs' actions.[23] Of special note, the combination of AGs with AME inhibitors can be a potentially

effective tactic to revive the usefulness of these drugs against AG-resistant strains. This was inspired by the clinical success encountered by the co-administration of β-lactams and β-lactamase inhibitors.[24] The search for Eis inhibitors enabled the development of a high-throughput screening (HTS) method that facilitated the identification of 25 active compounds out of 23,000 tested.[22] While waiting for HTS to be applied to the other classes of AMEs, existing AME inhibitors could be utilized in the meantime. These include the APH(3')-IIIa inhibitor ankyrin repeat protein,[25-26] the APH(2")-IVa inhibitor quercetin,[27] the APH(9)-Ia inhibitor CKI-7, which was co-crystallized with APH(3')-IIIa,[28] and the bifunctional enzyme AAC(6')-Ie/APH(2")-Ia inhibitor aranosin.[29] The 3-(dimethylamino)propylamine moiety was also found to be an essential scaffold for ANT(2")-Ia and APH(3')-IIIa inhibitors.[30]

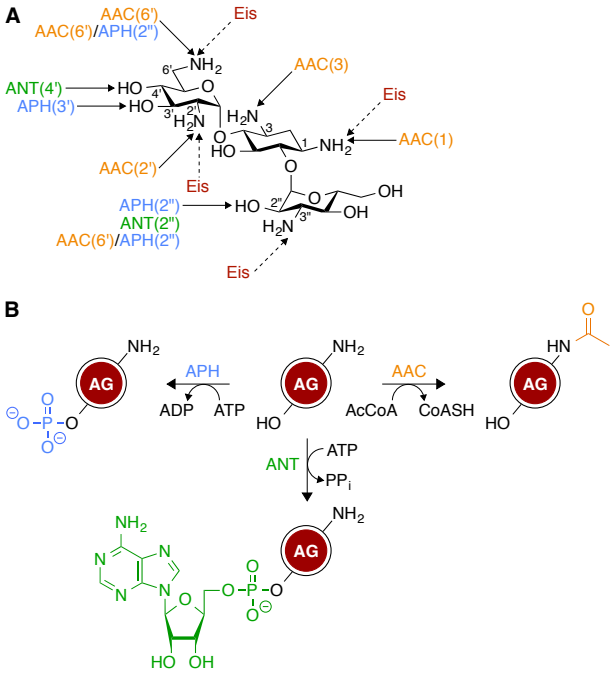

Figure 1.2. A. Sites that are targeted by the different AMEs. Unlike other AMEs that are regiospecific, Eis can multi-acetylate AGs. **B.** Chemical modifications catalyzed by AMEs.

Also worth mentioning is the development of AGs that could both tightly bind to the bacterial ribosome and disrupt the protein synthesis machinery and also be poor substrates of AMEs. This has eventually led to the synthesis of:

i) Structurally constrained AGs – Originally designed to resemble the locked conformation of AG when bound to the bacterial A-site, a variety of rigidified NEO, PAR, NEA, and KANA derivatives were synthesized (Figure 1.3).[31-37] Although they all displayed a decreased antibacterial activity compared to the parent AGs, the NEO and the KANA-restricted derivatives (through methylene linkers between the 2'-NH and 5"-C as well as the 2'-oxygen and 5-oxygen, respectively) were still quite active, with MIC values ranging from 2.5 to 64 μg/mL. Additionally, the NEO-restricted derivatives were poor substrates of *Staphylococcus aureus* ANT(4') and *Mycobacterium tuberculosis* AAC(2')-Ic.

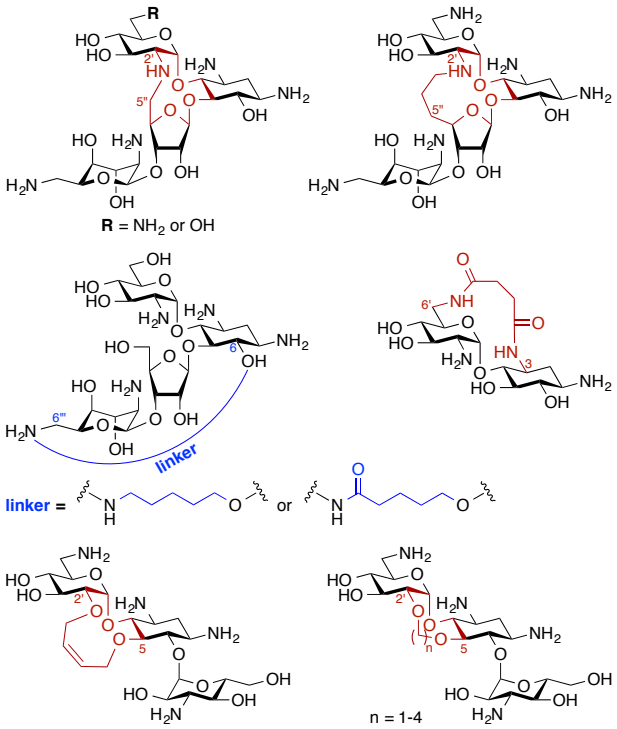

Figure 1.3. Structures of conformationally constrained AGs.

ii) AG dimers – Following evidence that dimerized parent AGs may have improved binding affinity towards RNA,[38] series of homo- and heterodimeric AGs were developed with the goal of investigating their ability to target the bacterial A-site.[39-43] In addition, some NEA dimers, linked at the 5-position *via* amides and 1,2-hydroxyamines (Figure 1.4), could evade the action of the AMEs AAC(6')-Ii, APH(3')-IIIa, and AAC(6')-Ie/APH(2")-Ia better than the parent compounds.[39] Furthermore, a TOB homodimer was shown to be a poor substrate of TOB-targeting AMEs AAC(6')-Ie/APH(2")-Ia, AAC(6')-Ib', and ANT(4').[43] The use of AG dimers has, however, not been limited to targeting bacterial ribosome. In fact, AG dimers also found application as binders of RNA hairpin loops,[44-45] as binders of the dimerization initiation site of the HIV-1 genomic RNA,[46] the HIV-1 Rev response element,[47] and HIV-1 trans-acting responsive sequence.[48] AG monomers and dimers have also found to be useful as inhibitors of anthrax lethal factor.[49-51]

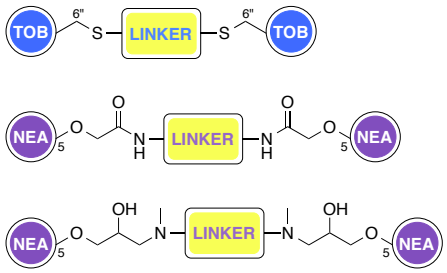

Figure 1.4. Representative TOB and NEA dimers with different linker attachments. *Note*: NEO-NEO, NEO-TOB, KAN-KAN, and KAN-TOB dimers have also been reported in the literature.[38, 41-43, 47]

iii) Guanidinylated AGs – By replacing the amine or hydroxyl moieties with a guanidine functionality in TOB, AMK, KANA, NEO, NEA, PAR, and APR, the Nizet and Tor groups were able to develop a library of AG derivatives, with most of them displaying an enhanced antibacterial activity, which correlated with higher affinity to bacterial A-site.[52]

We will discuss herein the antibacterial modes of action of AGs as well as some of the novel applications of AGs that have been investigated in the last decade, including as antifungal agents, as amphiphiles, and as potential treatment of genetic diseases arising from premature termination codons (PTCs). New ways to alleviate AG-induced ototoxicity will also be examined, with reference to the solely non-toxic AG APR and the prospective clinical candidate plazomicin (PLZ).

1.2. AMINOGLYCOSIDES MODE OF ACTION: BINDING TO THE RIBOSOME

AGs have long been known to exert their antibacterial functions by binding to the bacterial ribosome and interfering with protein translation. To further probe their mechanism of action, different approaches have been developed and employed in the past decades, including fluorescence-based assays,[3, 53-56] computational simulations,[57-58] microarray assays,[59-63] and X-ray crystallography.[4, 64-65] As a result, AGs have been demonstrated to bind not only to the ribosomal decoding A-site on the 16S rRNA, causing miscoding in the nascent polypeptide, but also to the helix 69 (h69) in the large 50S ribosomal subunit, which is critical in the processes of mRNA/tRNA translocation and ribosome recycling.

1.2.1. Aminoglycosides binding to the A-site

As a canonical model of AG binding, the interactions between AGs and the decoding A-site on the 30S ribosomal subunit have been extensively studied. AGs bind to a highly conserved set of nucleotides on helix 44 (h44) of the 16S rRNA (Figure 1.5A). The carbohydrate rings of AGs stack to the RNA, thereby stabilizing the bound complex at the

A-site by hydrogen-bonding and H_2O-mediated interactions.[57, 65-67] For 4,6-disubstituted 2-DOS AGs, the presence of a 4'-OH or a 2'-NH_2 group on ring I was reported to be critical in assisting proper targeting of the ribosome by the antibiotics. However, the substitution pattern on ring III was found to have minimal effect on drug targeting.[67] In the case of 4,5-disubstituted 2-DOS AGs, the stacking effect of ring I was complemented by rings III and IV, which enhanced AG-rRNA complex stabilization.[66] Appending of an aromatic moiety at the 2"-position of PAR was found to improve the drug susceptibility of bacterial resistant strains, thereby providing further details for the mechanisms of AG binding.[57]

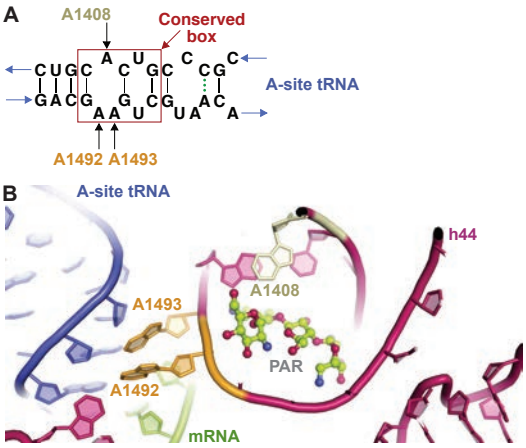

Figure 1.5. A. Representation of the internal loop structure of h44. **B.** Representation of h44 of the 16S rRNA showing residues destacking upon AG binding.

Binding of AGs to the 16S rRNA was reported to extrude the A1492 and A1493 residues on h44, conformationally rearranging them from an intra-helical to an extra-helical state in the rRNA. Such change disturbed the fidelity of aminoacyl-tRNA selection.[68] rRNA mutagenesis, X-ray crystallography, and determination of MIC studies revealed the residues that were critical in maintaining proper AG binding (A1492 and A1493) and stabilizing the destacked helix (A1408) (Figure 1.5B).[54-55] These results were also confirmed by fluorescence-based studies where S12, a ribosomal protein in the 30S

complex, was fluorescently-tagged to investigate NEO and h44 interactions.[56] Other residues, such as the purine/pyrimidine switches 1411•1489 and 1410•1490, were reported to have minimal effect on MIC values while 1409•1491 was found to be critical for AG susceptibility.[69]

In addition to the bacterial ribosomes, AGs have also been known to bind with lower affinity to the mammalian ribosomes, causing undesired side effects. In the aim of achieving higher selectivity of AGs towards their bacterial target, both AG and ribosome modifications have been investigated. 4',6'-*O*-acetal and 4'-*O*-ether modifications of PAR have been shown to impart greater sensitivity to A1408G, G1491C, and G1491A mutations, characteristic of prokaryotic-eukaryotic ribosome differences.[70] Applying nucleobase-conjugated AGs as probes, the A-site was reported to discriminate its ligand structures and conformations.[71] Conversely, in a study where KANA, TOB, NEA, and NEO derivatives were examined in a microarray-based assay against a library of internal loops in a two-dimensional combinatorial screening analysis, AGs were found to be non-selective and each preferentially bound to a different internal loop. For instance, KANA preferably bound to 1x1 internal loops with C•A mismatches, and the stability of the internal loop structure correlated with the binding affinity to AGs.[60-63] Anderson and Mecozzi further investigated the minimum sequence required for PAR binding to the A-site *via* a computational approach.[58] A combination of molecular dynamics, free-energy calculations, and *in vitro* binding assays showed that the 11-nucleotide:10-nucleotide duplex RNA was minimal to provide stable PAR binding, whereas smaller dupleces lost the complex stability and the accessibility for PAR.[58]

1.2.2. Aminoglycosides binding to h69

Although most AGs bind to the decoding A-site and introduce amino acids from near-cognate aminoacyl-tRNAs into the nascent polypeptides, this effect alone was postulated to be insufficient justification of AGs' antibacterial effect. Instead, some AGs, including NEO, PAR, and TOB, have been identified to have a secondary binding site at the major groove of h69 of the 23S rRNA of the 50S ribosomal subunit.[64, 72] Crystallography data revealed that h69 forms direct contact with the A-/P-site tRNAs, as well as the decoding center, by looping around the interface of the two subunits and forming an inter-subunit bridge (B2). Due to the vital position of h69 in the 3D structure, the binding of AGs to h69 hinders the ribosomal movement/global conformational rearrangement when the 30S rotates around the 50S ribosomal subunit in racquet-like movement around the L1 stalk domain.[73] This concerted movement, assisted by ribosome recycling factor (RRF) and GTPase elongation factor G (EF-G), occurs in multiple steps during protein translation, especially translocation and ribosome recycling processes. Therefore, AGs' mechanism of inhibiting the global conformational rearrangement is a vital contribution to their antibacterial properties.[4]

During translocation, the aminoacyl-tRNA first orients itself perpendicularly to the 30S and 50S subunits at the A-site, which is considered the classical configuration. Post peptide bond formation and prior to translocation, intermediate states where the 3'-terminus and the acceptor stems of tRNAs proceed to the next site on the large subunit while the anticodon stems remain fixed on the 30S subunit are referred to as the "hybrid" states.[74-75]

Two distinct hybrid-state intermediates have been elucidated by the Blanchard's group *via* single-molecule fluorescence resonance energy transfer (smFRET).[76] Studies have shown that AGs binding to h69 halted the pre-translocation complex at post peptidyl transfer. The dynamics of AG binding to pre-translocation complex revealed high-affinity (h44) and low-affinity (h69) binding sites on the ribosome. While most AGs bind to h44 only and stabilize the classical state, NEO was shown to stabilize the hybrid states at the low-affinity site upon saturation of h44.[3] To further study NEO inhibition on the ribosomal global conformational rearrangement, pre-steady state smFRET and dynamics studies demonstrated that NEO binding to h69 excluded RRF binding to the ribosome and attenuated the 30S subunit rotation with respect to the large subunit that normally promotes the conformational switch from the classical to the hybrid configuration. Crystal structures also confirmed NEO binding to h69, where the latter forms an inter-subunit bridge B2 and interacts with helices h24 and h45 of the 30S subunit.[64]

At the end of each translation cycle is the dissociation of the ribosome complex, where the same racquet-like movement is involved as in translocation. RRF binds to h69 and extrudes it away from the inter-subunit surface, causing the 30S subunit to dissociate from the 50S. However, AG binding to h69 makes the complex inaccessible to the RRF, and therefore, locked in the bound form, inhibiting ribosome recycling.[4] Confirming previous results, Agris and co-workers further compared the affinity of NEO and GEN to *Escherichia coli* and human h69. They reported that AGs bind to human h69 with lower affinity than to *E. coli* h69, which shed light into AG antibiotics target selectivity.[72]

AGs are structurally diverse, and therefore, bound to function by different mechanisms. Puglisi and co-workers reported the various mechanisms of APR, GEN, and PAR, which were confirmed by nuclear magnetic resonance (NMR) spectroscopy.[53] APR was found not to displace A1492 and A1493 residues at the decoding center but rather to block the translocation process. GEN and PAR, on the other hand, exhibited a different mode of action whereby they destacked h44, leading to significant miscoding in the nascent polypeptide.

Tracing back the efforts that have been put forth in the investigation of how AGs perform their antibiotic functions, a greater picture has been revealed. However, the unobserved part of the iceberg still remains elusive yet inviting. Along this line, more untouched functions of AGs are starting to be discovered. In addition to causing amino acid misincorporation and inhibiting translocation and ribosome recycling, Foster and Champney reported that AGs hinder the 30S ribosome assembly, which brings up an unexplored mechanism of AG antibiotics.[77] Any further knowledge we gain on the mechanism of action of AGs is certainly a step towards defeating bacterial infections, especially in the rapidly emergence resistant bacterial strains.

1.3. AMPHIPHILIC AMINOGLYCOSIDES

Owing to the recrudescence of antibiotic resistance by pathogenic bacteria and the promise of cationic amphiphiles as potent antimicrobial agents with new mechanisms of action, a novel class of antibacterial agents known as amphiphilic AGs came into being. Several groups have devoted tremendous efforts in the development of AG derivatives that bear in

their structure hydrophobic moieties connected to the cationic hydrophilic AG. Linear alkyl chains, ranging from C_6 to C_{20}, have been introduced through an amide bond at the 5"-position of NEO,[78-81] and the 6"-position of KAN[82] and TOB.[83] They have also been linked to TOB and PAR as thioethers at the 6"- and 5"-positions, respectively.[84-86] Other hydrophobic residues investigated include (i) amino acids/peptides, which have been attached to the nitrogen atom of AGs through an amide bond,[79] a lysine moiety,[87] or a triazole ring;[88-89] and (ii) aromatic rings, attached at the oxygen atom, to form polyethers and/or polycarbamates of NEA, PAR, NEO, KAN, and AMK.[90-93] This led to the discovery of potent amphiphilic AGs with revived antibacterial activity. For example, the C_{16} and C_{18} lipid chains conferred to NEO a 32-fold improvement in antibacterial activity against MRSA, while the C_{16} lipid chain decreased the MIC of KAN from 128 to 2 μg/mL against Canadian clinical isolates of MRSE, and the C_{14} lipid chain rendered TOB 64 times more active against *E. coli* BL21 (DE3) (Eis) and *Streptococcus mutans* UA159. Aromatic rings also considerably ameliorated the MIC values of NEO, KAN, NEA, and PAR.

Amphiphiles, such as cationic peptides, have been shown to exert their antimicrobial activities by disrupting the bacterial membranes *via* three main models: the toroidal, barrel-stave, and carpet models.[94] With the aim of investigating the mode of action of antibacterial amphiphilic AGs, the Garneau-Tsodikova and Fridman groups showed that amphiphilic AGs in the form of 6"-thioether TOB analogues target the bacterial membrane rather than the traditional bacterial ribosome.[84] Similar results were also observed by the Chang[95] and the Mingeot-Leclercq[96] groups, who synthesized 5"-derivatized NEO as well as 3'- and 6-modified NEA, respectively.

1.4. AMINOGYCOSIDES AS ANTIFUNGAL AGENTS

AGs have long been used for the treatment of bacterial infections in humans and animals, but their ability to bind to the eukaryotic ribosomes, though with lower affinity when compared to the prokaryotic ribosomes, has been a continuous step back. This limitation has, however, been exploited to explore new targets of AGs. Recently, Lee and co-workers have investigated the activities of PAR, NEO, RIB, and STR against six crop pathogenic oomycetes (*Phytophthora* and *Pythium* species) and ten common fungi.[97] All four AGs manifested modest to excellent antioomycete activity, with non-existent activity against several true fungal species. PAR displayed the strongest *in vitro* and *in vivo* inhibitory effect on various plant pathogens, including *P. capsici* and *P. infestans*, which are responsible for red pepper and tomato late blight diseases, respectively. Even though fungi are most often associated with crop diseases, they still remain an important problem in human and veterinary medicine that needs to be addressed.

Pythiosis is an infectious disease caused by the fungus *P. insidiosum* that affects dogs, cats, horses, and even humans. The *in vitro* susceptibility of 24 *P. insidiosum* isolates was measured against four naturally occurring AGs (PAR, GEN, NEO, and STR).[98] With *in vitro* MIC values ranging from 32 to 128 μg/mL, which are all higher than the safe plasma concentration of 30 μg/mL, these AGs could not be used therapeutically. It has, however, been observed that when used in conjunction with compounds that increase their cellular uptake in fungi, AGs could exert their fungicidal activity at lower, and possibly safer, concentrations. This is the case of HYG, a structurally unusual AG produced by *S.*

hygroscopicus that kills bacteria and fungi through protein biosynthesis inhibition. The membrane-disrupting agent polymyxin B was found to work synergistically with HYG, enabling this latter to inhibit the growth of *Saccharomyces cerevisiae* cells at a lower concentration than that expected from its own MIC value.[99]

Fungal and oomycete infections are responsible for huge economic loss generated from plant diseases. Current strategies to control these infections include the direct application of chemical fungicides. Although potentially useful as agrofungicides, the majority of AG antibiotics are clinically used for the treatment of human bacterial pathogens. Their involvement in plant disease management could then promote bacterial resistance, reduce the soil concentration of the agrofungicide AG, or change its structure. To overcome this problem, AG derivatives possessing antifungal activities with no antibacterial capabilities were pursued.

KANB is a classical AG antibiotic isolated from the soil bacterium *S. kanamyceticus* and has long been used for its broad-spectrum activity against Gram-negative and Gram-positive bacteria. One of its analogue, FG08 (Figure 1.6), which bears a 3"-OH group, a linear C_8 alkyl chain at the 4"-position, and is deoxygenated at the 6"-position, showed little to no antibacterial activity, but inhibited the growth of various yeasts, oomycetes, and true fungi, with *in vitro* MIC values between 3.9 and 31.3 μg/mL.[100] The antibacterial to antifungal activity "switch" in FG08 was attributed to the octyl chain, which conferred some amphiphilic properties to the AG. The susceptibility studies of *Fusarium graminearum*, a fungus responsible for the crop disease Fusarium Head Blight (FHB), to

FG08 revealed that at concentration close to *in vitro* MIC, FG08 afforded prophylactic protection to FHB-susceptible wheat seedlings against *F. graminearum*. FG08 was also capable of suppressing FHB disease. FG08 was shown to exert its antifungal activity through permeation of the fungal membrane.[100-101] This property of certain AGs to disrupt the membrane of fungi has also been observed with bacteria.

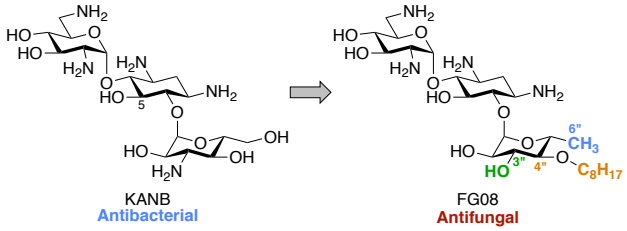

Figure 1.6. Modifications at the 3"-, 4"-, and 6"-positions of the antibacterial KANB result in the antifungal agent FG08.

1.5. READING THROUGH THE FAULTY "STOPS" AT THE PREMATURE TERMINATION CODONS

Pathogenic PTCs result from various mutations, including nonsense mutations, insertions or deletions, and/or alternative splicing events. In these diseases, PTCs are introduced prior to the natural stop codons, thereby leading to the production of truncated and, often times, defective proteins. AG interaction with eukaryotic ribosomes also sparked their new application as PTC suppressing compounds. AG binding to the mammalian 18S rRNA A-site, which is homologous to the 16S rRNA in bacterial ribosome complex, has been proposed to promote near-cognate aminoacyl-tRNA misincorporation at PTC site and allow random read-through for full-length protein production in in-frame PTC diseases (Figure 1.7).[102-103] Various AGs, including parent drugs and their derivatives, have been exploited for their read-through promoting activities in PTC diseases such as cystic fibrosis

(CF), Duchenne muscular dystrophy (DMD), Rett syndrome (RTT), and other PTC disorders (Figure 1.8).

1.5.1. Cystic fibrosis (CF)

CF arises from mutations in the *cystic fibrosis transmembrane conductance regulator* (*CFTR*) gene, which encodes a transmembrane cAMP-gated chloride channel in the epithelium. Studies have shown that several parent AGs, such as AMK and GEN, promote read-through of the PTC and increase the level of functional CFTR in mouse models and patient samples.[104-106] Furthermore, co-administration of AGs with poly-L-aspartic acid showed enhancement of the PTC suppression of GEN by 20-40%.[107] A combination of the two drugs increased the level and duration of PTC suppression as well as reduced the toxicity of GEN. In addition to parent AGs, their derivatives have also been exploited for higher efficacy and lower toxicity. Several AG derivatives, such as NB30, NB54, NB74, NB84, and NB124 (Figure 1.8) have been reported to suppress PTC at higher potency and lower toxicity compared to parent AGs.[108-110]

1.5.2. Duchenne muscular dystrophy (DMD)

DMD presents lethal X-linked pathology that lacks the protein dystrophin in the muscle fibers, leading to progressive muscle degeneration. Nonsense mutations in the genetic sequence of dystrophin account for about 15% of all DMD cases.[111] Glucocorticoids were the only beneficial treatment but possessed significant side effects, calling for more efforts to develop AGs as treatments for DMD.[112]

As a result of the enormous size of dystrophin, an extensive number of PTCs has been identified. GEN-treated mdx mouse showed rescued vascular parameters monitored by nitric oxide-dependent vascular functions.[113] A study in patient samples also confirmed GEN as an effective PTC suppressing compound.[114]

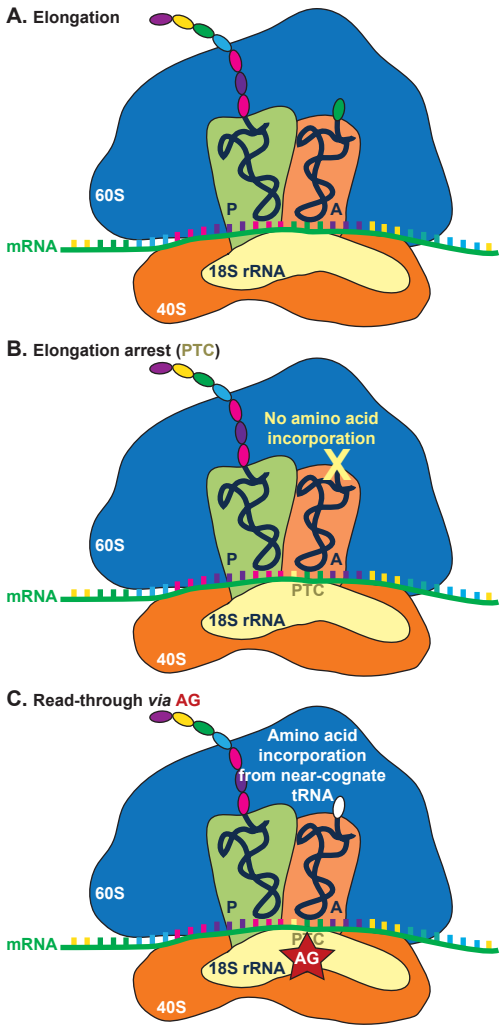

Figure 1.7. Proposed mechanism of AG-induced PTC read-through. **A.** Eukaryotic ribosome complex during normal protein translation elongation. **B.** Elongation arrest at the PTC site due to nonsense mutations results in translation abortion and truncated protein product. **C.** Binding of AG to PTC site allows random incorporation of an amino acid from a near-cognate aminoacyl tRNA and read-through at the PTC site.

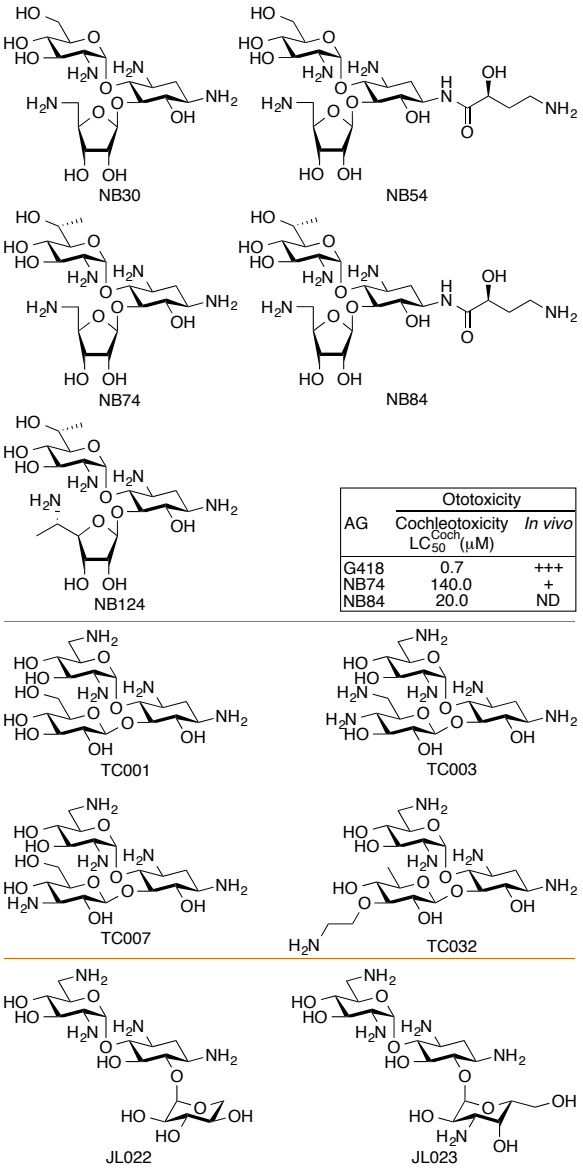

Figure 1.8. Structures of synthetic AG derivatives used for PTC-associated diseases. *Note*: Some of the NB series molecules have been shown to display reduced ototoxicity compared to G418.

As AGs exhibit various efficacies under distinct conditions, patients with different genetic variations at PTC can be subjected to different treatments. For example, PTCs with TGA mutations generally show better therapeutic response to GEN than patients with nonsense mutations TAA or TAG.[115]

1.5.3. Rett syndrome (RTT)

In contrast to DMD that only affects males, RTT is an X-linked PTC disorder solely impacts females. The PTCs for RTT are usually found in the *MeCP2* gene, which encodes methyl CpG-binding protein 2 (MeCP2) involved in epigenetic control of gene expressions. Common mutations in RTT were investigated in transiently transfected HEK-293 cells. The read-through activity was recovered by multiple AGs, including GEN and G418, and weakly by AMK, while PAR was reported to have no read-through promoting activity for these mutations in RTT.[116-117] However, it was also reported that these AGs, though showing PTC suppressing properties *in vitro*, had no read-through activity effect at therapeutic dose.[116] As the most prevalent mutation, R168X was also tested against PAR derivatives NB30, NB54, and NB84. Even though NB30 was not as promising, NB54 and NB84 both showed better efficiency than GEN as PTC suppressing drugs.[118-119]

1.5.4. Spinal muscular atrophy (SMA)

SMA is a neurodegenerative disorder that results from the absence of *survival motor neuron-1 (SMN1)* and symptomized by progressive atrophy of the limb and trunk muscles. *SMN* genes are present in two nearly identical copies (*SMN1* and *SMN2)* that differ by a C (*SMN1*) to T (*SMN2*) transition, leading to an alternative splicing pattern of SMN1 of the mRNA. The PTC in SMN1 results in a truncated non-functional protein that cannot be functionally compensated by SMN2.[120] As AGs are used to suppress PTCs, studies have also utilized AGs to treat SMA to restore functional protein production.[121] The Lorson's group tested 20 synthetic AGs that belong to either the 4,5- or 4,6-disubstituted 2-DOS

families. Six of them, TC001, TC003, TC007, TC032, JL022, and JL023 (Figure 1.8) were shown to increase the number of "gems", which is indicative of the alleviation of SMA disease progression, and functional protein level.[121] One of the six compounds, TC007, was further characterized in an animal model and proved to partially restore phenotype.[122-123]

1.5.5. Other PTC diseases

Type I Usher disease,[124-125] congenital muscular dystrophy (CMD),[126] ataxia-telangiectasia (A-T),[127] coagulation factor VII deficiency,[128] mucopolysaccharidosis type I-Hurler disease,[129] various types of cancer,[130-131] and other types of genetic disorders[132-133] have been investigated for the full-length protein production response after treating with AGs or their derivatives. Overall, GEN and G418 are the two most commonly tested AGs that improve PTC read-through. The response to AG treatment is dose- and context-dependent.[115]

Long-term AG treatment, which produces significant toxicity and bacterial resistance, has promoted the development of AG derivatives that possess higher potency and less toxicity. For instance, NB74 was reported to have a half-maximal lethal concentration (LC_{50}) of 25.8 mM in HEK-293 cells, which is about 10 times higher than the LC_{50} for GEN at 2.5 mM and 20 times higher than that for G418 at 1.3 mM.[110] NB74 was also shown to decrease cochleotoxicity (LC_{50} = 140.0 μM) compared to G418 (LC_{50} = 0.7 μM) (Figure 1.8).[134] There have been discoveries made on other read-through promoting compounds in order to achieve lower toxicity than parent AGs, for instance the organic compound PTC124. However, the lower potency and large variations in the cellular response within each

treatment has limited the use of PTC124 as a general treatment for multiple PTC diseases.[135-136] Therefore, the research on AGs supressing PTC, especially by their derivatization for improved potency and reduced toxicity, remains promising and inviting.

1.6. NEW WAYS TO ALLEVIATE AMINOGLYCOSIDE TOXICITY

Toxicity has always been and still remains a serious impediment to the long-term clinical use of AGs. Indeed, a few years after the discovery of STR and its introduction in the therapeutic regimen of tuberculosis, patients' kidneys and inner ear impairment were observed, resulting in AG-induced nephrotoxicity and ototoxicity, respectively.[137]

Nephrotoxicity arises from the small accumulation of AG drugs in the kidney cortex as a result of their uptake in the epithelial cells of the renal proximal tubules, following their glomerular filtration and excretion from the bloodstream by the urinary system.[138] Nephrotoxicity is a reversible process due in part to the regeneration capability of tubular cells[139] and the ability of dialysis to diminish AG accumulation in the kidneys. Ototoxicity, on the other hand, leads to permanent and irreversible hearing loss. AGs' damage to the inner ear has been shown to be directed to the vestibular organ[140] and the outer hair cells located in the cochlea.[141-142] It was reported that ≤15% of AG-treated patients developed vestibulotoxicity, while 2 to 25 % experienced cochleotoxicity.[143-144] Another estimate of ototoxicity incidence in patients administered AGs was shown to lie between 3 to 33%.[142]

Approaches to reduce or protect against AG-induced nephrotoxicity have previously been reviewed.[145] Since it is less aggressive than its ototoxicity counterpart, we will briefly focus

on understanding the mechanisms of AG-induced ototoxicity for a better appreciation of current ways utilized to alleviate it. A more detailed presentation of the mechanisms of AG ototoxicity has recently been reported.[137]

1.6.1. Mechanisms of ototoxicity

Following their uptake by inner ear sensory hair cells,[146-150] parenterally and topically administered AGs appear to induce ototoxicity either through the formation of reactive oxygen species,[151] activation of cochlear *N*-methyl-D-aspartate (NMDA) receptors,[152] or increase of nitric oxide synthase activity.[153-154] Individuals carrying the maternally inherited mutations A1555G or C1494T, which are both localized on the A-site of the human mitochondrial 12S rRNA, have also been shown to be more vulnerable to AG ototoxicity.[155-158] With the mitochondrion appearing to be a common denominator in all these mechanisms, mitochondrial protein synthesis may then be an essential target in AG ototoxicity.

Böttger and co-workers engineered hybrid bacterial ribosomes, whose decoding site mimiced that of the human mitochondrial 12S rRNA, and also contained either the A1555G or C1494T congenital deafness mutations.[159-160] The protein translation fidelity in these hybrid mitochondrial ribosomes (mitoribosomes) appeared to be disturbed in the presence of AGs. This misreading process could then lead to hair cell death, *i.e.* AG ototoxicity. Francis and co-workers, however, recently showed that inhibition of the cytosolic, rather than mitochondrial, protein synthesis better compares to AG-induced hearing loss.[161] *In*

vivo studies reported by Baasov and co-workers tipped the scale towards mitochondrial protein synthesis inhibition as the major contributor to AG ototoxicity.[134]

Several antioxidants, including salicylate,[162] aspirin,[163] *N*-acetylcysteine,[164-165] mitoquinone,[166] dexamethasone,[167] melatonin,[167] tacrolimus,[167] SkQR1,[168] have been shown to bear otoprotective properties when used in conjunction with AGs. The use of NMDA receptor antagonists has also been shown to alleviate AG-induced ototoxicity.[169]

Novel AG derivatives with reduced toxicity have also been designed based on the correlation that has been shown between the AGs' structural scaffold and their toxicity. It was reported that reducing the number of amino groups on AGs may lead to reduced toxicity.[170] Furthermore, a decrease in basicity of the amino groups, as a result of neighbouring group effect, was shown to also influence AG toxicity.[171]

1.6.2. Apramycin

Apramycin (APR, Figure 1.1) is an AG produced by the microorganism *S. tenebrarius*[172] with unique structural features that allow it to escape bacterial resistance other legacy AGs are usually subjected to. It is a potent antibiotic with growth inhibitory action against Gram-positive and Gram-negative bacteria.[173] It has found applications in veterinary medicine, but its use in humans is currently prohibited. Recent findings have shown that APR does not display the characteristic ototoxicity generally observed with AGs.[174] As a matter of fact, in a mice organ of Colti explant model, APR was found not to trigger the loss of hair cells in the base of cochlear at a concentration of 0.2 mM, a dose at which GEN completely

destroyed those hair cells. Minimal hair cells loss was only noticeable at 2 mM APR. Even in *in vivo* ototoxicity studies performed in guinea pig by measuring the auditory brain response at 12 kHz and the loss of hair cells, APR was less toxic than GEN. Since the ototoxicity of AGs has been correlated to their limited selectivity in preferentially binding bacterial ribosomes over mammalian ones,[159-160] it was interesting to find that APR does not significantly upset the mitochondrial ribosome as the other AG antibiotics do. Indeed, while APR exhibited comparable protein synthesis inhibitory activities in bacterial and hybrid human cytosolic ribosomes with GEN, TOB, KAN, and NEO, it perturbed the protein synthesis in hybrid human mitochondrial (wild-type and A1555G mutant) ribosomes to a much lesser extent. These results were further confirmed in eukaryotic rabbit reticulocyte ribosomes and *in vitro* mitochondrial *in organelle* translation assay. Analysis of the crystal structure of the APR-*Thermus thermophiles* 30S subunit h44 complex, together with the aprosamine-induced misreading of mitohybrid ribosomes, revealed that ring III of APR may prevent A1492 residue to puck out and may thus be essential in poorly inducing misreading in mitochondria. In the future, it will be fascinating to develop APR derivatives that retain these key structural features that will allow them to overcome ototoxicity and see if they will be able to find applications in the treatment of human bacterial infections.

1.6.3. New AG: Plazomicin

Plazomicin (PLZ), originally known as ACHN-490, is a semi-synthetic "neoglycoside" developed by Achaogen (San Francisco, CA, U.S.A.) that has shown great promise in alleviating nephrotoxicity and ototoxicity. Derived from SIS, PLZ has been shown to

exhibit enhanced *in vitro* potency against AG-susceptible and AG-resistant pathogens.[175] It was active against most Enterobacteriaceae species at a concentration below 4 μg/mL.[175] Indeed, it displayed an $MIC_{50/90}$ value of 0.5/1 μg/mL against 3050 *E. coli* clinical isolates from New York[176] and 1/1 μg/mL against 26 *Enterobacter* spp. gathered from Athens, Greece.[177] Interestingly, it even exhibited an MIC_{90} value of 1 μg/mL against a large collection of unique-patient *Klebsiella pneumoniae* isolates, including those producing carbapenemases (KPC) (*bla*$_{KPC}$-containing isolates), which was at least 32-fold lower than the clinically used AGs AMK, GEN, and TOB.[176, 178] However, PLZ was found to be inactive against any Enterobacteriaceae isolates carrying the ribosomal methyltransferase-encoding genes *ArmA* and/or *RmtC*.[175, 179] It was also inactive against *Providencia stuartii* (MIC >64 μg/mL), as a result of the inactivation by the AAC(2')-I enzyme. In general, PLZ has been shown to overcome the action of most AG resistance enzymes.[175]

When evaluated against nocosomial pathogens *Acinetobacter baumannii* and *Pseudomonas aeruginosa*, PLZ was moderately active with $MIC_{50/90}$ of 8/16 μg/mL and 8/32 μg/mL, respectively[180] and quite active against AG-resistant staphylococci ($MIC_{50/90}$ = 1/1 μg/mL).[175]

In light of these promising *in vitro* results, the *in vivo* efficacy of PLZ was tested in animals.[181] In a septicemia model, PLZ was able to increase the survival rate of mice infected with *E. coli* ATCC25922 (ED_{50} = 0.6 mg/kg) and *P. aeruginosa* ATCC27853 (ED_{50} = 8.3 mg/kg) over 7 days as a function of the dose administered. A murine neutropenic thigh model also confirmed that PLZ was capable of treating bacterial

infections caused by *E. coli* (susceptible and MDR), *K. pneumoniae* (susceptible, MDR, and strains expressing KPC), *P. aeruginosa* (susceptible), *Serratia marcescens* (with KPC phenotype), and *S. aureus* (MDR).

1.7. PERSPECTIVE AND CONCLUSIONS

AGs are broad-spectrum antibiotics that have long suffered from bacterial resistance and toxicity. While enormous efforts have been directed towards developing new strategies to minimize these accompanied side effects, novel applications of AGs as antifungal and genetic regulating compounds are also being investigated.

The incessant need to better understand AGs' mechanisms of action on the bacterial ribosomes has led researchers to the discovery of the h69 binding site, which could be another potential target of AGs and could be useful to develop novel AG drugs. The discovery of AME inhibitors and their use in combination with AGs also remain an interesting avenue to explore for counteracting bacterial resistance.

In addition to their traditional role as antibacterial agents, AGs have also emerged as potential antifungal agents and we believe that in the future, it will be important to pay attention to the derivatization of AGs as cationic amphiphiles for the development of novel fungicides. The capacity of certain AGs to bind to eukaryotic ribosomes has also been exploited for the treatment of parasitic diseases and PTC disorders. Although more attention had been directed towards CF and DMD, it will be worthy investigating how parent AGs and their derivatives could help in treating other PTC disorders. However, it

should not be forgotten that ototoxicity is an intrinsic side effect of AGs. Priority should then be given to those parent compounds, such as APR, that have demonstrated limited toxicity to mammalian cells.

There are currently only six AGs (AMK, GEN, NEO, PAR, STR, and TOB) that are approved by the US Food and Drug Administration for clinical use. However, with the renaissance experienced by AGs in the past decades, notably with the discovery of PLZ and its satisfactory results in clinical trials, there is great hope that new clinically useful AGs can still be discovered. Together with the promising use of AGs described herein, it thus becomes apparent that AGs remain a valuable potential source of drugs.

1.8. ACKNOWLEDGEMENT

Our work on aminoglycoside antibiotics is funded by a National Institute of Health (NIH) grant AI090048 (S.G.-T.) as well as startup funds from the College of Pharmacy at the University of Kentucky (S.G.-T.). We thank all of those working on aminoglycosides including those that we could not cite due to the scope of the original review article.

This chapter is adapted from my published review article (under my previous maiden name Yijia Li) referenced as Fosso, M. Y.; Li, Y.; Garneau-Tsodikova, S., New trends in the use of aminoglycosides. *MedChemComm* **2014,** *5*(8),1075-91.

1.9. AUTHORS' CONTRIBUTIONS

Y.L. contributed to the write up of sections 1.2 and 1.5 and reformatting the published review article into Chapter 1. M.Y.F. contributed to the write up of introduction, conclusions and sections 1.3, 1.4, and 1.6. S.G.-T. contributed to proof-reading and modifying the published review and this formatted chapter.

Chapter 2. Expanding aminoglycoside resistance enzyme regiospecificity by mutation and truncation

Aminoglycosides (AGs) are broad-spectrum antibiotics famous for their antibacterial activity against Gram-positive and Gram-negative bacteria, as well as *Mycobacteria*. In the U.S.A., the most prescribed AGs, including amikacin (AMK), gentamicin (GEN), and tobramycin (TOB), are vital components of the treatment for resistant bacterial infections. Arbekacin (ABK), a semi-synthetic AG, is widely used for the treatment of resistant *Pseudomonas aeruginosa* and methicillin-resistant *Staphylococcus aureus* in Asia. However, the rapid development of bacterial resistance is limiting the clinical application of AG antibiotics. Of all bacterial resistance mechanisms against AGs, the acquisition of AG-modifying enzymes (AMEs) by the bacteria is the most common. It was previously reported that a variant of a bifunctional AME, the AG 6'-*N*-acetyltransferase-Ie/AG-2"-*O*-phosphotransferase-Ia (AAC(6')-Ie/APH(2")-Ia), containing a D80G point mutation and a truncation after amino acid 240 modified ABK and AMK at a new position, the 4"'-amine, therefore, displaying a new change in regiospecificity. In this study, we aim to verify the altered regiospecificity of this bifunctional enzyme by mutation and truncation for the potential of derivatizing AGs with chemoenzymatic reactions. With the three variant enzymes in this study that contains either mutation only (D80G), truncation only (1-240), or mutation and truncation (D80G-1-240), we characterize their activity by profiling their substrate promiscuity, determine their kinetic parameters, and perform mass spectrometry in order to see how and where ABK and AMK were acetylated by these enzymes. We find that the three mutant enzymes possessed distinct acetylation regiospecificity compared to

the bifunctional AAC(6')-Ie/APH(2")-Ia enzyme and the functional AAC(6')-Ie domain (AAC(6')/APH(2")-1-194).

2.1. INTRODUCTION

The broad-spectrum aminoglycoside (AG) antibiotics are active against Gram-positive and Gram-negative bacteria, as well as *Mycobacteria*.[1-4] Their broad-spectrum feature has given AGs a vital position in clinical settings for the treatment of severe bacterial infections. Amikacin (AMK), gentamicin (GEN), and tobramycin (TOB) are currently approved in the U.S.A. for systemic administration (Figure 2.1). On the other hand, the systemic use of kanamycin (KAN) is limited to the treatment of multidrug-resistant (MDR) tuberculosis. Neomycin B (NEO) is most commonly added to antibiotic ointments for topical applications. In addition to being used as antibiotics, AGs are also currently heavily investigated as antifungal agents[5-10] as well as potential treatments for genetic disorders caused by premature termination codons, including but not limited to, cystic fibrosis and Duchene muscular dystrophy.[3, 11-15]

Arbekacin (ABK, Figure 2.1), although not currently prescribed in the U.S.A., has been widely used in Asia for decades due to its excellent efficacy against MDR strains of *Pseudomonas aeruginosa*, *Acinetobacter baumannii*, and methicillin-resistant *Staphylococcus aureus* (MRSA).[16] ABK is a semi-synthetic AG that has regained popularity over the past few decades. By appending an (*S*)-4-amino-2-hydroxybutyryl (AHB) group onto its precursor dibekacin, ABK was shown to possess better antimicrobial

activity than AMK and GEN, and to be less prone to the development of bacterial resistance compared to other AHB-lacking AGs.

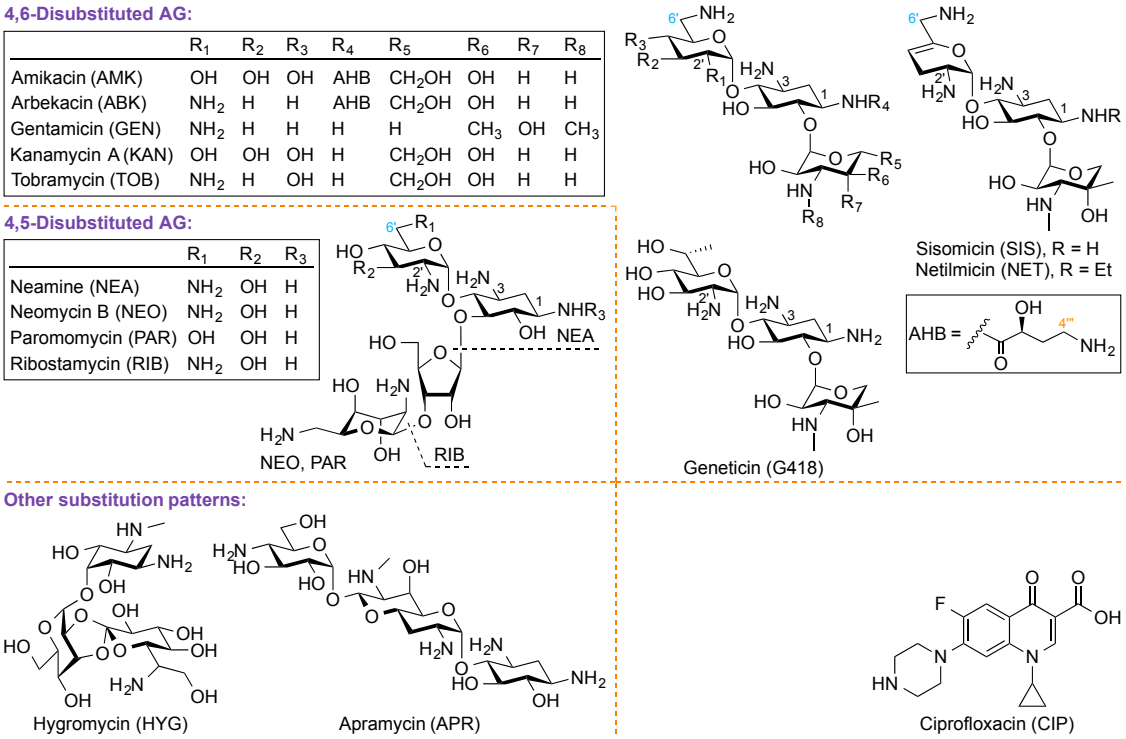

	R_1	R_2	R_3	R_4	R_5	R_6	R_7	R_8
Amikacin (AMK)	OH	OH	OH	AHB	CH_2OH	OH	H	H
Arbekacin (ABK)	NH_2	H	H	AHB	CH_2OH	OH	H	H
Gentamicin (GEN)	NH_2	H	H	H	H	CH_3	OH	CH_3
Kanamycin A (KAN)	OH	OH	OH	H	CH_2OH	OH	H	H
Tobramycin (TOB)	NH_2	H	OH	H	CH_2OH	OH	H	H

	R_1	R_2	R_3
Neamine (NEA)	NH_2	OH	H
Neomycin B (NEO)	NH_2	OH	H
Paromomycin (PAR)	OH	OH	H
Ribostamycin (RIB)	NH_2	OH	H

Figure 2.1. Structures of the various AGs and CIP tested in this chapter.

As with most antibiotics, the extensive use of AGs led to the accelerated development of bacterial resistance to these drugs. Bacteria can develop resistance to AGs by (i) changing their cell envelope composition, resulting in reduced drug permeability, (ii) upregulating their efflux pumps, resulting in a decreased intracellular drug concentration, (iii) modifying the ribosome, preventing binding of AGs to their target, and (iv) acquiring AG-modifying enzymes (AMEs), also preventing binding of the chemically modified drugs to the ribosome target.[17-22] AMEs, which represent the most common resistance mechanisms to AGs, can be classified into three families based on the distinct chemistry they catalyze: AG

N-acetyltransferases (AACs), AG *O*-phosphotransferases (APHs), and AG *O*-nucleotidyltransferases (ANTs). AACs, the most common AMEs detected in bacteria that are resistant to AGs, catalyze the transfer of an acetyl group from acetyl-coenzyme A (AcCoA) onto the amine functionalities present on AG molecules. Studies have revealed that most AACs are regiospecific and modify only one amine moiety on AGs, as often designated in their names.[23] One exception to this rule is Eis (enhanced intracellular survival), an AG multiacetylating protein upregulated in strains of *M. tuberculosis* displaying resistance to KAN.[24-31] Research has shown that some acetylated AGs, after being "inactivated" by AACs, still retain antibacterial activity. Therefore, having additional resistance enzymes that further modify AGs at different positions can help bacteria to completely inactivate AGs, avoiding toxic effects from these AG metabolites. The ability of Eis to multiacetylate a variety of AGs at various positions poses special challenges when it comes to combating bacterial resistance. Eis protein homologues are also found in other *mycobacterial* strains[29] as well as *Anabaena variabilis*,[30] *Bacillus anthracis*,[32] *Gordonia bronchialis*,[33] *Kocuria rhizophila*,[33] and *Tsukamurella paurometabola*.[33]

Research efforts were inspired by the discovery of a new ABK metabolite in an ABK-resistant MRSA strain in Japan, and subsequently led to the identification of a variant of the AAC(6')-Ie/APH(2")-Ia enzyme, from here on denoted as AAC(6')/APH(2") for simplicity.[34-37] The reported variant enzyme contained a D80G point mutation in the AAC(6') domain of this bifunctional protein, which was reported to introduce a natural proteolytic cleavage after amino acid 240, resulting in a mutated and truncated protein.

Compared to the wild-type (wt) protein that acetylates only at the 6'-position, the mutant truncated protein displayed a switch in regiospecificity to the 4'''-amine of ABK and AMK, which has not be observed in AACs before.[35-36] The unique regiospecificity of the variant enzyme could provide special protection to the bacteria under exposure to AGs, as it would modify and inactivate AG antibiotics at a special position that is distinct from what the common resistance enzymes modify.

Herein, we set off to verify the change in regiospecificity and examine whether both the D80G mutation and truncation are necessary for this change in regiospecificity. We first cloned, expressed, and purified various enzymes, including the AAC(6')/APH(2")-wt (previously cloned),[38] the AAC(6')/APH(2")-D80G (with mutation only), the AAC(6')/APH(2")-1-240 (with truncation only), and the AAC(6')/APH(2")-D80G-1-240 (with mutation and truncation) (Figures 2.2A and 2.3 and Tables 2.1-2.3). We then determined the substrate profiles of these enzymes with a panel of 14 AGs (ABK, AMK, apramycin (APR), geneticin (G418), GEN, hygromycin (HYG), KAN, neamine (NEA), NEO, netilmicin (NET), paromomycin (PAR), ribostamycin (RIB), sisomicin (SIS), and TOB) and 1 fluoroquinolone (ciprofloxacin, CIP) (Figure 2.1 and Table 2.4). We also determined the kinetic parameters for the AAC(6')/APH(2")-wt and the three different mutant enzymes with 7 selected AGs (ABK, AMK, KAN, NEA, NEO, SIS, and TOB) (Figures 2.4-2.7 and Table 2.5). After seeing the difference in the enzymatic regiospecificity between the AAC(6')/APH(2")-wt and mutant enzymes by performing mass spectrometry (MS) (and tandem mass spectrometry (MS^2)), we cloned an additional AAC(6')/APH(2")-1-194 protein, which was previously reported to be the functional

AAC(6')-Ie domain (Figure 2.2A and Tables 2.1-2.3).[39] We compared the activity of AAC(6')/APH(2")-wt, AAC(6')/APH(2")-1-240, AAC(6')/APH(2")-D80G, AAC(6')/APH(2")-D80G-1-240, and AAC(6')/APH(2")-1-194 on purified reaction mixtures containing acetylated ABK and AMK in order to see how and where these AG molecules were being modified by the AAC(6')/APH(2")-wt and mutants (Table 2.6 and Figures 2.8-2.10).

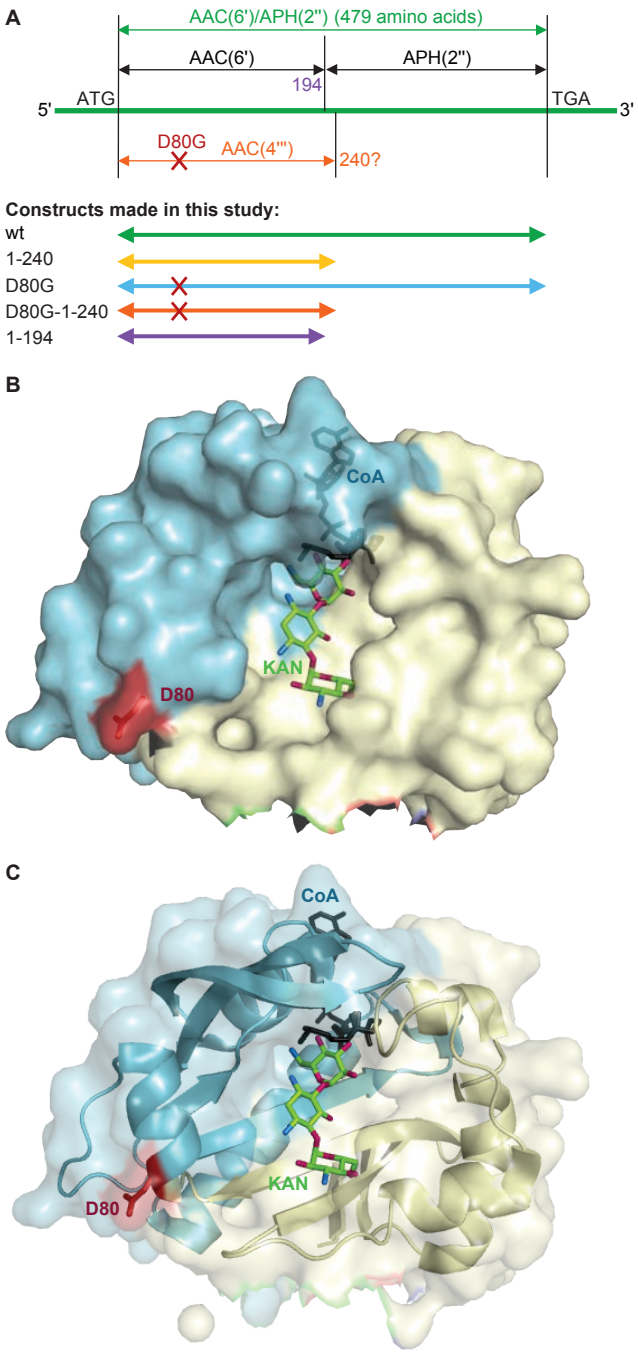

Figure 2.2. A. Schematic diagram of all mutant enzyme constructs generated and used in this study, including schematic diagram of AAC(6')/APH(2")-wt in green, as well as the truncated AAC(6')/APH(2")-1-240 in yellow, the mutated AAC(6')/APH(2")D80G in turquoise, the mutated/truncated AAC(6')/APH(2")-D80G-1-240 in orange, and the truncated AAC(6')/APH(2")-1-194 in purple. A red X denotes the D80G single point mutation. **B and C.** Crystal structures of the AAC(6') domain (PDB ID: 4QC6)[40] of the bifunctional enzyme AAC(6')/APH(2") in surface (**B**) and cartoon (**C**) representations with the amino acids 1-79 in off white, D80 residue in red, and amino acids 81-179 in pale turquoise. The substrate KAN (green) is represented in its stick form with nitrogen and oxygen atoms colored blue and red, respectively. The CoA derivative (black) is on the backside of the structure.

2.2. RESULTS AND DISCUSSION

2.2.1. Molecular cloning and expression of AAC(6')/APH(2")-wt and its mutant enzymes

As postulated in previous studies,[34-37] the change in regiospecificity of an AAC(6')/APH(2") mutant enzyme from the 6'- to 4"'-position could result from a D80G mutation and a D80G-induced truncation at amino acid 240. According to the published AAC(6') domain structure (PDB ID: 4QC6),[40] D80 is a residue that lies on the surface of this globular protein and belongs to the beginning of an α-helix (Figures 2.2B and C). Mutation of this aspartate into a glycine was predicted to introduce a strong α -helix break, which in turn was suggested to abruptly change the protein conformation during folding, thereby introducing a proteolytic cleavage after amino acid 240 in the APH(2") domain of the bifunctional enzyme.[36] Previous research on domain dissecting of this bifunctional AME[39] and crystallographic knowledge on each of the two domains[40-41] has revealed that the functional AAC(6') and APH(2") domains span from amino acids 1-194, and from 175 to 479, respectively. The overlapped linker region between the two domains (amino acids 175-194) had been proven to be critical for the activities for both domains.[39] Therefore, the resulting truncated protein would contain the linker domain and 46 residues from the APH(2") domain in addition to the AAC(6') domain. Even though we were not successful in determining crystal structures to demonstrate how the D80G mutation and/or 1-240 truncation would impact the protein conformation, we postulate that if the D80G mutation were to shift the rest of protein conformation during folding, the rest of the protein after the D80 residue, as represented by the pale turquoise portion, would change and impact the shape and size of the substrate binding pocket, as the residues after D80 compose half of

the AG binding site and the entire CoA binding site. Although structures of the bifunctional enzyme and of the AAC(6') domain have been modeled/determined, attempts at crystallizing the AAC(6')/APH(2")-D80G-1-240 proved unsuccessful so far. It is therefore difficult to prove how the protein would fold as a result of the mutation and/or truncation, especially since the D80G mutation occurred so early in the protein sequence.

In order to verify whether both mutation and truncation are required for the change in AAC regiospecificity, we cloned three mutant enzymes that contained mutation only (AAC(6')/APH(2")-D80G), truncation only (AAC(6')/APH(2")-1-240), and both mutation and truncation (AAC(6')/APH(2")-D80G-1-240) with $NHis_6$ tag. Expression in BL21 (DE3) cells and purification with Ni^{II}-NTA resin yielded soluble proteins with yields between 6.3-13.9 mg/L of LB broth culture (Figures 2.2A and 2.3 and Tables 2.1-2.3).

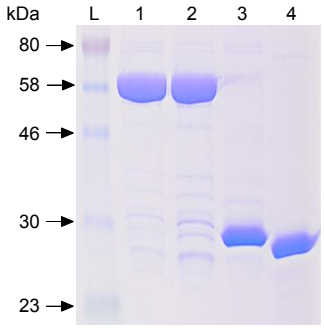

Figure 2.3. Coomassie blue-stained 15% Tris-HCl SDS-PAGE gel showing purified $NHis_6$-tagged AAC(6')/APH(2") (59.0 kDa, lane 1), AAC(6')/APH(2")-D80G (59.0 kDa, lane 2), AAC(6')/APH(2")-1-240 (30.9 kDa, lane 3), and AAC(6')/APH(2")-D80G-1-240 (30.9 kDa, lane 4). 6 μg of protein was loaded into each lane.

Table 2.1. Primers used for the PCR amplification of the *aac(6')/aph(2")* gene for various constructs.[a,b]

Gene	5' primer #	5' primer	3' primer #	3' primer
aac(6')/aph(2")-wt	1	GATAAACATATGAATATAG TTGAAAATGAAATATG	2	TATATTCTCGAGTCAATCTTTA TAAGTCCTTTTATAAATTTC
aac(6')/aph(2")-1-240	1	GATAAACATATGAATATAG TTGAAAATGAAATATG	3	ATTATACTCGAGTTATTCTTTT GCATA
aac(6')/aph(2")-D80G	4	TATAAAATGTATggcGAGTT ATATACT	5	AGTATATAACTCgccATACATTT TATA
aac(6')/aph(2")-1-194	1	GATAAACATATGAATATAG TTGAAAATGAAATATG	6	ATTATCCTCGAGTCACTCAATT AAATATTTCAT

[a]The introduced restriction sites are underlined for each relevant primer with 5' and 3' primers introducing an *Nde*I and an *Xho*I restriction sites, respectively. [b]The D80G mutation is in lower-case for each primer.

Table 2.2. SOE PCR strategies to generate all new AAC(6')/APH(2") constructs used in this study.

Construct	PCR round	5' primer	3' primer	DNA template	PCR product	PCR product code	Expected size (bp)
aac(6')/aph(2")-1-240	1	1	3	*aac(6')/aph(2")-wt (CHis)*	*aac(6')/aph(2")-1-240 (NHis)*		750
aac(6')/aph(2")-D80G	1	1	5	*aac(6')/aph(2")-wt (CHis)*	*N*-terminal half of *aac(6')/aph(2")-D80G*	a	252
	1	4	2	*aac(6')/aph(2")-wt (CHis)*	*C*-terminal half of *aac(6')/aph(2")-D80G (NHis)*	b	1216
	2	1	2	PCR products a and b	*aac(6')/aph(2")-D80G (NHis)*		1470
aac(6')/aph(2")-D80G-1-240 (NHis)	1	1	5	*aac(6')/aph(2")-wt (CHis)*	*N*-terminal half of *aac(6')/aph(2")-D80G*	a	252
	1	4	3	*aac(6')/aph(2")-wt (CHis)*	*C*-terminal half of *aac(6')/aph(2")-D80G-1-240 (NHis)*	d	496
	2	1	3	PCR products a and d	*aac(6')/aph(2")-D80G-1-240 (NHis)*		750
aac(6')/aph(2")-1-194	1	1	6	*aac(6')/aph(2")-wt (CHis)*	*aac(6')/aph(2")-1-194 (NHis)*		603

Table 2.3. Purification yields of AAC(6')/APH(2") and mutant and/or truncated proteins.[a]

Protein	Yield (mg/L)
AAC(6')/APH(2") (NHis)	10.1
AAC(6')/APH(2")-1-240 (NHis)	13.9
AAC(6')/APH(2")-D80G (NHis)	6.3
AAC(6')/APH(2")-D80G-1-240 (NHis)	6.9
AAC(6')/APH(2")-1-194 (NHis)	7.2

[a]Protein yields were calculated based on absorbance at 280 nm.

2.2.2. Establishment of the substrate profiles of AAC(6')/APH(2")-wt and its three mutant enzymes by UV-Vis assays

In order to examine whether the AAC(6')/APH(2")-wt and its three mutant enzymes have different or similar substrate profiles, we performed UV-Vis assays with 14 AGs (ABK, AMK, APR, G418, GEN, HYG, KAN, NEA, NEO, NET, PAR, RIB, SIS, and TOB) and 1 fluoroquinolone (CIP). We found that the AAC(6')/APH(2")-wt and its mutant enzymes

were all most active against AMK, KAN, NEA, and TOB, and mildly active against ABK, GEN, NEO, NET, RIB, and SIS. These enzymes were not active against APR, G418, HYG, PAR, and CIP (Table 2.4). These results contradict the previous reports on AAC(6')/APH(2")-D80G-1-240 stating that this specific mutant was devoid of AAC(6') activity,[36] as we found that AGs possessing 6'-amines were substrates of our mutant enzymes, whereas the AGs that do not possess 6'-amines, but instead comprise hydroxyl groups at the 6'-position, were not substrates of these mutant enzymes, indicating the mutant enzymes were likely to possess 6'-acetyltransferase activity. Additionally, AAC(6')/APH(2")-wt enzyme was previous reported to be capable of *O*-acetylating AGs, such as PAR, that lack 6'-amine.[42] However, we did not observe such activity in our study. Given that ABK and AMK were the only AGs that possessed AHB groups, it was not clear whether acetylation was happening at the 6'-, 4'"-, or another amine position. We therefore later relied on MS and MS^2 to decipher the position(s) modified by all of our enzymes (see below).

Table 2.4. Substrate promiscuity for AAC(6')/APH(2")-wt and mutant constructs, including AAC(6')/APH(2")-1-240, AAC(6')/APH(2")-D80G, and AAC(6')/APH(2")-D80G-1-240.

AG	wt	1-240	D80G	D80G-1-240
ABK	~	--	~	--
AMK	✓	✓	✓	✓
APR	×	×	×	×
G418	×	×	×	×
GEN	--	--	~	~
HYG	×	×	×	×
KAN	✓	✓	✓	✓
NEA	✓	✓	✓	✓
NEO	~	~	~	~
NET	--	--	--	--
PAR	×	×	×	×
RIB	--	--	--	--
SIS	~	~	~	~
TOB	✓	✓	✓	✓
CIP	×	×	×	×

Activity is based on absorbance observed at 412 nm. All enzymes used in this assay are $NHis_6$-tagged constructs. × = not a substrate, -- = poor substrate, ~ = moderate substrate, ✓ = great substrate.

2.2.3. Determination of kinetic parameters for AAC(6')/APH(2")-wt and its three mutant enzymes

Next, we determined the kinetic parameters for AAC(6')/APH(2")-wt and its three mutant enzymes in order to gain insights into potential differences in enzyme behavior. We selected seven AGs (ABK, AMK, KAN, NEA, NEO, SIS, and TOB) that were assessed to be good substrates of the AAC(6')/APH(2")-wt and of its mutants in our substrate profiling experiments, and determined the K_m, k_{cat}, and k_{cat}/K_m values (in μM, min^{-1}, and $\mu M^{-1}min^{-1}$, respectively) by fitting to a non-linear regression Michaelis-Menten equation (Figures 2.4-2.7 and Table 2.5). In general, we found that for AAC(6')/APH(2")-wt enzyme, the substrates that showed the lowest and highest K_m values were KAN (2.98 ± 0.67 μM) and NEO (102 ± 20 μM), respectively. While KAN consistently displayed the lowest K_m values to all four enzymes, the substrates that displayed highest K_m values were NEO (102 ± 20 μM) for AAC(6')/APH(2")-wt, ABK (146 ± 17 μM) for AAC(6')/APH(2")-1-240; NEO (307 ± 51 μM) for AAC(6')/APH(2")-D80G, and ABK (331 ± 108 μM) for AAC(6')/APH(2")-D80G-1-240. As implied by the definition of K_m values, the full-length enzymes shared similar preference in terms of binding efficiencies, so did the two truncated enzymes. As for the enzyme turnover rate (k_{cat}), the values generally did not change drastically from AAC(6')/APH(2")-wt to its three mutants. Combining the binding affinity and enzyme turnover rate, we found that in some cases, *i.e.,* with AMK as a substrate, mutation seemed to have slightly improved enzyme efficiencies. In other cases, with TOB as substrate, mutation did not cutback the overall enzyme efficiencies, but truncation did.

Table 2.5. Kinetic parameters determined for AAC(6')/APH(2")-wt and the mutant enzymes, including AAC(6')/APH(2")-1-240, AAC(6')/APH(2")-D80G, and AAC(6')/APH(2")-D80G-1-240, with various AGs.

AGs		AAC(6')/APH(2")-wt	AAC(6')/APH(2")-1-240	AAC(6')/APH(2")-D80G	AAC(6')/APH(2")-D80G-1-240
ABK	K_m	77.9 ± 21.4	146 ± 17	109 ± 58	331 ± 108
	k_{cat}	2.43 ± 0.14	2.55 ± 0.11	2.12 ± 0.36	5.16 ± 0.76
	k_{cat}/K_m	0.031 ± 0.009	0.017 ± 0.002	0.019 ± 0.011	0.016 ± 0.006
AMK	K_m	30.7 ± 5.6	65.8 ± 6.6	31.1 ± 3.5	26.4 ± 5.2
	k_{cat}	3.16 ± 0.20	7.75 ± 0.37	9.17 ± 0.34	6.59 ± 0.53
	k_{cat}/K_m	0.103 ± 0.020	0.118 ± 0.013	0.295 ± 0.035	0.250 ± 0.053
KAN	K_m	2.98 ± 0.67	1.11 ± 0.28	0.779 ± 0.286	1.24 ± 0.35
	k_{cat}	8.02 ± 0.57	5.64 ± 0.45	6.16 ± 0.73	9.09 ± 0.90
	k_{cat}/K_m	2.69 ± 0.64	5.10 ± 1.35	7.91 ± 3.05	7.33 ± 2.20
NEA	K_m	8.12 ± 1.56	7.63 ± 0.57	11.7 ± 1.3	7.21 ± 1.14
	k_{cat}	12.3 ± 0.7	8.33 ± 0.18	8.72 ± 0.29	6.82 ± 0.30
	k_{cat}/K_m	1.51 ± 0.30	1.09 ± 0.09	0.744 ± 0.084	0.946 ± 0.155
NEO	K_m	102 ± 20	107 ± 19	307 ± 51	140 ± 19
	k_{cat}	13.9 ± 1.1	7.33 ± 0.54	22.4 ± 2.0	11.9 ± 0.7
	k_{cat}/K_m	0.136 ± 0.029	0.068 ± 0.013	0.073 ± 0.014	0.084 ± 0.013
SIS	K_m	49.9 ± 6.0	13.9 ± 3.7	67.9 ± 9.1	45.8 ± 5.6
	k_{cat}	12.9 ± 0.6	4.15 ± 0.30	11.7 ± 0.7	10.5 ± 0.5
	k_{cat}/K_m	0.259 ± 0.033	0.298 ± 0.082	0.172 ± 0.025	0.229 ± 0.030
TOB	K_m	15.0 ± 4.3	16.4 ± 1.7	7.46 ± 1.87	15.2 ± 3.0
	k_{cat}	15.3 ± 1.7	10.7 ± 0.7	11.1 ± 0.9	9.38 ± 1.00
	k_{cat}/K_m	1.02 ± 0.32	0.651 ± 0.080	1.48 ± 0.39	0.618 ± 0.140

All AGs presented in this table were found to be good substrates of the different AAC(6')/APH(2") (NHis) constructs according to our substrate profiling experiment results. K_m, k_{cat}, and k_{cat}/K_m values are presented in μM, min^{-1}, and ($\mu M^{-1}min^{-1}$), respectively.

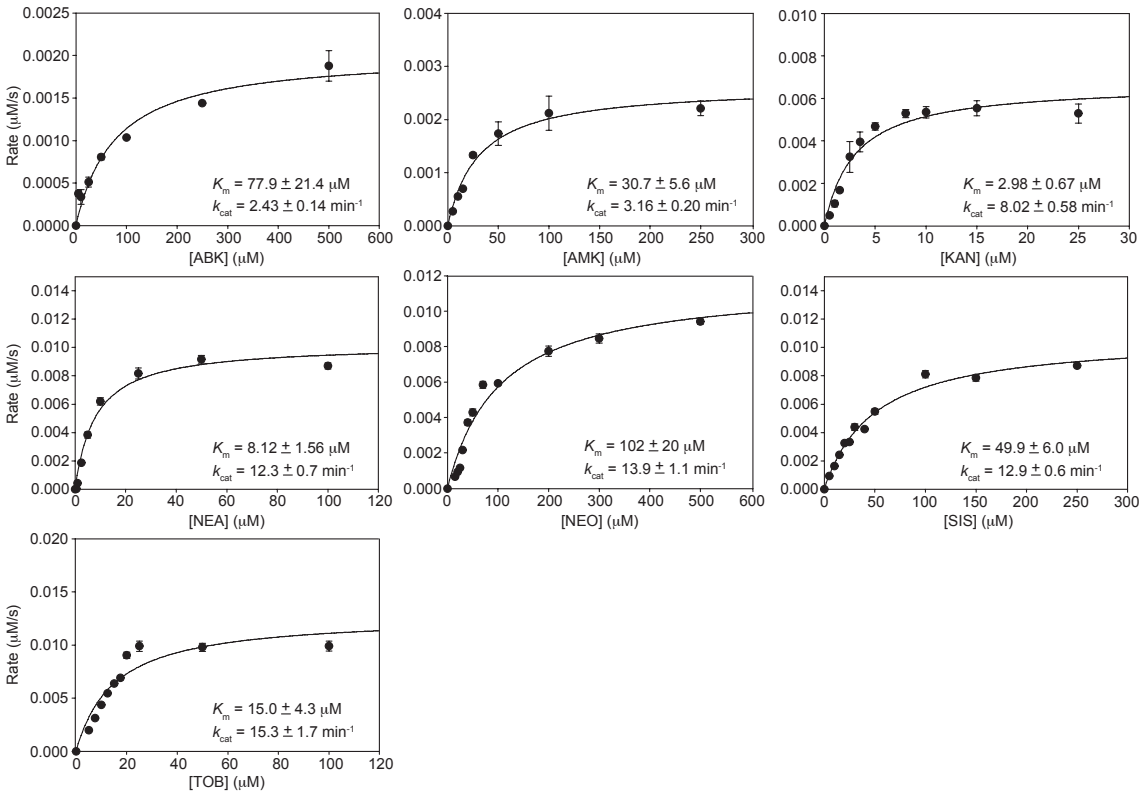

Figure 2.4. Kinetic curves for AAC(6')/APH(2")-wt (NHis) with various AGs. Insets include the K_m and k_{cat} values from a non-linear regression fit to the Michaelis-Menten equation.

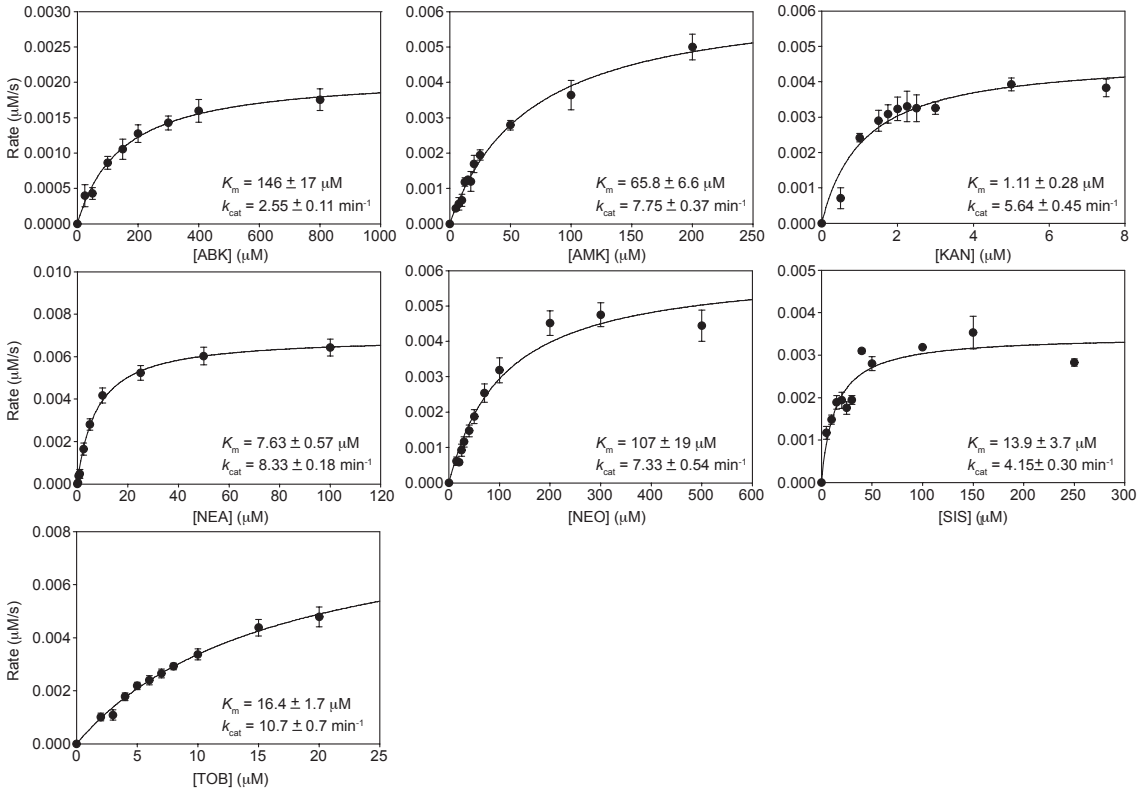

Figure 2.5. Kinetic curves for AAC(6')/APH(2")-1-240 (NHis) with various AGs. Insets include the K_m and k_{cat} values from a non-linear regression fit to the Michaelis-Menten equation.

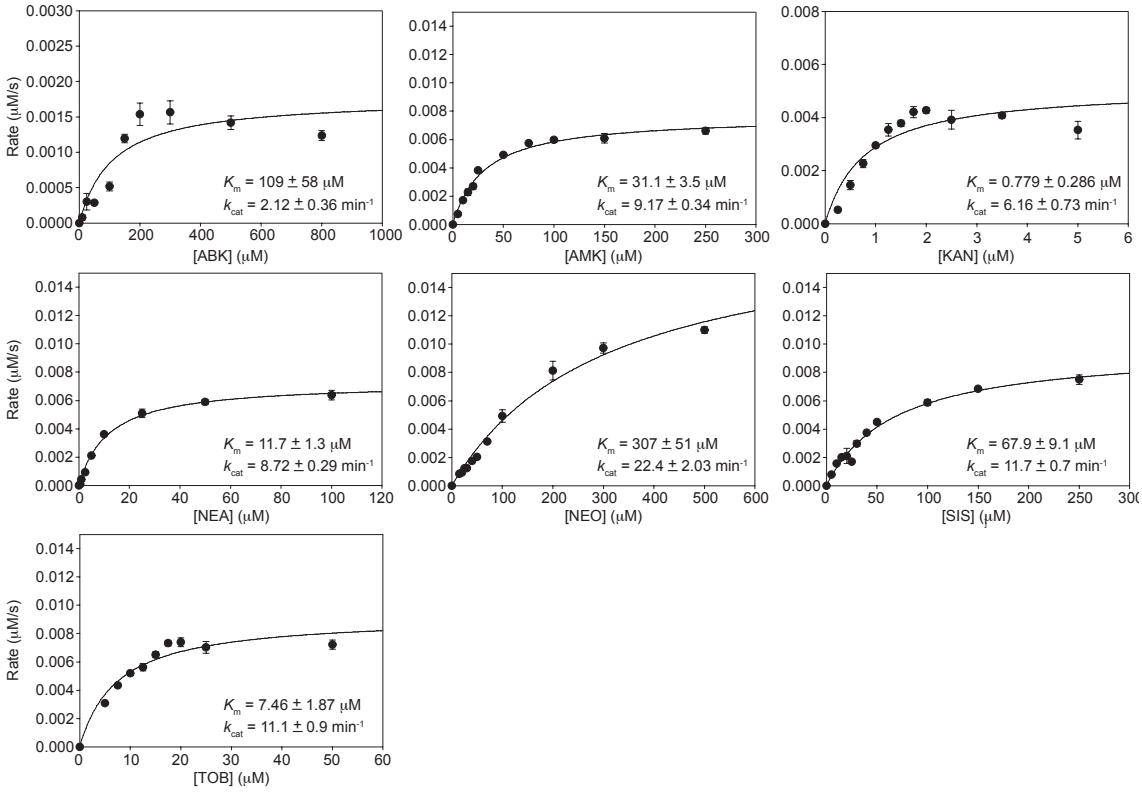

Figure 2.6. Kinetic curves for AAC(6')/APH(2")-D80G (NHis) with various AGs. Insets include the K_m and k_{cat} values from a non-linear regression fit to the Michaelis-Menten equation.

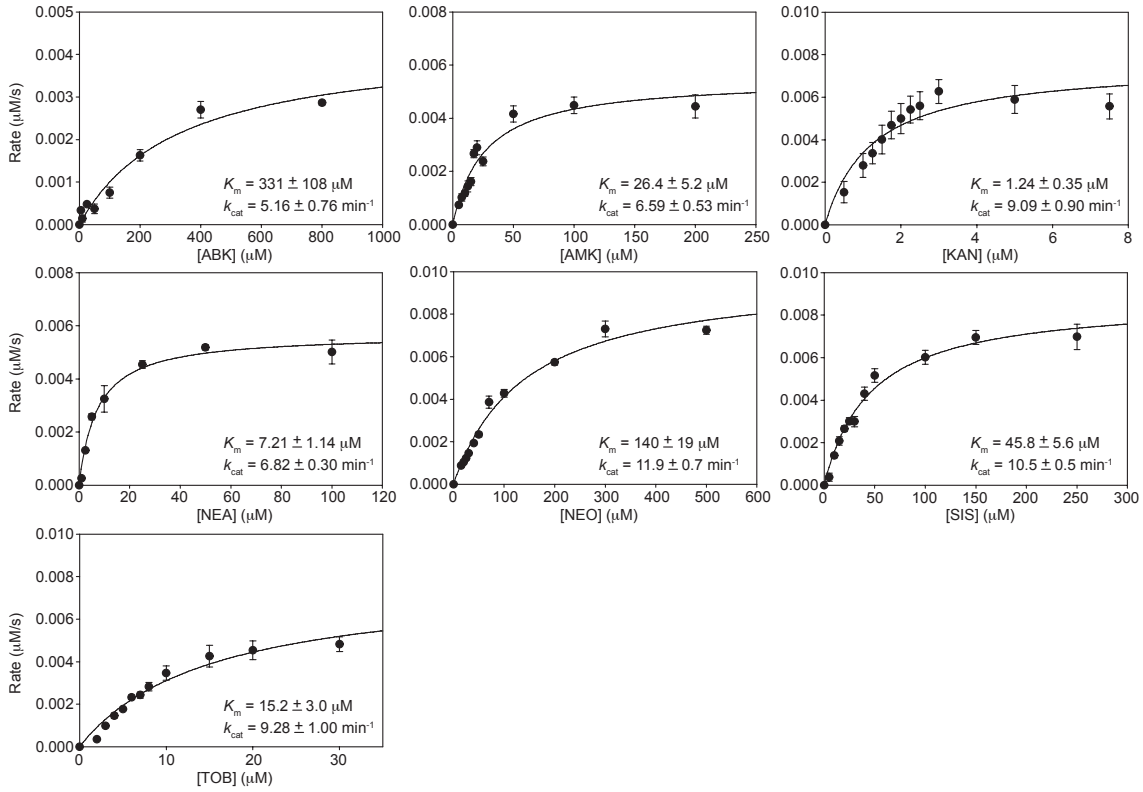

Figure 2.7. Kinetic curves for AAC(6')/APH(2")-D80G-1-240 (NHis) with various AGs. Insets include the K_m and k_{cat} values from a non-linear regression fit to the Michaelis-Menten equation.

The enzyme activities we observed in this study were overall consistent to those presented in previously reported studies on the wt and truncated AAC(6')/APH(2") enzymes kinetics.[38-39, 42-43] The difference observed in the mutant enzymes with the occurrence of mutation and/or truncation was not significant enough to indicate substantial difference between enzyme mechanisms. It was interesting to note that despite ABK would be considered as "the natural substrate" for the AAC(6')/APH(2")-D80G-1-240 enzyme, we found all four enzymes to display low efficiency towards ABK as a substrate. The D80G mutant enzyme also showed potential indications of slight substrate inhibition in the Michaelis-Menten plots, which might suggest that the mutation could facilitate alternative binding modes to the enzyme that interfere with catalysis (Figure 2.6).

2.2.4. Determination by MS and MS^2 of the position(s) acetylated on ABK and AMK by AAC(6')/APH(2")-wt and its three mutant enzymes

Since the substrate profile and the kinetic parameters of the AAC(6')/APH(2")-wt and D80G mutant and/or 1-240 truncated enzymes did not reveal significant difference between the four enzymes, we further looked into more sensitive techniques such as MS and MS^2 to decipher the potential switch in regioselectivity of these enzymes. We first incubated ABK with a single enzyme (AAC(6')/APH(2")-wt, 1-240, D80G, or D80G-1-240) and 1.5 or 3 eq. of AcCoA. Theoretically, 1.5 eq. of AcCoA would be sufficient for at least one acetylation and 3 eq. of AcCoA would be sufficient for at least two acetylations on each AG molecule.

As summarized in Figures 2.8-2.10 and Table 2.6, we found that the AAC(6')/APH(2")-wt enzyme modifies ABK solely on the 6'-position with either 1.5 or 3 eq. of AcCoA, indicated by only an AcABK peak at 595.3297 *m*/*z* and a fragmentation pattern aligning with that of 6'-AcABK in MS^2. This strict regiospecificity displayed by AAC(6')/APH(2")-wt enzyme agreed with previous findings.[38] ABK modified by AAC(6')/APH(2")-1-240, D80G, or D80G-1-240 with 1.5 eq. of AcCoA resulted in only 6'-AcABK according to MS and MS^2. However, each reaction with 3 eq. of AcCoA yielded not only 6'-AcABK, but also 6',4'''-diAcABK (637.3403 *m*/*z*). This suggested that AAC(6')/APH(2")-1-240, D80G, and D80G-1-240 enzymes preferred the 6'-position, but were also able to modify the 4'''-amine given excess amount of AcCoA, expanding their original regiospecificity to a novel position, the 4'''-amine. Similar activities were observed among the three mutant enzymes.

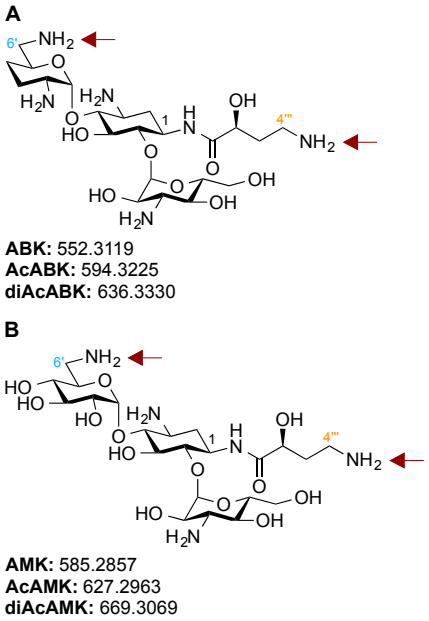

Figure 2.8. Structures of **A.** ABK and **B.** AMK with the potential acetylation sites of interest in this study (6'- and 4'''-amine positions) denoted with red arrows. The exact mass of the parent ABK and AMK, monoacetylated ABK (AcABK) or AMK (AcAMK), and diacetylated ABK (diAcABK) and AMK (diAcAMK) are also listed under the structure.

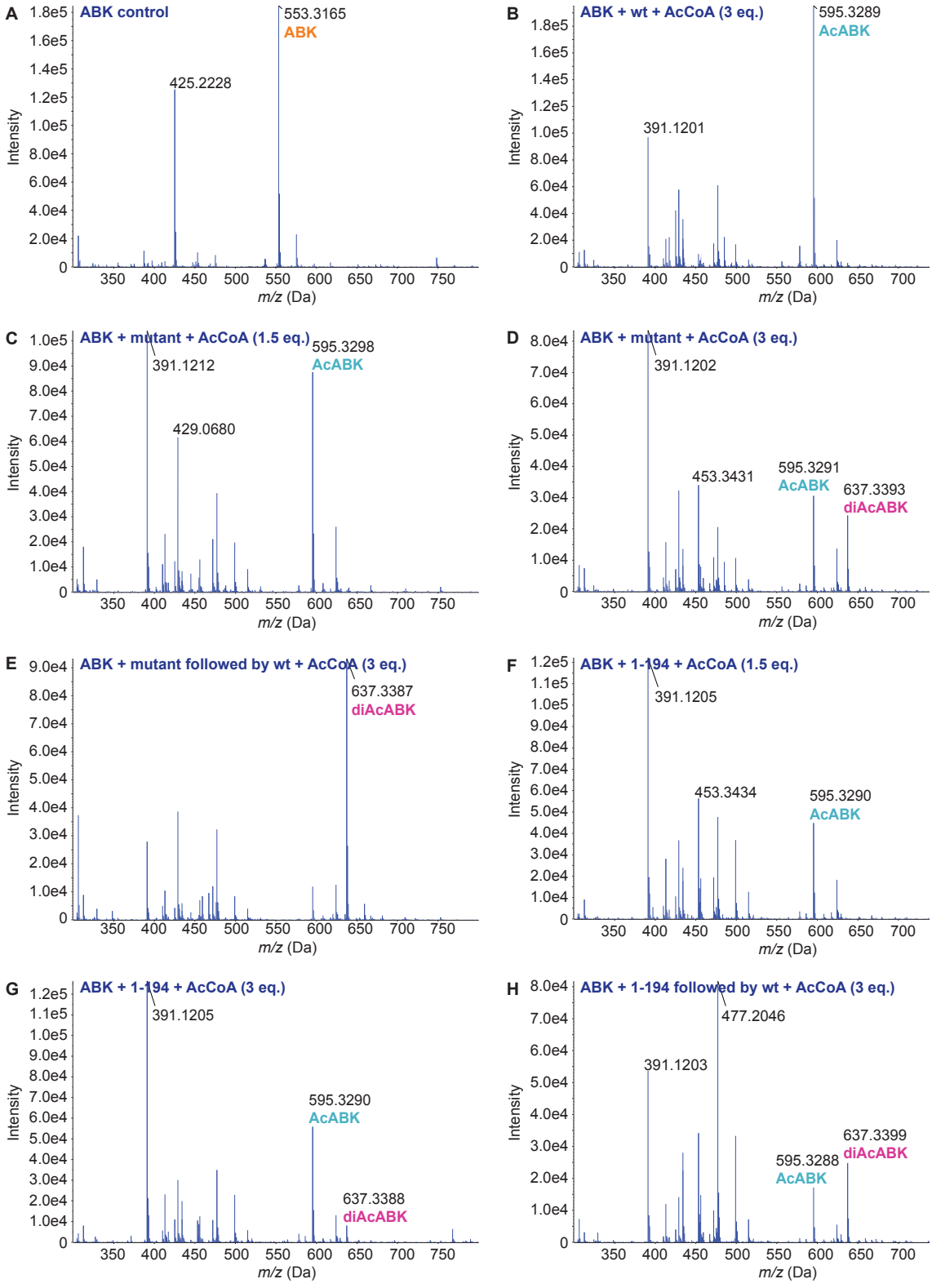

Figure 2.9. Representative mass spectra of ABK control and ABK modified with various amount of AcCoA by various enzymes generated in this study either individually or sequentially. **A.** ABK control. **B.** ABK + AAC(6')/APH(2")-wt + AcCoA (3 eq.). **C.** ABK + AAC(6')/APH(2")-D80G-1-240 + AcCoA (1.5 eq.) (Note: using other mutant enzymes gave the same spectra). **D.** ABK + AAC(6')/APH(2")-D80G-

1-240 + AcCoA (3 eq.) (Note: using different mutant enzymes gave the same spectra). **E.** ABK + AAC(6')/APH(2")-D80G-1-240 followed by wt + AcCoA (3 eq.) (Note: using various mutant enzymes first followed by wt and using the wt enzyme followed by various mutant enzymes gave the same spectra). **F.** ABK + AAC(6')/APH(2")-1-194 + AcCoA (1.5 eq.). **G.** ABK + AAC(6')/APH(2")-1-194 + AcCoA (3 eq.). **H.** ABK + AAC(6')/APH(2")-1-194 followed by wt + AcCoA (3 eq.) (Note: using wt enzyme first followed by 1-194 enzyme gave the same spectra). The expected *m/z* ratios for ABK, AcABK, and diAcABK $[m + H]^+$ were 553.3192, 595.3297, and 637.3403.

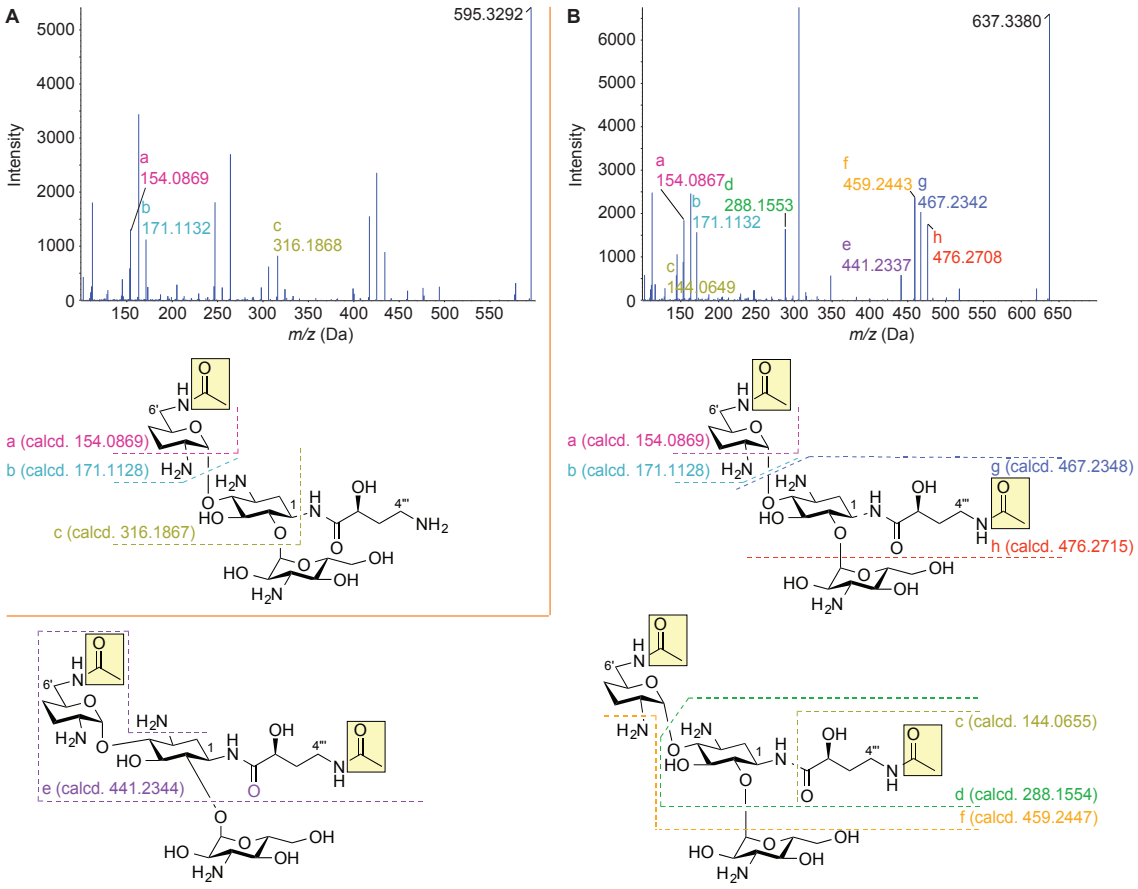

Figure 2.10. Representative tandem mass spectra (MS^2) of **A.** AcABK and **B.** diAcABK with predicted fragmentation. Fragments with *m/z* ratios between 100 to 600 for AcABK and between 100 to 700 for diAcABK were collected. The fragments of interests in each panel that indicated the position of acetylation were labeled both in the spectra and in the structure of AcABK and diAcABK with their calculated *m/z* ratios. Note: Each predicted fragment above or below a dash line was indicated with the corresponding calculated *m/z* ratio placed above or below the dash line, respectively.

Table 2.6. Summary of mass spectrometry results obtained by using a single enzyme or sequentially using two enzymes.[a]

AG	Enzyme 1	Enzyme 2	AcCoA (eq.)	AG	6'-AcAG	6',4'''-diAcAG
ABK	×	×	×	✓		
	wt	×	1.5		✓	
	wt	×	3		✓	
	1-240	×	1.5		✓	
	1-240	×	3		++	++
	D80G	×	1.5		✓	
	D80G	×	3		++	++
	D80G-1-240	×	1.5		✓	
	D80G-1-240	×	3		++	++
	1-194	×	1.5		✓	
	1-194	×	3		++	--
	wt	1-240	3		--	++
	wt	D80G	3		--	++
	wt	D80G-1-240	3		--	++
	wt	1-194	3		++	++
	1-240	wt	3		--	++
	D80G	wt	3		--	++
	D80G-1-240	wt	3		--	++
	1-194	wt	3		++	++
AMK	×	×	×	✓		
	wt	×	1.5		✓	
	wt	×	3		+	--
	1-240	×	1.5		✓	
	1-240	×	3		+	--
	D80G	×	1.5		✓	
	D80G	×	3		+	--
	D80G-1-240	×	1.5		✓	
	D80G-1-240	×	3		+	--
	1-194	×	1.5		✓	
	1-194	×	3		✓	
	wt	1-240	3		++	+
	wt	D80G	3		++	+
	wt	D80G-1-240	3		++	+
	wt	1-194	3		++	--
	1-240	wt	3		++	+
	D80G	wt	3		++	+
	D80G-1-240	wt	3		++	+
	1-194	wt	3		++	--

[a] Reactions with a single enzyme were performed for 24 h prior to processing, whereas sequential reactions were performed by reacting with enzyme 1 for 24 h followed by enzyme 2 for 24 h.

× = enzyme or AcCoA not used in the reaction; ✓ = the only species detected; ++ = this species is of high abundance; + = this species is of moderate abundance; -- = this species is of very low abundance.

Next, we incubated ABK with two different enzymes sequentially with either AAC(6')/APH(2")-wt as enzyme 1 (E1) then followed by AAC(6')/APH(2")-1-240, D80G, or D80G-1-240 as enzyme 2 (E2), or one of the mutant enzymes as E1 and wt as E2. The results were similar. We found that most of the ABK had been converted to 6',4'''-diAcABK. Although previous research reported that the acetylation of AGs at a certain position can hinder further acetylation at other positions, *i.e.*, it was reported that acetylation of NEO and SIS at their 3-position hindered the subsequent acetylation at 6'-

position,[38] we did not observe such phenomenon in this study regarding the 6'- and 4'''-modification of ABK. The fact that we observed similar activity among all three mutant enzymes, either by one enzyme or by two enzymes sequentially, suggested that the D80G mutation and the 1-240 truncation were not both required for the expanded regiospecificity. Even though the D80G-1-240 enzyme could be the naturally occurring variant in the producing bacteria due to the D80G mutation, enzymes with either mutation or truncation alone, when expressed heterologously, can show altered regiospecificity, as indicated by MS and MS^2 results.

Structurally, the D80G mutation was first postulated to significantly change protein conformation.[35-37] If the D80G mutation were to cause the protein conformation to be significantly altered during protein folding (*i.e.*, five sixth of AAC(6')/APH(2")-D80G will fold differently from the wt protein conformation), the AAC(6')/APH(2")-D80G conformation could have an expanded active site in order to accommodate the substrate, ABK, to bind in various orientations and be modified at two distinct amine appendages. According to the published modeling/structure of AAC(6')/APH(2"), the substrate binding cavities of AAC(6') and APH(2") was reported to lie on the same side of the protein. Such close arrangement inspired suspicions that the two active sites facilitate substrate binding/channeling cooperatively. Given such rigid arrangement, the proteolytic cleavage at amino acid residue 240 that resulted from the mutation in the distant D80 residue might not in fact be random. The D80G mutation possibly altered protein conformation that rearranged the two active sites relative to each other might account for the alternative binding of ABK in the AAC(6') active site.[40] Similarly, since AAC(6')/APH(2")-1-240

would contain an extra portion of the linker domain and the 46 residues from the APH(2") domain, this fairly large segment would also be highly possible of disrupting the native protein conformation of the AAC(6') portion by interacting with amino acid residues in the AAC(6') domain. Therefore, we postulated that the structural change in protein folding resulting from either the D80G mutation, the appendage of the linker region and the 46 residues from APH(2"), or a combination on both could enlarge the enzymes' substrate binding site to allow the acetylation of ABK at the 4"'-position.

In order to test this hypothesis, we cloned and expressed the functional AAC(6') domain, which included residues 1-194 from the original AAC(6')/APH(2") bifunctional enzyme, herein denoted as AAC(6')/APH(2")-1-194 to test whether the AAC(6') domain alone would show the expanded regiospecificity. We included the linker region (175-194) in this construct in order to obtain a functional AAC(6'), but left out the 46 residues from the APH domain. We first modified ABK with AAC(6')/APH(2")-1-194 with 1.5 eq. of AcCoA and observed only 6'-AcABK in MS and MS^2 (Figures 2.9 and 2.10). The reaction containing ABK, AAC(6')/APH(2")-1-194, and 3 eq. of AcCoA still yielded mostly 6'-AcABK. Sequentially modifying ABK with either AAC(6')/APH(2")-wt followed by 1-194, or AAC(6')/APH(2")-1-194 followed by wt resulted in both 6'-AcABK and 6',4"'-diAcABK as shown by MS and MS^2. The results generated by using AAC(6')/APH(2")-1-194 enzyme were considerably different from those with AAC(6')/APH(2")-1-240, D80G, and D80G-1-240 enzymes. We found that the ability of AAC(6')/APH(2")-1-194 at acetylating ABK at the 4"'-position was significantly lower compared to that of the other three mutant

enzymes, confirming that the extra 46 residues from the APH(2") domain in our truncated enzymes indeed assisted the expansion of regiospecificity, as did the D80G mutation.

Due to the structural similarities between ABK and AMK, we next obtained the MS and MS^2 spectra for the same reactions with AMK instead of ABK in order to see whether the expansion of regiospecificity applies to AMK (Table 2.6 and Figures 2.8 and 2.11-2.12). We found that AMK, when modified by a single enzyme (AAC(6')/APH(2")-wt, 1-240, D80G, D80G-1-240, or 1-194) with 1.5 eq. of AcCoA, was converted to 6'-AcAMK only (628.3036 *m*/*z*). When AMK was co-incubated with a single enzyme (AAC(6')/APH(2")-wt, 1-240, D80G, and D80G-1-240) and 3 eq. of AcCoA, we identified the majority of the product being 6'-AcAMK and trace amount of 6',4'"-diAcAMK (670.3141 *m*/*z*) whereas AAC(6')/APH(2")-1-194 with 3 eq. of AcCoA converted AMK to 6'-AcAMK only. This agreed with previous observation that AAC(6')/APH(2")-1-194 enzyme was more limited in its ability to acetylate AGs at various amine positions compared to AAC(6')/APH(2")-1-240, D80G, and D80G-1-240 enzymes.

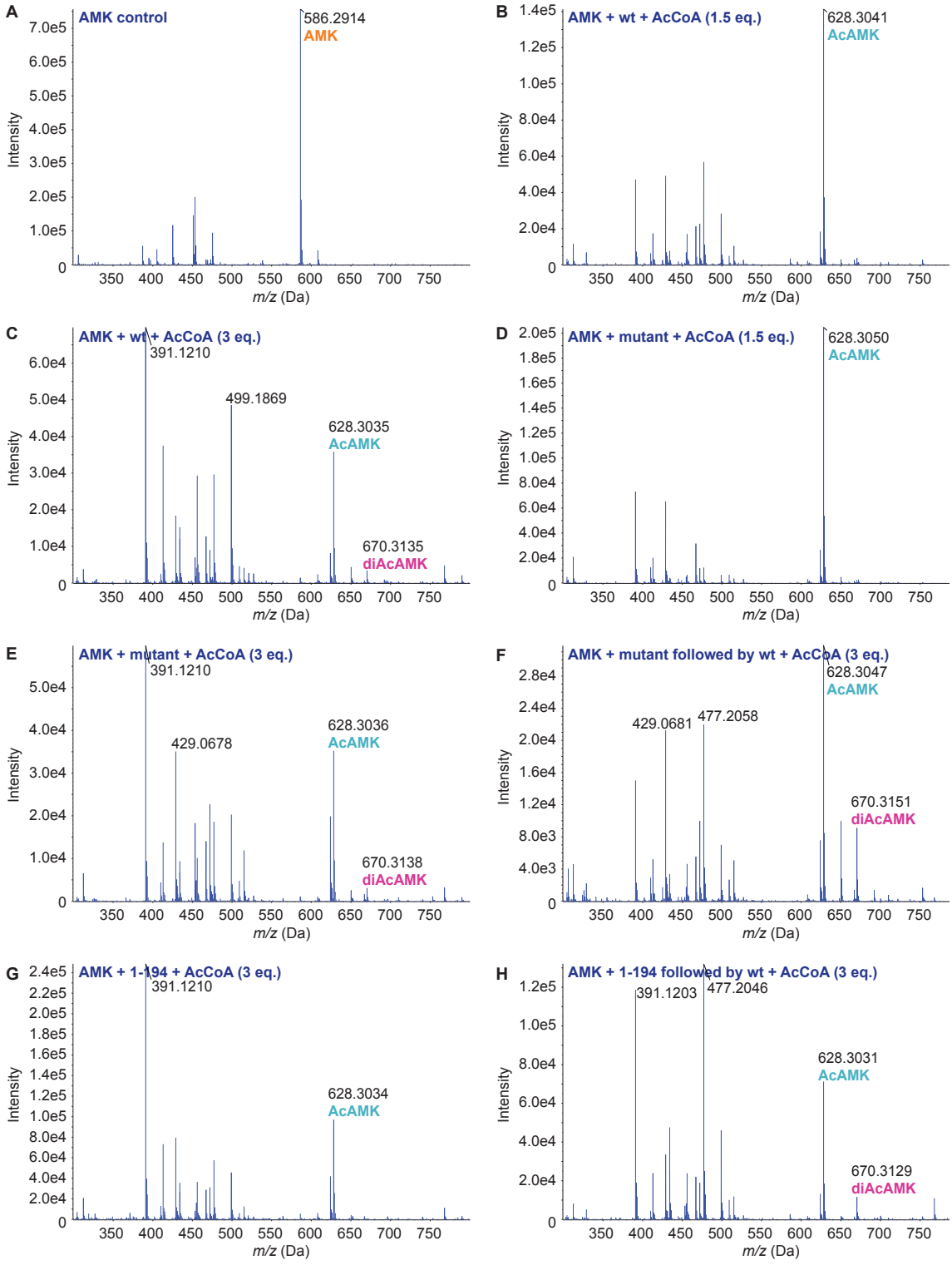

Figure 2.11. Representative mass spectra of AMK control and AMK modified with various amount of AcCoA by various enzymes generated in this study either individually or sequentially. **A.** AMK control. **B.** AMK + AAC(6')/APH(2")-wt + AcCoA (1.5 eq.). **C.** AMK + AAC(6')/APH(2")-wt + AcCoA (3 eq.). **D.** AMK + AAC(6')/APH(2")-D80G-1-240 + AcCoA (1.5 eq.) (Note: using other mutant enzymes gave the same spectra). **E.** AMK + AAC(6')/APH(2")-D80G-1-240 + AcCoA (3 eq.) (Note: using different

mutant enzymes gave the same spectra). **F.** AMK + AAC(6')/APH(2")-D80G-1-240 followed by wt + AcCoA (3 eq.) (Note: using various mutant enzymes first followed by wt and using the wt enzyme followed by various mutant enzymes gave the same spectra). **G.** AMK + AAC(6')/APH(2")-1-194 + AcCoA (3 eq.) (Note: using AcCoA (1.5 eq.) gave the same spectra). **H.** AMK + AAC(6')/APH(2")-1-194 followed by wt + AcCoA (3 eq.) (Note: using wt enzyme first followed by 1-194 enzyme gave the same spectra). The expected *m/z* ratios for AMK, AcAMK, and diAcAMK $[m + H]^+$ were 586.2930, 628.3036, and 670.3141.

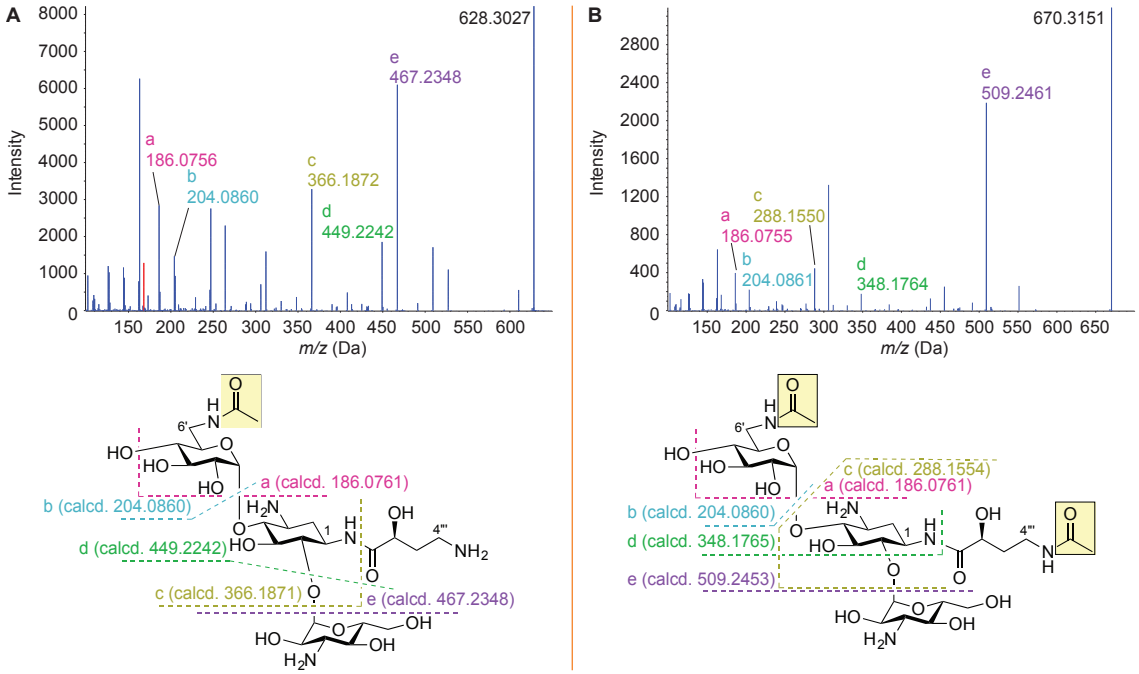

Figure 2.12. Representative tandem mass spectra (MS^2) of **A.** AcAMK and **B.** diAcAMK with predicted fragmentation. Fragments with *m/z* ratios between 100 to 650 for AcAMK and between 100 to 700 for diAcAMK were collected. The fragments of interests in each panel that indicated the position of acetylation were labeled both in the spectra and in the structure of AcAMK and diAcAMK with their calculated *m/z* ratios. Note: Each predicted fragment above or below a dash line was indicated with the corresponding calculated *m/z* ratio placed above or below the dash line, respectively.

At the same time, we used two different enzymes to sequentially modify AMK. We realized that no matter whether we used AAC(6')/APH(2")-wt as E1 and AAC(6')/APH(2")-1-240, D80G, or D80G-1-240 as E2, or AAC(6')/APH(2")-1-240, D80G, or D80G-1-240 as E1 and AAC(6')/APH(2")-wt as E2, the results were similar. We observed 6'-AcAMK as a major product and 6',4"'-diAcAMK as a minor product. No significant difference was observed between the three different mutant enzymes. However,

when we used AAC(6')/APH(2")-wt as E1 and AAC(6')/APH(2")-1-194 as E2, or AAC(6')/APH(2")-1-194 as E1 and AAC(6')/APH(2")-wt as E2, we observed different results: most of the AMK was converted into 6'-AcAMK and only trace amount of 6',4"'-diAcAMK was detected. Once again, this supported our previous observation that AAC(6')/APH(2")-1-240, D80G, and D80G-1-240 were much more efficient at acetylating the 4"'-position after the enzyme regiospecificity was expanded. In addition, the different results observed between the acetylation of ABK and AMK by the same enzyme revealed an interesting phenomenon. Even though ABK and AMK structurally only differed by their 2'-, 3'-, and 4'-substitutions on ring I, the enzymes were able to discriminate one AG over the other, as the expanded acetylation activity at the 4"'-location for ABK was much more efficient compared to that for AMK.

In addition to MS and MS^2, nuclear magnetic resonance (NMR) spectroscopy would also be a great tool to elucidate where and how ABK and AMK are being acetylated by AAC(6')/APH(2")-wt and its various mutant enzymes. However, with the limited amount of ABK that we received as a gift from Dr. Sergei Vakulenko (University of Notre Dame, U.S.A.) and the inability to obtain ABK from the U.S.A. market, MS remained the better and only instrument available to us to elucidate various enzyme behaviors with respect to ABK as a substrate.

Acetylation of AGs by various AACs usually abolishes the antibacterial effect of these antibiotics. Therefore, acquiring these resistance enzymes can provide bacteria with advantages at surviving the presence of a xenobiotic. However, previous research has also

demonstrated that some AG metabolites, even after being chemically modified by AMEs, can still retain antibacterial activities. For instances, 6'-AcNEO has been shown to still possess antibacterial activity against *Bacillus subtilis*.[38] Various ABK metabolites, including 2'-, 6'-, and 3''-AcABK have also been reported to retain weak to moderate antibacterial activities.[44-46] In such circumstance, a single acetylation does not completely eliminate the antibacterial effect of AGs. Therefore, possessing any additional enzymes that are capable of acetylating at a secondary site on AGs and further inactivate these drugs can provide the bacteria substantial survival advantages. In the case of AAC(6')/APH(2'')-D80G-1-240, MRSA acquired/developed this mutant enzyme that further modifies the 4'''-amine in addition to the 6'-amine. As a result, the bacteria can better survive ABK treatment in case the 6'-acetylated ABK still retains any antibacterial activity.

In our study, we also used disk diffusion assays to examine whether ABK metabolites by various enzyme constructs generated in this study possess any antibacterial effect against a susceptible strain of *E. coli* MC 1061. We found that ABK metabolites modified with one enzyme alone (AAC(6')/APH(2'')-wt, 1-240, or D80G-1-240), or with two enzymes sequentially (AAC(6')/APH(2'')-1-240 followed by wt, or D80G-1-240 followed by wt) displayed no visible zone of inhibition, suggesting that these ABK metabolites retained no detectable antibacterial activity against this strain of bacteria by this assay. Another possibility to consider is that the acetylated ABK metabolites (6'-AcABK and 6',4'''-diAcABK) may become less membrane permeable due to the chemical modification on the molecules by acetylation. If so, the ABK metabolites might become unable to cross the bacteria cell envelope and membrane to reach its target in the cytoplasm even if the ABK

metabolites might still be able to act on the ribosome and interfere with protein translation. In such scenario, we would not be able to observe any zones of inhibition produced by these ABK metabolites despite their inhibitory activity on the ribosome. The absence of a zone of inhibition with these ABK metabolites also suggested no product inhibition of these AAC(6')/APH(2") enzymes.

2.3. CONCLUSIONS

In this study, we explored the possibility of expanding AAC(6')/APH(2")-wt regiospecificity by introducing a D80G point mutation and/or 1-240 truncation (Tables 2.1-2.3 and Figures 2.2-2.3). Even though AAC(6')/APH(2")-D80G-1-240 may be the naturally occurring mutant enzyme as a result of the D80G mutation in the MRSA strain where this mutant enzyme was originally discovered, we found that the three mutant enzymes we cloned in this study (AAC(6')/APH(2")-1-240, AAC(6')/APH(2")-D80G, and AAC(6')/APH(2")-D80G-1-240) showed similar substrate promiscuity (Table 2.4) and kinetic efficiency against various AGs (Table 2.5 and Figures 2.4-2.7). MS and MS^2 with purified reaction mixtures with ABK as a substrate revealed that the three mutant enzymes showed preference to acetylate AGs at their 6'-amine positions, but can also modify the 4'"-position given excess amount of AcCoA (Table 2.6 and Figures 2.8-2.10). This was not a complete switch of regiospecificity from the 6'- to the 4'"-position as reported before,[35-37] but rather an expansion, which the presence of mutation only or truncation only can also alter the protein catalysis in such way described above. We postulated the D80G mutation and/or 1-240 truncation could cause alteration in protein conformation during protein

during protein folding, resulting in an enlarged AG binding site that would accommodate ABK binding from various orientations.

Moreover, we also found that these three mutant enzymes did not display the same activity with AMK as a substrate as did with ABK (Table 2.6 and Figures 2.8 and 2.11-2.12). Even though the mutant enzymes still displayed preference for 6'-amine of AMK, the ability to modify AMK at the 4'''-position was significantly lower compared to that when modifying ABK. This suggested an uncharacterized mechanism by which the enzymes were able to discriminate between ABK and AMK even though the two AG structures are extremely similar.

Overall, bacteria evolved to possess AAC(6')/APH(2'')-D80G-1-240, a variant enzyme of AAC(6')/APH(2'') with expanded regiospecificity, to further protect the bacteria from any AG metabolites that might retain antibacterial activity after chemical modification and inactivation by AACs. The findings in this study can help us better understand the bacterial resistance mechanisms associated with AG antibiotics in order to better combat resistant bacteria.

2.4. MATERIALS AND METHODS

2.4.1. Materials and instrumentation

The pET28 vector was purchased from Novagen (Gibbstown, NJ), TOP10 and BL21 (DE3) chemically competent *E. coli* cells were purchased from Invitrogen (Carlsbad, CA). Reagents for cloning, including restriction endonucleases, T4 DNA ligase, and Phusion

DNA polymerase (accompanied with appropriate buffers), were purchased from New England BioLabs (Ipswich, MA). DNA primers for PCR were purchased from Sigma-Aldrich (Milwaukee, WI) and Integrated DNA Technologies (Coralville, IA). DNA sequencing was performed by Eurofins Genomics. AcCoA and DTNB were purchased from Sigma-Aldrich. AMK, GEN, KAN, NEA, NET, SIS, and TOB were bought from AK Scientific (Mountain View, CA). APR, G418, HYG, PAR, and RIB were purchased from Sigma-Aldrich. NEO was purchased from Tokyo Chemical Industry Co. Ltd. ABK was a generous gift from Dr. Sergei Vakulenko (University of Notre Dame, U.S.A.). CIP was purchased from Sigma-Aldrich. Ni^{II}-NTA used for affinity chromatography was purchased from Qiagen.

E. coli cultures were grown in Thermo Scientific MaxQ 6000 incubators, and OD measurements were taken on a Thermo Spectronic Genesys 20. Centrifugation was performed by using a Thermo Sorvall^{TM} RC 6 Plus centrifuge. Cell disruption was achieved by sonication using a Qsonica sonicator ultrasonic processor (Newtown, CT). UV-Vis assays for the determination of kinetic parameters and substrate profiling were performed on a SpectraMax M5 plate reader. Mass spectra were recorded in positive mode using an AB SCIEX TripleTOF^{TM} 5600 (AB SCIEX, Redwood city, CA) mass spectrometer and a Shimadzu HPLC system equipped with a DGU-20A/3R degasser, LC-20AD binary pumps, CBM-20A controller, and a SIL-20A/HT autosampler (Shimadzu, Kyoto, Japan).

2.4.2. Cloning of $NHis_6$-tagged *aac(6')/aph(2")-1-240, aac(6')/aph(2")-D80G, aac(6')/aph(2")-D80G-1-240, and aac(6')/aph(2")-1-194* genes in pET28a

The wt AAC(6')/APH(2") DNA was previously cloned into pET22b and pET28a vectors to generate plasmid encoding for $CHis_6$ and $NHis_6$-tagged proteins.[38] Here, the *aac(6')/aph(2")-1-240*, *aac(6')/aph(2")-D80G*, *aac(6')/aph(2")-D80G-1-240*, and *aac(6')/aph(2")-1-194* genes were cloned into pET28a using the primers and cloning strategies listed in Tables 2.1-2.2, and Figure 2.2A, respectively. All genes were amplified by polymerase chain reaction (PCR) using the AAC(6')/APH(2")-wt DNA from the pAAC(6')/APH(2")-pET22b vector. PCR products were confirmed *via* agarose gel electrophoresis and purified by gel extraction (Qiagen QIAquick Gel Extraction Kit). The PCR amplified genes and empty pET28a vector were digested by using *Nde*I and *Xho*I for 4 h at 37 °C and purified using Qiagen QIAquick PCR purification kit. The purified inserts and digested vector were ligated using T4 DNA ligase (5:1/insert:vector) overnight at rt to generate plasmids pAAC(6')/APH(2")-1-240-pET28a, pAAC(6')/APH(2")-D80G-pET28a, pAAC(6')/APH(2")-D80G-1-240-pET28a, and pAAC(6')/APH(2")-1-194-pET28a, which were directly transformed into *E. coli* TOP10 chemically competent cells for DNA isolation (Qiagen QIAprep Spin Miniprep Kit). After confirming the existence of desired gene insert into the pET28a vector by double digestion of the isolated DNA with *Nde*I and *Xho*I and DNA sequencing (Eurofins MWG Operon), the isolated plasmids were transformed into *E. coli* BL21 (DE3) chemically competent cells for protein expression and purification.

2.4.3. Overexpression and purification of AAC(6')/APH(2")-wt, AAC(6')/APH(2")-1-240, AAC(6')/APH(2")-D80G, AAC(6')/APH(2")-D80G-1-240, and AAC(6')/APH(2")-1-194 NHis$_6$-tagged proteins

The *E. coli* BL21 (DE3) transformed with the pAAC(6')/APH(2")-1-240-pET28a, pAAC(6')/APH(2")-D80G-pET28a, pAAC(6')/APH(2")-D80G-1-240-pET28a, and pAAC(6')/APH(2")-1-194-pET28a constructs were inoculated into 2 × 1L of LB broth supplemented with 50 μg/mL of KAN and stirred at 200 rpm at 37 °C until the attenuance at 600 nm reached 0.5. Then, each culture was induced with 1 mM IPTG (final concentration) and incubated at 20 °C overnight (200 rpm). Cells were harvested by centrifugation at 5,000 rpm for 10 min at 4 °C and lysed in buffer A (50 mM Na_2HPO_4 (pH 8.0 adjusted at rt), 300 mM NaCl, 10% glycerol) by sonication 2 min × 3 cycles, alternating between 2 s "on" and 10 s "off" for each cycle, resting for 2 min in between cycles) on ice. After removal of the cell debris by centrifugation at 16,000 rpm for 45 min at 4 °C, each enzyme was purified *via* Ni^{II}-NTA affinity chromatography by washing and eluting with buffer A containing imidazole in a gradient fashion (10 mL of 5 mM imidazole, 3 × 5 mL of 20 mM imidazole, 3 × 5 mL of 40 mM imidazole, and 3 × 5 mL of 250 mM imidazole). After analysis by SDS-PAGE, fractions containing pure protein were combined and dialyzed in 50 mM HEPES (pH 7.5 adjusted at rt) and 10% glycerol and stored at 4 °C or flash-frozen at -80 °C. By comparing the enzyme activity from the 4 °C and the -80 °C protein stocks, we found that being stored at 4 °C does not result in noticeable loss in enzymatic activities of the enzymes involved in this study compared to the enzymes stored at -80 °C. A sample SDS-PAGE gel of AAC(6')/APH(2")-wt, AAC(6')/APH(2")-1-240,

AAC(6')/APH(2")-D80G, and AAC(6')/APH(2")-D80G-1-240 is shown in Figure 2.3 with yields provided in Table 2.3.

2.4.4. Establishment of the substrate profiles of AAC(6')/APH(2")-wt, AAC(6')/APH(2")-1-240, AAC(6')/APH(2")-D80G, and AAC(6')/APH(2")-D80G-1-240 by UV-Vis assays

In order to test whether the AAC(6')/APH(2")-wt and mutant enzymes could modify various AGs, we established their substrate profiles by UV-Vis assays. We tested a panel of 14 AGs (ABK, AMK, APR, G418, GEN, HYG, KAN, NEA, NEO, NET, PAR, RIB, SIS, and TOB) and 1 fluoroquinolone (CIP). Acetylation reactions were monitored by using a colorimetric UV-Vis assay in 96-well plates at 37 °C. Each reaction (200 μL total) contained 50 mM MES (pH 6.6 adjusted at rt), 2 mM DTNB, 150 μM AcCoA, 100 μM of various AG substrate, and were initiated by the addition of 5 μM enzyme (stored in 50 mM HEPES (pH 7.5) and 10% glycerol). The reaction progress was monitored by recording the absorbance at 412 nm every 20 s for 20 min. As presented in Table 2.4, whether the AG (or CIP) tested was a great, moderate, poor substrate, or not a substrate was arbitrarily determined in this study based on the absorbance at 412 nm (absorbance >0.8 was categorized as great substrate, absorbance of 0.4-0.8 was categorized as moderate substrate, absorbance of 0.1-0.4 was categorized as poor substrate, and absorbance <0.1 was categorized as not a substrate).

2.4.5. Determination of kinetic parameters for AAC(6')/APH(2")-wt, AAC(6')/APH(2")-1-240, AAC(6')/APH(2")-D80G, and AAC(6')/APH(2")-D80G-1-240

In order to determine the kinetic parameters of various enzymes with respect to AGs, we tested 7 selected AGs that were tested to be good substrates of the four enzymes in previous substrate profiling experiment (ABK, AMK, KAN, NEA, NEO, SIS, and TOB) by UV-Vis assays in 96-well plates for 15 min at 37 °C. Reactions contained 50 mM MES pH 6.6 (adjusted at rt), 2 mM DTNB, 0.05 μM enzyme, AcCoA (the concentration of AcCoA in the determination of kinetic parameters for each AG equals 1.5 eq. of the highest AG concentration) and were initiated by the addition of 50 μL of AG substrate of various concentrations to make the total reaction volume 200 μL. All experiments were performed in triplicates and the kinetic parameters were then calculated based on Lineweaver-Burke plots generated by using the Sigma Plot software version 9.0 (Table 2.5 and Figures 2.4-2.7).

2.4.6. Mass spectrometry

In order to confirm the number of acetylation events and their positions, we subjected purified enzymatic reactions to mass spectrometry and tandem mass spectrometry. We performed reactions with 1 eq. of ABK or AMK modified by a single enzyme generated in this study with 1.5 eq. of AcCoA in order to see the preferred position of each enzyme (1.5 eq. of AcCoA allowed for acetylation of one position on AG by the enzyme to be visualized by mass spectrometry), or with 3 eq. of AcCoA in order to see whether each enzyme is capable to transferring multiple acetyl groups onto one AG molecule. We then performed

sequential modification reactions where we set up reactions with 1 eq. of ABK or AMK with 3 eq. of AcCoA and a first enzyme (either the wt or any of the three mutants generated in this study). After completion of the reaction (24 h at 37 °C), we added a second enzyme (either any of the three mutants or the wt enzyme) and let the reaction go for an additional 24 h at 37 °C in order to see whether the wt and mutants have different preference about the site of modification/acetylation on ABK and AMK. Each reaction (50 μL total) contained MES pH 6.6 (50 mM), AGs (100 μM) (either ABK or AMK), AcCoA (150 or 300 μM), and various enzymes by themselves or in sequential orders (5 μM each). Reaction mixtures were subjected to cation solid phase extraction (Alltech, catalog # 209800), and eluted with 2% NH_4OH. Elution fractions were dried in a vacuum centrifuge and redissolved in ddH_2O (50 μL). 15 μL of each sample was directly injected using the ESI method with mobile phase composed of 0.1% formic acid in H_2O onto the mass spectrometer. Species between *m*/*z* of 300 to 800 Da were collected by MS (Figures 2.9-2.10). Species of interest with specific *m*/*z* ratios, including ABK (exact mass 552.3119 Da), monoacetylated ABK (exact mass 594.3225 Da), diacetylated ABK (exact mass 636.3330 Da), AMK (exact mass 585.2857 Da), monoacetylated AMK (exact mass 627.2963 Da), and diacetylated AMK (exact mass 669.3069 Da), were collected and fragmented *via* tandem MS, as presented in Table 2.6 and Figures 2.8 and 2.11-2.12.

2.4.7. Disk diffusion assays

In order to assess the antibacterial activity of AME-modified ABK metabolites, we performed disk diffusion assays with reaction mixtures containing ABK modified by either

a single enzyme individually (*i.e.*, AAC(6')/APH(2")-wt, AAC(6')/APH(2")-1-240, or AAC(6')/APH(2")-D80G-1-240), or two enzymes sequentially (*i.e.*, AAC(6')/APH(2")-1-240 followed by AAC(6')/APH(2")-wt, or AAC(6')/APH(2")-D80G-1-240 followed by AAC(6')/APH(2")-wt). Reaction conditions were as described in the MS experiments. After completion of the reactions (24 h at 37 °C), 15 μL of the reaction mixtures were spotted onto a sterile filter disks (~0.6 cm), air dried for 15 min, then placed on the LB-agar surface. A fresh dilution of an overnight culture of *E. coli* MC 1061 strain in soft LB-agar (100 μL culture in 10 mL of soft LB-agar) was thinly layered onto the hard LB-agar surface. The presence or absence of zones of inhibition were visually inspected after overnight incubation at 37 °C.

2.5. ACKNOWLEDGMENT

This work was supported by startup funds from the University of Kentucky as well as by a National Institutes of Health (NIH) Grant AI090048 (to S.G.-T.). We thank Dr. Wenjing Chen for cloning of the pAAC(6')-1-194 and Dr. Jamie Horn for helping the development of the mass spectrometry methods that we used.

This chapter is adapted from a published article referenced as Holbrook, S. Y.; Garneau-Tsodikova, S. Expanding aminoglycoside resistance enzyme regiospecificity by mutation and truncation. *Biochemistry* **2016,** *55* (40), 5726-37.

2.6. AUTHORS' CONTRIBUTIONS

S.Y.L.H. was involved in performing all experiment, writing up of the manuscript and later modifying the manuscript into this dissertation chapter. S.G.-T. contributed in the writing and proof-reading of the manuscript and later proof-reading the modified dissertation chapter.

Chapter 3. Inhibition of aminoglycoside acetyltransferase resistance enzymes by metal salts

Aminoglycosides (AGs) are clinically relevant antibiotics used to treat infections caused by both Gram-negative and Gram-positive bacteria, as well as *Mycobacteria*. As with all current antibacterial agents, resistance to AGs is an increasing problem. The most common mechanism of resistance to AGs is the presence of AG-modifying enzymes (AMEs) in bacterial cells, with AG acetyltransferases (AACs) being the most prevalent. Recently, it was discovered that Zn^{2+} metal ions displayed an inhibitory effect on the resistance enzyme AAC(6')-Ib in *Acinetobacter baumannii* and *Escherichia coli*. In this study, we explore a wide array of metal salts (Mg^{2+}, Cr^{3+}, Cr^{6+}, Mn^{2+}, Co^{2+}, Ni^{2+}, Cu^{2+}, Zn^{2+}, Cd^{2+}, and Au^{3+} with different counter ions) and their inhibitory effect on a large repertoire of AACs (AAC(2')-Ic, AAC(3)-Ia, AAC(3)-Ib, AAC(3)-IV, AAC(6')-Ib', AAC(6')-Ie, AAC(6')-IId, and Eis). We identify AMEs in clinical isolates of various bacterial strains (two strains of *A. baumannii*, three of *Enterobacter cloacae*, and four of *Klebsiella pneumoniae*) and one representative of each strain purchased from the American Type Culture Collection. Lastly, we determine the MIC values for amikacin and tobramycin in combination with a zinc pyrithione complex.

3.1. INTRODUCTION

Aminoglycosides (AGs) are broad-spectrum bactericidal antibiotics that are used clinically for the treatment of serious bacterial infections.[1-2] These antibiotics were originally isolated from *Streptomyces* and *Micromonosporas*,[3] and display activity against Gram-positive, aerobic Gram-negative pathogenic bacteria, and *Mycobacteria*. Since the discovery of

streptomycin, the first-in-class AG isolated, many generations of AGs have been discovered with improved efficacy. This property has kept them clinically relevant despite their inherent oto- and nephrotoxicity. Currently, amikacin (AMK), gentamicin (GEN), and tobramycin (TOB) are the most commonly prescribed AGs for systemic administration in the U.S.A. against bacterial infections (Figure 3.1).[4] Another AG, kanamycin (KAN), is also used systemically, but only to treat resistant strains of *M. tuberculosis* in patients who show no response to first-line anti-tuberculosis treatments. Other AGs, such as neomycin B (NEO), are found in antibiotic ointment formulations for topical use.[5]

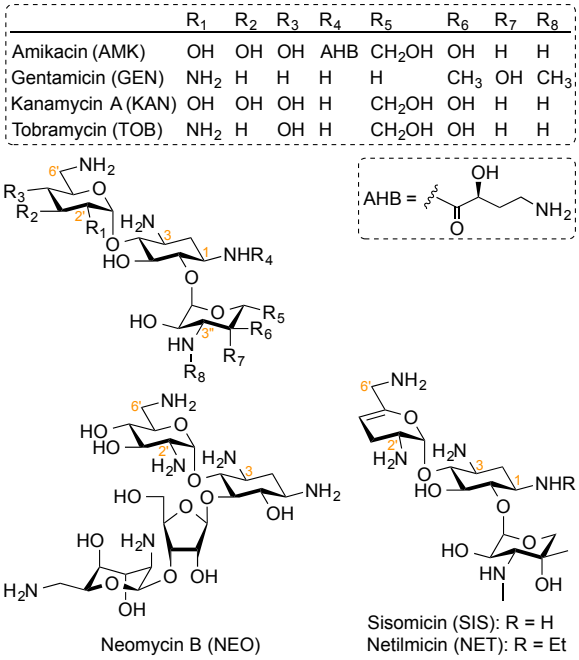

Figure 3.1. Structures of the AGs tested in this study.

The increased importance and popularity of AGs has, unfortunately, led to lapses in antimicrobial stewardship. This, coupled with patient non-compliance to their prescribed drug regimen, has accelerated the development of resistance against AGs and reduced the

effective agents available for combating ever-evolving pathogens. The most common mechanism of bacterial resistance to AGs is the acquisition of AG-modifying enzymes (AMEs).[6-7] Based on the reactions they catalyze, AMEs can be classified as AG *N*-acetyltransferases (AACs), AG *O*-phosphotransferases (APHs), or AG *O*-nucleotidyltransferases (ANTs), amongst which AACs are responsible for the majority of resistant infections. AACs modify AG substrates and disrupt their binding to the ribosome by transferring the acetyl group from acetyl-coenzyme A (AcCoA) onto amine moieties of the AG scaffolds. Although most AACs are regiospecific and only modify a single amino group, the unique enhanced intracellular survival (Eis) protein upregulated in resistant *M. tuberculosis* strains, is capable of acetylating AG substrates at several different positions.[8-10]

In an effort to overcome bacterial resistance, a large amount of time and money has been invested towards the development of inhibitors to these resistance enzymes. Most commonly, small organic molecules have been explored for this purpose. For example, *in silico* and high-throughput screening were used to identify small organic molecules capable of inhibiting AAC(6')-Ib[11] and Eis,[12] respectively. Traditional synthesis was utilized to identify 7-hydroxytropolone as an inhibitor of ANT(2"),[13] and to generate a library of 45 non-carbohydrate molecules containing a 1,3-diamine scaffold commonly found in AGs, which were found to be competitive inhibitors of ANT(2")-Ia and APH(3')-IIIa.[14] Bisubstrate inhibitors comprised of an AG (GEN or neamine) linked to an AcCoA-like molecule were also found to inhibit various AAC(3) and AAC(6') resistance enzymes.[15-16]

Interestingly, Zn^{2+} metal ions were recently reported to inhibit AAC(6')-Ib and reduce AMK resistance in *Acinetobacter baumannii* and *Escherichia coli.*[17] Inspired by this study, we aimed to decipher whether metal ions could be used to inhibit a larger repertoire of AACs in a variety of bacterial strains. Herein, we explore the possibility of using Zn^{2+} and other ions (Mg^{2+}, Cr^{3+}, Cr^{6+}, Mn^{2+}, Co^{2+}, Ni^{2+}, Cu^{2+}, Cd^{2+}, and Au^{3+} in different salt forms) to inhibit various AACs, including AAC(2')-Ic (from *M. tuberculosis*),[18-19] AAC(3)-Ia (from *Serratia marcescens*),[20] AAC(3)-Ib from the bifunctional AAC(3)-Ib/AAC(6')-Ib' (from *Pseudomonas aeruginosa*),[21-22] AAC(3)-IV (from *E. coli*),[23] AAC(6')-Ib' from the bifunctional AAC(3)-Ib/AAC(6')-Ib' (from *P. aeruginosa*),[21-22] AAC(6')-Ie from the bifunctional enzyme AAC(6')-Ie/APH(2")-Ia (from *Staphylococcus aureus*),[24-26] AAC(6')-IId from the bifunctional ANT(3")-Ii/AAC(6')-IId (from *S. marcescens*),[27-28] and Eis (from *M. tuberculosis*).[8] We identify various AME genes present in clinical isolates of *A. baumannii*, *Enterobacter cloacae*, and *Klebsiella pneumoniae* and compare their resistance enzyme profile to their susceptibility to a variety of clinical antibiotics. We also present MIC data for AMK and TOB in combination with a zinc complex, zinc pyrithione (ZnPT).

3.2. RESULTS

3.2.1. *In vitro* inhibition of AACs by metal salts

To determine the inhibitory effect of different metal salts on the *N*-acetylating activity of AACs with various AGs, we first performed UV-Vis assays in 96-well plates (Figures 3.2 and 3.3, and Table 3.1). Amongst the metal ions (Mg^{2+}, Cr^{3+}, Cr^{6+}, Mn^{2+}, Co^{2+}, Ni^{2+}, Cu^{2+}, Zn^{2+}, Cd^{2+}, and Au^{3+}) selected, Cu^{2+} salts ($Cu(OAc)_2$, $Cu(NO_3)_2$, $CuSO_4$) showed the most inhibitory activity against AACs in general. The presence of Zn^{2+} and Cd^{2+} ions also

resulted in generally lower AAC activity, with the exception of AAC(2')-Ic that was not well inhibited by Zn^{2+} or Cd^{2+}. Eis also seemed to remain uninhibited by Zn^{2+} salts when tested with AMK, and by $ZnSO_4$ when tested with other AGs. Actually, AAC(2')-Ic was, in general, only effectively inhibited by Cu^{2+} and Au^{3+}. Interestingly, we noted that in general Ni^{2+} ($NiCl_2$ and $NiSO_4$) exerted moderate inhibition against the AAC(6') enzymes, but not AAC(6')-Ie (when tested with KAN or NEO) or other AACs. On the other hand, Au^{3+} inhibited all AACs tested with the exception of AAC(6')-Ie where only 6'-*N*-acetylation of KAN was inhibited, and AAC(3)-Ib in the presence of GEN and sisomicin (SIS) where 3-*N*-acetylation was not inhibited. We also explored whether different anions affected the inhibitory ability of the same metal cation, yet with the Ni^{2+}, Zn^{2+}, Cu^{2+}, and Cd^{2+} ions that we tested in different salt forms, we did not observe a noticeable difference in the enzyme activities amongst the different anions.

Additionally, with few exceptions, we did not observe a difference in the metals' inhibitory effect amongst various AGs across all enzymes studied. In addition, Eis showed the most reduction in activity in response to Au^{3+}, which made Au^{3+} more effective as an inhibitor for Eis than Cd^{2+} and some Zn^{2+} salts. It was also noticeable that $ZnSO_4$ did not inhibit Eis activity as much as the other Zn^{2+} salts did when tested with other AGs. This trend was also observed with AAC(3)-IV, suggesting that the SO_4^{2-} ion may deteriorate the inhibitory effect of Zn^{2+}. For the different AAC(3) enzymes, Zn^{2+} and Cd^{2+} showed the second best inhibitory effect after Cu^{2+}, even though the AAC(3)-IV activity was higher when tested with $ZnSO_4$ than when tested with other Zn^{2+} salts. Au^{3+} was also found to exert decent

inhibition of the AAC(3) enzymes with the exception of AAC(3)-Ib when tested with GEN and SIS.

Figure 3.2. The inhibition of AAC enzymes by various metal salts with and without physiological concentration of NaCl. Activities with metal ion inhibitors are presented as a percentage of the activity of each AAC with AG without metal salts. The clinical relevant AGs, AMK, GEN, and TOB, are presented here. Other AGs, KAN, NEO, NET, and SIS, are presented in Figure 3.3. *As $AuCl_3$ precipitated in HEPES pH 7.5 buffer with DTDP in the reaction mixture, it was not tested against AAC(6')-Ib' and AAC(6')-IId, and is therefore not presented in this figure. AAC(6')-Ib' and AAC(6')-IId were also not tested with the Cu^{2+} salts in the presence of 100 mM NaCl due to solubility issues.

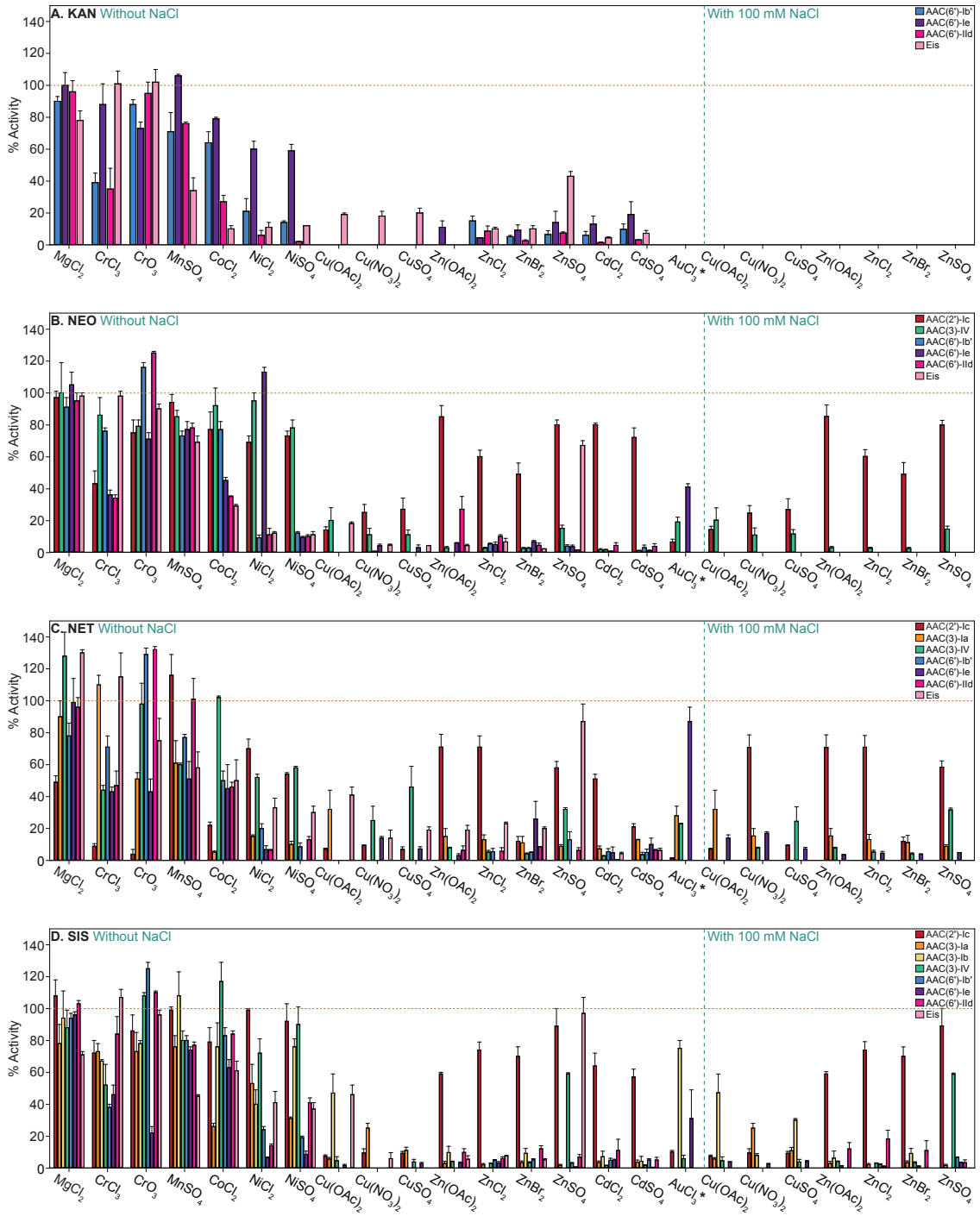

Figure 3.3. The inhibition of AAC enzymes by various metal salts with and without physiological concentration of NaCl. Activities with metal ion inhibitors are presented as a percentage of the activity of each AAC with AG without metal salts. The AGs that are not presented in Figure 3.2, KAN, NEO, NET, and SIS, are presented here. *As $AuCl_3$ precipitated in HEPES pH 7.5 buffer with DTDP in the reaction mixture, it was not tested against AAC(6')-Ib' and AAC(6')-IId, and is therefore not presented in this figure. AAC(6')-Ib' and AAC(6')-IId were also not tested with the Cu^{2+} salts in the presence of 100 mM NaCl due to solubility issues.

Table 3.1. Summary of inhibition of various AAC enzymes by metal salts in combination with different AGs (*Note*: these data are presented in Figures 3.2 and 3.3).

Enzyme	**AG**	**Metal**									
		$MgCl_2$	$CrCl_3$	CrO_3	$MnSO_4$	$CoCl_2$	$NiCl_2$	$NiSO_4$	$Cu(OAc)_2$	$Cu(NO_3)_2$	$CuSO_4$
AAC(2')-Ic[a]	GEN	94 ± 9	72 ± 1	61 ± 2	102 ± 5	80 ± 10	96 ± 1	80 ± 6	17 ± 1	20 ± 4	15 ± 2
	NEO	97 ± 4	43 ± 8	75 ± 8	94 ± 5	77 ± 11	69 ± 4	73 ± 3	14 ± 2	25 ± 5	27 ± 7
	NET	49 ± 4	8.9 ± 1.6	3.9 ± 3.0	116 ± 13	22 ± 2	70 ± 6	54 ± 1	7.0 ± 0.7	9.4 ± 0.3	7.0 ± 1.5
	SIS	108 ± 10	72 ± 8	86 ± 10	99 ± 2	79 ± 9	99 ± 1	92 ± 11	7.3 ± 0.9	9.4 ± 2.6	9.2 ± 1.2
	TOB	90 ± 5	--	49 ± 4	89 ± 2	53 ± 4	78 ± 1	65 ± 4	9.3 ± 1.2	17 ± 8	12 ± 6
AAC(3)-Ia[a]	GEN	84 ± 4	110 ± 6	79 ± 7	64 ± 9	66 ± 2	51 ± 2	69 ± 6	--	--	--
	NET	90 ± 10	110 ± 6	51 ± 4	61 ± 14	5.2 ± 0.7	15 ± 1	10 ± 2	32 ± 12	--	--
	SIS	78 ± 12	73 ± 5	73 ± 12	76 ± 7	26 ± 2	53 ± 12	31 ± 1	5.6 ± 1.0	25 ± 3	11 ± 2
AAC(3)-Ib[a]	GEN	104 ± 25	61 ± 8	63 ± 16	66 ± 18	53 ± 9	31 ± 7	31 ± 1	--	--	--
	SIS	94 ± 17	67 ± 1	78 ± 2	108 ± 15	76 ±15	40 ± 9	76 ± 5	47 ± 12	--	--
AAC(3)-IV[a]	GEN	95 ± 6	37 ± 5	76 ± 5	73 ± 7	80 ± 9	36 ± 3	69 ± 8	--	--	4.0 ± 0.1
	NEO	100 ± 19	86 ± 11	79 ± 4	85 ± 4	92 ± 11	95 ± 5	78 ± 5	20 ± 8	11 ± 4	11 ± 3
	NET	128 ± 15	44 ± 3	98 ± 13	60 ± 1	102 ± 1	52 ± 2	58 ± 1	--	25 ± 9	46 ± 13
	SIS	88 ± 11	53 ± 13	108 ± 2	80 ± 6	117 ± 12	72 ± 9	90 ± 11	4.6 ± 2.5	--	3.8 ± 1.6
	TOB	105 ± 7	80 ± 4	55 ± 3	48 ± 2	126 ± 4	76 ± 7	84 ± 3	--	6.9 ± 1.2	--
AAC(6')-Ib'[b]	AMK	93 ± 5	85 ± 3	108 ± 6	92 ± 5	21 ± 1	3.9 ± 0.5	6.5 ± 0.5	--	--	--
	GEN	90 ± 4	73 ± 19	111 ± 4	86 ± 3	95 ± 5	35 ± 3	32 ± 4	--	--	--
	KAN	90 ± 3	39 ± 6	88 ± 3	71 ± 12	64 ± 7	21 ± 8	14 ± 1	--	--	--
	NEO	91 ± 6	76 ± 2	116 ± 3	73 ± 3	77 ± 5	9.1 ± 1.7	12 ± 1	--	0.59 ± 0.17	--
	NET	77 ± 8	71 ± 7	129 ± 4	77 ± 2	50 ± 6	20 ± 3	8.2 ± 2.5	--	--	--
	SIS	94 ± 3	38 ± 2	125 ± 4	80 ± 3	83 ± 5	24 ± 2	19 ± 1	--	--	--
	TOB	103 ± 1	56 ± 1	100 ± 4	74 ± 6	79 ± 2	11 ± 2	15 ± 3	4.7 ± 0.4	5.5 ± 1.0	--
AAC(6')-Ie[a]	AMK	104 ± 1	57 ± 9	75 ± 1	100 ± 4	84 ± 4	10 ± 5	8.9 ± 0.4	--	--	--
	GEN	93 ± 3	77 ± 8	65 ± 6	85 ± 4	70 ± 2	18 ± 3	12 ± 2	--	--	--
	KAN	100 ± 8	88 ± 13	73 ± 4	106 ± 1	79 ± 1	60 ± 5	59 ± 4	--	--	--
	NEO	105 ± 8	36 ± 3	71 ± 4	77 ± 5	45 ± 2	113 ± 3	9.3 ± 0.7	--	4.1 ± 1.0	2.9 ± 1.7
	NET	99 ± 15	43 ± 3	43 ± 8	51 ± 11	45 ± 15	6.8 ± 2.4	--	--	14 ± 1	7.2 ± 1.4
	SIS	96 ± 2	46 ± 6	22 ± 4	74 ± 2	63 ± 5	6.5 ± 0.4	8.6 ± 2.0	1.6 ± 0.7	--	2.7 ± 0.8
	TOB	92 ± 7	109 ± 6	76 ± 14	130 ± 15	125 ± 8	32 ± 1	33 ± 3	7.9 ± 5.0	13 ± 2	7.9 ± 0.3
AAC(6')-IId[b]	AMK	96 ± 6	63 ± 2	72 ± 4	28 ± 2	3.1 ± 1.2	0.72 ± 0.18	--	--	--	--
	GEN	119 ± 6	77 ± 9	122 ± 4	87 ± 5	86 ± 4	47 ± 9	38 ± 8	--	--	--
	KAN	96 ± 7	35 ± 13	95 ± 7	76 ± 1	27 ± 4	6 ± 3	2.0 ± 0.1	--	--	--
	NEO	95 ± 5	34 ± 2	125 ± 1	78 ± 3	35 ± 0.4	11 ± 4	9.9 ± 1.1	--	--	--
	NET	96 ± 6	47 ± 9	132 ± 2	101 ± 13	46 ± 3	6.5 ± 0.4	13 ± 2	--	--	--
	SIS	103 ± 2	84 ± 11	110 ± 1	77 ± 2	84 ± 2	14 ± 1	41 ± 3	--	--	--
	TOB	90 ± 23	26 ± 2	130 ± 15	110 ± 29	38 ± 15	12 ± 2	16 ± 3	--	--	--
Eis[a]	AMK	73 ± 9	110 ± 1	87 ± 6	55 ± 5	41 ± 5	50 ± 2	41 ± 4	23 ± 10	22 ± 5	18 ± 2
	KAN	78 ± 6	101 ± 8	102 ± 8	34 ± 8	10 ± 2	11 ± 3	12 ± 0.1	19 ± 1	18 ± 3	20 ± 3
	NEO	98 ± 2	98 ± 3	90 ± 3	69 ± 4	29 ± 1	12 ± 1	11 ± 2	18 ± 1	4.5 ± 0.6	4.2 ± 0.1
	NET	130 ± 2	115 ± 15	75 ± 14	58 ± 10	50 ± 13	33 ± 6	30 ± 4	41 ± 5	14 ± 5	19 ± 2
	SIS	71 ± 2	107 ± 5	96 ± 3	45 ± 1	61 ± 6	41 ± 7	37 ± 4	46 ± 6	5.9 ± 3.7	--
	TOB	68 ± 1	130 ± 8	107 ± 8	109 ± 11	12 ± 5	26 ± 4	20 ± 5	28 ± 5	13 ± 1	13 ± 2

-- Indicates that no enzymatic activity was detected.
X Indicates that the Au^{3+} precipitated in HEPES pH 7.5 buffer in the presence of DTDP.
[a] Reactions monitored by absorbance of reacted DTNB at 412 nm.
[b] Reactions monitored by absorbance of reacted DTDP at 324 nm.

Table 3.1 cont. Summary of inhibition of various AAC enzymes by metal salts in combination with different AGs (*Note*: these data are presented in Figures 3.2 and 3.3).

Enzyme	AG	Metal						
		$Zn(OAc)_2$	$ZnCl_2$	$ZnBr_2$	$ZnSO_4$	$CdCl_2$	$CdSO_4$	$AuCl_3$
AAC(2')-Ic[a]	GEN	87 ± 4	73 ± 13	57 ± 3	83 ± 7	88 ± 2	74 ± 1	--
	NEO	85 ± 7	60 ± 4	49 ± 7	80 ± 3	80 ± 1	72 ± 6	6.5 ± 1.7
	NET	71 ± 8	71 ± 7	12 ± 3	58 ± 4	51 ± 3	21 ± 2	1.5 ± 0.1
	SIS	59 ± 1	74 ± 5	70 ± 6	89 ± 11	64 ± 8	57 ± 5	10 ± 1
	TOB	60 ± 3	62 ± 8	32 ± 5	66 ± 5	63 ± 6	44 ± 5	38 ± 1
AAC(3)-Ia[a]	GEN	4.2 ± 1.1	--	2.1 ± 1.1	6.8 ± 2	3.7 ± 0.8	3.9 ± 0.9	--
	NET	15 ± 5	13 ± 3	11 ± 4	8.8 ± 1.1	7.3 ± 1.7	13 ± 0.2	28 ± 6
	SIS	2.8 ± 1.4	2.0 ± 0.8	3.3 ± 1.1	1.6 ± 0.7	3.3 ± 1.1	3.6 ± 1.4	--
AAC(3)-Ib[a]	GEN	7.7 ± 4.2	1.9 ± 0.7	--	--	--	--	74 ± 9
	SIS	9.7 ± 3.9	--	9.2 ± 3.1	--	7.1 ± 3.4	4.2 ± 3.1	75 ± 5
AAC(3)-IV[a]	GEN	3.2 ± 0.3	1.9 ± 0.3	2.9 ± 0.4	27 ± 3	1.4 ± 0.3	1.2 ± 0.3	--
	NEO	2.8 ± 0.8	2.5 ± 0.7	2.4 ± 0.7	15 ± 2	1.6 ± 0.7	1.1 ± 0.1	19 ± 3
	NET	7.9 ± 0.4	5.2 ± 1.1	4.1 ± 0.6	32 ± 1	2.8 ± 0.3	3.6 ± 1.5	23 ± 0.3
	SIS	4.1 ± 0.2	2.9 ± 0.3	3.4 ± 0.5	59 ± 1	1.5 ± 0.3	0.7 ± 0.3	5.8 ± 2.2
	TOB	1.5 ± 0.3	2.9 ± 0.6	2.7 ± 0.4	39 ± 5	0.7 ± 0.4	1.1 ± 0.4	20 ± 3
AAC(6')-Ib'[b]	AMK	8.8 ± 2.7	1.3 ± 0.6	1.6 ± 0.2	7.5 ± 4.0	--	--	X
	GEN	--	16 ± 4	5.5 ± 1.5	8.6 ± 0.2	2.4 ± 0.6	--	X
	KAN	--	15 ± 3	5.1 ± 0.8	6.5 ± 2.4	6.0 ± 2.4	9.7 ± 3.4	X
	NEO	--	5.2 ± 0.6	2.6 ± 0.4	3.8 ± 0.9	1.5 ± 0.4	2.9 ± 1.6	X
	NET	--	5.5 ± 2.0	5.1 ± 0.2	13 ± 5	5.5 ± 1.9	5.0 ± 2.1	X
	SIS	--	4.8 ± 0.5	5.1 ± 0.7	3.0 ± 0.5	4.8 ± 1.3	5.0 ± 0.8	X
	TOB	--	13 ± 1	2.2 ± 0.1	4.3 ± 1.2	1.5 ± 0.4	2.3 ± 0.2	X
AAC(6')-Ie[a]	AMK	1.7 ± 0.4	8.5 ± 0.8	2.9 ± 2.1	9.7 ± 1.4	9.3 ± 1.7	7.5 ± 2.1	54 ± 7
	GEN	--	12 ± 2	4.9 ± 1.8	5.7 ± 1.7	4.9 ± 0.9	0.61 ± 0.21	38 ± 13
	KAN	11 ± 4	4.4 ± 0.1	9.2 ± 3.3	14 ± 7	13 ± 5	19 ± 8	--
	NEO	5.8 ± 0.3	4.9 ± 1.6	6.6 ± 0.8	3.5 ± 1.0	0.67 ± 0.10	0.99 ± 0.44	41 ± 2
	NET	3.0 ± 1.2	--	26 ± 11	--	4.9 ± 3.5	10 ± 4	87 ± 9
	SIS	3.1 ± 0.7	3.2 ± 0.9	--	0.62 ± 0.05	4.9 ± 0.6	0.44 ± 0.10	31 ± 18
	TOB	10 ± 2	16 ± 3	4.7 ± 1.6	--	6.8 ± 3.3	5.3 ± 2.3	106 ± 30
AAC(6')-IId[b]	AMK	13 ± 5	1.5 ± 0.5	2.9 ± 0.3	2.4 ± 0.7	0.91 ± 0.36	1.1 ± 0.1	X
	GEN	--	20 ± 2	12 ± 1	29 ± 4	13 ± 6	12 ± 2	X
	KAN	--	8.6 ± 3.2	2.5 ± 0.6	7.4 ± 0.7	1.4 ± 0.4	3.1 ± 0.1	X
	NEO	27 ± 8	9.9 ± 1.1	4.4 ± 1.4	1.4 ± 0.2	4.3 ± 1.7	3.7 ± 1.7	X
	NET	6.3 ± 2.8	5.7 ± 2.3	8.6 ± 0.02	6.3 ± 1.7	0.34 ± 0.02	6.5 ± 0.4	X
	SIS	9.8 ± 2.3	5.9 ± 1.1	12 ± 2	6.8 ± 1.6	11 ± 7	5.0 ± 1.7	X
	TOB	--	11 ± 2	17 ± 3	10 ± 4	8.5 ± 1.8	8.1 ± 1.7	X
Eis[a]	AMK	57 ± 2	57 ± 2	48 ± 1	60 ± 12	23 ± 4	23 ± 2	3.9 ± 1.7
	KAN	--	10 ± 1	10 ± 2	43 ± 3	4.4 ± 0.6	7.2 ± 1.8	--
	NEO	4.2 ± 0.8	6.5 ± 2.2	2.1 ± 0.2	67 ± 3	--	--	--
	NET	19 ± 3	23 ± 1	20 ± 1	87 ± 11	4.2 ± 0.9	6.3 ± 1.4	--
	SIS	5.5 ± 2.2	7.5 ± 0.4	5.1 ± 0.8	97 ± 10	--	--	--
	TOB	5.4 ± 2.1	5.5 ± 1.1	4.9 ± 1.2	68 ± 10	--	3.0 ± 0.4	--

-- Indicates that no enzymatic activity was detected.
X Indicates that the Au^{3+} precipitated in HEPES pH 7.5 buffer in the presence of DTDP.
[a] Reactions monitored by absorbance of reacted DTNB at 412 nm.
[b] Reactions monitored by absorbance of reacted DTDP at 324 nm.

To investigate if the metal salts would react similarly under physiological conditions, we tested our best overall inhibitor candidates, Cu^{2+} and Zn^{2+} salts, in the presence of 100 mM NaCl (Figures 3.2 and 3.3). We observed no significant difference between the enzyme activity with and without physiological concentration of NaCl in the presence of different metal ions. AAC(6')-Ie, as well as AAC(6')-Ib' and AAC(6')-IId (with Zn^{2+} salts), showed complete inhibition when tested against AMK and KAN in the presence of NaCl, indicating

that at physiological conditions these metal salts could be even better inhibitors. It is important to note that AAC(6')-Ib' and AAC(6')-IId were not tested with Cu^{2+} salts due to solubility issues.

We next determined the half maximum inhibitory concentration (IC_{50}) values for selected salts that showed complete inhibition in our UV-Vis assays (Table 3.2 and Figure 3.5). With the exception of AAC(3)-IV in the presence of NEO where the IC_{50} values for $ZnCl_2$, $Zn(OAc)_2$, and $ZnBr_2$ were 44 ± 19 μM, 34 ± 8 μM, and 17 ± 5 μM, respectively, Zn^{2+} salts were found to display low IC_{50} values ranging from 0.04 ± 0.01 μM to 7.8 ± 1.7 μM against all enzymes. For the inhibition of AAC(3)-IV by Cd^{2+} salts, IC_{50} values of 7.3 ± 2.7 μM and 8.7 ± 1.7 μM were determined for $CdCl_2$ in the presence NEO and $CdSO_4$ in the presence of netilmicin (NET), respectively. Cd^{2+} salts were found to be much better inhibitors of AAC(6')-Ib' and Eis with IC_{50} values ranging from 0.41 ± 0.03 μM to 0.79 ± 0.10 μM. $AuCl_3$ was found to display the biggest range of IC_{50} values (0.010 ± 0.003 μM to 121 ± 26 μM).

Finally, to elucidate the potential mechanism by which these metal ions inhibit the AAC activities, we tested whether the effect metal ions exert on AAC activity is reversible. We added EDTA to the reactions to chelate the metal inhibitors and found that the presence of EDTA can restore enzyme activity against AG substrates, potentially by chelating the metal ions and preventing them from interfering with the enzymatic reaction between the AACs and AGs (a representative graph was shown in Figure 3.5).

Table 3.2. IC_{50} values of some for the various metal ions that have shown complete inhibition in UV-Vis assays against various AACs in combination with different AGs.

Enzyme	AG	Metal ion	IC_{50} (μM)
AAC(2')-Ic[a]	GEN	$AuCl_3$	12 ± 3
AAC(3)-Ia[a]	GEN	$ZnCl_2$	1.4 ± 0.3
AAC(3)-Ib[a]	SIS	$ZnCl_2$	0.13 ± 0.02
		$ZnSO_4$	1.4 ± 0.2
AAC(3)-IV[a]	NEO	$ZnCl_2$	44 ± 19
		$Zn(OAc)_2$	34 ± 8
		$ZnBr_2$	17 ± 5
		$CdCl_2$	7.3 ± 2.7
	NET	$CdSO_4$	8.7 ± 1.7
	TOB	$CuSO_4$	0.35 ± 0.14
AAC(6')-Ib'[b]	AMK	$CdSO_4$	0.41 ± 0.08
		$AuCl_3$	0.41 ± 0.07
	SIS	$Zn(OAc)_2$	7.8 ± 1.7
AAC(6')-Ie[a]	SIS	$ZnBr_2$	0.41 ± 0.08
	TOB	$ZnSO_4$	5.2 ± 1.3
Eis[a]	KAN	$AuCl_3$	7.7 ± 2.3
	NET	$AuCl_3$	18 ± 1
	SIS	$CdCl_2$	0.78 ± 0.09
		$CdSO_4$	0.79 ± 0.10
		$AuCl_3$	121 ± 26
	TOB	$Zn(OAc)_2$	0.04 ± 0.01
		$CdCl_2$	0.41 ± 0.03
		$AuCl_3$	0.010 ± 0.003

[a] Reactions were monitored by recording the absorbance at 412 nm with DTNB. [b]Reactions were monitored by recording the absorbance at 324 nm with DTDP.

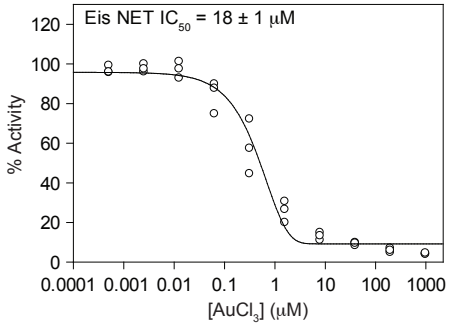

Figure 3.4. Representative IC_{50} plot. The example provided is that of the IC_{50} value of $AuCl_3$ against Eis in combination with NET.

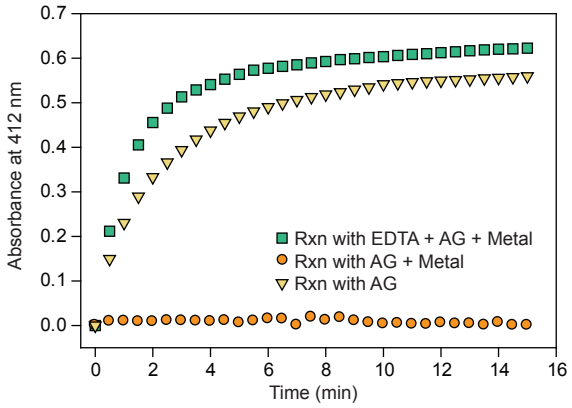

Figure 3.5. Representative graph demonstrating that addition of EDTA restored the ability of AACs to acetylate AGs as the metal ions were chelated. The green squares represent the reaction where EDTA chelated the metal ions. The orange circles indicate the reaction where the *N*-acetylation of AGs was inhibited by metal ions. The yellow triangles represent the standard *N*-acetylation of AGs by AACs.

3.2.2. Profiling of resistance enzymes in clinical isolates of various bacterial strains

To gain a better understanding of the profile of AMEs that are present in the different bacterial strains involved in our study, we performed PCR with primers that amplify the genes for four different AMEs, AAC(6')-Ib, AAC(3)-IV, ANT(2")-Ia, and APH(3')-Ia, in twelve bacterial strains from ATCC and clinical isolates (Figure 3.6). In all the *A. baumannii* strains (ATCC 19606, clinical isolates #75 and #81), we identified the presence of *aac(6')-Ib* and *aph(3')-Ia*. In the *E. cloacae* ATCC 13047 strain, we did not find any of the four AME genes. However, we found *ant(2")-Ia* gene in *E. cloacae* clinical isolates #41 and #61, and *aph(3')-Ia* in clinical isolate #52. For the five *K. pneumoniae* strains, we found *aac(6')-Ib*, *aac(3)-IV*, and *aph(3')-Ia* in clinical isolate strains #22, #34, and #44. The *K. pneumoniae* ATCC 27736 strain only possessed *aph(3')-Ia*. Clinical isolate #24 possessed *aac(6')-Ib* and *aac(3)-IV*.

3.2.3. Activity of AGs in combination with ZnPT in various bacterial strains

Since Zn^{2+} was overall a great metal ion inhibitor in our study, we decided to further investigate Zn^{2+} for its effect on the MIC values of AMK or TOB against strains of *A. baumannii*, *E. cloacae*, and *K. pneumoniae*. After discovering that $ZnCl_2$ had no effect on the MIC values of AMK and TOB against *A. baumannii*, possibly due to poor intracellular Zn^{2+} concentration, we decided to use ZnPT, an organic zinc complex, that was previously reported to have improved membrane permeability.[17] This study showed that the presence of ZnPT significantly reduced the MIC values of AMK and TOB in most of the twelve bacterial strains that we tested (Tables 3.3 and 3.4).

Table 3.3. MIC values of AMK (μg/mL) in the presence of various concentrations of ZnPT against various Gram-negative bacterial strains.

	A. baumannii			*E. cloacae*				*K. pneumoniae*				
[ZnPT] (μM)	ATCC 19606	#75	#81	ATCC 13047	#41	# 52	#61	ATCC 27736	#22	#24	#34	#44
80	≤0.06	NG	NG	NG	NG	NG	NG	NG	NG	NG	NG	NG
40	≤0.06	NG	NG	NG	NG	NG	NG	0.5	NG	NG	NG	NG
20	0.25	≤0.25	0.25	NG	NG	NG	4	0.5	NG	4	NG	NG
10	0.5	>128	1	0.5	1	NG	4	2	8	4	NG	NG
5	2	>128	2	2	8	1	4	4	8	4	0.25	1
2.5	2	>128	1	2	8	>2	8	8	32	8	0.5	16
1.25	2	>128	1	2	8	>2	>8	8	32	16	0.5	16
0	4	>128	4	2	8	>2	>8	16	32	16	2	>16

NG = no growth.

Table 3.4. MIC values of TOB (μg/mL) in the presence of various concentrations of ZnPT against various Gram-negative bacterial strains.

	A. baumannii			*E. cloacae*				*K. pneumoniae*				
[ZnPT] (μM)	ATCC 19606	#75	#81	ATCC 13047	#41	# 52	#61	ATCC 27736	#22	#24	#34	#44
80	NG	NG	NG	NG	NG	NG	NG	NG	NG	NG	NG	NG
40	≤0.0313	NG	NG	NG	NG	NG	8	≤0.0313	NG	NG	NG	NG
20	≤0.0313	NG	NG	NG	>8	NG	8	≤0.0313	NG	NG	NG	NG
10	≤0.0313	NG	NG	1	>8	4	>8	≤0.0313	8	4	NG	8
5	0.5	>8	1	1	>8	4	>8	0.5	128	128	0.0094	128
2.5	0.5	>8	1	1	>8	8	>8	0.5	>128	128	0.038	128
1.25	1	>8	1	1	>8	8	>8	0.5	>128	128	0.075	128
0	1	>8	2	1	>8	8	>8	2	>128	128	0.038	>128

NG = no growth.

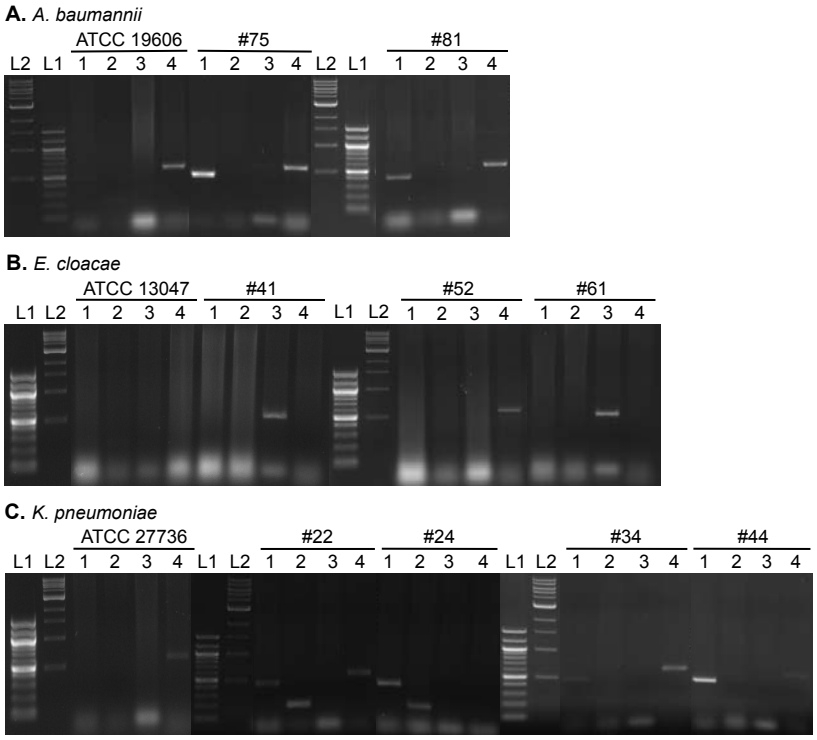

Figure 3.6. Agarose gels of PCR reactions probing for AME genes in various ATCC strains and clinical isolates. Strains of **A.** *A. baumannii*, **B.** *E. cloacae*, and **C.** *K. pneumoniae* tested for *aac(6')-Ib* (lanes 1), *aac(3)-IV* (lanes 2), *ant(2")-Ia* (lanes 3), and *aph(3')-Ia* (lanes 4) genes. L1 and L2 represent 100 bp and 1 kb DNA ladders, respectively. Expected band sizes are as follow: *aac(6')-Ib* = 482 bp; *aac(3)-IV* = 230 bp; *ant(2")-Ia* = 534 bp; and *aph(3')-Ia* = 624 bp.

Against *A. baumannii* ATCC 19606 as well as clinical isolate #81, the MIC value of AMK was reduced from 4 μg/mL to 0.25 μg/mL in the presence of 20 μM ZnPT (Table 3.3). With the same amount of ZnPT, the MIC value of AMK was reduced from >128 μg/mL to ≤0.25 μg/mL against *A. baumannii* clinical isolate #75. The same trend held true against the *E. cloacae* and *K. pneumoniae* strains. Against *E. cloacae* clinical isolate #41, the MIC value of AMK was reduced from 8 μg/mL to 1 μg/mL in the presence of 10 μM ZnPT. Against the other strains (*E. cloacae* ATCC 13047, #52, and #61), the AMK MIC values were reduced from 2 μg/mL to 0.5 μg/mL, >2 μg/mL to 1 μg/mL, and >8 μg/mL to 4 μg/mL in the presence of 5-10 μM ZnPT, respectively. Against *K. pneumoniae* strains, 4-

32-fold reductions in the MIC values of AMK were observed in the presence of 5-20 μM ZnPT.

The reduction in MIC values in the presence of ZnPT was also observed for TOB against most strains tested (Table 3.4). Against the different *A. baumannii* strains, the MIC values of TOB were reduced from 1 μg/mL to ≤0.0313 μg/mL (ATCC 19606), and from 2 μg/mL to 1 μg/mL (clinical isolate #81) in the presence of 10 μM and 1.25 μM ZnPT, respectively. Yet, against clinical isolate #75, the MIC value of TOB went from >8 μg/mL to no growth in the control wells, suggesting that ZnPT had no effect on the MIC of TOB in this strain. This was similarly observed against the *E. cloacae* ATCC 13047 and clinical isolates #41 and #61. Against the *E. cloacae* clinical isolate #52, the MIC value of TOB was reduced from 8 μg/mL to 4 μg/mL with 5 μM ZnPT. Against *K. pneumoniae* ATCC 27736 and clinical isolates #22, #24, and #44, 10 μM ZnPT effectively reduced the MIC values of TOB from 2 μg/mL to ≤0.0313 μg/mL, >128 μg/mL to 8 μg/mL, 128 μg/mL to 4 μg/mL, and >128 μg/mL to 8 μg/mL, respectively. Against *K. pneumoniae* clinical isolate #34, the MIC value of TOB was reduced from 0.038 μg/mL to 0.0094 μg/mL in the presence of 5 μM ZnPT.

3.3. DISCUSSION

To investigate their inhibitory effect on eight AACs, we tested a panel of nine metal ions (in different salt forms) and studied their interference in modifying seven AGs (AMK, GEN, KAN, NEO, NET, SIS, and TOB) (Figures 3.2 and 3.3, and Table 3.1). By UV-Vis assays, we demonstrated that Cu^{2+} is overall the best at inhibiting the different AACs

studied. We found Zn^{2+} and Cd^{2+}, which also showed significant inhibition of most enzymes, to be the second best candidates as AAC inhibitors. Although metal salts were found to be good inhibitors of AACs, the inherent toxicity of some of these metals can render them less desirable regardless of their high inhibitory effect. Despite Zn^{2+} salts falling short in their inhibitory ability compared to Cu^{2+} salts, Zn^{2+} salts remain more desirable for their potential development into clinical AAC inhibitors as they are amongst the least toxic metal salts based on LD_{50} values (*e.g.*, 794 mg/kg in rats oral intake for $Zn(OAc)_2$ compared to 501 mg/kg for $Cu(OAc)_2$; and 1710 mg/kg in rats oral intake for $ZnSO_4$ compared to 361 mg/kg for $NiSO_4$, 482 mg/kg for $CuSO_4$, and 280 mg/kg for $CdSO_4$). Even though Zn^{2+} and Cd^{2+} showed similar inhibitory activity *in vitro* and displayed similar ranges of IC_{50} values (0.04 ± 0.01 μM to 44 ± 19 μM for Zn^{2+} salts compared to 0.41 ± 0.03 μM to 8.7 ± 1.7 μM for Cd^{2+} salts; Table 3.2), Zn^{2+} salts remain more clinically relevant, as Cd^{2+} salts display higher toxicity (LD_{50} values of 107 mg/kg and 280 mg/kg for $CdCl_2$ and $CdSO_4$, respectively, in rats oral intake).

It is known that Cl^- salts are inherently more toxic than some other salt forms. Within the Zn^{2+} salt family, the toxicity of $ZnCl_2$ and $Zn(OAc)_2$ (LD_{50} values of 359 mg/kg, 794 mg/kg, 1447 mg/kg, and 1710 mg/kg for $ZnCl_2$, $Zn(OAc)_2$, $ZnBr_2$, and $ZnSO_4$, respectively, in rats oral intake) and the failure of the less toxic $ZnSO_4$ at inhibiting some AACs render $ZnBr_2$ the most desirable amongst the Zn^{2+} salts studied. Within the Cu^{2+} salts, NO_3^- seems to be a safer counter ion than SO_4^{2-} and OAc^- (LD_{50} values of 482 mg/kg, 501 mg/kg, and 940 mg/kg for $CuSO_4$, $Cu(OAc)_2$, and $Cu(NO_3)_2$, respectively). As for gold salts, even though gold is generally known to be toxic and expensive, it is currently part of therapies for

diseases such as rheumatoid arthritis.[29] Given that no other metal ions worked as well as gold at inhibiting the AAC(2')-Ic enzyme, gold should not be dismissed as a potential candidate to combat the resistance associated with this enzyme.

Having established Zn^{2+} salts as top candidates for AAC inhibition, we set to determine their effect on the activity of AGs in various bacterial strains of *A. baumannii*, *E. cloacae*, and *K. pneumoniae*. Prior to working in bacterial cells, we demonstrated that the presence of NaCl, at concentration mimicing that of physiological conditions, did not interfere with the inhibitory effect of the metal ion salts on AACs (Figures 3.2 and 3.3). We also showed that in the presence of EDTA, the inhibitory effect of the metal ions on the AACs could be reversed as EDTA, a strong metal chelating agent, sequestered the metal ions from the enzymatic reactions (Figure 3.5).

Within each bacterial species selected for our studies with Zn^{2+} salts, we included one commercially purchased ATCC strain as well as a few clinical isolates. We chose some clinical isolates displaying susceptibility to the three commonly prescribed AGs (AMK, GEN, and TOB) and some displaying resistance to these drugs (Table 3.5). Overall, all clinical isolates selected displayed a complex resistance profile to a variety of clinically relevant antibiotics, including different classes and generations of β-lactams, fluoroquinolones, tetracycline, etc. With their specific resistance against AGs in mind, we probed these strains for four AME genes, *aac(6')-Ib*, *aac(3)-IV*, *ant(2")-Ia*, and *aph(3')-Ia* (Figure 3.6). The *aph(3')-Ia* gene was found to be the most prevalent, and was present in eight out of twelve strains. The second most prevalent AME gene was *aac(6')-Ib*, which

was present in seven strains. In addition, different species seemed to possess distinct profiles of AME genes. All *A. baumannii* strains tested possessed *aac(6')-Ib* and *aph(3')-Ia*, but not *aac(3)-IV* and *ant(2")-Ia*. In the five *K. pneumoniae* strains, we found that *aac(6')-Ib*, *aac(3)-IV*, and *aph(3')-Ia* were the most predominant AME genes, whereas *ant(2")-Ia* was not found. In contrast to the first two bacterial species, which mostly rely on *aph(3')-Ia* and *aac(6')-Ib* for resistance, the *E. cloacae* that were tested clearly possessed a different set of AMEs. None of the *E. cloacae* strains tested encoded either AACs, only one clinical isolate contained *aph(3')-Ia*, and two contained *ant(2")-Ia*. These data, when compared to the MIC values of AMK and TOB (Tables 3.3 and 3.4), suggested that these strains possess additional AMEs that we did not probe for, or alternative resistance mechanisms.

Table 3.5. Resistance profiles of clinical isolates (isolate # into parenthesis) against the three AGs used for treatment of systemic infections in the U.S.A. as well as other clinically relevant antibiotics.

Strain	AMK	GEN	TOB	AZA	CFPM	CFX	CFZ	CEFX	CIP	LEV	MEM	NTF	TET
A. baumannii (75)	>128	>8	>8	>16	>16	>16	>16	>32	0.2	>4	>8	>64	>8
A. baumannii (81)	4	8	≤2	>16	>16	>16	>16	>32	>2	>4	>8	>64	>8
E. cloacae (41)	8	>8	>8	>16	>16	>16	>16	>32	1	≤1	>8	64	>8
E. cloacae (52)	1-2	8	>8	>16	16	>16	8	>32	>2	>4	>8	32	8
E. cloacae (61)	4-8	>8	8	>16	≤1	>16	>16	16	>2	>4	≤1	>64	8
K. pneumoniae (22)	32	>8	>8	>16	>16	>16	>16	>32	>2	>4	≤1	>64	>8
K. pneumoniae (24)	16	8	>8	>16	16	>16	>16	>32	>2	>4	2	>64	4
K. pneumoniae (34)	1	≤2	≤2	≤2	≤1	≤4	2	>32	≤0.5	≤1	≤1	64	≤2
K. pneumoniae (44)	16	>8	>8	>16	≤1	>16	>16	>32	>2	>4	>8	>64	>8

AZA = aztreonam; CFPM = cefepime; CFX = cefoxitin; CFZ = ceftazidime; CEFX = ceftriaxone; CIP = ciprofloxacin; LEV = levofloxacin; MEM = meropenem; NTF = nitrofurantoin; TET = tetracycline.

When we tried to determine the MIC values of AMK and TOB against *A. baumannii* in the presence of $ZnCl_2$, we quickly realized that the Zn^{2+} salts studied had no effect on the MIC values of these AGs. We postulated that this could possibly be due to poor intracellular Zn^{2+} concentration resulting from the poor membrane permeability of these salts. We therefore decided to use ZnPT, a membrane permeable organic zinc complex. We found ZnPT to significantly reduce the MIC values for both AGs in most strains tested. Of the *A.*

baumannii strains, the ATCC 19606 and clinical isolate #81 are both susceptible to AMK. Co-treating with 40 μM of ZnPT reduced the MIC value of AMK by 67-fold against the ATCC 19606 strain, whereas using 20 μM of ZnPT reduced the MIC value of AMK by 16-fold against clinical isolate #81. The most significant effect was observed against clinical isolate #75, which was resistant to AMK (>128 μg/mL) and became highly sensitive to this AG (≤0.25 μg/mL) in the presence of 20 μM ZnPT. Against *E. cloacae* and *K. pneumoniae* strains, which were all sensitive or displayed intermediate level of resistance to AMK to start with, the MIC values of AMK showed as much as a 32-fold reduction with 20 μM ZnPT. The resistance profile to TOB is different from that to AMK in the strains that we studied. Most of the *K. pneumoniae* strains (#22, #24, and #44) are resistant to TOB while ATCC 27736 and clinical isolate #34, as well as all *A. baumannii* and *E. cloacae* strains are susceptible to this AG. Although not as significant as those observed in AMK, the reductions in the MIC values of TOB were still observed against most of these strains. Although we established the benefit of co-administering metal ions with AGs for the purpose of re-activating AGs in resistance bacterial strains, we believe that it is critical to not dismiss the bacteriostatic attribute of ZnPT. We postulate that in addition to the inhibitory effect from the Zn^{2+}, there may also be a synergistic effect from the bacteriostatic feature of ZnPT. Further studies outside of the scope of this chapter will be required to help elucidate the intracellular mechanism of ZnPT in the presence or absence of AGs.

3.4. CONCLUSIONS

In sum, we showed that Zn^{2+} and other metal ions are capable of inhibiting the AG *N*-acetyltransferase activity of a variety of AACs *in vitro*. Developing metal salts into AAC inhibitors for combinatorial therapies with AGs is potentially a promising avenue for improving the clinical outcomes of AGs in treatment of resistant bacterial infections resulting from the action of AAC enzymes. The mechanism(s) by which these metal ions inhibit AACs is still unknown. Future studies aimed at elucidating the potential mechanism(s) underlying this inhibition would further enhance our understanding and help combat bacterial resistance in clinical therapeutic regiments.

3.5. MATERIALS AND METHODS

3.5.1. Materials and instrumentation

With the exception of AAC(3)-Ia for which the cloning, overexpression, and purification is described below, all of the enzymes involved in this study, AAC(2')-Ic,[8] AAC(3)-Ib,[30] AAC(3)-IV,[31] AAC(6')-Ie/APH(2")-Ia,[31] AAC(6')-Ib',[30] AAC(6')-IId,[32] and Eis[8] were expressed and purified as previously described. Herein, AAC(6')-Ie/APH(2")-Ia was studied solely for its AAC(6') activity and is referred to as AAC(6')-Ie throughout the manuscript. The *S. marcescens* genomic DNA used to clone AAC(3)-Ia was a gift from Dr. Paul H. Roy (Université Laval, QC, Canada). Primers for PCR were purchased from IDT (Coralville, IA). Ladders for DNA agarose gels as well as cloning enzymes, including Phusion DNA polymerase, restrictive endonucleases, and T4 DNA ligase were purchased from New England BioLabs (NEB; Ipswich, MA). The pET28a vector was purchased from Novagen (Gibbstown, NJ). TOP10 and BL21 (DE3) chemically competent *E. coli* cells

were purchased from Invitrogen (Carlsbad, CA). The Ni^{II}-NTA resin used for affinity chromatography was purchased from Qiagen (Valencia, CA). The AcCoA, DTDP, DTNB, all metal salts ($MgCl_2$, $CrCl_3$, CrO_3, $MnSO_4$, $CoCl_2$, $NiCl_2$, $NiSO_4$, $Cu(OAc)_2$, $Cu(NO_3)_2$, $CuSO_4$, $Zn(OAc)_2$, $ZnCl_2$, $ZnBr_2$, $ZnSO_4$, $CdCl_2$, $CdSO_4$, and $AuCl_3$), and the AGs AMK, GEN, and SIS were purchased from Sigma-Aldrich (Milwaukee, WI). The AGs KAN, NEO, NET, and TOB were purchased from AK Scientific (Mountain View, CA). 96-Well plates were purchased from Thermo Fisher Scientific (Waltham, MA). UV-Vis assays were monitored on a multimode SpectraMax M5 plate reader.

Previously identified bacterial strains were obtained from the ATCC, including *A. baumannii* ATCC 19606, *E. cloacae* ATCC 13047, and *K. pneumoniae* ATCC 27736. Clinical isolates of *A. baumannii* (isolates #75 and #81), *E. cloacae* (isolates #41, #52, and #61), and *K. pneumoniae* (isolates #22, #24, #34, and #44) were obtained from the microbiology laboratory at the University of Kentucky Hospital System. Known resistance profiles of the clinical isolates are presented in Table 3.5.

3.5.2. Cloning, overexpression, and purification of AAC(3)-Ia (NHis)

The *aac(3)-Ia* gene was PCR amplified from *S. marcescens* genomic DNA by using forward primer 5'-CGATACCATATGTTACGCAGCAGCAACGATG-3' and reverse primer 5'-TTGAACCTCGAGTTAGGTGGCGGTAC-3'. The amplified fragment was digested by using the *Nde*I and *Xho*I restriction enzymes (cut sites are underlined in the primer sequences) and ligated into the linearized pET28a vector. The ligated pAAC(3)-Ia-pET28a plasmid was transformed into *E. coli* TOP10 chemically competent cells for

plasmid replication and then into *E. coli* BL21 (DE3) chemically competent cells for protein overexpression. After confirmation of its DNA sequence, a fresh transformant of the pAAC(3)-Ia-pET28a plasmid was grown in LB broth (KAN 50 μg/mL) (3 L) at 37 °C with shaking at 200 rpm until the optical density at an attenuance of 600 nm reached 0.6. The protein expression was induced with 1 mM IPTG (final concentration). After induction, bacteria were kept growing overnight at 20 °C. The desired AAC(3)-Ia protein was then purified using Ni^{II}-NTA affinity column chromatography in 25 mM Tris-HCl pH 8.0 (adjusted at rt), 200 mM NaCl, and 10% glycerol with a gradient of imidazole (10 mL of 5 mM, 3 × 5 mL each of 20 mM, 40 mM and 200 mM). Pure fractions, as determined by SDS-PAGE (Figure 3.7), were dialyzed in Tris-HCl (50 mM, pH 8.0), NaCl (300 mM), and glycerol (10%), flash-frozen in liquid nitrogen and stored at -80 °C after concentrating using an Amicon (10,000 MWCO) ultra centrifugal filter cellulose protein concentrator. Protein purification yielded 0.5 mg of AAC(3)-Ia per L of culture.

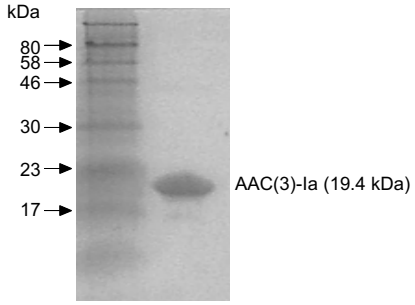

Figure 3.7. SDS-PAGE gel of $NHis_6$-tagged AAC(3)-Ia (19.4 kDa) purified by Ni^{II}-NTA chromatography.

3.5.3. Determination of inhibition of AAC enzymes by various metal salts

To determine the inhibition of various AACs by different metal salts, we performed UV-Vis assays in 96-well plates. Each reaction (200 μL) contained metal salts (1 mM), AGs

(100 μM), AcCoA (500 μM for Eis and 150 μM for all other AACs), indicator (DTNB or DTDP, 2 mM), and enzyme (0.5 μM for AAC(6') enzymes, AAC(3)-Ib, AAC(3)-Ia, and Eis or 0.125 μM for AAC(2')-Ic and AAC(3)-IV) in the appropriate buffer (100 mM K_2HPO_4 for AAC(2')-Ic, 50 mM Tris-HCl pH 8.0 for Eis, 50 mM MES pH 6.6 for AAC(3)-Ia, AAC(3)-Ib, AAC(3)-IV, and AAC(6')-Ie, and 50 mM HEPES pH 7.5 for AAC(6')-Ib' and AAC(6')-IId). The pH of all buffers was adjusted at rt. Reactions were carried out at 25 °C for all enzymes except for AAC(6')-Ie where reactions were performed at 37 °C. DTNB was used to monitor reaction progress with all enzymes, except with AAC(6')-Ib' and AAC(6')-IId where DTDP was used. Reactions containing DTDP were monitored at 324 nm (ε = 19,800 $M^{-1}cm^{-1}$) and those containing DTNB were monitored at 412 nm (ε = 14,150 $M^{-1}cm^{-1}$). Absorbance was recorded every 30 s for 20 min. Enzyme activities were determined by calculating the initial reaction rates using the first 2-5 min of the reaction (Figures 3.2 and 3.3, and Table 3.1). NEO and TOB are not substrates of AAC(3)-Ia and AAC(3)-Ib. In addition, NET is not a substrate of AAC(3)-Ib. Therefore, these AGs were not tested with the two AAC(3)s listed above. All experiments were performed in triplicate.

3.5.4. Determination of potential inhibition mechanism using EDTA

To investigate whether the inhibition of various AACs by different metal ions is reversible and establish whether AAC enzyme activity could be restored by sequestering the metal ions from the reactions, we performed assays with EDTA, which served as a strong metal ion scavenger. Reactions (200 μL) contained metal salt (1 mM), AG (100 μM), AcCoA (150 μM), DTNB (2 mM), EDTA (2 μM, pH 8.0), and AAC(3)-Ib (0.5 μM) or AAC(3)-IV (0.125 μM). Reactions were carried out in 50 mM MES pH 6.6. The AAC(3)-Ib enzyme

was tested with SIS and the metal salts $Cu(OAc)_2$, $ZnCl_2$, and $AuCl_3$. AAC(3)-IV was tested with TOB and the salts $Cu(OAc)_2$, $ZnCl_2$, $CdSO_4$, and $AuCl_3$. After the addition of the enzyme, the absorbance of each reaction was recorded every 30 s for 20 min (Figure 3.5). All reactions were performed in triplicate. Three control reactions were performed in which the following components were lacking: (i) EDTA (which represented the inhibited reactions), (ii) EDTA and metal salts (which represented the standard *N*-acetylation reactions of AGs by AACs to which all other reactions were compared in this study), and (iii) EDTA and AGs (which showed that the metal salts did not interfere with the assay conditions).

3.5.5. Inhibition of AACs by metal salts at near physiological salt concentration

To establish if the metal inhibition of AACs is unaffected by the salt concentration found physiologically, experiments were performed in the presence of 100 mM NaCl. Experiments with Cu^{2+} and Zn^{2+} were performed as above for each enzyme, except for Eis as its activity is inhibited in the presence of salt, and therefore, was not tested with NaCl. AAC(6')-Ib' and AAC(6')-IId were not tested with the Cu^{2+} salts in the presence of NaCl due to solubility issues. Results of these control experiments are presented in Figures 3.2 and 3.3.

3.5.6. Determination of IC_{50} values by UV-Vis assays

For selected metal salts that showed complete inhibition of the AAC activities against certain AGs, we determined the IC_{50} values in combination with the corresponding AGs. Assays were performed in 96-well plates with DTNB or DTDP as indicators for specific

enzymes as described above. The metal salts were dissolved in appropriate buffers (100 μL) for each enzyme and a five-fold dilution was performed, making the final concentration of the metal salts range from 2.6 pM to 1 mM in the assay. AG and enzyme in buffer (50 μL) were then added into each well and incubated for 10 min to allow potential positioning or binding of the substrate and/or inhibitor into the enzyme active site. Reactions were then initiated by the addition of AcCoA and indicator (50 μL). Reactions with AAC(6')-Ie were performed at 37 °C. All other enzymatic reactions were performed at 25 °C. Absorbance at 412 nm (for DTNB) or 324 nm (for DTDP) was recorded every 30 s for 20 min. Initial rates of reaction were calculated using the first 10 min of the reaction and expressed as a percentage of the rate of the reaction containing no metal salt inhibitors. IC_{50} values were then calculated using a Hill plot fit with KaleidaGraph 4.1. Experiments were performed in duplicate or triplicate. The data with standard errors are summarized in Table 3.2 and a sample graph for the IC_{50} value of $AuCl_3$ against Eis with NET is presented in Figure 3.4.

3.5.7. Identification of AMEs in twelve bacterial strains

To determine the AME genes present in each of the twelve bacterial strains selected (three strains of *A. baumannii*, four of *E. cloacae*, and five of *K. pneumoniae*), colonies were picked and subjected to PCR analysis. Primer probes used for the *aac(6')-Ib*, *aac(3)-IV*, *ant(2'')-Ia*, and *aph(3')-Ia* genes were as previously reported.[33] An initial 5 min at 95 °C was used to lyse the bacterial cells and denature the DNA. For 35 cycles the samples were subjected to 2 min at 95 °C, 1 min at 58 °C, and 1 min at 72 °C. After the 35 cycles, the reactions were held at 72 °C for 10 min and then analyzed on a 1.5% agarose gel. Expected

band sizes were 482 bp (*aac(6')-Ib*), 230 bp (*aac(3)-IV*), 534 bp (*ant(2")-Ia*), and 624 bp (*aph(3')-Ia*) (Figure 3.6).

3.5.8. Determination of MIC values for combinations of metals and AGs

MIC values were determined using the double-microdilution method. Various concentrations of AGs were combined with different concentrations of ZnPT (0-80 μM) and bacteria were grown for 16 h prior to MIC value determination. The AG concentrations used varied with each bacterial strain as follow: AMK (0.06-32 μg/mL) with *A. baumannii* ATCC 19606, (0.25-128 μg/mL) with #75, (0.015-8 μg/mL) with #81, (0.063-16 μg/mL) with *E. cloacae* ATCC 13047, (0.015-8 μg/mL) with #41, (0.004-2 μg/mL) with #52, (0.015-8 μg/mL) with #61, (0.031-16 μg/mL) with *K. pneumoniae* ATCC 27736, (0.125-64 μg/mL) with #22, (0.031-16 μg/mL) with #24, (0.004-2 μg/mL) with #34, and (0.031-16 μg/mL) with #44; TOB (0.031-16 μg/mL) with *A. baumannii* ATCC 19606, (0.015-8 μg/mL) with #75, (0.004-2 μg/mL) with #81, (0.008-4 μg/mL) with *E. cloacae* ATCC 13047, (0.015-8 μg/mL) with #41, (0.015-8 μg/mL) with #52, (0.015-8 μg/mL) with #61, (0.031-16 μg/mL) with *K. pneumoniae* ATCC 27736, (0.25-128 μg/mL) with #22, (0.25-128 μg/mL) with #24, (0.0006-0.3 μg/mL) with #34, and (0.25-128 μg/mL) with #44. For combinational studies, the concentration of AGs was varied horizontally on the plate, while the metal concentration was varied vertically on the plate. Observed bactericidal concentrations were then compared to that of AG or ZnPT (Tables 3.3 and 3.4).

3.6. ACKNOWLEDGEMENTS

This work was supported by start-up funds from the College of Pharmacy at the University of Kentucky (S.G.-T) and by a National Institutes of Health (NIH) Grant AI090048 (S.G.-T.). We thank Vanessa R. Porter for preliminary cloning of AAC(3)-Ia.

This chapter is adapted from my published article (under my previous maiden name Yijia Li) referenced as Li, Y.; Green, K. D.; Johnson, B. R.; Garneau-Tsodikova, S. Inhibition of aminoglycoside acetyltransferase resistance enzymes by metal salts. *Antimicrob. Agents and Chemother.* **2015,** *59* (7), 4148-56.

3.7. AUTHORS' CONTRIBUTIONS

Y.L. performed most of the UV-Vis assays, wrote up the manuscript, and later modified this manuscript into dissertation chapter. B.R.J. performed part of the UV-Vis assay, IC_{50} assay, and EDTA chelation assay. K.D.G. performed part of the UV-Vis assays and all of PCR probing for AMEs, MIC assays, and combination assay. S.G.-T. contributed in the study design and write-up of manuscript and later proof-reading the formatted dissertation chapter.

Chapter 4. Nucleoside triphosphate cosubstrates control the substrate profile and efficiency of aminoglycoside 3'-*O*-phosphotransferase type IIa

Aminoglycosides (AGs) are broad-spectrum antibiotics that play an important role in the control and treatment of bacterial infections. Despite the great antibacterial potency of AGs, resistance to these antibiotics has been limiting their clinical applications. The AG 3'-*O*-phosphotransferase of type IIa (APH(3')-IIa) encoded by the *neo*^{R} gene is a common bacterial AG resistance enzyme that inactivates AG antibiotics. This enzyme is used as a selection marker in molecular biology research. APH(3')-IIa catalyzes the transfer of the γ-phosphoryl group of ATP to an AG at its 3'-OH group. Although APH(3')-IIa has been reported to utilize exclusively ATP as a cosubstrate, we demonstrate that this enzyme can utilize a broad array of NTPs. By substrate profiling, TLC, and enzyme kinetics experiments, we probe AG phosphorylation by APH(3')-IIa with an extensive panel of substrates and cosubstrates (13 AGs and 10 NTPs) for the purpose of gaining a thorough understanding of this resistance enzyme. We find, for the first time, that the identity of the NTP cosubstrate dictates the set the AGs modified by APH(3')-IIa and the phosphorylation efficiency for different AGs.

4.1. INTRODUCTION

The 2-deoxystreptamine aminoglycosides (2-DOS AGs, Figure 4.1A) are broad-spectrum antibiotics that display excellent potency against Gram-positive and Gram-negative bacteria as well as *Mycobacteria*.[1-4] As one of the most effective weapons in the combat against bacterial infections, these aminocyclic sugars are classified as 4,5- or 4,6-disubstituted AGs based on the positions of substitution on the 2-DOS core.[5] In the U.S.A.,

amikacin (AMK), gentamicin (GEN), and tobramycin (TOB) are administered systemically.[6] European countries also employ netilmicin (NET) and sisomicin (SIS) in their antibacterial regimens.[7] Kanamycin (KAN) is used globally against drug-resistant *M. tuberculosis* infections. In addition to their use as antibiotics, AGs have been widely explored as therapeutic options for premature termination codon (PTC) diseases for the ability of these drugs to promote readthrough of a PTC to allow biosynthesis of functional full-length proteins.[8-12]

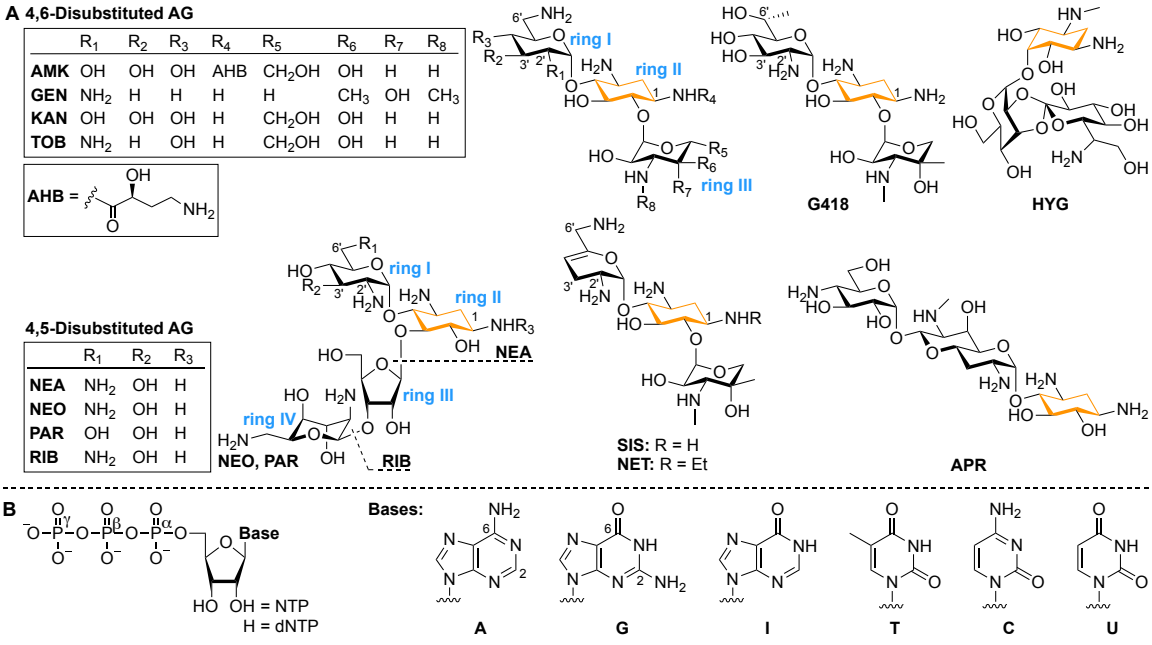

	R_1	R_2	R_3	R_4	R_5	R_6	R_7	R_8
AMK	OH	OH	OH	AHB	CH_2OH	OH	H	H
GEN	NH_2	H	H	H	H	CH_3	OH	CH_3
KAN	OH	OH	OH	H	CH_2OH	OH	H	H
TOB	NH_2	H	OH	H	CH_2OH	OH	H	H

	R_1	R_2	R_3
NEA	NH_2	OH	H
NEO	NH_2	OH	H
PAR	OH	OH	H
RIB	NH_2	OH	H

Figure 4.1. Structures of **A.** AGs with their 2-DOS core highlighted in orange, and **B.** (d)NTPs used in this chapter.

Unfortunately, incorrect or non-compliant use of antibiotics or overuse of certain antibiotics gave rise to one of the greatest global health threats: antibiotic resistance. Bacteria can acquire resistance to AG antibiotics *via* three mechanisms: by changing the cell wall composition, modifying the antibiotic target (in this case the ribosome), and

acquiring or upregulating AG-modifying enzymes (AMEs).[13] AMEs represent the prevalent mechanism of AG resistance. AMEs are represented by three types of enzymes, each catalyzing a distinct chemistry: AG *N*-acetyltransferases (AACs), AG *O*-nucleotidyltransferases (ANTs), and AG *O*-phosphotransferases (APHs).[14] APHs transfer a phosphoryl group from an NTP (Figure 4.1B) onto a specific OH group of an AG yielding a phosphorylated AG and an NDP.[15-16] This transfer occurs with the regiospecificity dictated by the specific class of the APH indicated in the enzyme name according to the AME nomenclature. Such phosphorylation abrogates AG binding to the ribosome, making the bacteria highly resistant to that AG.

Harnessing their AG resistance function, researchers have been using APH enzymes as antibiotic selection markers in recombinant DNA technology. A subject of the present study, APH(3')-IIa, encoded by the neomycin resistance (*neo*^{R}) gene *aph(3')-IIa*, has been used as an AG resistance marker in molecular biology for decades, providing robust selection in AG-containing media.[17-19]

A key issue to considering AGs as therapies or genetic selection tools is their modification by APHs. Therefore, a systematic investigation of the substrate-cosubstrate profile of APH enzymes is necessary. As indicated by the nomenclature, APH(3')-IIa and other APH(3') enzymes phosphorylate AGs at their 3'-OH group. A partial AG substrate profile of APH(3')-IIa was previously reported.[20-21] It was previously reported that APH(3')-IIa used exclusively ATP, whereas another APH(3') enzyme, APH(3')-Ia, also transferred a phosphate from GTP.[22] In fact, GTP was used in some *in vitro* studies of these enzymes.[22-

[26] In contrast to APH(3'), some APH(2") enzymes, such as APH(2")-Ia,[27] APH(2")-If,[28] and APH(2")-IIIa[27], showed a clear preference for GTP. The study of APH(3')-IIa described herein addresses the enzyme activity for different substrate-cosubstrate pairs in order to help us better understand this resistance enzyme.

4.2. RESULTS AND DISCUSSION

4.2.1. Determination of AG profile of APH(3')-IIa with various NTPs

To examine whether and if so, how different NTPs may dictate the AG substrate profile of APH(3')-IIa, we measured its AG phosphorylation activity by a well-established UV-Vis assay. In this assay, we monitored the conversion of NADH to NAD^+ by lactate dehydrogenase (LDH) coupled with pyruvate kinase (PK), converting the NDP coproduct of the AG phosphorylation back to NTP (Figure 4.2).[20, 22, 26, 29] We tested 13 AGs (AMK, apramycin (APR), GEN, geneticin (G418), hygromycin (HYG), KAN, neamine (NEA), neomycin B (NEO), NET, paromomycin (PAR), ribostamycin (RIB), SIS, and TOB) along with 9 NTPs (ATP, dATP, GTP, dGTP, UTP, dUTP, dCTP, TTP, and ITP). Due to the lack of a commercially available CTP of sufficient purity for this assay, we had to exclude CTP from our assay. In addition to ATP, we found APH(3')-IIa to use 7 out of the 9 (d)NTPs tested as cosubstrates. We discovered that purine-containing NTPs generally supported phosphorylation of a larger number of AGs than did pyrimidine-containing NTPs. When ATP was used as a cosubstrate, APH(3')-IIa phosphorylated 7 AGs (AMK, G418, KAN, NEA, NEO, PAR, and RIB), amongst which PAR and RIB have not been reported previously (Table 4.1). Interestingly, when using GTP as a cosubstrate, we noticed that while KAN, NEA, NEO, PAR, and RIB could be readily phosphorylated by APH(3')-

IIa, the enzyme displayed a much lower activity for G418 and no activity for AMK. Among the purine-containing NTPs, ITP supported the narrowest AG profile, with only NEA, NEO, PAR, and RIB being efficiently phosphorylated. It was also notable that KAN, while being efficiently phosphorylated with ATP or GTP as cosubstrates, was a poor substrate when the enzyme was provided with ITP.

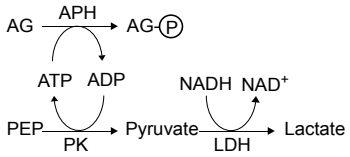

Figure 4.2. Schematic of the coupled UV-Vis assay used in this study for determination of substrate and cosubstrate profiles and kinetics.

Table 4.1. AG substrate profile of APH(3')-IIa with various (d)NTPs.

	AMK	APR	GEN	G418	HYG	KAN	NEA	NEO	NET	PAR	RIB	SIS	TOB
ATP	✓	✗	✗	✓	✗	✓	✓	✓	✗	✓	✓	✗	✗
GTP	✗	✗	✗	--	✗	✓	✓	✓	✗	✓	✓	✗	✗
UTP	✗	✗	✗	✗	✗	--	✓	✓	✗	✓	✓	✗	✗
ITP	✗	✗	✗	✗	✗	--	✓	✓	✗	✓	✓	✗	✗
dATP	--	✗	✗	✓	✗	✓	✓	✓	✗	✓	✓	✗	✗
dGTP	--	--	✗	✓	--	✓	✓	✓	✗	✓	✓	✗	✗
dCTP	✗	✗	✗	✗	✗	✗	--	--	✗	--	--	✗	✗
dUTP	✗	✗	✗	✗	✗	✓	✓	✓	✗	✓	--	✗	✗
TTP	✗	✗	✗	✗	✗	✗	--	--	✗	--	--	✗	✗

✓ = Absorbance at 340 nm > 0.1, -- = Absorbance at 340 nm between 0.05-0.1, ✗ = Absorbance at 340 nm < 0.05.

Even though UTP was a pyrimidine-containing NTP, potentially interacting suboptimally with the base binding site compared to a purine-containing NTP, such as ITP, the AG substrate profile for UTP was identical to that observed for ITP. These observations indicate that different perturbations of base structure and size can have similar effects of limiting the substrate profile.

To test the effect of the 2'-OH group on the ribose ring, we compared the AG profiles for NTP and dNTP as cosubstrates. We found that the AG profiles of the enzyme were similar

for dATP and ATP, dGTP and GTP, and dUTP and UTP. As one minor exception, with dUTP the enzyme was slightly more active with KAN and slightly less active with RIB than with UTP. We found that the dNTPs that were cosubstrates for the most limited sets of AGs were dCTP and TTP (note that TTP naturally contains a deoxyribose sugar). This was not surprising since both dNTPs contained a monocyclic base that may not engage optimally with the enzyme NTP binding site.

4.2.2. Thin-layer chromatography

In order to visualize directly the phosphoryl transfer activity of APH(3')-IIa, we performed TLC experiments (Table 4.2 and Figures 4.3 and 4.4). We first used ATP as a representative cosubstrate and carried out reactions with all 13 AGs. For the AGs that were observed to be modified by the UV-Vis assay, we made two time-point observations, at 2 h and at 24 h. For the other AGs, we quenched the reactions only after 24 h. For each AG, we also included an AG substrate standard as well as a full reaction that we quenched immediately after initiating it (time 0) to confirm that the reaction conditions did not interfere with AG migration on TLC plates.

Table 4.2. Summary of TLC results based on whether each AG was phosphorylated by various (d)NTPs with APH(3')-IIa enzyme.

	AMK	APR	GEN	G418	HYG	KAN	NEA	NEO	NET	PAR	RIB	SIS	TOB
ATP	✓	✗	✗	✓	✗	✓	✓	✓	✗	✓	✓	✗	✗
GTP	✓	✗	✗	✗	✗	✓	✓	✓	✗	✓	✓	✗	✗
CTP	p	✗	✗	✗	✗	✓	✓	✓	✗	✓	✓	✗	✗
UTP	✓	✗	✗	✗	✗	✓	✓	✓	✗	✓	✓	✗	✗
ITP	✓	✗	✗	✗	✗	✓	✓	✓	✗	✓	✓	✗	✗
dATP	✓	✗	✗	✓	✗	✓	✓	✓	✗	✓	✓	✗	✗
dGTP	p	✗	✗	✓	✗	p	✓	✓	✗	✓	✓	✗	✗
dCTP	✗	✗	✗	✗	✗	✓	✓	✓	✗	✓	✓	✗	✗
TTP	✓	✗	✗	✓	✗	✓	✓	p	✗	✓	✓	✗	✗
dUTP	✗	✗	✗	✓	✗	✓	✓	✓	✗	✓	✓	✗	✗

✓ = phosphorylated, p = partially phosphorylated, ✗ = not phosphorylated.

Upon the enzymatic modification of the AGs that were previously found to be accepted by the enzyme as a substrate (AMK, G418, KAN, NEA, NEO, PAR, and RIB) we observed product species with significantly larger R_f values than those of the respective substrates. The AGs that were not observed to be substrates by the UV-Vis assay (APR, GEN, HYG, NET, SIS, and TOB) did not display a shift in their R_f values after enzymatic reactions. These AGs were either highly structurally distinct (APR, HYG) or they did not contain a 3'-OH group (GEN, NET, SIS and TOB). These observations were in agreement with the AG phosphorylation results obtained by the UV-Vis assay.

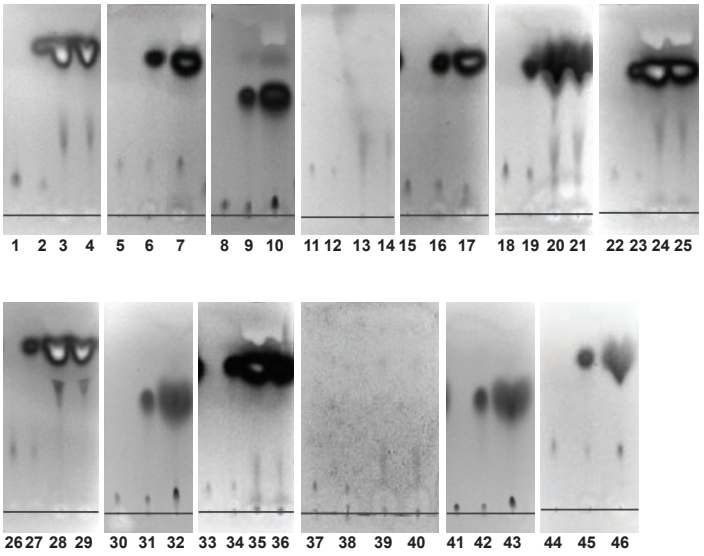

Lane	AG	Time (h)	R_f	Lane	AG	Time (h)	R_f
1	AMK	-	0.17	**26**	NEO	-	0.29
2		0	0.17	**27**		0	0.29
3		2	0.37	**28**		2	0.62
4		24	0.38	**29**		24	0.62
5	APR	-	0.24	**30**	NET	-	0.07
6		0	0.24	**31**		0	0.07
7		24	0.25	**32**		24	0.09
8	GEN	-	0.06	**33**	PAR	-	0.12
9		0	0.05	**34**		0	0.12
10		24	0.06	**35**		2	0.21
11	G418	-	0.22	**36**		24	0.21
12		0	0.22	**37**	RIB	-	0.11
13		2	0.33	**38**		0	0.11
14		24	0.33	**39**		2	0.26
15	HYG	-	0.15	**40**		24	0.26
16		0	0.15	**41**	SIS	-	0.02
17		24	0.13	**42**		0	0.03
18	KAN	-	0.18	**43**		24	0.05
19		0	0.19	**44**	TOB	-	0.30
20		2	0.27	**45**		0	0.29
21		24	0.27	**46**		24	0.28
22	NEA	-	0.19				
23		0	0.19				
24		2	0.37				
25		24	0.38				

Figure 4.3. Pictures of TLC plates of APH(3')-IIa reacting with ATP and various AGs as well as the corresponding R_f values for each lane.

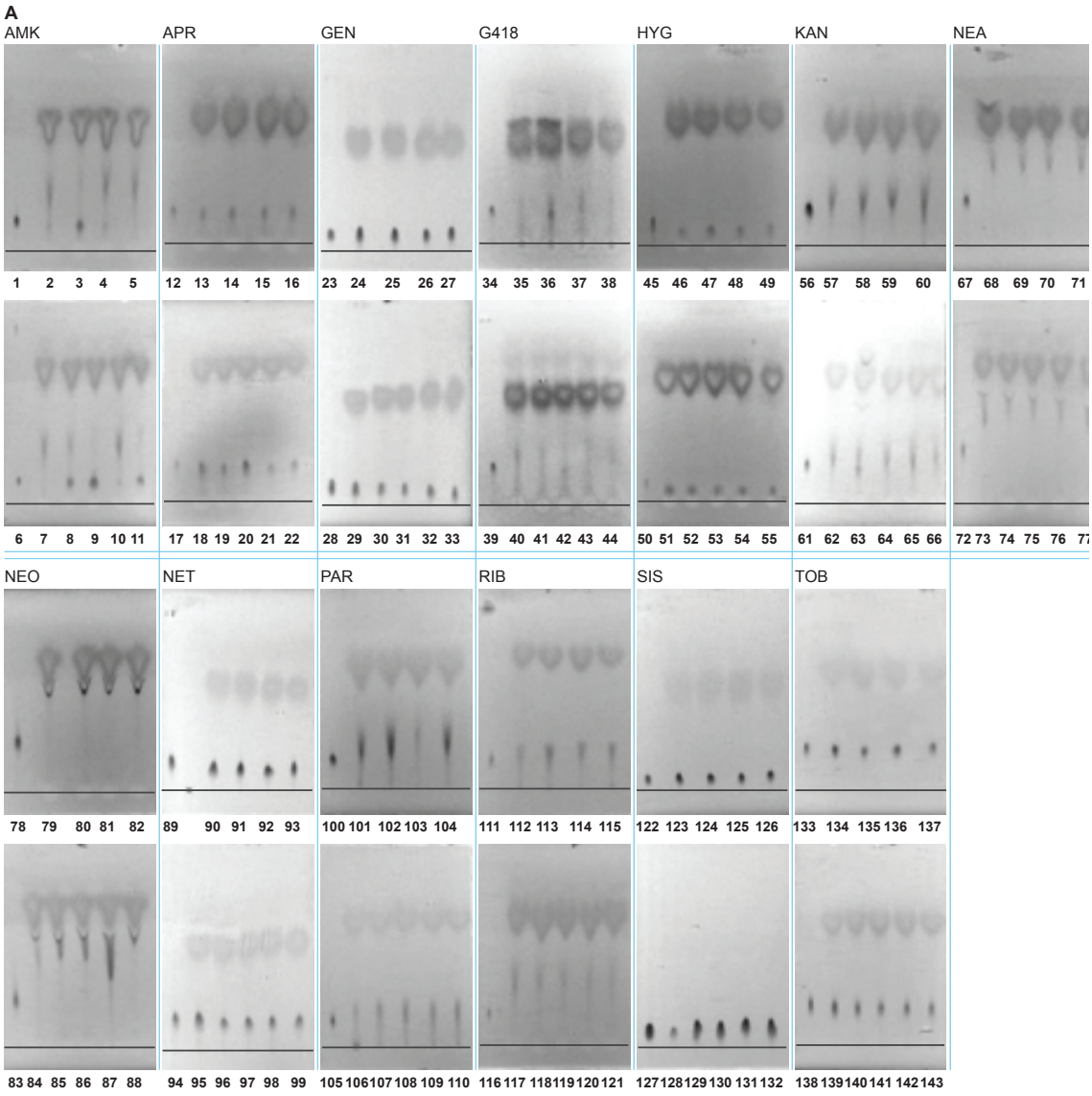

Figure 4.4A. Pictures of TLC plates of APH(3')-IIa reacting with various (d)NTPs and AGs. The corresponding R_f values for each lane are listed in Figure 4.4B presented on next page. *Note*: TLC images with ATP and the corresponding R_f values are summarized in Figure 4.3.

B

Lane	AG	NTP	R_f	Lane	AG	NTP	R_f	Lane	AG	NTP	R_f	Lane	AG	NTP	R_f	Lane	AG	NTP	R_f
1	AMK	-	0.17	34	G418	-	0.17	67	NEA	-	0.27	100	PAR	-	0.15	133	TOB	-	0.29
2		GTP	0.32	35		GTP	0.17	68		GTP	0.57	101		GTP	0.20	134		GTP	0.29
3		CTP	0.15, 0.38	36		CTP	0.17	69		CTP	0.57	102		CTP	0.22	135		CTP	0.62
4		UTP	0.33	37		UTP	0.19	70		UTP	0.57	103		UTP	0.24	136		UTP	0.62
5		ITP	0.33	38		ITP	0.22	71		ITP	0.57	104		ITP	0.22	137		ITP	0.07
6		-	0.11	39		-	0.17	72		-	0.20	105		-	0.14	138		-	0.07
7		dATP	0.31	40		dATP	0.26	73		dATP	0.50	106		dATP	0.20	139		dATP	0.09
8		dGTP	0.11, 0.33	41		dGTP	0.28	74		dGTP	0.52	107		dGTP	0.20	140		dGTP	0.12
9		dCTP	0.11	42		dCTP	0.17	75		dCTP	0.52	108		dCTP	0.22	141		dCTP	0.12
10		TTP	0.31	43		TTP	0.26	76		TTP	0.51	109		TTP	0.20	142		TTP	0.21
11		dUTP	0.11	44		dUTP	0.26	77		dUTP	0.45	110		dUTP	0.20	143		dUTP	0.21
12	APR	-	0.18	45	HYG	-	0.13	78	NEO	-	0.30	111	RIB	-	0.15				
13		GTP	0.18	46		GTP	0.10	79		GTP	0.58	112		GTP	0.21				
14		CTP	0.18	47		CTP	0.10	80		CTP	0.58	113		CTP	0.26				
15		UTP	0.18	48		UTP	0.10	81		UTP	0.58	114		UTP	0.26				
16		ITP	0.15	49		ITP	0.10	82		ITP	0.58	115		ITP	0.02				
17		-	0.19	50		-	0.08	83		-	0.25	116		-	0.03				
18		dATP	0.19	51		dATP	0.06	84		dATP	0.55	117		dATP	0.05				
19		dGTP	0.19	52		dGTP	0.06	85		dGTP	0.55	118		dGTP	0.30				
20		dCTP	0.18	53		dCTP	0.06	86		dCTP	0.55	119		dCTP	0.29				
21		TTP	0.18	54		TTP	0.08	87		TTP	0.20, 0.56	120		TTP	0.28				
22		dUTP	0.18	55		dUTP	0.08	88		dUTP	0.58	121		dUTP	0.18				
23	GEN	-	0.08	56	KAN	-	0.21	89	NET	-	0.16	122	SIS	-	0.08				
24		GTP	0.08	57		GTP	0.25	90		GTP	0.15	123		GTP	0.08				
25		CTP	0.08	58		CTP	0.25	91		CTP	0.15	124		CTP	0.08				
26		UTP	0.09	59		UTP	0.27	92		UTP	0.15	125		UTP	0.09				
27		ITP	0.09	60		ITP	0.27	93		ITP	0.16	126		ITP	0.09				
28		-	0.09	61		-	0.19	94		-	0.18	127		-	0.09				
29		dATP	0.09	62		dATP	0.28	95		dATP	0.18	128		dATP	0.09				
30		dGTP	0.09	63		dGTP	0.28	96		dGTP	0.20	129		dGTP	0.09				
31		dCTP	0.09	64		dCTP	0.19, 0.26	97		dCTP	0.18	130		dCTP	0.09				
32		TTP	0.09	65		TTP	0.26	98		TTP	0.17	131		TTP	0.09				
33		dUTP	0.09	66		dUTP	0.26	99		dUTP	0.17	132		dUTP	0.09				

Figure 4.4B. R_f values for each lane of TLC sample listed in Figure 4.4A presented on the previous page. *Note*: TLC images with ATP and the corresponding R_f values are summarized in Figure 4.3.

As the UV-Vis assay relies on the activity of a coupled enzyme, PK, for conversion of the NDP product back to the respective NTP, the inability to observe activity by this assay for some nucleotides could be due to the NDP specificity of PK, and not APH(3')-IIa. Therefore, we performed TLC with the rest of NTP cosubstrates (24 h time point only, Table 4.2 and Figure 4.4). As expected, we found that for all the cosubstrates that were shown to support phosphorylation by the UV-Vis assay, the reaction was also observed by TLC. In addition, we observed that APH(3')-IIa transferred a phosphoryl group from CTP (not tested in previous UV-Vis substrate profile assays) as well as dCTP and TTP, indicating that the minimal UV-Vis signal from the coupled enzyme assay was due to PK not accepting dCDP and TDP as substrates. Indeed, we did not observe the activity of PK when we tested this enzyme with dCDP and TDP in the absence of APH(3')-IIa and AG. Furthermore, we observed phosphorylation of AGs in some AG-NTP combinations where

no phosphorylation was observed previously in substrate profiling experiment, including AMK with GTP, UTP, ITP, dATP, and dGTP (partial), G418 with dUTP, and KAN with UTP and ITP. This likely occurred due to the much higher reactant and enzyme concentrations as well as a longer reaction time used in the TLC assays.

4.2.3. Determination of enzyme kinetics by UV-Vis assays

To characterize quantitatively the reaction kinetics for different substrates and cosubstrates, we determined the Michaelis-Menten kinetic parameters (K_m and k_{cat}) for APH(3')-IIa with respect to representative AGs using ATP, GTP, and UTP as cosubstrates at a fixed saturating concentration (2 mM). We chose NEO and KAN as representative 4,5- and 4,6-disubstituted AGs, as they were shown to be good substrates for most NTP cosubstrates. We also selected the 4,6-disubstituted AGs AMK and G418, because APH(3')-IIa displayed the highest variation in its phosphorylation activity with these AGs among different NTPs as cosubstrates. Because APH enzymes characterized to date follow either an ordered sequential mechanism, where the NTP binds the enzyme prior to the AG, or a random sequential mechanism,[15] K_m in these experiments can be interpreted in terms of the binding affinity of the AG to the enzyme-NTP complex.

We found that with ATP as a cosubstrate, APH(3')-IIa displayed the highest affinity for KAN with a K_m value of 3.1 ± 0.9 μM (Table 4.3 and Figure 4.5). Of note, even though APH(3')-IIa is often referred to as the product of the *neo*^{R} gene, the K_m value for NEO is nearly 6-fold higher, 17 ± 4 μM. APH(3')-IIa displayed similar maximum turnover rates of phosphorylation of NEO and KAN (k_{cat} = 49 ± 3 min^{-1} and 34 ± 2 min^{-1}, respectively). As

a result, when using ATP as a cosubstrate, the enzyme was found to be more efficient with KAN ($k_{cat}/K_m = 11 \pm 3$ min^{-1}μM^{-1}) than with NEO ($k_{cat}/K_m = 2.9 \pm 0.7$ min^{-1}μM^{-1}). APH(3')-IIa showed much lower binding affinities for G418 ($K_m = 113 \pm 12$ μM) and AMK ($K_m = 1040 \pm 260$ μM) than for NEO and KAN. A likely structural explanation for the lack of affinity for AMK and G418 is that the bulky substitutions, such as the (*S*)-4-amino-2-hydroxybutyryl (AHB) group at the 1-position of AMK might not fit well into the substrate binding pocket (Figure 4.7A). The 6'-amino group of KAN and presumably NEO is bound in a negatively-charged environment of the C-terminal carboxyl group, Asp154 and Asp157. G418 does not contain a 6'-amino group, lacking a positive charge at this position. In addition, the 3"-amino group of G418 is methylated and does not bear a positive charge, unlike its non-methylated counterpart in KAN and NEO. This amino group in KAN is in a negatively-charged environment of Glu230 (Figure 4.7A). The absence of positive charges at 6'- and 3"-positions in G418 is predicted to disfavor its binding. Despite the drastically higher K_m values, the maximum turnover rates for G418 ($k_{cat} = 89 \pm 3$ min^{-1}) and AMK ($k_{cat} = 51 \pm 7$ min^{-1}) were found to be comparable to those for NEO and KAN, indicating that the geometry of the phosphoryl transfer reaction was unchanged. Consequently, the catalytic efficiencies of the enzyme with AMK ($k_{cat}/K_m = 0.049 \pm 0.014$ min^{-1}μM^{-1}) and G418 ($k_{cat}/K_m = 0.79 \pm 0.09$ min^{-1}μM^{-1}) were lower than with NEO and KAN.

Table 4.3. Kinetic parameters of APH(3')-IIa with respect to AGs.

AG	NTP	K_m (μM)	k_{cat} (min^{-1})	k_{cat}/K_m (min^{-1}μM^{-1})
KAN	ATP	3.1 ± 0.9	34 ± 2	11 ± 3
	GTP	69 ± 9	6.3 ± 0.3	0.09 ± 0.01
	UTP	40 ± 6	2.8 ± 0.1	0.07 ± 0.01
NEO	ATP	17 ± 4	49 ± 3	2.9 ± 0.7
	GTP	23 ± 5	43 ± 2	1.9 ± 0.4
	UTP	5.4 ± 1.1	10.0 ± 0.4	1.9 ± 0.4
G418	ATP	113 ± 12	89 ± 3	0.79 ± 0.09
	GTP	2,172 ± 732	12 ± 2	0.006 ± 0.002
AMK	ATP	1,040 ± 260	51 ± 7	0.05 ± 0.01

Interestingly, when we switched the cosubstrate from ATP to GTP, we observed a change in the AG binding preference. With GTP, APH(3')-IIa had the highest affinity for NEO (K_m = 23 ± 5 μM), which was similar to that observed with ATP. Furthermore, the enzyme turnover and overall efficiency (k_{cat} = 43 ± 2 min^{-1} and k_{cat}/K_m = 1.9 ± 0.4 $min^{-1}\mu M^{-1}$) were similar to those observed with ATP as the cosubstrate. These observations indicate that GTP binds the enzyme and acts as a phosphoryl donor similarly to ATP in the presence of NEO. With GTP, the enzyme had a much weaker, 20-fold lower affinity for KAN (K_m = 69 ± 9 μM) than it did with ATP (see next section for structural rationale). GTP also had a deleterious (6-fold) effect on the maximum turnover rate of phosphoryl transfer from GTP to KAN: k_{cat} = 6.3 ± 0.3 min^{-1}. It is possible that the dissociation of GDP, if rate limiting, as observed for APH(3')-IIIa,[30-31] was slower than that of ADP. The different k_{cat} values for the same AG and different NTP cosubstrates can be rationalized as a consequence of minor shifts in the positioning and orientation of the γ-phosphate of different NTPs, the differences in K_m values suggest that an allosteric effect of these small changes on interactions of the AG with the enzyme.

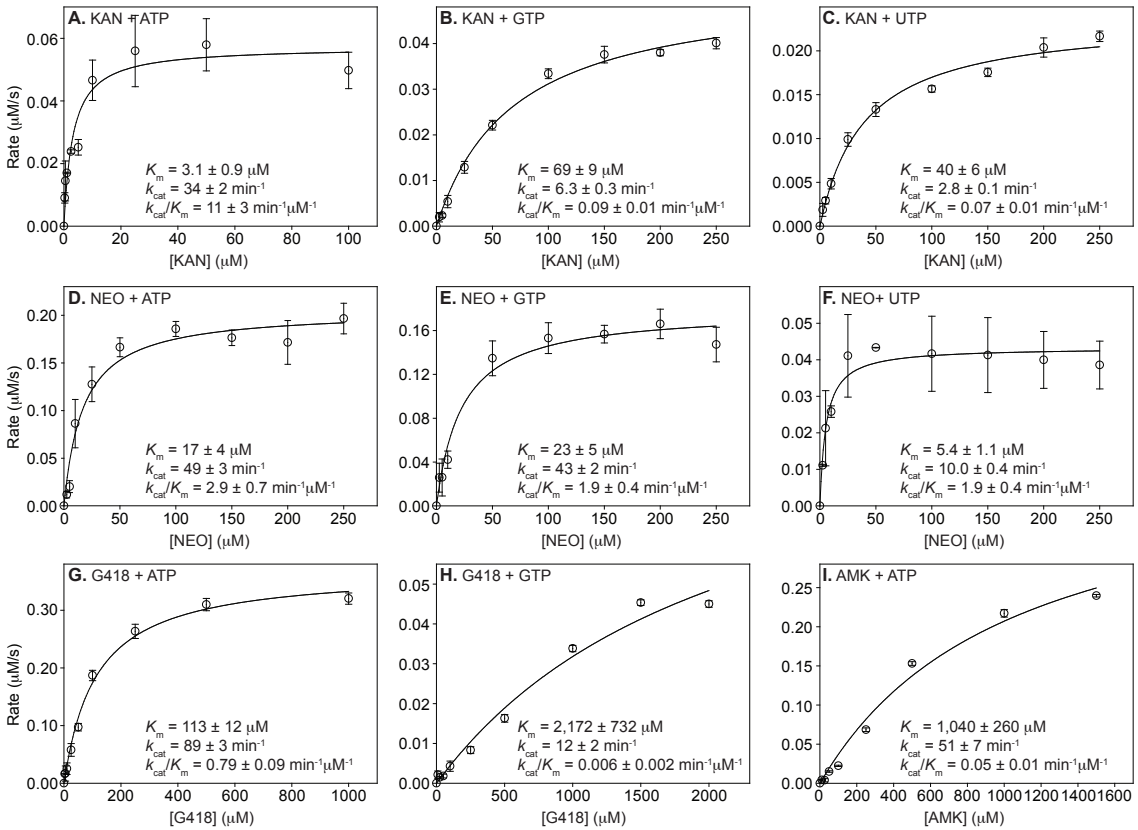

Figure 4.5. Michaelis-Menten graphs with the determined kinetics parameters of APH(3')-IIa with various AG substrates and NTP cosubstrates.

When GTP was used as a cosubstrate with G418, the K_m value for G418 was 20-fold higher (K_m = 2172 ± 732 μM) than that measured with ATP as a cosubstrate, indicating that G418 was a poor substrate for this enzyme. With the much larger K_m and smaller k_{cat} (12 ± 2 min^{-1}) values, the catalytic efficiency for G418 with GTP became more than 100-fold smaller than that with ATP as a cosubstrate (k_{cat}/K_m = 0.006 ± 0.002 min^{-1}μM^{-1}). Phosphoryl transfer from GTP to AMK was below the detection limit. This again indicated that the minor chemical differences in NTP transmit to both the catalytic center and the AG binding pocket. Overall, these kinetic measurements were consistent with those observed during the substrate profile determination (Table 4.1).

When we explored the enzyme kinetics for UTP as a cosubstrate, we found that APH(3')-IIa displayed higher binding affinity and lower turnover rates than with GTP for both KAN and NEO, which resulted in similar overall catalytic efficiencies to those observed with GTP. It is possible that the pyrimidine base of UTP, while having a favorable allosteric effect on the AG binding site, resulted in a slower dissociation of UDP. Alternatively, the change from a purine to a pyrimidine base may have resulted in slight mispositioning of the γ-phosphate group, slowing the phosphoryl transfer step. APH(3')-IIa did not accept G418 and AMK as substrates when UTP was used.

The underlying assumption of these kinetic measurements is that the observed coupled reaction is not rate-limited by a coupled enzyme, PK, acting on the NDP product of the reaction of interest. We tested this directly by carrying out representative kinetic assays for all relevant nucleotides with 2x higher concentrations of the coupled enzymes than those used in the above measurements (Figure 4.6). The progress curves with the original and with the doubled concentrations of the coupled enzymes were the same within experimental uncertainty, indicating that, indeed, the above kinetics were not affected by potential variations in activity of PK with different NDP substrates.

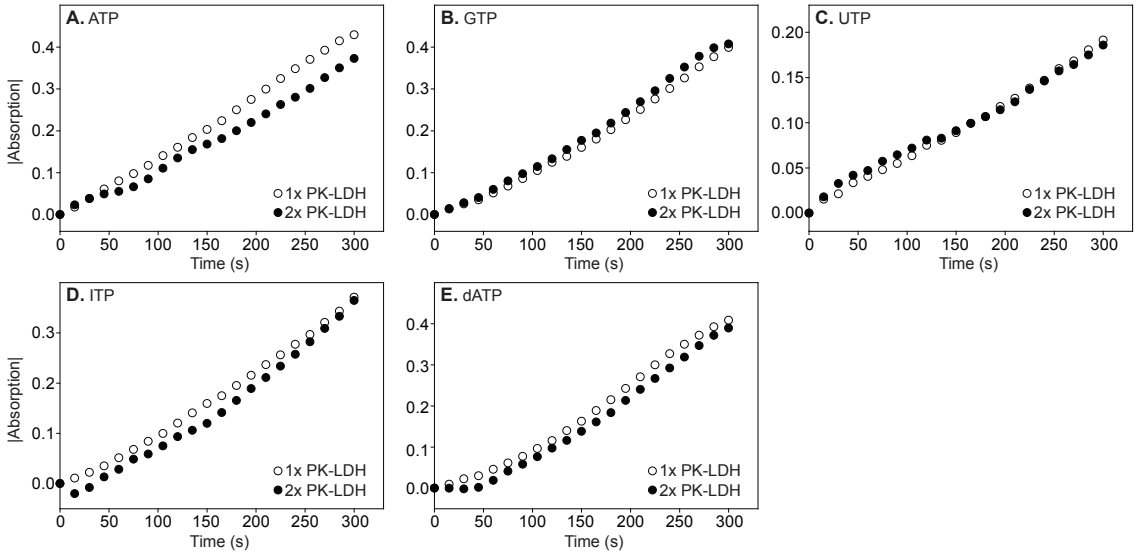

Figure 4.6. Time course reaction for each NTP with APH(3')-IIa enzyme with either 1× or 2× PK-LDH concentration in the reaction in order to prove that APH(3')-IIa kinetics shown in Table 4.3 and Figure 4.5 were not limited by the coupled reaction used in UV-Vis assays.

4.2.4. Structural insight into the NTP effect of the AG profile

We examined available crystal structures of APH(3')-IIa in complex with KAN (PDB ID: 1ND4)[25] as well as two crystal structures of APH(3')-IIIa, a thoroughly characterized homologous APH, in complexes with ADP and KAN (PDB ID: 1L8T)[32] and with ADP and NEO (PDB ID: 2B0Q)[32] to help us understand the effects of NTP on the AG profile.

The structures of APH(3')-IIa in complex with KAN and that of APH(3')-IIIa in complex with ADP and KAN are highly superimposable (Figure 4.7A). Nevertheless, differences can be observed between the two superimposed structures, specifically at the different accommodation of KAN ring III of the two proteins. For instance, APH(3')-IIa contains a salt bridge formed by Glu160 and Arg229 that is absent in APH(3')-IIIa. The salt bridge could help stabilize the flexible loop (Asp150-Phe165 in APH(3')-IIIa)[32] at the AG-binding site in a closed form upon KAN binding. Another difference in binding of KAN ring III between the two enzymes is in that the larger Asp227 in APH(3')-IIa than Ser227 in

APH(3')-IIIa positions ring III of KAN further away from the protein core, consequently forcing the AG-gating flexible loop outward into a seemingly looser conformation in APH(3')-IIa.

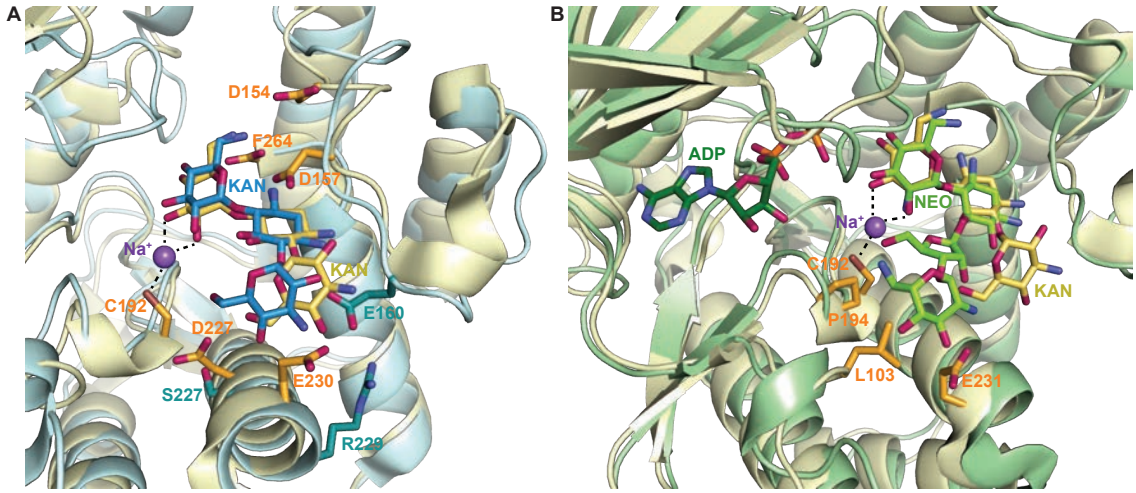

Figure 4.7. Computational superimposition of the protein structures of **A.** APH(3')-IIa (in beige) with KAN (in bright yellow) bound (PDB ID: 1ND4)[25] and APH(3')-IIIa (in pale blue) with KAN (in teal) bound (PDB ID:1L8T).[32] D154, D157, D227, E230, and F264 in APH(3')-IIa are shown in bright orange. S227 in APH(3')-IIIa as well as the two residues forming the salt bridge, E160 and R229, are shown in dark teal. **B.** APH(3')-IIa (in beige) with KAN (in bright yellow) bound (PDB ID: 1ND4)[25] and APH(3')-IIIa (in pale green) with ADP (in dark green) and NEO (in bright green) bound (PDB ID:2B0Q).[32] L103, C192, P194, and E231 of APH(3')-IIa are shown in bright orange. The Na^+ ion coordinating C192 and the 2'- and 3'-OH of KAN is shown in purple.

Next, we superimposed the crystal structures of APH(3')-IIa in complex with KAN and APH(3')-IIIa in complex with ADP and NEO (Figure 4.7B). Please note that NEO is a 4,5-disubstited AG with rings III and IV positioned in a different orientation from that of ring III of the 4,6-disubstituted KAN. APH(3')-IIIa was previously reported to be the most substrate promiscuous amongst all APH(3') enzymes.[32-33] For APH(3')-IIa , the 2'- and 3'-OH of KAN are coordinated, through a Na^+ ion, to the side chain of Cys192. This highly restrained binding mode, not observed for APH(3')-IIIa, could be an AG-selection mechanism for APH(3')-IIa. The AGs that do not satisfy this coordination, such as NEO,

which bears an NH_2 group instead of OH at its 2'-position, may be less favored than KAN. In addition, we can see that Leu103, Pro194, and Cys192 in APH(3')-IIa form a hydrophobic wall that may prevent binding of NEO, which contains an extra ring (IV). Specifically, Leu103, Pro194, and Glu231 sterically clash the with ring IV of NEO bound to APH(3')-IIIa in the superimposition. This steric hindrance may contribute to the reason why NEO is a less favored substrate than KAN for APH(3')-IIa when using ATP as a cosubstrate. This surface, especially Pro194, is located close to the ATP binding site, apparently to bind AGs in a U-shaped conformation. Due to this proximity, the binding of a different NTP may induce structural shifts propagated via this surface to the AG-binding cavity to affect AG selection.

In addition, we compared APH(3')-IIa to another APH enzyme known for its dual cosubstrate specificity, APH(2")-IVa.[34] We superimposed the crystal structure of APH(3')-IIa (PDB ID: 1ND4)[25] with the two structures of APH(2")-IVa bound to adenosine (PDB ID: 4DT8) and guanosine (PDB ID: 4DT9) (Figures 4.8 and 4.9).[34] The dual nucleotide specificity in APH(2")-IVa was attributed to a shift in the hydrogen bonding network when adenine was replaced by guanine. Specifically, the N6 of adenine donates a hydrogen to the carbonyl oxygen of Thr96 of APH(2")-IVa and the N1 of adenine accepts the hydrogen from the amide nitrogen of Ile96 of APH(2")-IVa (Figure 4.9A). The O6 and N1 of guanine form hydrogen bonds with the amide nitrogen and carbonyl oxygen Ile98, respectively (Figure 4.9B). We asked if a similar shift could occur with APH(3')-IIa. We found potential hydrogen bond donors and acceptors for both adenine and guanine in this case as well. The N6 and N1 of adenine could serve as hydrogen bond donor and acceptor, respectively, to

interact with the backbone oxygen of Gly95 and the backbone nitrogen of Val97 in APH(3')-IIa (Figure 4.9C). On the other hand, guanine could interact with APH(3')-IIa by forming hydrogen bonds between O6, N1, and N2 and the backbone nitrogen and oxygen of Val97, as well as the backbone oxygen of Gly99 (hydrogen bond accepter) of APH(3')-IIa, respectively (Figure 4.9D). This structural model provides a potential explanation for the broad cosubstrate promiscuity of APH(3')-IIa.

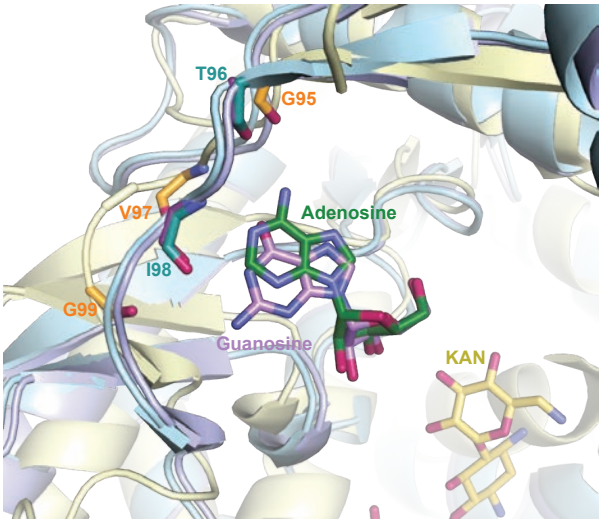

Figure 4.8. Superimposition of APH(3')-IIa (in pale yellow) with KAN (in bright yellow) bound (PDB ID: 1ND4)[25] and two crystal structures of APH(2")-IVa with adenosine (APH(2")-IVa in light blue, adenosine in dark green, PDB ID: 4DT8) and guanosine (APH(2")-IVa in light purple, guanosine in purple, PDB ID: 4DT9) bound.[34] Residues of APH(3')-IIa are colored in orange whereas the residues in APH(2")-IVa are colored in teal and dark purple. The specific interactions between each enzyme and nucleoside are shown in four separate panels in Figure 4.9.

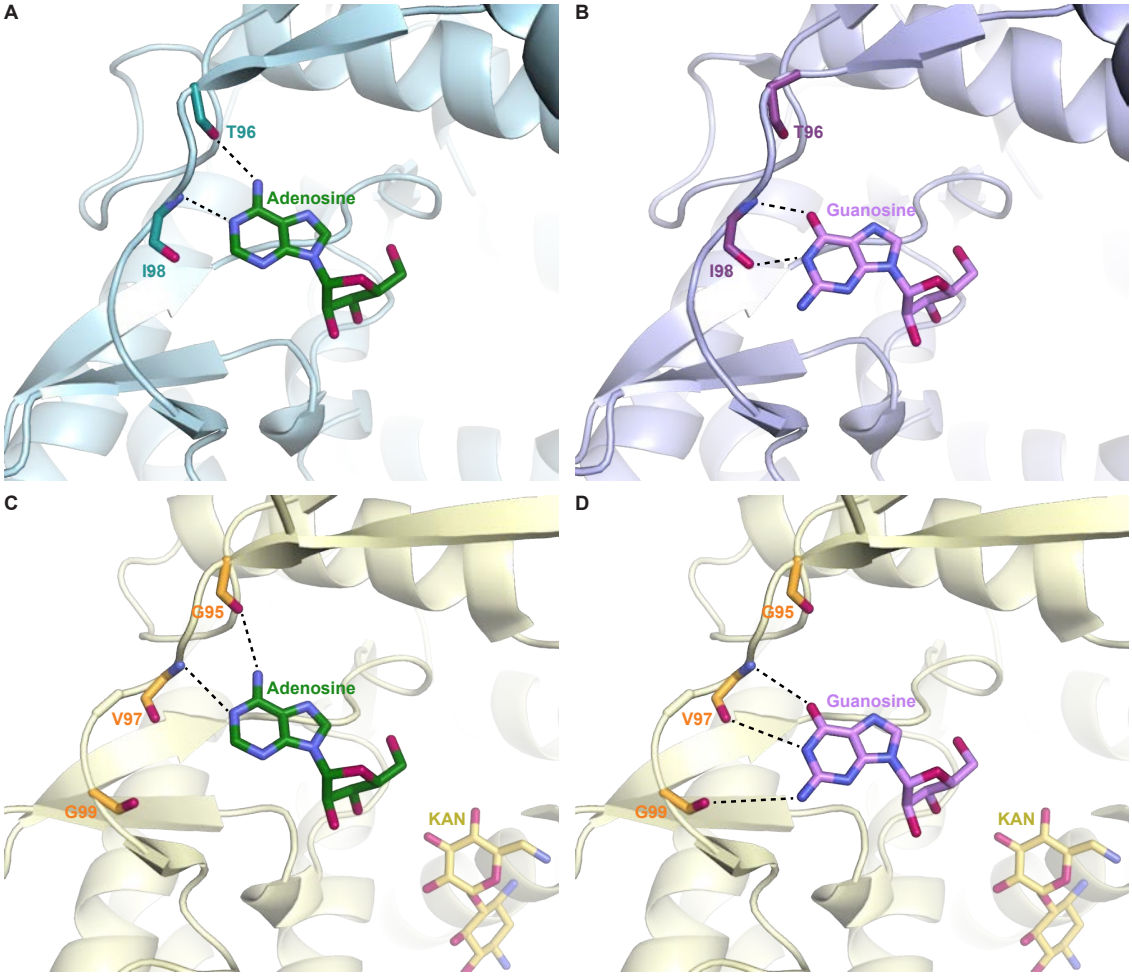

Figure 4.9. Superimposition of crystal structures of APH(3')-IIa with KAN (PDB ID: 1ND4)[25] and APH(2")-IVa with adenosine and guanosine (PDB IDs: 4DT8 and 4DT9, respectively)[34]. **A.** APH(2")-IVa (in light teal) and adenosine in dark green with the backbones of T96 and I98 colored in dark teal, **B.** APH(2")-IVa (in light purple) and guanosine in purple with the backbone of T96 and I98 colored in dark purple, **C.** APH(3')-IIa (in pale yellow) with KAN (in bright yellow) and the adenosine from APH(2")-IVa structure in dark green and the backbone of G95, V97, and G99 in orange, **D.** APH(3')-IIa (in pale yellow) with KAN (in bright yellow) and the guanosine from APH(2")-IVa structure in purple and the backbone of G95, V97, and G99 in orange.

4.3. CONCLUSIONS

In this chapter, we investigated for the first time how cosubstrate NTPs define the AG profile for APH(3')-IIa. A complex dependence of the AG profile on the identity of the base of the NTP strongly suggests allosteric communication between the cosubstrate and the substrate binding sites. Even though ATP is the most abundant NTP *in vivo*, this study

indicates other NTPs should not be disregarded as potential cosubstrates in the context of AG antibiotic overuse.

4.4. MATERIALS AND METHODS

4.4.1. Materials and instrumentation

The enzymes and buffers used for the molecular cloning of APH(3')-IIa, were purchased from New England BioLabs (NEB; Ipswich, MA), whereas primers for PCR were purchased from Sigma-Aldrich (Milwaukee, WI). All AGs used in this study were purchased from AK Scientific (Union City, CA). ATP, dATP, dCTP, GTP, UTP, TTP, and ITP were purchased from Sigma-Aldrich. dGTP and dUTP were purchased from Promega (Madison, WI). TLC plates (silica gel 60 F254 coated) were purchased from VWR (Radnor, PA). UV-Vis assays were performed on a SpectraMax M5 plate reader. Kinetics parameters were determined using SigmaPlot 13.0 (SysStat Software, San Jose, CA).

4.4.2. Cloning, expression, and purification of APH(3')-IIa

Cloning of *aph(3')-IIa*-pET28a was performed in *E. coli* TOP10. The *aph(3')-IIa* gene was PCR amplified by using the forward primer 5'-GCGTTTCATATGATTGAACAAGATGG-3' and reverse primer 5'-CCAGAGCTCGAGTCAGAAGAACTCGTC-3' using the pcDNA3.1 vector from Invitrogen. After PCR, the amplified *aph(3')-IIa* gene (817 bp) was purified, digested, with *Nde*I and *Xho*I (restriction sites are underlined above) and ligated into an *Nde*I/*Xho*I digested pET28a vector. The DNA sequence was confirmed (sequencing performed by Eurofins Genomics, Louisville, KY). The *aph(3')-IIa*-pET28a vector was transformed into

E. coli BL21 (DE3). An overnight culture was grown at 37 °C from a fresh transformant colony. The protein was overexpressed starting with a 1% inoculum in Luria-Bertani (LB) broth (2 L) containing KAN (50 μg/mL) at 37 °C with shaking at 200 rpm until the attenuance of 0.6 at 600 nm. The protein expression was then induced with IPTG (1 mM) and the cells were grown overnight at 25 °C with shaking at 200 rpm. The cell pellet was resuspended in 50 mL of lysis buffer (25 mM Tris-HCl, pH 8.0, 200 mM NaCl, and 10% glycerol) and the cells were lysed by intermittent sonication. The protein was purified using Ni^{II}-NTA affinity column chromatography in lysis buffer with a gradient of imidazole (10 mL of 5 mM, 3×5 mL of 20 mM, 40 mM, and 250 mM). Pure fractions were then dialyzed in 3×2 L of Tris-HCl (50 mM, pH 8.0), NaCl (300 mM) and 10% glycerol before being concentrated to 100 μM using a 10 kDa molecular weight cut-off Millipore Amicon Ultra centrifugual device. The pure 32.1 kDa $NHis_6$-tagged protein was flash-frozen in liquid nitrogen and stored at -80 °C. Protein yield was 8 mg per L of culture.

4.4.3. Determination of AG profile of APH(3')-IIa with various NTPs

To determine the substrate profiles of APH(3')-IIa for different NTP cosubstrates, we used a protocol previously described.[20, 22, 26, 29] In a 96-well plate, each 200 μL reaction contained AG (100 μM), Tris-HCl (50 mM, pH 8.0), $MgCl_2$ (10 mM), KCl (40 mM), NADH (0.5 mg/mL freshly prepared), phosphoenolpyruate (PEP, 2.5 mM), NTP (2 mM), PK-LDH (4 μL of 10 mg/mL solution) (P0294, Sigma Aldrich), and APH(3')-IIa (1 μM), which was added last to the plate to initiate the reaction. The assay was carried out at 37 °C and absorbance at 340 nm was recorded every 30 s for 20 min to monitor the disappearance of NADH. After subtraction from the final absorbance of each reaction that measured for

a control reaction in the absence of AG, the absorbance values greater than 0.1 were considered significant and indicated accordingly in Table 4.1. The AGs for which the corrected absorbance values were in the range of 0.05-0.1 were considered poor substrates for a given NTP. The AGs for which the absorbance values were below 0.05 were considered not to be substrates for APH(3')-IIa.

4.4.4. Thin-layer chromatography

The TLC assays with stains that detected AGs and their phosphorylated products were performed in order to confirm directly that the reactions we observed from the UV-Vis assay resulted from phosphorylation of AGs. We first used ATP as a representative NTP. Each reaction contained Tris-HCl (50 mM, pH 8.0), AG (1 mM), NTP (2 mM), $MgCl_2$ (10 mM), KCl (40 mM), and APH(3')-IIa (5 μM). The eluent system for each AG consisted of different ratios of MeOH and NH_4OH as follows: 3:2/MeOH:NH_4OH for AMK and NEO, 5:2 for APR, HYG, and SIS, 15:2 for GEN, G418, NET, and TOB, 7:3 for KAN, and 3:1 for NEA, PAR, and RIB. TLC plates for most AGs were stained with ninhydrin, with the exception of G418 and RIB, which were stained with 10% sulfuric acid in MeOH. The stained plates were heated for visualization (Figure 4.3). We then performed TLC for the rest of (d)NTPs in the same reaction condition (24 h reactions). The results were summarized in Figure 4.4.

4.4.5. Determination of enzyme kinetics by UV-Vis assays with respect to AGs

The reaction conditions were the same as those described in the AG profile by UV-Vis assay section and the data collected were processed as previous published.[5] The first 3 min

were used to determine the initial rate of reaction. The best-fit kinetic parameters with respect to each AG are summarized in Table 4.3 with the Michaelis-Menten curves shown in Figure 4.5.

4.4.6. Validation of PK efficiency in kinetics UV-Vis assays

To confirm that kinetic parameters determined for APH(3')-IIa in the UV-Vis assay with PK-LDH were not affected by the activity of PK, we used NEO as a representative AG and performed time course reactions containing 1x and 2x (compared to the concentration of the coupled enzymes used in the kinetic assays above) with each relevant nucleotide cosubstrate. Specifically, each reaction contained NEO (250 μM) and the rest of the ingredients at concentrations described in the kinetics assays. We used either 1x (as in the kinetics analysis) or 2x PK-LDH to test whether the concentration of PK-LDH in our kinetics analysis was limiting the rate of APH(3')-IIa enzymes (Figure 4.6).

4.5. ACKNOWLEDGEMENT

This work was supported by a grant from the National Institutes of Health (NIH AI090048) (to S.G.-T.).

This chapter is adapted from a published article herein referenced as Holbrook, S. Y. L.; Gentry, M. S.; Tsodikov, O. V.; Garneau-Tsodikova, S. Nucleoside triphosphate cosubstrates control the substrate profile and efficiency of aminoglycoside 3'-*O*-phosphotransferase type IIa. *MedChemComm* **2018,** Epub ahead of print.

4.6. AUTHORS' CONTRIBUTIONS

S. Y. L. H. was responsible for experimental design, performing all enzymatic experiments, and writing up the manuscript. S. G.-T. and M. S. G. both contributed in experimental design. O. V. T. assisted in structural insights. All authors contributed to the proof-reading of the manuscript. S. Y. L. H formatted the manuscript into this book chapter and S. G.-T. further proof-read the dissertation chapter.

Chapter 5. Evaluation of aminoglycoside and carbapenem resistance in a collection of drug-resistant *Pseudomonas aeruginosa* clinical isolates

Pseudomonas aeruginosa, a Gram-negative bacterium, is a member of the ESKAPE pathogens and one of the leading causes of healthcare-associated infections worldwide. Aminoglycosides (AGs) are recognized for their efficacy against *P. aeruginosa*. The most common resistance mechanism against AGs is the acquisition of AG-modifying enzymes (AMEs) by the bacteria, including AG *N*-acetyltransferases (AACs), AG *O*-phosphotransferases (APHs), and AG *O*-nucleotidyltransferases (ANTs). In this study, we obtained 122 multidrug-resistant *P. aeruginosa* clinical isolates and evaluated the antibacterial effects of six AGs and two carbapenems alone against all clinical isolates, and in combination against eight selected strains. We further probed for four representatives of the most common AME genes (*aac(6')-Ib*, *aac(3)-IV*, *ant(2'')-Ia*, and *aph(3')-Ia*) by PCR and compared the AME patterns of these 122 clinical isolates to their antibiotic resistance profile. Amongst the diverse antibiotics resistance profile displayed by these clinical isolates, we found correlations between the resistance to various AGs as well as between the resistance to one AG and the resistance to carbapenems. PCR results revealed that the presence of *aac(6')-Ib* renders these isolates more resistant to a variety of antibiotics. The correlation between resistance to various AGs and carbapenems partially reflects the complex resistance strategies adapted in these pathogens and encourages the development of strategic treatment for each *P. aeruginosa* infection by considering the genetic information of each isolated bacteria.

5.1. INTRODUCTION

Pseudomonas aeruginosa is a member of a group of Gram-negative (-) and Gram-positive (+) bacterial pathogens known as ESKAPE (where E stands for *Enterococcus faecium* (+), S for *Staphylococcus aureas* (+), K for *Klebsiella pneumoniae* (-), A for *Acinetobacter baumannii* (-), P for *Pseudomonas aeruginosa* (-), and E for *Enterobacter* species (-)) due to their ability to escape a broad array of antimicrobial agents.[1] Its pathogenicity, transmission, and resistance have caused the currently available antibiotics to rapidly lose activity against these pathogens.[2-7]

As an opportunistic pathogen, *P. aeruginosa* is a leading cause of healthcare-associated infections and poses great threat in critically ill and immunocompromised patients.[8-9] According to the Center for Diseases Control and Prevention, *P. aeruginosa* is estimated to cause 51,000 infections in U.S.A. every year amongst which 13% are caused by multidrug-resistant strains. It is the most common cause of nosocomial pneumonia (17%); third most common cause of urinary track infections (7%); fourth most common cause of surgical site infections (8%); as well as the fifth common isolate overall from all sites (9%).[10] *P. aeruginosa* is also one of the greatest challenges faced by military healthcare professionals, since it is often isolated among antibiotic-resistant bacteria in such settings in patients with military injuries and wounds.[11]

Due to their excellent efficacy against Gram-negative bacteria, aminoglycosides (AGs) are widely used to treat infections caused by *P. aeruginosa*. In addition to AMK, GEN, and TOB that are currently approved in the U.S.A. for systemic administration, netilmicin

(NET) and sisomicin (SIS) are widely employed in AG treatment regiments in European countries. Apramycin (APR), which is currently used in veterinary treatment, is another AG that has shown excellent antibacterial efficacy, limited toxicity, and was found to be less prone to the development of resistance over time.[12-14] Nonetheless, resistance has quickly developed to these antimicrobial agents with a significant portion of clinical isolates identified now resistant to clinically used AG antibiotics.[14-16] Resistance to AGs results from a variety of mechanisms including (i) changes in bacterial cell envelope composition, (ii) modification on RNA target, (iii) upregulation of efflux pumps, and (iv) acquisition of AG-modifying enzymes (AMEs), with the last accounting for most of the resistance cases. AMEs comprise three different types of enzymes: AG *N*-acetyltransferases (AACs), AG *O*-nucleotidyltransferases (ANTs), and AG *O*-phosphotransferases (APHs). These enzymes transfer an acetyl, a nucleotidyl, or a phosphate group onto AGs, respectively. AACs, which target the 6'-, 2'-, and 3-amine moieties on AG molecules, are the most common AMEs in resistant organisms. A more recently discovered multiacetylating AAC, the enhanced intracellular survival protein (Eis),[17-22] could become highly problematic in the future with its ability to acetylate more than one site on AGs. Most APHs, on the other hand, attack the 3'- and 2"-positions. ANTs are the least common AMEs and attack the 4'- or the 2"-hydroxyl groups.[23]

Our laboratory, as well as many other research groups, is dedicated to developing AG antibiotics and understanding resistance mechanisms.[24-39] Previously, researchers have observed discrepant results over whether AG and carbapenem combination therapies yield positive outcomes for the killing of *P. aeruginosa*.[40-43] In an effort to understand in greater

detail the underlying resistance mechanisms in *P. aeruginosa*, in this study, we obtained 122 multidrug-resistant *P. aeruginosa* clinical isolates from the University of Kentucky Hospital System and evaluated the *in vitro* activity of various clinically-relevant AGs, including AMK, APR, GEN, NET, SIS, and TOB, and two carbapenem antibiotics, meropenem (MEM) and imipenem (IPM), against these clinical isolates. We evaluated the bactericidal effect of AG and carbapenem alone against all clinical isolates, and in combination against eight selected strains. We have also performed PCR probing for four of the most common AME genes, *aac(6')-Ib*, *aac(3)-IV*, *ant(2")-Ia*, and *aph(3')-Ia*, and compared the AME patterns of these 122 clinical isolates to their antibiotic resistance profiles.

5.2. RESULTS AND DISCUSSION

5.2.1. Susceptibility of various antibiotics against 122 *P. aeruginosa* clinical isolates

We first determined the MIC values of various AGs (AMK, APR, NET, SIS, and TOB) and MEM against all 122 *P. aeruginosa* strains (Table 5.1).[44-45] The breakpoint concentrations for APR are yet to be determined. Therefore, for all analyses in this study, APR was not categorized based on susceptibility or resistance. As summarized in Table 5.2, 117 strains were susceptible to AMK and only 3 strains were resistant to AMK. The susceptibility of all strains showed a similar distribution to GEN, NET, SIS, and TOB: ~55% of the strains susceptible and ~40% resistant. Approximately 60% of these 122 strains were susceptible to MEM and less than 20% of them were resistant to MEM.

Table 5.1. MIC values (μg/mL) of various AGs and MEM against all clinical isolates studied.

Strain #	AGs							Strain #	AGs						
	AMK	APR	GEN[a]	NET	SIS	TOB	MEM		AMK	APR	GEN[a]	NET	SIS	TOB	MEM
1	2	4	≤2	1	≤0.25	1	1	**62**	4	16	≤2	16	4	0.5	1
2	2	8	8	2	0.5	1	1	**63**	2	4	16	8	16	2	2
3	16	2-4	>8	>128	>128	128	16	**64**	4	8	>8	>128	>128	32	4
4	1	2	≤2	0.5	≤0.25	0.5	1	**65**	8	16	>8	>128	>128	32	2-4
5	1-2	8	8	1	≤0.25	0.5	≤0.25	**66**	4	2	128	>128	>128	32	4
6	0.5	8	≤2	0.5	≤0.25	0.5	≤0.25	**67**	1-2	1-2	≤2	2	0.5	≤0.25	≤0.25
7	2	4-8	>8	4	≤0.25	64-128	2-4	**68**	4	8	4	16	4	0.5	≤0.25
8	1	4	>8	2	128	128	2-4	**69**	2	8	≤2	4-8	1-2	≤0.25	1
9	4	2	≤2	4	1	0.5	0.5	**70**	2	8	≤2	4	2-4	0.5-1	0.5
10	0.5-1	2	≤2	≤0.25	≤0.25	0.5	≤0.25	**71**	4	8	>8	16	>128	32	4
11	1	4	>8	2	>128	64	2-4	**72**	4	8	>8	16	>128	64	2
12	0.5	2	≤2	≤0.25	≤0.25	1	0.5	**73**	8	16-32	>8	32	>128	>128	16
13	8	8	>8	>128	>128	128	2	**74**	2-4	4	≤2	8	2	0.5-1	2
14	4	8	≤2	4	2	0.5	1	**75**	8	16	>8	16	>128	16-32	4-8
15	8	16	>8	>128	>128	64	16	**76**	1	2-4	≤2	8	2-8	4-8	8
16	8	8	>8	>128	>128	64	16	**77**	2-4	4-8	≤2	4	2	0.5	0.5
17	1	4	≤2	4	1	1	2	**78**	8	8	≤2	8	2-4	0.5-2	0.5
18	1	4	≤2	2	2	1	≤0.25	**79**	1	2	1	2	1	64	4
19	1-2	4	≤2	1-4	1-2	1	≤0.25	**80**	1-2	4	4	4	1	0.5	0.5
20	4	8	>8	>128	>128	64	4	**81**	8	8	>8	16	>128	16-32	4
21	2	4	≤2	4	2	1-2	0.5	**82**	8	8	>8	16	>128	64	4
22	1	4	≤2	2	2	0.5	≤0.25	**83**	4	8	>8	8	128	16	4
23	2-4	4-8	>8	8-16	>128	64	2	**84**	2	2	≤2	4	128	4	2
24	1	2-4	≤2	2	1-2	0.5-1	0.5-1	**85**	16	32	>8	32	4-8	4	2
25	2	4	≤2	4	1	1	≤0.25	**86**	0.5-1	4	≤2	2	0.5	≤0.25	≤0.25
26	128	>128	>8	>128	>128	>128	0.5	**87**	8	8	>8	8	>128	128	≤0.25
27	16	8	>8	>128	>128	64	16	**88**	2	4-8	4	8	1	≤0.25	≤0.25
28	32	8	>8	>128	>128	128	16	**89**	2	2	≤2	2	0.5	≤0.25	1
29	4	8	≤2	2	1	1	0.5	**90**	32-64	8	>8	>128	>128	>128	4
30	2	8	≤2	4	2	1	0.5	**91**	2	8	>8	>128	>128	32	4
31	4	4-8	≤2	8	1	1	2	**92**	0.5	2	≤2	0.5	1	≤0.25	2
32	2	4	≤2	4	1-2	0.5	8	**93**	2	8	≤2	4	2	0.5	2
33	4	4	≤2	4	1-2	0.5-1	32-64	**94**	2	8	>8	16-32	>128	64	4-8
34	4	4	≤2	4	1-2	0.5-1	≤0.25	**95**	4-8	32	>8	>128	>128	64	4
35	8	8	>8	>128	>128	64	2	**96**	2	4	≤2	4-8	2	≤0.25	≤0.25
36	4	4-8	≤2	8-16	2	0.5	2	**97**	4	8	≤2	4	2	≤0.25	≤0.25
37	4	4-8	2	8	4	0.5	1-2	**98**	8	8	>8	>128	>128	64	2
38	4	8-16	1	8-16	2	0.5	4	**99**	8	8	≤2	8	2-4	0.5	0.5
39	8	16	>128	>128	>128	64	4	**100**	8	8	>8	>128	>128	32	4
40	4	8	2	4	2	1	≤0.25	**101**	2	4	≤2	4	4	4	2
41	4-8	4	1	1-2	2-4	2	≤0.25	**102**	8	8	≤2	>128	128	1-2	2
42	1	1	≤2	1	0.5	0.5	≤0.25	**103**	4	8	≤2	8	1-2	0.5	0.5
43	8	8	>8	>128	>128	64	4	**104**	4	8-16	≤2	8	2	≤0.25	≤0.25
44	1	2	8	2	1	1	4	**105**	8	8-16	>8	16	>128	64	8
45	1	2	≤2	2	1	2	0.5	**106**	4	4-8	≤2	16	>128	16	4
46	1	1	>8	2	1	32	2	**107**	16	16	>8	16	8	2	≤0.25
47	1-2	4	1	4	1	0.5	0.5	**108**	8	16	>8	32	>128	32	8
48	16	8-16	≤2	16	4	0.5	≤0.25	**109**	8-16	8	>8	>128	>128	64	16
49	4	4	≤2	8	2	0.5	≤0.25	**110**	0.5	0.5-1	≤2	≤0.25	≤0.25	≤0.25	8
50	8	4-8	4	>128	>128	8	64	**111**	8	16	≤2	128	>128	32	16
51	32	2	2	64-128	32	8	128	**112**	4	8	>8	4	4-8	4	≤0.25
52	8	8-16	4	8	4	0.5	4	**113**	8	8	>8	128	128	32	2
53	2	4-8	≤2	16	4	0.5	≤0.25	**114**	16	16	>8	>128	128	32-64	>128
54	4	8	≤2	8	2	0.5	≤0.25	**115**	16	16-32	≤2	128	128	16-32	2
55	0.5-1	2-4	≤2	4	2	0.5	4	**116**	16	16	>8	32	16	8-16	1
56	2-4	8-16	>8	>128	>128	32	2	**117**	8-16	16	>8	>128	>128	32	4
57	4	16	8	32	4	1	2	**118**	4	4	≤2	4	2	≤0.25	4
58	2	8	≤2	8	2	0.5	0.5	**119**	64	8-16	>8	>128	>128	128	>128
59	1-2	8	≤2	4-8	2	≤0.25	≤0.25	**120**	4	4	128	>128	>128	64	8
60	8	16	>8	>128	>128	32	2-4	**121**	8	4-8	>8	>128	>128	64	64
61	4	4	≤2	128	64	≤0.25	0.5	**122**	8	8	≤2	64	>128	4	8-16

S, I, and R are depicted as green, yellow, and orange cells respectively. The resistance cutoff values for various antibiotics against *P. aeruginosa* are: AMK (S ≤16, I = 32, R ≥64), GEN (S ≤4, I = 8, R ≥16), MEM (S ≤2, I = 4, R ≥8), NET (S ≤8, I = 16, R ≥32), and TOB (S ≤4, I = 8, R ≥16) according to the CLSI.[44] The resistance cutoff values for SIS against *P. aeruginosa* are not established in the U.S.A. and are considered to be S ≤4 and R >4.[46] [a] Most MIC values for GEN against the strains studied were obtained from the University of Kentucky Hospital System.

Table 5.2. Susceptibility of 122 *P. aeruginosa* clinical isolate strains to various antibiotics.

	Susceptible (S)		Intermediate (I)		Resistant (R)	
Antibiotic	No. of strains	%	No. of strains	%	No. of strains	%
AMK	117	95.9	2	1.0	3	2.5
GEN	68	55.8	5	4.1	49	40.2
NET	66	54.1	15	12.3	41	33.6
SIS	65	53.3	--	--	57	46.7
TOB	70	57.4	3	2.5	49	40.2
MEM	72	59.0	27	22.1	23	18.9

The resistance cutoff values for various antibiotics against *P. aeruginosa* are AMK (S ≤16, I = 32, R ≥64), GEN (S ≤4, I = 8, R ≥16), NET (S ≤8, I = 16, R ≥32), TOB (S ≤4, I = 8, R ≥16), and MEM (S ≤2, I = 4, R ≥8) according to the CLSI. The resistance cutoff values for SIS against *P. aeruginosa* are not established in the U.S.A. and are considered to be S ≤4 and R >4 in this study. APR is not included in this analysis due to lack of established resistance cutoff.

To further explore if the resistance to these antibiotics occur mostly individually or in groups of antibiotics, we next categorized the *P. aeruginosa* strains studied based on the number of antibiotics that they were resistant to (Figure 5.1). We found that over half of the strains (58 strains) were susceptible to all of the antibiotics tested in this study. We observed that simultaneous resistance to all six antibiotics is rare (1 strain only). Moreover, we found 20 strains that concurrently resisted the action of four antibiotics.

In order to establish the correlations between the susceptibility/resistance to one antibiotic to the resistance to another drug in these *P. aeruginosa* strains, we further categorized these clinical isolates based on their susceptibility/resistance to each individual antibiotic (AMK, GEN, NET, SIS, TOB, and MEM) and analyzed their resistance patterns to other antibiotics within this group. First, we separated the 122 strains based on their susceptibility/resistance to a first antibiotic, then analyzed the median MIC values, range of MIC values, and the resistance rate for a second antibiotic within each group (Table 5.3). Then, we plotted the MIC values of the second antibiotic based on the susceptibility/resistance to the first antibiotic in order to see the distribution of the MIC values of all the clinical isolates. The data based on GEN susceptibility/resistance were presented in Figure 5.2, whereas those

based on the susceptibility/resistance to the rest of the antibiotics were displayed in Figures 5.3 and 5.4.

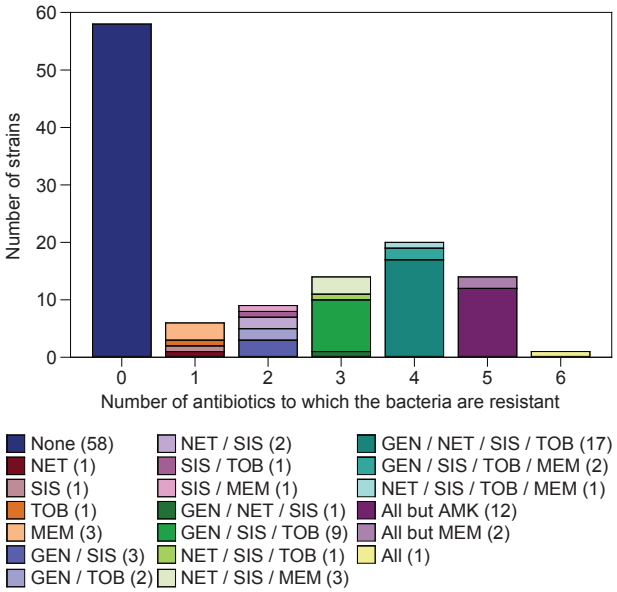

Figure 5.1. Number of strains grouped by the number of antibiotics to which the *P. aeruginosa* strains are resistant. The specific antibiotic to which each strain is resistant to are marked in the legend with the number of strains with each resistance profile in parentheses. The resistance cutoff values for each antibiotic are as follow: AMK (S ≤16, I = 32, R ≥64), GEN (S ≤4, I = 8, R ≥16), MEM (S ≤2, I = 4, R ≥8), NET (S ≤8, I = 16, R ≥32), and TOB (S ≤4, I = 8, R ≥16) according to the CLSI.[44] The resistance cutoff values for SIS against *P. aeruginosa* are not established in the U.S.A. and are considered to be S ≤4 and R >4 in this study based on ref 45.

Table 5.3. Summary of the median MIC values, the range of MIC values, and the rate of resistance to each antibiotic based on the susceptibility to AMK, GEN, NET, SIS, TOB, and MEM.

	AMK susceptible (n = 117)			AMK resistant (n = 3)		
	MIC (μg/mL)			MIC (μg/mL)		
Antibiotic	Median	Range	Resistance rate %	Median	Range	Resistance rate %
GEN	≤2	≤2 - >8	38.5	>8	>8	100
NET	8	≤0.25 - >128	60.7	>128	>128	100
SIS	4	≤0.25 - >128	38.5	>128	>128	100
TOB	2	≤0.25 - >128	38.5	>128	≥128	100
MEM	1	≤0.25 - >128	17.1	4	0.5 - >128	33
	GEN susceptible (n = 69)			GEN resistant (n = 49)		
	MIC (μg/mL)			MIC (μg/mL)		
Antibiotic	Median	Range	Resistance rate %	Median	Range	Resistance rate %
AMK	2	0.5 - 32	0	8	1-128	6.1
NET	4	≤0.25 - >128	10.1	>128	2 - >128	67.4
SIS	2	≤0.25 - >128	14.5	>128	≤0.25 - >128	95.9
TOB	0.5	≤0.25 - 64	6.3	64	2 - >128	91.8
MEM	0.5	≤0.25 - >128	11.6	4	≤0.25 - >128	30.6
	NET susceptible (n = 66)			NET resistant (n = 41)		
	MIC (μg/mL)			MIC (μg/mL)		
Antibiotic	Median	Range	Resistance rate %	Median	Range	Resistance rate %
AMK	2	0.5 - 8	0	8	1-128	7.3
GEN	≤2	≤2 - >8	12.1	>8	≤2 - >8	80.5
SIS	2	≤0.25 - >128	12.1	>128	1 - >128	97.6
TOB	0.75	≤0.25 - 128	10.6	64	≤0.25 - >128	12.2
MEM	0.5	≤0.25 - 64	6.1	4	≤0.25 - >128	41.5
	SIS susceptible (n = 65)			SIS resistant (n = 57)		
	MIC (μg/mL)			MIC (μg/mL)		
Antibiotic	Median	Range	Resistance rate %	Median	Range	Resistance rate %
AMK	2	0.5 - 16	0	8	1-128	5.3
GEN	≤2	≤2 - >8	3.1	>8	≤2 - >8	82.5
NET	4	≤0.25 - >128	1.4	>128	2 - >128	70.2
TOB	0.5	≤0.25 - >128	4.6	32	≤0.25 - >128	80.7
MEM	0.5	≤0.25 - 64	4.6	4	≤0.25 - >128	35.1
	TOB susceptible (n = 70)			TOB resistant (n = 49)		
	MIC (μg/mL)			MIC (μg/mL)		
Antibiotic	Median	Range	Resistance rate %	Median	Range	Resistance rate %
AMK	2	1 - 128	0	8	1-128	2.0
GEN	≤2	≤2 - >8	5.7	>8	≤2 - >8	91.8
NET	4	≤0.25 - >128	7.1	>128	2 - >128	57.6
SIS	2	≤0.25 - 128	11.4	>128	≤0.25 - >128	93.9
MEM	0.5	≤0.25 - 64	5.7	4	≤0.25 - >128	32.7
	MEM susceptible (n = 73)			MEM resistant (n = 23)		
	MIC (μg/mL)			MIC (μg/mL)		
Antibiotic	Median	Range	Resistance rate %	Median	Range	Resistane rate %
AMK	4	0.5 - 128	1.4	8	0.5 - 64	4.4
GEN	≤2	≤2 - >8	20.6	>8	≤2 - >8	65.2
NET	4	≤0.25 - >128	16.4	128	≤0.25 - >128	73.9
SIS	2	≤0.25 - >128	24.7	>128	≤0.25 - >128	87.0
TOB	1	≤0.25 - >128	16.4	32	≤0.25 - >128	69.6

* Intermediate (I) strains are not included in this analysis. Results of APR are not shown in this table due to lack of susceptibility cutoff standards.

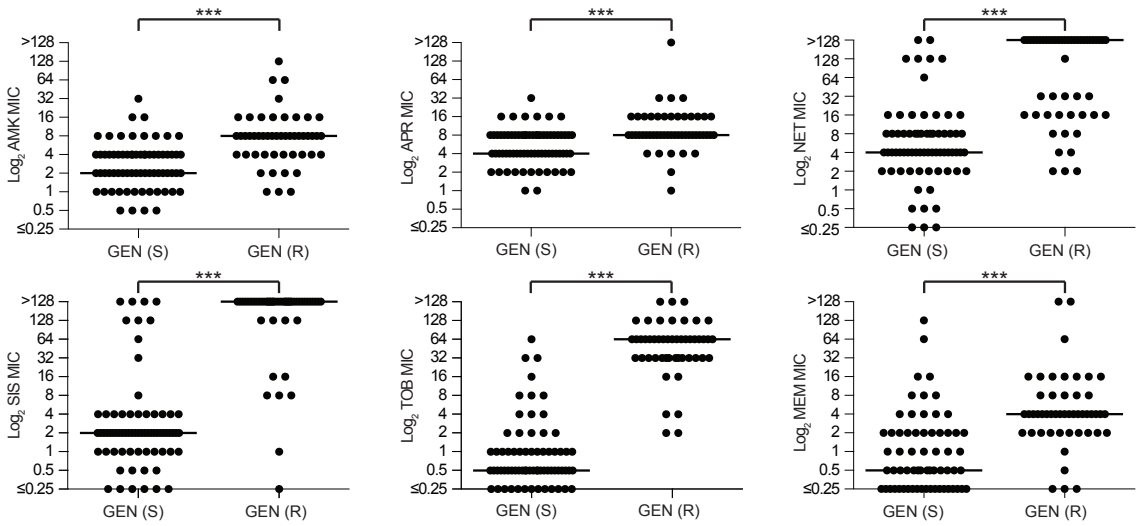

Figure 5.2. Distribution of MIC values of each antibiotic based on the susceptibility to GEN. The median MIC of each antibiotic is marked by a horizontal bar. Additional distribution plots of MIC values of each antibiotic based on the susceptibility to other antibiotics (NET and SIS, and TOB and MEM) are presented in Figures 5.3-5.4. We did not plot the MIC values of each antibiotic based on the susceptibility to AMK as the vast majority of the 122 *P. aeruginosa* strains tested are susceptible to AMK and only 3 strains are resistant to this AG. Significance was defined as P value ≤0.05 (0.033 (*), 0.002 (**), <0.001 (***)).

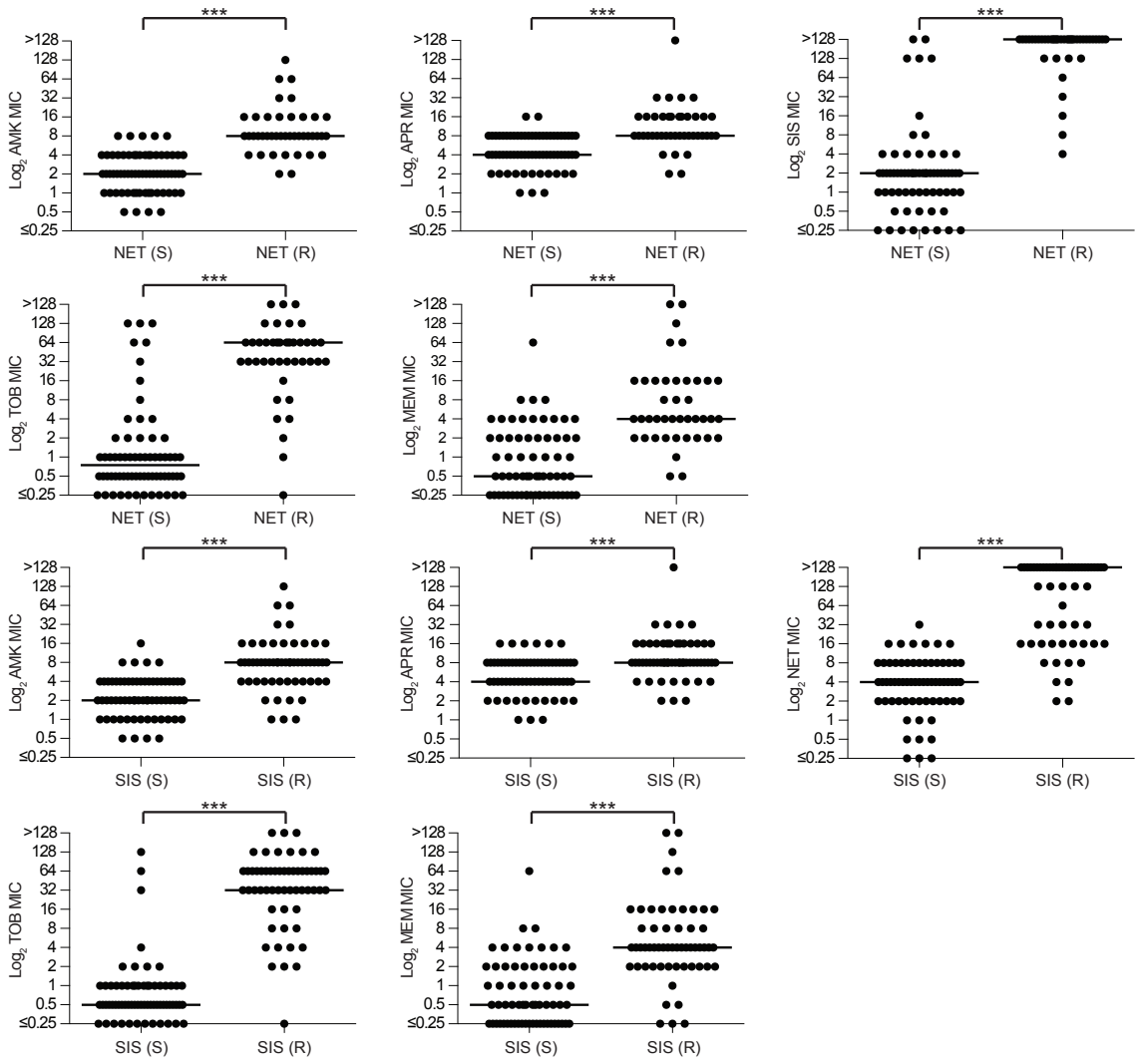

Figure 5.3. Distribution of MIC values of each antibiotic based on the susceptibility to NET and SIS. The median MIC value of each antibiotic is marked by a horizontal bar. *Note*: Additional distributions of MIC values of each antibiotic based on the susceptibility to other antibiotics (GEN, and TOB and MEM) are presented in Figures 5.2 and 5.4, respectively. We did not plot the MIC values of each antibiotic based on the susceptibility to AMK as the vast majority of the 122 *P. aeruginosa* strains tested are susceptible to AMK and only 3 strains are resistant to this AG. Significance was defined as P value ≤0.05 (<0.001 (***)).

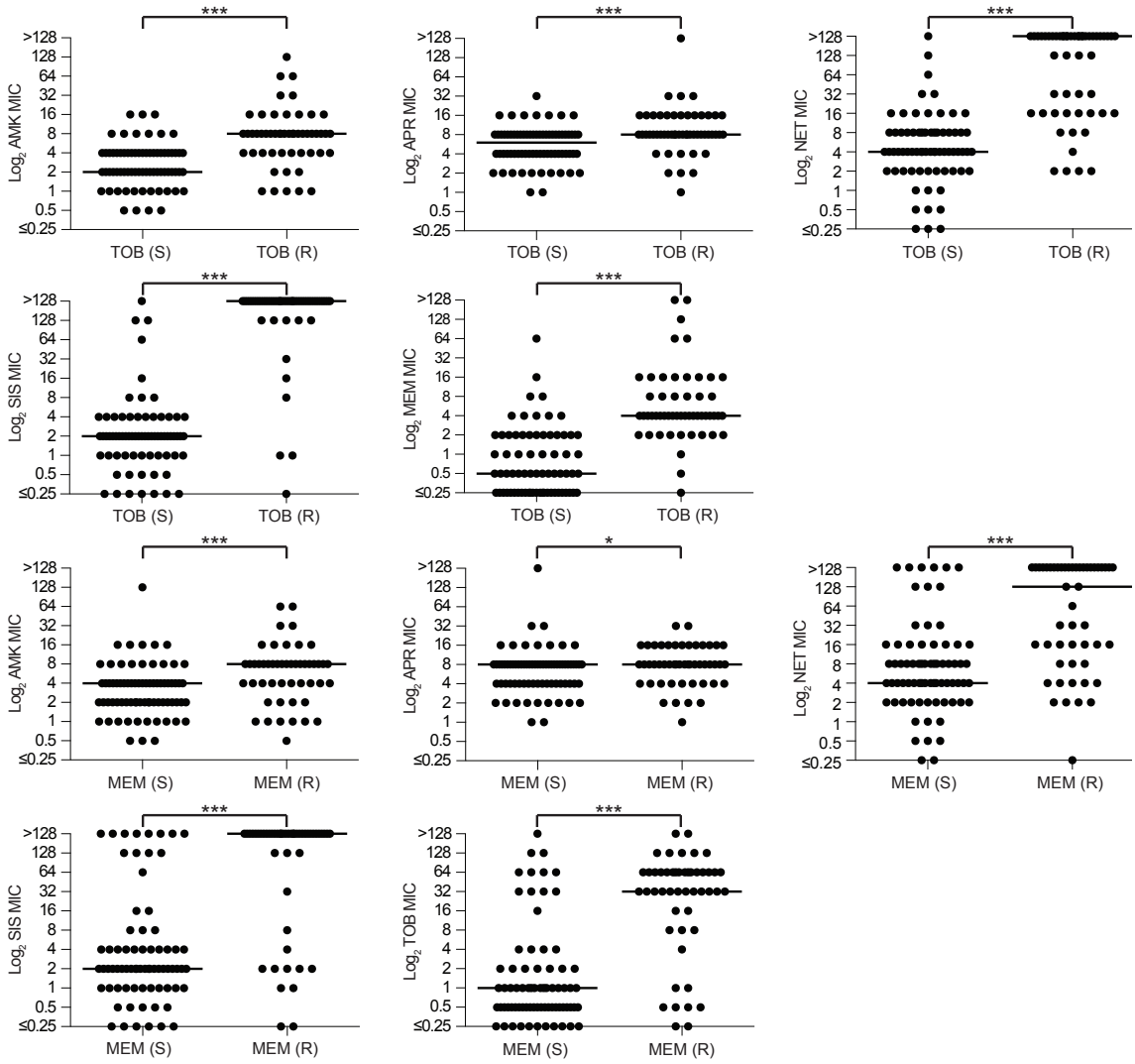

Figure 5.4. Distribution of MIC values of each antibiotic based on the susceptibility to TOB and MEM. The median MIC value of each antibiotic is marked by a horizontal bar. *Note*: Additional distributions of MIC values of each antibiotic based on the susceptibility to other antibiotics (GEN, and NET and SIS) are presented in Figures 5.2-5.3, respectively. We did not plot the MIC values of each antibiotic based on the susceptibility to AMK as the vast majority of the 122 *P. aeruginosa* strains tested are susceptible to AMK and only 3 strains are resistant to this AG. Significance was defined as P value ≤0.05 (0.033 (*), <0.001 (***)).

Taking GEN as an example, we found that within the GEN-susceptible group (n = 69 strains), the median MIC values for AMK, APR, NET, SIS, TOB, and MEM were 2, 4, 4, 2, 0.5, and 0.5 μg/mL, respectively, which were lower than those in the GEN-resistant group (n = 49 strains) where the median MIC values for the above antibiotics were 8, 8,

>128, >128, 64, and 4 μg/mL, respectively (Table 5.3). We observed that the range of MIC values in GEN-susceptible and GEN-resistant categories did not differ much, potentially due to the large sample size in this study. However, the resistance rates to the other five antibiotics in the GEN-resistant groups were prominently higher than in the GEN-susceptible groups. The differences in median MIC values and overall distributions of MIC values between the GEN-susceptible and GEN-resistant groups can be clearly observed in Figure 5.2. For instance, the median MIC values for NET, SIS, TOB, and MEM were all significantly different (≥8-fold difference) between the GEN-susceptible (lower median MIC) and GEN-resistant (higher median MIC) groups. In contrast, the median AMK and APR MIC values between the GEN-susceptible and GEN-resistant groups only differed by 4-fold and 2-fold, respectively. Similarly, the overall distributions of MIC values (looking at individual dots on the plots) of NET, SIS, TOB, and MEM were significantly different between the GEN-susceptible and GEN-resistant groups, whereas these differences were less extensive for AMK and practically absent for APR.

It is important to note that the trends observed in resistance rates, median MIC values, and overall distributions of MIC values in the GEN-susceptible and GEN-resistant groups were also observed when the data were analyzed based on the susceptibility/resistance to all other antibiotics (Table 5.3, Figures 5.3-5.4), with the exception of the resistance rates to TOB between the NET-susceptible (10.6%) and NET-resistant (12.2%) groups, which were not significantly different from each other (Table 5.3). Furthermore, in the case of AMK, we observed that the median MIC values and the resistance rates to all other antibiotics in the AMK-resistant group looked profoundly different from those in the

AMK-susceptible group. However, the small sample size of the AMK-resistant group (3 strains) would not necessarily allow us to generalize this observation to most *P. aeruginosa* strains.

Based on the results above, we postulated that the correlations observed between the susceptibility/resistance to one AG with that of other AGs could be explained by different resistance mechanisms affecting multiple AGs, which was not surprising given that the presence of AMEs is the most common resistance mechanism against AG antibiotics. For instance, if the bacteria acquired an AME, the most common mechanism of resistance to AGs, then it would likely be resistant to any AGs that can be inactivated by this particular AME due to the structural similarities between the AG molecules. Furthermore, given that all AGs tested in this study possess a 6'-amine group, except for APR, it is not hard to explain what we observed in Table 5.3 and Figures 5.1-5.4, where we found that the strains that are resistant to one AG also have higher resistance rates and overall higher MIC values to other AGs. Moreover, the correlations established between the resistance to MEM and those to AGs, which are two distinct classes of antibiotics with discrete chemical structures, although not surprising, may suggest the presence of other resistance mechanisms that are less structurally specific, and therefore, work against different classes of antibiotics. Another possibility to explain this phenomenon is the resistance elements to various antibiotics that could have accumulated simultaneously in bacteria, *i.e.*, the resistance element to carbapenems could have accumulated inside these *P. aeruginosa* isolates at the same time as resistance elements to AG antibiotics develop.[47] Furthermore, since both classes of antibiotics are often used in patients infected with *P. aeruginosa*, the resistance

to both classes of antibiotics could potentially result from previous antibiotics exposure.[48-50]

5.2.2. Screen for AME genes by PCR

Having established that half of the *P. aeruginosa* clinical isolates studied displayed resistance to AGs, we further investigated whether the observed AG resistance could be explained by the presence of one or multiple AME resistance genes. Therefore, we performed PCR with lysed bacteria probing for four of the most common AME genes (*aac(6')-Ib*, *aac(3)-IV*, *ant(2")-Ia*, and *aph(3')-Ia*) as previously described.[51] A representative PCR result for each gene is presented in Figure 5.5 and a summary of the AMEs present in all clinical isolates is presented in Table 5.4.

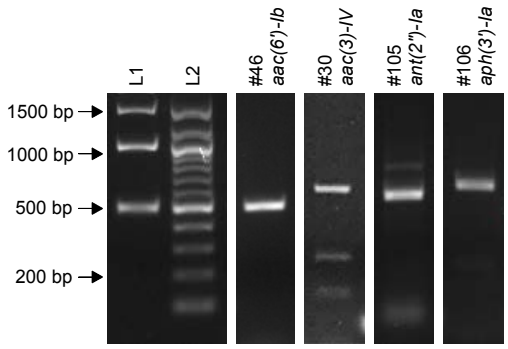

Figure 5.5. Sample agarose gel of representative PCR products for each AME gene probed. L1 and L2 represent 1-kb and 100-bp ladders, respectively. The expected sizes for each AME gene are 482 bp, 230 bp, 534 bp, and 624 bp for *aac(6')-Ib*, *aac(3)-IV*, *ant(2")-Ia*, and *aph(3')-Ia*, respectively.

Table 5.4. Patterns of the four common AME genes in all clinical *P. aeruginosa* strains as detected by PCR.

Strain	AME				Strain	AME			
	aac(6')-Ib	*aac(3)-IV*	*ant(2'')-Ia*	*aph(3')-Ia*		*aac(6')-Ib*	*aac(3)-IV*	*ant(2'')-Ia*	*aph(3')-Ia*
1	0	0	0	1	**62**	0	0	0	1
2	0	0	0	1	**63**	0	0	0	0
3	0	0	0	1	**64**	1	0	0	0
4	0	0	0	1	**65**	1	0	0	0
5	0	0	0	1	**66**	0	0	0	0
6	0	0	0	0	**67**	0	0	0	1
7	0	0	1	1	**68**	0	1	0	0
8	1	0	1	1	**69**	1	0	0	1
9	0	0	0	1	**70**	0	0	0	1
10	0	1	0	1	**71**	0	0	0	1
11	0	1	1	0	**72**	1	0	0	1
12	0	1	0	1	**73**	0	0	0	1
13	1	1	0	0	**74**	0	0	0	1
14	0	0	0	0	**75**	0	0	0	1
15	1	1	0	0	**76**	1	0	0	1
16	1	0	0	0	**77**	0	0	0	1
17	1	0	0	1	**78**	0	0	0	1
18	0	0	0	1	**79**	1	0	0	1
19	0	0	0	1	**80**	0	0	0	1
20	1	0	0	1	**81**	0	0	0	1
21	0	1	0	0	**82**	1	0	0	0
22	0	0	0	0	**83**	0	0	0	1
23	0	0	0	1	**84**	0	0	0	1
24	0	0	0	1	**85**	0	0	0	0
25	0	0	0	0	**86**	1	0	0	1
26	0	0	0	1	**87**	0	0	0	1
27	0	0	0	1	**88**	0	0	0	1
28	1	1	0	0	**89**	0	0	0	0
29	0	1	0	0	**90**	0	0	0	1
30	0	1	0	0	**91**	1	0	0	1
31	1	1	1	0	**92**	0	0	0	1
32	0	1	0	1	**93**	0	0	0	1
33	1	1	0	0	**94**	0	0	1	1
34	1	0	0	1	**95**	1	0	0	1
35	1	0	0	1	**96**	0	0	0	1
36	0	0	0	1	**97**	0	0	0	1
37	0	0	0	1	**98**	1	0	0	0
38	0	0	0	1	**99**	0	0	0	1
39	1	0	0	1	**100**	1	0	0	1
40	0	0	0	0	**101**	1	0	0	1
41	0	0	0	0	**102**	1	0	0	1
42	0	0	0	0	**103**	0	0	0	1
43	0	0	0	0	**104**	1	0	0	1
44	0	0	0	0	**105**	1	0	1	1
45	0	0	0	0	**106**	1	0	0	1
46	1	0	0	0	**107**	0	0	0	1
47	0	0	0	0	**108**	1	0	0	1
48	0	0	0	1	**109**	1	0	0	1
49	1	0	0	1	**110**	0	0	0	1
50	0	0	0	1	**111**	1	0	0	1
51	0	0	0	0	**112**	0	0	0	1
52	1	0	0	0	**113**	1	0	0	1
53	1	0	0	1	**114**	1	0	0	1
54	1	0	0	0	**115**	1	0	1	1
55	0	0	0	1	**116**	1	0	0	1
56	1	0	0	1	**117**	1	0	0	1
57	0	0	0	0	**118**	0	0	0	1
58	1	0	0	1	**119**	1	0	0	1
59	0	0	0	1	**120**	1	0	0	1
60	1	0	0	0	**121**	1	0	0	1
61	1	0	0	1	**122**	1	0	0	1

0	Denotes that the AME gene is not present by PCR.
1	Denotes that the AME gene is present by PCR.

Overall, 50 (41.0%), 13 (10.7%), 7 (5.7%), and 86 (70.5%) of the 122 *P. aeruginosa* clinical isolates possessed *aac(6')-Ib*, *aac(3)-IV*, *ant(2")-Ia*, and *aph(3')-Ia* genes, respectively. These statistics agree with the common understanding of *aac* and *aph* being the most common AME genes and *ant* being the least common. Contrary to what was observed in a previous study that identified *aac(6')-Ib* as the most common AME in *Klebsiella pneumoniae* strains,[51] we found *aph(3')-Ia* to be the most common AME gene harbored by the *P. aeruginosa* clinical isolates in our study. The 122 clinical isolates displayed 11 different AME patterns (Table 5.5). There were 17 strains (13.9%) that contained no AME genes. 58 strains (47.5%) contained one AME gene only, among which, 9 (7.4%), 4 (3.3%), and 45 (36.9%) strains contained *aac(6')-Ib* only, *aac(3)-IV* only, and *aph(3')-Ia* only, respectively. Not surprisingly, zero strains contained *ant(2")-Ia* by itself. Furthermore, 43 (35.3%) strains contained two AME genes: 4 (3.3%) strains contained the combination of *aac(6')-Ib* and *aac(3)-IV*, 33 (27.0%) strains contained *aac(6')-Ib* and *aph(3')-Ia*, 1 (0.8%) strain contained *aac(3)-IV* and *ant(2")-Ia*, 3 (2.5%) strains contained *aac(3)-IV* and *aph(3')-Ia*, and 2 (1.6%) strains contained *ant(2")-Ia* and *aph(3')-Ia*. There were also 4 (2.5%) strains that possessed three AME genes: either *aac(6')-Ib*, *aac(3)-IV*, and *ant(2")-Ia* (1 (0.8%) strain; #31 in Table 5.4) or *aac(6')-Ib*, *ant(2")-Ia*, and *aph(3')-Ia* (3 (2.5%) strains; #8, #105, and #115 in Table 5.4). It is important to note that none of the clinical isolates studied contained all four AME genes probed for.

Table 5.5. The median MIC values of each antibiotic based on the presence and absence of different AME gene patterns.

AME pattern	No. of strains	AMK Median MIC (μg/mL)		APR Median MIC (μg/mL)		GEN* Median MIC (μg/mL)		NET Median MIC (μg/mL)		SIS Median MIC (μg/mL)		TOB Median MIC (μg/mL)		MEM Median MIC (μg/mL)	
		Patten present	Pattern absent	Patten present	Pattern absent	Patten present	Pattern absent	Patten present	Pattern absent	Patten present	Pattern absent	Patten present	Pattern absent	Patten present	Pattern absent
No AMEs	17	2	4	4	8	≤2	≤2	4	8	2	4	1	4	0.5	2
AAC(6')-Ib only	9	8	4	8	8	>8	≤2	>128	8	>128	4	32	1	4	2
AAC(3)-IV only	4	3	4	8	8	≤2	≤2	4	8	2	4	1	2	0.5	2
APH(3)-Ia only	45	4	4	8	8	≤2	4	8	8	2	16	1	8	1	2
AAC(6')-Ib + AAC(3)-IV	4	8	4	8	8	>8	≤2	>128	8	>128	4	64	2	16	2
AAC(6')-Ib + APH(3')-Ia	33	4	4	8	8	>8	≤2	128	8	>128	2	32	1	2	1
AAC(3)-IV + ANT(2")-Ia	1	1	4	4	8	>8	≤2	2	8	>128	4	64	2	4	2
AAC(3)-IV + APH(3')-Ia	3	1	4	2	8	≤2	≤2	≤0.25	8	≤0.25	4	0.5	2	0.5	2
ANT(2")-Ia + APH(3')-Ia	2	2	4	8	8	>8	≤2	18	8	-	4	96	2	6	2
AAC(6')-Ib + AAC(3)-IV + ANT(2")-Ia	1	4	4	8	8	≤2	≤2	8	8	1	4	1	2	2	2
AAC(6')-Ib + ANT(2")-Ia + APH(3')-Ia	3	8	4	16	8	>8	≤2	16	8	128	4	64	2	4	2

*Most GEN MIC values were obtained from the University of Kentucky Hospital System, ranging from ≤2 to >8.

Note: - indicates that it was impossible to determine the median MIC value as the values involved were a combination of ≤0.25 and >128.

In order to determine if the presence of the AME genes found in the clinical isolates correlated with the MIC values that were observed for the AGs and to see if they had a potential influence on the MIC values of MEM, we categorized all *P. aeruginosa* strains based on their AME gene patterns and compared the median MIC values of each antibiotic between the pattern present and the pattern absent groups (*e.g.*, for the group of strains that contained *aph(3')-Ia* only, the pattern present group consisted of the 45 strains that possessed only *aph(3')-Ia*, whereas the pattern absent group included the rest of the 77 *P. aeruginosa* strains that either did not contain this gene or contained other AME genes in addition to *aph(3')-Ia*) (Table 5.5).

For the no AME group, the median TOB and MEM MIC values showed a mild difference (4-fold) between the pattern present and absent groups, not surprisingly with the pattern present (no AMEs) group showing lower MIC values. No significant difference (≥8-fold) was observed between the pattern present and absent groups for other antibiotics in this no AME group.

For the three different groups that possessed a single AME gene, the group that contained *aac(6')-Ib* only showed significant differences (≥8-fold) in the median MIC values of GEN, NET, SIS, and TOB between the pattern present and absent groups, with the median MIC values of the pattern absent group for each of the four antibiotics lying in the susceptible range and the pattern present median MIC values falling in the resistant range for each antibiotics. The other single AME gene pattern groups did not display as significant a contrast with the exceptions of a mild difference (4-fold) in the median MEM MIC values

between the *aac(3)-IV* only pattern present and absent groups, and 8-fold differences in the median MIC values of SIS and TOB between the *aph(3')-Ia* only pattern present and absent groups. Counterintuitively, the *aph(3')-Ia* only pattern present group displayed lower MIC values than those in the pattern absent group for SIS and TOB. These interesting observations may suggest that AAC(6')-Ib could be the most significant AME contributing to the resistance to AGs in this study. Additionally, considering the subtle differences in the chemical structures of these AGs, AMK and APR are the only two AGs in this study that possess 3' hydroxyl groups to be targeted by APH(3')-Ia, yet, differences in the median MIC values in the *aph(3')-Ia* only pattern present and absent groups were not observed for those AGs. However, for SIS and TOB, which contain hydrogen atoms at their 3' position, and therefore, do not allow inactivation by the APH(3')-Ia enzyme, the 8-fold lower in the median MIC values observed between the *aph(3')-Ia* only pattern present and absent groups potentially indicate that other resistance mechanisms are contributing to resistance to these AG antibiotics in the *P. aeruginosa* clinical isolates tested.

In the five different groups that possessed two AME genes, substantial differences could be observed between the pattern present and absent groups for GEN, NET, SIS, TOB, and MEM, with the exceptions of the median MEM MIC values between the pattern present and absent groups harboring *aac(6')-Ib* and *aph(3')-Ia* or *aac(3)-IV* and *ant(2'')-Ia*, the median GEN MIC values for the groups harboring *aac(3)-IV* and *aph(3')-Ia*, and the median NET and SIS MIC values for the groups harboring *ant(2'')-Ia* and *aph(3')-Ia*. As for the two groups that contained three AME genes, the only significant differences between the pattern present and absent groups were observed in median GEN, SIS, and

TOB MIC values for the *P. aeruginosa* strains that contained *aac(6')-Ib*, *ant(2")-Ia, and aph(3')-Ia*. Another interesting observation was that the one strain containing *aac(6')-Ib*, *aac(3)-IV*, and *ant(2")-Ia* showed slightly lower MIC to SIS and TOB in the pattern present group when compared to the pattern absent group. However, the differences between the MIC values were not significant (≤4-fold difference). Additionally, having only one strain in the pattern present group also made it hard to generalize this observation to all *P. aeruginosa* strains harboring this particular AME pattern. In addition to the above observations, it is also important to note that none of these AME patterns correlated with significant differences in median AMK and APR MIC values between the pattern present and absent groups, which agrees with previous studies suggesting that AMK and APR are less vulnerable to AMEs and, therefore, less prone to developing resistance due to the acquisition of AMEs.[51] These two AGs can, therefore, greatly help patients infected with resistance microorganisms. Furthermore, the much weaker correlation between MEM MIC values and AME gene patterns could easily be explained by the structural difference between AGs and carbapenems and the fact that AMEs do not chemically modify carbapenems.

Although these *P. aeruginosa* clinical isolates possessed diverse patterns of AME genes, we next decided to further analyze the clinical isolates harboring three of the most significant/common AME patterns: *aac(6')-Ib*, *aph(3')-Ia*, and *aac(6')-Ib* + *aph(3')-Ia*. We first separated all the clinical isolates based on the exclusive (gene only) and non-exclusive (gene present) presence and absence (gene absent) of the three gene patterns above and compared the MIC value distributions of each antibiotic (Figures 5.6-5.8). These findings

are in agreement with the previous observations from Table 5.5 and with a previous report stating that *aph(3')-Ia* in combination with another AME correlated with higher resistance rates against various antibiotics.[51] It is also important to note that the presence of AME genes studied does not necessarily equate to the expression and function of the AME proteins. Therefore, the presence of certain AME genes, if the gene was not expressed, would not contribute to a resistant phenotype.

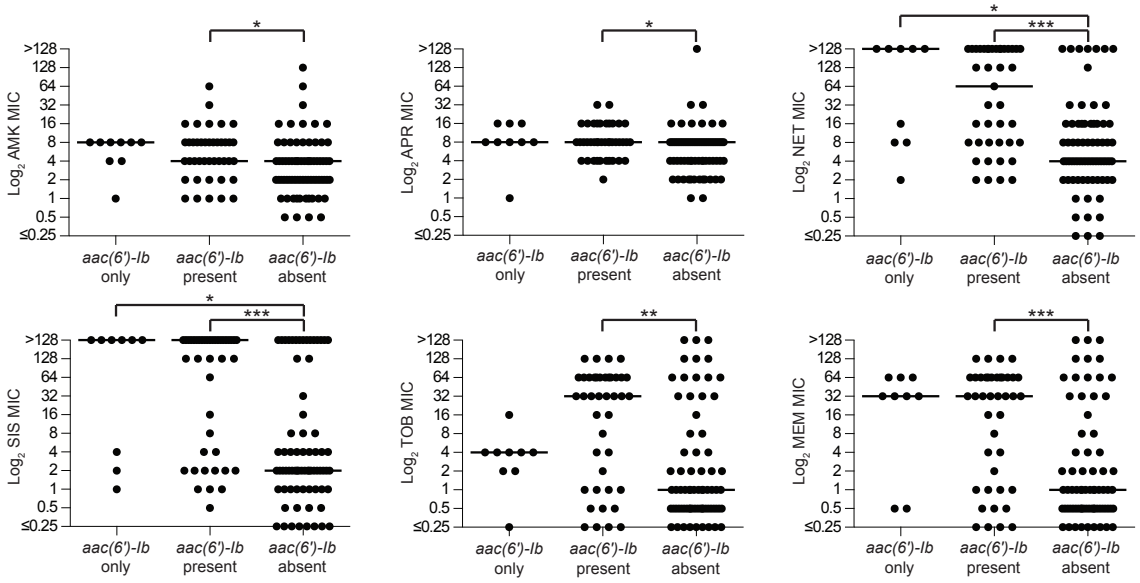

Figure 5.6. Distribution of MIC values of each antibiotic grouped by the presence or absence of the *aac(6')-Ib* gene. The median MIC value in each group, *aac(6')-Ib* only, *aac(6')-Ib* present, and *aac(6')-Ib* absent, is represented by a horizontal bar. *Note*: Plots depicting the distribution of MIC values of each antibiotic group by the presence and absence of *aph(3')-Ia*, and *aac(6')-Ib* + *aph(3')-Ia* genes are presented in Figure 5.7. Significance was defined as P value ≤0.05 (0.033 (*), 0.002 (**), <0.001 (***)).

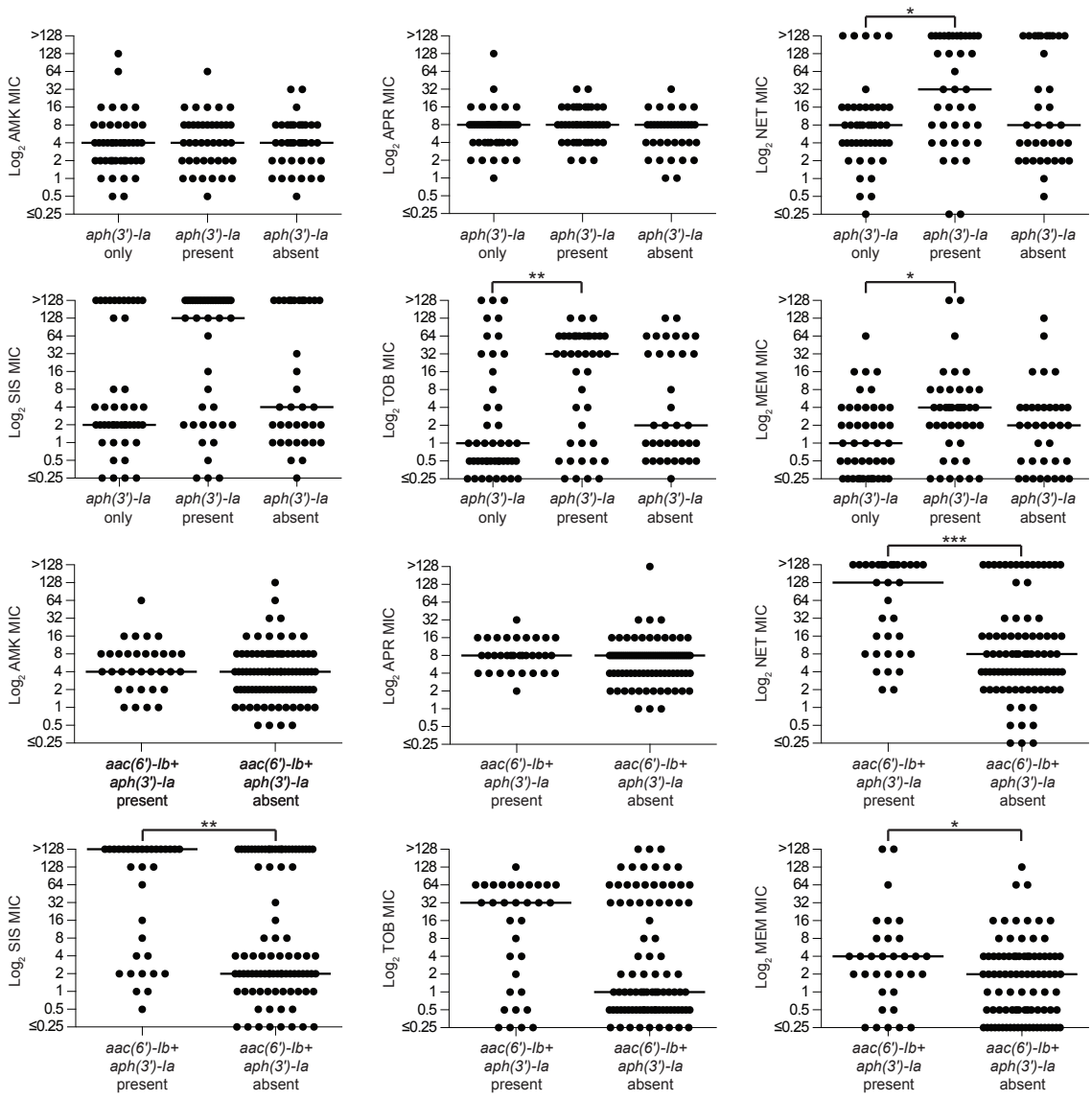

Figure 5.7. Distribution of MIC values of each antibiotic grouped by the presence and absence of *aph(3')-Ia*, and *aac(6')-Ib* + *aph(3')-Ia*. The median MIC value in each group is represented by a horizontal bar. *Note*: Additional plots depicting the distribution of MIC values of each antibiotic group by the presence and absence of *aac(6')-Ib* are presented in Figure 5.6. Significance was defined as P value ≤0.05 (0.033 (*), 0.002 (**), <0.001 (***)).

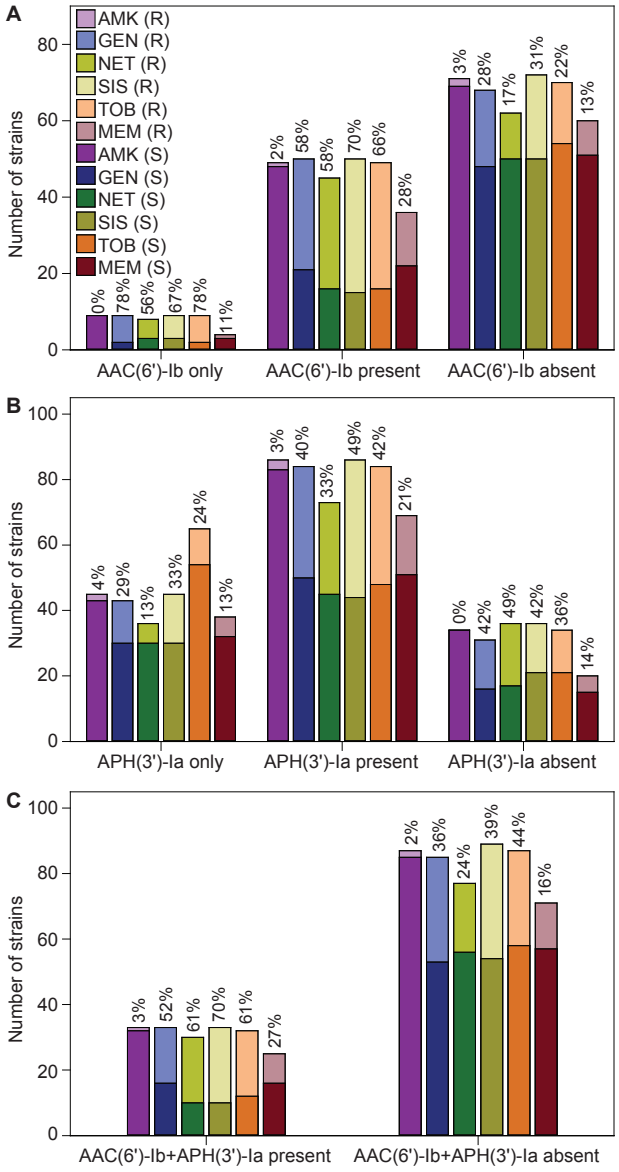

Figure 5.8. Number of *P. aeruginosa* clinical isolates harboring various AME gene patterns. **A.** *aac(6')-Ib*, **B.** *aph(3')-Ia*, and **C**. *aac(6')-Ib + aph(3')-Ia*. The percentage of *P. aeruginosa* strains, which are resistant to each antibiotic within each AME pattern group are marked at the top of each column.

Overall, the *P. aeruginosa* clinical isolates involved in this study showed great AME gene diversity and resistance profiles to various antibiotics. Recently, research groups have directed a lot of effort to the establishment of combination therapies and seen promising results in killing various ESKAPE pathogens.[52-54] We selected four *P. aeruginosa* strains

that were susceptible to AMK and MEM, susceptible to AMK and resistant to MEM, susceptible to MEM and resistant to AMK, and resistant to both AMK and MEM, and four that were susceptible to TOB and MEM, susceptible to TOB and resistant to MEM, susceptible to MEM and resistant to TOB, and resistant to both TOB and MEM, and performed combination studies to investigate potential synergistic effects between AGs (AMK and TOB) and carbapenems (MEM and IPM (*Note*: MIC values for IPM alone are presented in Table 5.6)) *via* standard checkerboard assays. Our results, however, suggested no synergistic effects between these two classes of antimicrobial agents with the fractional inhibitory concentration index (FICI) ranging from 0.625 to 2. This result added on to the existing dispute on whether AG and carbapenem combination therapy could be potentially helpful to patients with *P. aeruginosa* infections, and the answer is embedded in the intrinsic diversity of *P. aeruginosa* and the resistance mechanism(s) that it harbors.[40-43]

Table 5.6. MIC values of IPM (μg/mL) against selected *P. aeruginosa* clinical isolates.

Strain	MIC	S/R
1	4	I
15	16	R
26	2	S
28	16	R
33	32	R
50	64	R
99	2	S
116	>128	R

The resistance cutoff values for IPM against *P. aeruginosa* are ≤2 (S) and ≥8 (R) according to the Performance Standards for Antimicrobial Susceptibility Testing; Twenty-Fourth Informational Supplement from CLSI in 2014.[44]

5.3. CONCLUSIONS

By evaluating the resistance profile of various AGs and carbapenems of 122 *P. aeruginosa* clinical isolates, we found that the correlation in the resistance between two AGs, and the correlation between the resistance to AGs and that to carbapenems suggested a variety of

antibiotic resistance mechanisms in addition to the presence of AMEs. Specifically, we discovered that the presence of *aac(6')-Ib*, whether alone or in the presence of other AMEs, led to higher rates of resistance to various antibiotics involved in this study, whereas the presence of *aph(3')-Ia* did not, even though the latter was present at a higher frequency in these *P. aeruginosa* strains. However, these observations only revealed a small portion of the complex resistance mechanisms to various antibiotics. Thus, our study confirmed the unlikeliness of a single "standard treatment" for all *P. aeruginosa* infections. Instead, personalized therapies that take advantage of the genetic information of the isolated bacteria, such as resistance gene screening, should be utilized to aid in the selection of antimicrobial agents for determination of treatment regiment in order to account for the complex nature of *P. aeruginosa*.

5.4. MATERIALS AND METHODS

5.4.1. Materials and instrumentation

All *P. aeruginosa* strains involved in this study were obtained from the University of Kentucky Hospital System. All PCR reagents, including Phusion DNA polymerase, as well as ladders for DNA gel electrophoresis were purchased from New England BioLabs (NEB, Ipswich, MA). Primers used in PCR reactions and Mueller Hinton broth were purchased from Sigma-Aldrich (Milwaukee, WI). InstaGene Matrix was manufactured by Bio-Rad® (Hercules, CA). All antibiotics used in this study, including AGs (AMK, APR, GEN, NET, SIS, and TOB) and carbapenems (MEM and IPM) were purchased from AK Scientific (Mountain View, CA). Data were analyzed and plotted in Sigma Plot 12.3 and Prism 7.

5.4.2. Susceptibility testing for AGs and carbapenems

The MIC values of all AGs and MEM were determined against all 122 clinical isolates (Table 5.1), and the MIC values of IPM were determined for a small portion of the clinical isolate library (Table 5.6) comprising the strains used for MEM and IPM combination study with AGs. Using the broth microdilution method according to guidelines from the CLSI,[55] a 100 μL aliquot of a bacterial culture in its exponential phase were incubated with 100 μL of the various antibiotics (final concentration range of 0.5-128 μg/mL) for 16 h and then visually inspected for growth. The resistance breakpoint values for each of the various antibiotics against *P. aeruginosa* strains were as follows: AMK (S ≤16, I = 32, R ≥64), GEN (S ≤4, I = 8, R ≥16), NET (S ≤8, I = 16, R ≥32), TOB (S ≤4, I = 8, R ≥16), MEM (S ≤2, I = 4, R ≥8), and IPM (S ≤2, I = 4, R ≥8) according to the CLSI.[44] The resistance cutoff values for SIS against *P. aeruginosa* have not been established in U.S.A. and are considered to be S ≤4 and R >4 in this study.[45, 56] Statistical analyses were performed by using Prism 7 and all values were transformed to $\log_2$ scale prior to analysis. Comparisons between groups of clinical isolates susceptible or resistant to a certain antibiotic were made by two-tailed Mann-Whitney test. Significance was defined as P ≤0.05. Significance levels were defined in further detail as 0.033, 0.002, <0.001, which were marked in figures by *, **, and ***, respectively. Please note that in order to use the Mann-Whitney test for continuous variable, we considered all MIC values that were >128 μg/mL to be 256 μg/mL for the sake of the test and all that were ≤0.25 μg/mL to be 0.25 μg/mL.

5.4.3. Screen for AME genes by PCR

The presence of *aac(6')-Ib*, *aac(3)-IV*, *ant(2")-Ia*, and *aph(3')-Ia* genes was evaluated by PCR using specific primers, as previously described.[51, 57] A 40 μL aliquot of an overnight Mueller Hinton liquid culture of each *P. aeruginosa* strain were centrifuged at 13,000 rpm for 1 min to collect the bacteria, which were then mixed with 100 μL of InstaGene Matrix and heated up at 100 °C for 30 min. The PCR program was also previously described.[51, 57] The expected sizes were 482 bp, 230 bp, 534 bp, and 624 bp for *aac(6')-Ib*, *aac(3)-IV*, *ant(2")-Ia*, and *aph(3')-Ia*, respectively (Figure 5.7 and Table 5.4). Statistical analyses were performed by using GraphPad Instat and Prism 7 software as described in the section above. Comparisons between two groups or three groups of clinical strains were made by two-tailed Mann-Whitney test or Kruskal Wallis test.

5.4.4. Combination studies of AGs and carbapenem by checkerboard assays

In order to assess the interactions between AGs and carbapenem antibiotics, combination studies were performed using standard checkerboard assays with the concentration of AGs varied horizontally and that of MEM/IPM varied vertically. For each of AMK and TOB, we selected four distinct clinical isolates: one that was susceptible to both AG and MEM, one that was susceptible to AG and resistant to MEM, one that was resistant to AG and susceptible to MEM, and one that was resistant to both AG and MEM. The concentrations of antibiotics for each strain varied as follows: #1 (AMK: 0.008-4 μg/mL, MEM: 0.03-2 μg/mL, IPM: 0.13-8 μg/mL), #26 (AMK: 4 μg/mL, MEM: 0.06-4 μg/mL, IPM: 0.13-8 μg/mL), #50 (AMK: 0.03-16 μg/mL, MEM: 2-128 μg/mL, IPM: 2-128 μg/mL), #28 (AMK: 0.13-64 μg/mL, MEM: 0.5-32 μg/mL, IPM: 1-64 μg/mL), #99 (TOB: 0.004-2 μg/mL,

MEM: 0.06-4 μg/mL, IPM: 0.13-8 μg/mL), #116 (TOB: 0.06-32 μg/mL, MEM: 0.06-4 μg/mL), #33 (TOB: 0.004-2 μg/mL, MEM: 2-128 μg/mL, IPM: 1-64 μg/mL), and #15 (TOB: 0.25-128 μg/mL, MEM: 0.5-32 μg/mL, IPM: 1-64 μg/mL). The combination of TOB and IPM was not tested against strain #116 due to a higher than 128 μg/mL IPM MIC. After 16 h of incubation at 37 °C, bacterial growth was inspected visually and FICI values were calculated by adding the fractions of MIC of each drug in combination over MIC value of that drug alone for each of the two drugs. Drug interaction is defined as synergistic if FICI ≤0.5, indifferent if 0.5<FICI<4, antagonistic if FICI >4.[58]

5.5. ACKNOWLEDGEMENTS

This work was supported by NIH grant AI090048 (to S.G.-T.). S.Y.L.H. was in part supported by a University of Kentucky Presidential Fellowship. We thank Prof. David S. Burgess for sharing with us the clinical isolates that we used in this study.

This chapter is adapted from a published review article referenced as Holbrook, S. Y. L.; Garneau-Tsodikova, S. Evaluation of aminoglycoside and carbapenem resistance in a collection of drug-resistant *Pseudomonas aeruginosa* clinical isolates. *Microb. Drug Resist*. **2017**, doi: 10.1089/mdr.2017.0101.

5.6. AUTHORS' CONTRIBUTIONS

S.Y.L.H. performed all biological testing, write-up of the manuscript, and formatting the published manuscript into dissertation chapter. S.G.-T. contributed in the write-up and proof-reading the manuscript and later proof-reading the dissertation chapter.

Chapter 6. Repurposing antipsychotic drugs into antifungal agents: synergistic combinations of azoles and bromperidol derivatives in the treatment of various fungal infections

As the number of hospitalized and immunocompromised patients continues to rise, invasive fungal infections, such as invasive candidiasis and aspergillosis, threaten the life of millions of patients every year. The azole antifungals are currently the most prescribed drugs clinically that display broad-spectrum antifungal activity and excellent oral bioavailability. Yet, the azole antifungals have their own limitations and are unable to meet the challenges associated with increasing fungal infections and the accompanied development of resistance against azoles. Exploring combination therapy that involves the current azoles and another drug has been shown to be a promising strategy. Haloperidol and its derivative, bromperidol, were originally discovered as antipsychotics. Herein, we synthesize and report a series of bromperidol derivatives and their synergistic antifungal interactions in combination with a variety of current azole antifungals against a wide panel of fungal pathogens. We further select two representative combinations and confirm the antifungal synergy by performing time-kill assays. Furthermore, we evaluate the ability of selected combinations to destroy fungal biofilm. Finally, we perform mammalian cytotoxicity assays with the representative combinations against three mammalian cell lines.

6.1. INTRODUCTION

Fungal infections are an ever-growing global health problem. Even though fungal infections can affect both the healthy and the sick, they pose a much greater threat to

chronically ill and immunocompromised patients.[1] As the number of hospitalized and immunocompromised patients increases, the rise of fungal infections and the associated resistance problems are raising alarm. *Candida albicans* is a leading cause of fungal infections and accounts for up to 70% of total incidents worldwide.[2] Invasive candidiasis, a bloodstream infection of *Candida* species, is one of the most common nosocomial fungal diseases with an estimate of 350,000 incidents worldwide every year and a 30-55% mortality rate.[3-4] From 2000 to 2005, the number of invasive candidiasis in the U.S.A. rose by 52% and inevitably much more in less developed countries, such as Brazil and India. In addition to *Candida* species, some filamentous fungi, such as *Aspergillus*, also cause life-threatening infections. If left untreated, invasive aspergillosis can result in a 99% mortality rate, and therefore, is another fungal infection that is calling for immediate attention worldwide. For instance, the increasing use of corticosteroid in 4.8 million asthma patients is linked to over 400,000 patients developing chronic pulmonary aspergillosis.[5]

Fungi infect not only humans but also various food sources. From the Irish potato famine in the 19th century[6-7] to today's spread of *Puccina graminis tritici* Ug99, which is responsible for stem or black rust diseases on wheat,[8] fungal infections have never been solely a burden to clinical healthcare providers, but also to food production and quality control professionals. By infecting crops and livestock, fungi not only result in severe damage in the food production industry but can be spread to humans through food and cause diseases.

The challenges we face with fungal infections are evident and urgent, yet, our repertoire of antifungals is limited.[3] Currently, there are only few antifungal drugs for the treatment of systemic infections, including polyenes (*e.g.*, amphotericin B (AmB)), azoles (*e.g.*, fluconazole (FLC), itraconazole (ITC), ketoconazole (KTC), posaconazole (POS), and voriconazole (VOR); Figure 6.1A), and echinocandins (*e.g.*, caspofungin (CAS)), each of which has severe limitations. The intravenous drug AmB was the first antifungal agent approved for systemic use for invasive fungal infections over 50 years ago.[9] However, its dose-limiting toxicity and other adverse effects often result in interruption of treatment courses.[10] Another intravenous antifungal drug family, the echinocandins, was shown to possess lower toxicity and to be better tolerated than AmB in various formulations.[3] The broad-spectrum nature of the echinocandins has made them a better alternative to AmB for treating invasive fungal infections.

The azoles are the only class of oral antifungals identified due to their excellent oral bioavailability.[11-12] By targeting the sterol 14α-demethylase, azoles inhibit the biosynthesis of ergosterol, which is a vital component of the fungal cell membrane.[13-14] Inhibition of this enzyme causes the methylated sterol side products to accumulate inside the fungal cells, which is toxic to fungi and results in cell death. In addition to excellent bioavailability, the azole antifungals also exhibit fewer adverse effects than AmB. Consequently, the azole antifungals quickly became the most clinically prescribed antifungal class worldwide since their introduction to the market. However, azoles have their own limitations. Azoles inhibit cytochrome P450 enzymes, which results in undesired interference with the metabolism of numerous other drugs, making it difficult for patients

being treated with multiple concurrent medications.[15] Moreover, azoles are often found to be fungistatic towards many fungi, resulting in only temporary inhibition of fungal growth.[16] The lack of fungicidal activity has made it challenging to prevent fungal regrowth and the accompanied development of antimicrobial resistance to azoles.

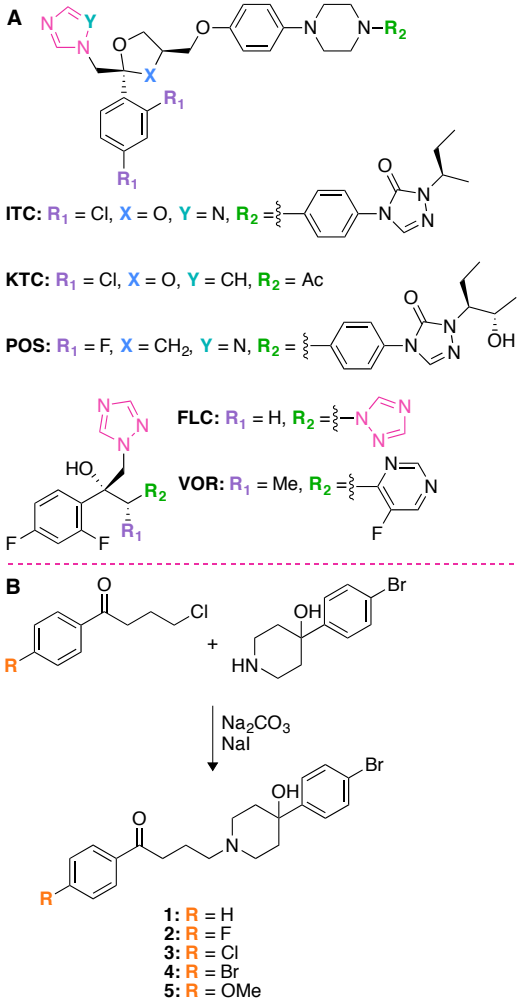

Figure 6.1. Structures of **A.** the common azole antifungals with the triazole pharmacophore highlighted in pink as well as **B.** the chemical synthesis of bromperidol series compounds (**1-5**) involved in this chapter.

Due to the clinical importance of azole antifungals, many research groups have tried to develop new azole antifungal therapies with broader antifungal spectra, reduced undesired

drug-drug interactions, and diminished other adverse effects. Besides developing new azole derivatives,[17-19] exploring various combination therapies that work synergistically with the current azole antifungals has proved fruitful.[20-22] For instance, various azoles were shown to display synergistic antifungal activity with a series of amphiphilic tobramycin derivatives with azoles inhibiting ergosterol biosynthesis and the tobramycin derivatives proposed to act on the fungal membrane integrity.[23-24] Sertraline, an antidepressant, was also found to work synergistically with FLC against cryptococcal infections.[25]

The benefits of repurposing existing drugs that have already been approved by the US Food and Drug Administration (FDA) for a new application against fungal infections extend beyond yielding potentially new antifungal therapies. The previous evaluations of the approved drugs from years of clinical studies can also provide valuable information about these drugs, such as their pharmacokinetics, pharmacodynamics, metabolism, and toxicity profiles. In the effort of repurposing existing drugs, several non-antifungal drugs were identified with antifungal activity and were summarized in a previous review article.[26] Haloperidol (trade name Haldol) is an FDA-approved oral antipsychotic that was recently discovered to possess antifungal activity towards a drug-sensitive *C. albicans* strain (*C. albicans* SC5314).[27] Bromperidol, a haloperidol derivative also with antipsychotic properties, was reported to kill mycobacteria in a synergistic manner with spectinomycin,[28] further suggesting that this antipsychotic drug may possess antimicrobial properties. Although the cellular antifungal target of haloperidol/bromperidol is still in debate, this antipsychotic drug can potentially be developed into a combination therapy with azoles as a new antifungal strategy.

Herein, we synthesized a series of bromperidol (**2**) and a series of its derivatives (**1** and **3-5**) (Figure 6.1B) and evaluated the combinational antifungal properties of these compounds with a variety of clinical azole antifungal drugs. We tested the combinations of five azoles (FLC, ITC, KTC, POS, and VOR) and compounds **1-5** against a wide selection of fungal strains, including seven *C. albicans*, one non-*albicans Candida* (*C. glabrata*), and one filamentous fungus (*A. terreus*). After assessing the synergistic effect between the azole antifungals and compounds **1-5**, we further performed time-kill assays to evaluate this antifungal strategy in a time- and dose-dependent manner. Moreover, we evaluated the combination of bromperidol (**2**) and selected azole antifungals for its ability to disrupt yeast biofilm in a representative *C. albicans* strain. Finally, we performed mammalian cytotoxicity assay with three selected mammalian cell lines in order to estimate the mammalian cytotoxicity exerted by the combinations of compounds **1-5** and azole antifungals.

6.2. RESULTS AND DISCUSSION

6.2.1. Chemical synthesis of bromperidol and its derivatives

In this study, we aim to evaluate the antifungal activity of the combination of common azole antifungals (FLC, ITC, KTC, POS, and VOR, Figure 6.1A) and bromperidol (**2**) as well as its derivatives (**1** and **3-5**) (Figure 6.1B) against nine fungal pathogens. Each of the nine fungal strains tested in this study also presents distinct biology and a complex resistance profile. The bromperidol series compounds (**1-5**) were synthesized by a reaction of 4-(4-bromophenyl)-4-hydroxypiperidine with different 4-chlorobutyrophenone

derivatives in the presence of sodium iodide and sodium carbonate (Figure 6.1B). The substituents at the R position of the five compounds varied in size and included a hydrogen atom, halogens (*e.g.*, fluorine, chlorine, and bromine), and a methoxy group.

6.2.2. Antifungal synergy of the combinations of azole antifungals and bromperidol series compounds 1-5 by checkerboard assays

Prior to evaluating the combinational antifungal effect of azoles and compounds **1-5**, we first determined the minimum inhibitory concentration (MIC) values of each drug against a variety of fungal pathogens to examine their innate antifungal effect and better gauge for an appropriate concentration range to use for the following checkerboard assay (Tables 6.1 and 6.3, displayed as MIC_{alone}). We first selected two representative *C. albicans* strains (strains *B* and *F*) (Table 6.1). *C. albicans* ATCC 10231 (strain *B*) is sensitive to most azoles whereas *C. albicans* ATCC 64124 (strain *F*) displays resistance to most azoles tested. The MIC values of the azole antifungals against some fungal strains determined in this study were in agreement with previously reported values.[17] Furthermore, we observed no antifungal effect for compounds **1-5** when tested alone.

We then tested the synergistic antifungal effects of the five azoles and compound **1-5** in combination by checkerboard assays and calculated the fractional inhibitory concentration index (FICI) against strains *B* and *F* (Table 6.1). The FICI cutoff values for determining synergy are: synergistic (SYN) if FICI $\leq$0.5, additive (ADD) if 0.5<FICI$\leq$4, antagonistic (ATG) if FICI >4.[29] In some cases where the FICI was >0.5, however, we observed a significant decrease in the MIC values of at least one of the drugs in the combinations. In

such cases, we further defined partial synergy (pSYN) as 0.5<FICI≤0.75 (indicating that both drugs showed reduction in MIC values and one drug showed ≥2-fold reduction in MIC value), and strong additive effect (ADD*) where one drug showed ≥2-fold reduction in MIC value. We deemed defining these two categories necessary, as with these combinations, we would still be able to use low level of azoles in combination to achieve a similar antifungal effect as using high concentrations of azoles alone, which would alleviate azole-induced toxicity and side effects. One thing to note is that due to the resistant nature of some fungal strains and the insufficient antifungal activity of the tested drugs, we were unable to achieve full inhibition of fungal growth with some drugs, therefore, resulting in unbound MIC values such as >32 μg/mL for most azoles and >128, >64, and >32 μg/mL for most bromperidol derivatives. In these cases, we considered the MIC values to be 32 μg/mL for the azoles and 128, 64, and 32 μg/mL for compounds **1-5**, respectively, in order to calculate a bound FICI value. However, this approximation would produce overestimated FICI values that are higher than the true FICI values if the real MIC values could be determined. Hence, the amount of synergy observed in this study (both in terms of the FICI value for each combination and in terms of the percentage of combinations with synergy) would be an underestimation of the real potential synergy.

Table 6.1. The combinational effect of various azoles and compounds **1-5** against two representative *C. albicans* strains.

Cpd	Azole	Strain	MIC alone (μg/mL) Azole	MIC alone (μg/mL) Cpd	MIC in combo (μg/mL) Azole	MIC in combo (μg/mL) Cpd	FICI	Interp.
1	FLC	*B*	>32	>64	32	64	2.00	ADD
		F	>32	>64	>32	>64	2.00	ADD
	ITC	*B*	1	>64	0.5	64	1.50	ADD
		F	>32	>64	>32	>64	2.00	ADD
	KTC	*B*	1	>64	1	>64	2.00	ADD
		F	8	>64	4	32	1.00	ADD
	POS	*B*	1	>64	0.5	16	0.75	pSYN
		F	>32	>64	2	8	0.19	SYN
	VOR	*B*	1	>64	0.5	8	0.63	pSYN
		F	>32	>64	8	32	0.75	pSYN
2	FLC	*B*	>32	128	32	64	1.50	ADD
		F	>32	128	32	64	1.50	ADD
	ITC	*B*	1	128	0.25	64	0.75	pSYN
		F	>32	128	2	64	0.56	pSYN
	KTC	*B*	1	>128	0.5	32	0.75	pSYN
		F	16	>128	4	64	0.75	pSYN
	POS	*B*	0.5	128	0.125	64	0.75	pSYN
		F	>32	128	4	4	0.16	SYN
	VOR	*B*	0.5	128	0.25	32	0.75	pSYN
		F	>32	128	4	8	0.19	SYN
3	FLC	*B*	>32	>32	32	16	1.50	ADD
		F	>32	>32	>32	>32	2.00	ADD
	ITC	*B*	1	>32	1	>32	2.00	ADD
		F	>32	>32	>32	>32	2.00	ADD
	KTC	*B*	2	>32	0.5	16	0.75	pSYN
		F	8	>32	4	0.5	0.52	pSYN
	POS	*B*	1	>32	0.5	4	0.63	pSYN
		F	>32	>32	2	4	0.19	SYN
	VOR	*B*	1	>32	0.25	16	0.75	pSYN
		F	>32	>32	4	16	0.63	pSYN
4	FLC	*B*	>32	>64	>32	>64	2.00	ADD
		F	>32	>64	>32	>64	2.00	ADD
	ITC	*B*	1	>64	0.5	64	1.50	ADD
		F	>32	>64	>32	>64	2.00	ADD
	KTC	*B*	2	>64	1	1	0.52	pSYN
		F	8	>64	4	1	0.52	pSYN
	POS	*B*	1	>64	0.5	32	1.00	ADD
		F	>32	>64	4	16	0.38	SYN
	VOR	*B*	1	>64	0.5	32	1.00	ADD
		F	>32	>64	4	32	0.63	pSYN
5	FLC	*B*	>32	>128	>32	>128	2.00	ADD
		F	>32	>128	>32	>128	2.00	ADD
	ITC	*B*	1	>128	1	>128	2.00	ADD
		F	>32	>128	>32	>128	2.00	ADD
	KTC	*B*	1	>128	1	>128	2.00	ADD
		F	8	>128	4	64	1.00	ADD
	POS	*B*	1	>128	1	>128	2.00	ADD
		F	>32	>128	2	8	0.13	SYN
	VOR	*B*	1	>128	0.5	32	0.75	pSYN
		F	>32	>128	8	128	1.25	ADD*

Strains: *B* = *C. albicans* ATCC 10231, *F* = *C. albicans* ATCC 64124.
The FICI cutoff values for determining synergy are: synergistic (SYN) if FICI ≤0.5, additive (ADD) if 0.5<FICI≤4, antagonistic (ATG) if FICI >4.
Note: Where the highest concentration of a compound or azole drug alone did not achieve optical growth inhibition, the MIC_{alone} value used in the FICI calculation is the highest concentration tested of that compound or azole drug.

Indicates synergy (SYN, both drugs showed ≥2-fold reduction in MIC value).
Indicates partial synergy (pSYN, both drugs showed decrease in MIC value and one drug showed ≥2-fold reduction in MIC value).
Indicates strong additive effect (ADD*, only one drug showed ≥2-fold reduction in MIC value).
Indicates weak additive effect (ADD, neither of the drugs showed ≥2-fold reduction in MIC value).

Of the 25 combinations tested against strains *B* and *F* in the first round, we found six combinations (24% of all combinations) to be synergistic with FICI values ranging from 0.13 to 0.5 against the azole-resistant strain *F*. The best combination with the lowest FICI value of 0.13 observed was compound **5** and POS, which showed decrease of MIC_{alone} of azole and compound **5** from >32 and >128 μg/mL to 2 and 8 μg/mL (16-fold reduction in MIC values for both drugs), respectively. The second-best combination discovered with an FICI value of 0.16 was with compound **2** and POS, which showed decrease of MIC_{alone} of

azole and compound **2** from >32 and 128 μg/mL to 4 (8-fold MIC reduction) and 4 μg/mL (32-fold MIC reduction), respectively. In these cases, we demonstrated that the combinations of azoles and bromperidol derivatives could synergistically inhibit the growth of an azole-resistant *C. albicans* that otherwise would not have responded to high concentrations of either drugs given in the assay. Amongst the six combinations that display synergy, four of them (compound **1** with POS, compound **2** with POS or VOR, and compound **3** with POS) were also found to display partial synergy ($0.5<FICI\leq0.75$) against strain *B*. Moreover, partial synergy was also observed against both strains *B* and *F* for the following combinations: compound **1** with VOR, compound **2** with ITC or KTC, compound **3** with KTC or VOR, and compound **4** with KTC. For example, with the combination of compound **2** and ITC against strain *F* (FICI = 0.56), inhibition of fungal growth could be achieved with 2 μg/mL of ITC (16-fold MIC reduction) and 64 μg/mL of compound **2** (1-fold MIC reduction). Partial synergy was also detected for compound **4** with VOR against strain *F* as well as for compound **5** with VOR against strain *B*. With the FICI values calculated in this study likely to be overestimated as explained above, these combinations with partial synergy also have great potentials for being developed into synergistic antifungal therapies.

Besides the combinations found to exert synergistic or partial synergistic effect between the azole antifungals and our bromperidol derivatives, we also found one combination to display strong additive effect, which is the combination of VOR and compound **5** against strain *F*. An FICI value of 1.25 indicated that this combination displayed additive effect. However, looking at the MIC values of each drug alone and in combination, we found a

significant decrease (4-fold reduction) in the MIC of VOR in combination compared to that of VOR alone even though the MIC value of compound **5** showed no further decrease from 128 μg/mL. This suggested that the addition of compound **5** significantly reduced the amount of VOR required to inhibit fungal growth, alleviating the toxicity and other undesired side effects of azole antifungals. The rest of the combinations (11 out of 25 combinations) displayed weak additive effect against both strains *B* and *F* with FICI values ranging from 1.00 to 2.00. No antagonism was found in any combinations tested in this study.

When we collected all FICI values for these 25 combinations in Table 6.2 and analyzed them in a heat map style table, it became clear that all synergistic combinations discovered so far involve either POS or VOR. Of the five combinations involving POS, 100% displayed synergy against the azole-resistant *C. albicans* strain *F*, and 60% displayed partial synergy against strain *B*. Of all the combinations involving VOR, only one combination (that with compound **2**) was found to be synergistic against strain *F*. Meanwhile, four combinations with VOR showed partial synergy against strains *B* (compounds **1-3** and **5**) and *F* (**1**, **3**, and **4**). This demonstrated that the combination of azoles and bromperidol derivatives showed better results with the more resistant fungal strain *F*. Besides POS and VOR, we found that three combinations, compounds **2-4** with KTC, showed partial synergy against both fungal strains, and one combination, compound **2** with ITC, displayed partial synergy against both fungal strains. All the combinations involving FLC only displayed weak additive effect. This suggested that POS and VOR might be the best candidates for developing combination therapy with compounds **1-5**.

Table 6.2. FICI values of the combinations of 5 azoles and compounds **1-5** against two *C. albicans* strains.

		FLC		ITC		KTC		POS		VOR	
Cpd	R	*B*	*F*	*B*	*F*	*B*	*F*	*B*	*F*	*B*	*F*
1	H	2.00	2.00	1.50	2.00	2.00	1.00	0.75	0.19	0.63	0.75
2	F	1.50	1.50	0.75	0.56	0.75	0.75	0.75	0.16	0.75	0.19
3	Cl	1.50	2.00	2.00	2.00	0.75	0.52	0.63	0.19	0.75	0.63
4	Br	2.00	2.00	1.50	2.00	0.52	0.52	1.00	0.38	1.00	0.63
5	OMe	2.00	2.00	2.00	2.00	2.00	1.00	2.00	0.13	0.75	1.25

Strains: *B* = *C. albicans* ATCC 10231, *F* = *C. albicans* ATCC 64124.
The FICI cutoff values for determining synergy are: synergistic (SYN) if FICI ≤0.5, additive (ADD) if 0.5<FICI≤4, antagonistic (ATG) if FICI >4.

Indicates synergy (SYN, both drugs showed ≥2-fold reduction in MIC value).
Indicates partial synergy (pSYN, both drugs showed decrease in MIC value and one drug showed ≥2-fold reduction in MIC value).
Indicates strong additive effect (ADD*, only one drug showed ≥2-fold reduction in MIC value).
Indicates weak additive effect (ADD, neither of the drugs showed ≥2-fold reduction in MIC value).

When looking at the five synergistic combinations of POS and compounds **1-5** against strain *F*, we noticed that smaller R substituents in our compounds seemed to correlate with lower FICI values. The FICI values increased as the size of the R substituent increased from fluorine to bromine in compounds **2-4**. This may indicate that the small size of a fluorine atom as the R substituent in our compounds may be optimal for interacting with its cellular target in fungal cells and increase in the size of the R substituent may cause loss of engagement with the target due to steric hindrance. This postulation could also be observed by looking at the overall number of combinations that show synergistic tendency (synergy or partial synergy) amongst all 25 combinations tested in the first round. Compound **2**, with a fluorine substituent, showed the highest number of combinations (four out of five combinations) with synergistic tendencies. This number decreases as the size of the R substituent increases (from fluorine to bromine in compounds **2-4**). Compound **5**, with a methoxy substituent, showed the best synergistic effect in combination with POS with the lowest FICI value identified in this study so far. Although methoxy group is the largest R group amongst all five compounds in this study, the presence of an oxygen atom and the lowest FICI value of 0.13 might suggest either potential hydrogen bonding

involved in the interaction of compound **5** with its target or methoxy group, as a strong electron donating group, increased the π–π interaction of the connected phenyl ring with the target protein/enzyme.

With POS and VOR appearing to be the best azoles to develop combinational antifungal therapy with compounds **1-5**, we further expanded our fungal collection and tested the combination of either POS or VOR and compounds **1-5** against seven additional strains in order to better assess the potential synergy against a wide variety of pathogenic fungi with distinct biological features (Table 6.3). Amongst these seven additional fungal strains were five extra *C. albicans* strains, one non-*albicans Candida* strain (*C. glabrata*, strain *H*), and one filamentous fungus (*A. terreus*, strain *I*). All of these fungi are resistant to POS and VOR, except for *A. terreus*, which is sensitive to both of these azoles. The checkerboard assay results for POS and VOR in combination with compounds **1-5** against strain *B* and *F* from Table 6.1 were also listed in Table 6.3 for easy comparison.

Of the ten combinations listed in Table 6.3, each against nine fungal strains, we found seven combinations to display synergistic interactions. Compound **2** in combination with POS or VOR showed synergy against strains *F*, *G*, and *I* or *F* and *G*, respectively. Compound **3** with either POS or VOR exhibited synergistic interactions against strain *F*. The other compounds, **1**, **4**, and **5**, all demonstrated synergistic interactions when combined with POS against strains *F*. Compounds **4** and **5** also were found to be synergistic with POS against strains *H* and *I*, respectively. Furthermore, all ten combinations exhibited partial synergy against at least one fungal strain, four of which also displayed strong

additive effect against a variety of fungal strains (compound **1** with POS or VOR, compound **3** with POS, and compound **5** with VOR). The best combination appeared to be compound **2** and POS, as this combination exhibited synergistic interactions against three fungal strains and partial synergy against four out of the nine fungal strains we tested. No combinations were discovered to have antagonistic interactions (FICI>4). Additionally, we found that more combinations involving POS showed synergistic or partially synergistic effect compared to the combinations involving VOR. For instance, all five combinations involving POS displayed synergy, whereas only two out of five combinations involving VOR tested exhibited synergistic interactions. These data demonstrated better synergy from developing combination antifungal therapy with POS and bromperidol series derivatives.

In addition to the various *C. albicans* strains, we also observed synergy in the non-*albicans Candida*, *C. glabrata*, and the filamentous fungus, *A. terreus*. Amongst the ten combinations against *C. glabrata* (strain *H*), we found one combination (compound **4** with POS) to display strong synergy, four combinations (compounds **1**, **2**, and **5** with POS as well as compound **2** with VOR) to display partial synergy, and one combination (compound **1** with VOR) to display strong additive effect. Amongst the ten combinations against *A. terreus* (strain *I*), we found two combinations (compounds **2** or **5** with POS) to be synergistic, one combination to display partial synergy, and one combination to display strong additive effect. Overall, these data further suggested that combining azoles and compounds **1-5** as an antifungal strategy would be effective against a variety of fungal pathogens and benefit patients suffering from different fungal infections.

Table 6.3. Combinational effect of POS or VOR with compounds **1-5** against a variety of fungal strains.

Cpd	Azole	Strain	MIC alone (μg/mL)		MIC combo (μg/mL)		FICI	Interp.	Azole	Strain	MIC alone (μg/mL)		MIC combo (μg/mL)		FICI	Interp.
			Azole	Cpd	Azole	Cpd					Azole	Cpd	Azole	Cpd		
1	POS	*A*	>32	>64	1	64	1.03	ADD*	VOR	*A*	>32	>64	2	64	1.06	ADD*
		B	1	>64	0.5	16	0.75	pSYN		*B*	1	>64	0.5	8	0.63	pSYN
		C	>32	>64	>32	>64	2.00	ADD		*C*	>32	>64	>32	>64	2.00	ADD
		D	>32	>64	0.25	64	1.01	ADD*		*D*	>32	>64	>32	>64	2.00	ADD
		E	>32	>64	>32	>64	2.00	ADD		*E*	>32	>64	>32	>64	2.00	ADD
		F	>32	>64	2	8	0.19	SYN		*F*	>32	>64	8	32	0.75	pSYN
		G	>32	>64	0.125	64	1.00	ADD*		*G*	>32	>64	0.125	64	1.00	ADD*
		H	>32	>64	2	32	0.56	pSYN		*H*	>32	>64	0.25	64	1.01	ADD*
		I	1	>64	0.25	64	1.25	ADD*		*I*	0.5	>64	0.5	>64	2.00	ADD
2	POS	*A*	>32	>128	8	64	0.75	pSYN	VOR	*A*	>32	>128	0.5	64	0.52	pSYN
		B	0.5	128	0.125	64	0.75	pSYN		*B*	0.5	128	0.25	32	0.75	pSYN
		C	>32	>128	>32	>128	2.00	ADD		*C*	>32	>128	>32	>128	2.00	ADD
		D	>32	>128	0.5	64	0.52	pSYN		*D*	>32	>128	1	64	0.53	pSYN
		E	>32	>128	>32	>128	2.00	ADD		*E*	>32	>128	>32	>128	2.00	ADD
		F	>32	128	4	4	0.16	SYN		*F*	>32	128	4	8	0.19	SYN
		G	>32	>128	0.0625	64	0.50	SYN		*G*	>32	>128	0.125	64	0.50	SYN
		H	>32	>128	0.25	64	0.51	pSYN		*H*	>32	>128	0.25	64	0.51	pSYN
		I	1	>128	0.25	32	0.5	SYN		*I*	0.5	>128	0.5	>128	2.00	ADD
3	POS	*A*	>32	>32	1	16	0.53	pSYN	VOR	*A*	>32	>32	8	16	0.75	pSYN
		B	1	>32	0.5	4	0.63	pSYN		*B*	1	>32	0.25	16	0.75	pSYN
		C	>32	>32	0.5	32	1.02	ADD*		*C*	>32	>32	16	16	1.00	ADD
		D	>32	>32	2	16	0.56	pSYN		*D*	>32	>32	16	16	1.00	ADD
		E	>32	>32	0.5	16	0.52	pSYN		*E*	>32	>32	16	16	1.00	ADD
		F	>32	>32	2	4	0.19	SYN		*F*	>32	>32	4	16	0.63	pSYN
		G	>32	>32	0.5	16	0.52	pSYN		*G*	>32	>32	2	8	0.31	SYN
		H	>32	>32	>32	>32	2.00	ADD		*H*	>32	>32	>32	>32	2.00	ADD
		I	0.5	>32	0.5	>32	2.00	ADD		*I*	0.25	>32	0.25	>32	2.00	ADD
4	POS	*A*	>32	>64	>32	>64	2.00	ADD	VOR	*A*	>32	>64	>32	>64	2.00	ADD
		B	1	>64	0.5	32	1.00	ADD		*B*	1	>64	0.5	32	1.00	ADD
		C	>32	>64	>32	>64	2.00	ADD		*C*	>32	>64	>32	>64	2.00	ADD
		D	>32	>64	>32	>64	2.00	ADD		*D*	>32	>64	>32	>64	2.00	ADD
		E	>32	>64	>32	>64	2.00	ADD		*E*	>32	>64	>32	>64	2.00	ADD
		F	>32	>64	4	16	0.38	SYN		*F*	>32	>64	4	32	0.63	pSYN
		G	>32	>64	>32	>64	2.00	ADD		*G*	>32	>64	>32	>64	2.00	ADD
		H	>32	>64	8	8	0.38	SYN		*H*	>32	>64	>32	>64	2.00	ADD
		I	0.5	>64	0.25	1	0.52	pSYN		*I*	0.25	>64	0.25	>64	2.00	ADD
5	POS	*A*	>32	>128	>32	>128	2.00	ADD	VOR	*A*	>32	>128	>32	>128	2.00	ADD
		B	1	>128	1	>128	2.00	ADD		*B*	1	>128	0.5	32	0.75	pSYN
		C	>32	>128	>32	>128	2.00	ADD		*C*	>32	>128	>32	>128	2.00	ADD
		D	>32	>128	>32	>128	2.00	ADD		*D*	>32	>128	>32	>128	2.00	ADD
		E	>32	>128	>32	>128	2.00	ADD		*E*	>32	>128	>32	>128	2.00	ADD
		F	>32	>128	2	8	0.13	SYN		*F*	>32	>128	8	128	1.25	ADD*
		G	>32	>128	>32	>128	2.00	ADD		*G*	>32	>128	>32	>128	2.00	ADD
		H	>32	>128	0.25	64	0.51	pSYN		*H*	>32	>128	>32	>128	2.00	ADD
		I	0.5	>128	0.125	32	0.50	SYN		*I*	0.25	>128	0.25	>128	2.00	ADD

Strains: *A* = *C. albicans* ATCC MYA-1003, *B* = *C. albicans* ATCC 10231, *C* = *C. albicans* ATCC MYA-1237, *D* = *C. albicans* ATCC MYA-2310, *E* = *C. albicans* ATCC MYA-2876, *F* = *C. albicans* ATCC 64124, *G* = *C. albicans* ATCC 90819, *H* = *C. glabrata* ATCC 2001, *I* = *A. terreus* ATCC MYA-3633.

The FICI cutoff values for determining synergy are: synergistic (SYN) if FICI ≤0.5, additive (ADD) if 0.5<FICI≤4, antagonistic (ATG) if FICI >4.

Note: Where the highest concentration of a compound or azole drug alone did not achieve optical growth inhibition, the MIC_{alone} value used in the FICI calculation is the highest concentration tested of that compound or azole drug.

Indicates synergy (SYN, both drugs showed ≥2-fold reduction in MIC value).

Indicates partial synergy (pSYN, both drugs showed decrease in MIC value and one drug showed ≥2-fold reduction in MIC).

Indicates strong additive effect (ADD*, only one drug showed ≥2-fold reduction in MIC value).

Indicates weak additive effect (ADD, neither of the drugs showed ≥2-fold reduction in MIC value).

6.2.3. Time-dependent antifungal activity of the combinations of azole antifungals and bromperidol series compounds

In order to confirm the synergistic interaction between our bromperidol series compounds and azole antifungals, we performed time-kill assays against strain *F* for two representative combinations (compound **2** and either POS or VOR) that displayed great synergy in previous checkerboard assays (Figure 6.2). In these time-kill assays, we evaluated the antifungal effect of each drug alone (POS, VOR, or compound **2**) as well as the two combinations (POS or VOR with compound **2**) at various concentrations (0.5×-8× MIC_{combo} of each drug). Overall, the combinations of POS or VOR and compound **2** showed fungistatic effect at 8× MIC_{combo} concentrations. The colony-forming unit (CFU)/mL values did not differentiate amongst various samples until after 6 h. In the first combination tested (POS + compound **2**), we saw significant growth in the growth control (increase in CFU/mL by 4 order of magnitude). Meanwhile, the POS or compound **2** alone samples showed slight inhibition of fungal growth similar to that of the 0.5× and 1× MIC_{combo} samples (increase in CFU/mL by about 1 order of magnitude). The combination sample with 4× MIC_{combo} showed stronger inhibition of fungal growth compared to the alone samples as well as the combination samples with less drugs. The combination sample with 8× MIC_{combo} showed complete inhibition of fungal growth and the CFU/mL value for this sample remained around 1×10^5 CFU/mL throughout 24 h. The growth of the fungus in each sample was further assessed by the addition of resazurin after the 24-h time point, which can be metabolized by live fungal cells and turns the solution from blue to pink. The combination of VOR and compound **2** showed a similar profile to that of the combination

of POS and compound **2**, except that the combination sample with 8× MIC_{combo} showed slight reduction in CFU/mL by about 1 log_{10} unit over 24 h.

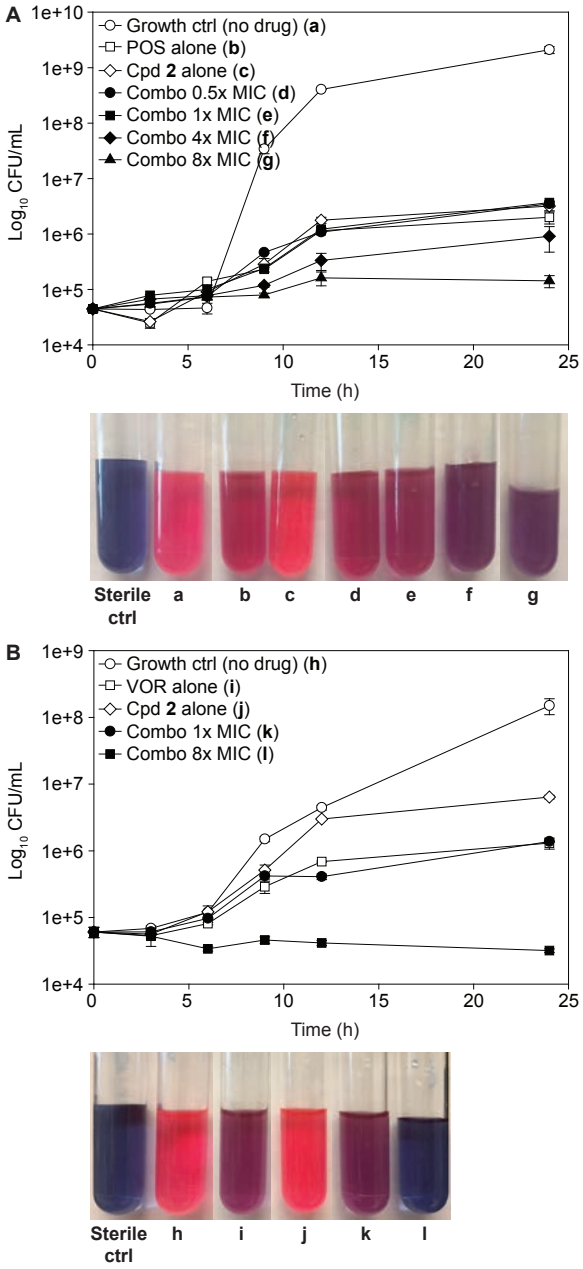

Figure 6.2. Time- and dose-dependent antifungal synergy of the combinations of **A.** POS or **B.** VOR and compound **2** at various concentrations against *C. albicans* ATCC 64124 (strain *F*). Each sample with resazurin added for visualization of fungal growth is presented underneath the growth curve for each combination.

6.2.4. Biofilm disruption with the combinations of representative azole antifungals and bromperidol series compounds

Recent discoveries suggest that fungi in biofilms display drastically different biology and antimicrobial susceptibility when compared to free living (planktonic) fungal cells.[30] Biofilm-forming (sessile) fungal cells are protected by extracellular matrices and display increased resistance against a variety of antifungal agents.[31-34] Using a water soluble metabolic dye, XTT (2,3-bis(2-methoxy-4-nitro-5-sulfo-phenyl)-2H-tetrazolium-5-carboxanilide), the metabolic activity of biofilm (sessile cells) can be measured in checkerboard format assays.[35] In this study, we selected two representative combinations (POS or VOR with compound **2**), which showed excellent synergy in the above checkerboard assay against strain *F*, and evaluated the antifungal effect that these combinations have on sessile cells (Table 6.4). We reported that the sessile cells of strain *F* are highly resistant to all drugs tested, including POS, VOR, and compound **2** alone with sessile MIC (SMIC) values of >32, >32, and >128 μg/mL, respectively. When tested in combination, both combinations failed to show strong synergy as observed in checkerboard assay in planktonic fungal cells. Instead, both combinations showed strong additive antifungal effect with FICI values of 1.02 (the SMIC value of compound **2** in combination did not decrease by much compared to that alone, the SMIC values of POS or VOR both decreased significantly from >32 to 0.5 μg/mL). This result suggested great antifungal potential of the combination of azoles and bromperidol series compounds as well as the more resistant nature of the sessile fungal cells compared to planktonic cells.

Table 6.4. Inhibition of biofilm formation with azoles and compound **2** combinations.

Cpd	Azole	Strain	SMIC alone (μg/mL)		SMIC combo (μg/mL)		FICI	Interp.
			Azole	Cpd	Azole	Cpd		
2	POS	*F*	>32	>128	0.5	128	1.02	ADD*
	VOR	*F*	>32	>128	0.5	128	1.02	ADD*

Strain *F* = *C. albicans* ATCC 64124.
The FICI cutoff values for determining synergy are: synergistic (SYN) if FICI ≤0.5, additive (ADD) if 0.5<FICI≤4, antagonistic (ATG) if FICI >4.
Since the highest concentration of compound **2** or azole alone did not achieve complete growth inhibition, the MIC_{alone} value used in the FICI calculation is the highest concentration tested of compound **2** or azole drugs.
ADD* indicates strong additive effect (one drug showed ≥2-fold reduction in MIC value).

6.2.5. Mammalian cytotoxicity of the combinations of representative azole antifungals and bromperidol series compounds

In addition to assessing the time-dependent killing and disruption of fungal biofilm, we also evaluated the mammalian cytotoxicity of azole antifungals and bromperidol (**2**) alone and in combination (Figure 6.3). In order to gain a better understanding of the toxicity profile towards different mammalian cells, we evaluated representative azoles (POS and VOR) and compound **2** against three different mammalian cell lines, including human bronchial epithelial cells BEAS-2B, human kidney epithelial cells HEK-293, and the murine macrophage J774A.1. Please note that as many xenobiotics stimulate cell growth instead of exerting toxicity at sub-IC_{50} concentrations,[23, 36-39] resulting in >100% cell survival in the treatment groups, we have considered these >100% cell survival data as no observed toxicity and expressed them as 100% cell survival. When testing the azole antifungals alone (Figure 6.3A), we observed no cytotoxic effect up to 4 μg/mL. At 8 μg/mL, we observed 80 ± 9% cell survival with J774A.1 cells, and at 16 μg/mL, we observed around 45 ± 12% and 46 ± 3% cell survival POS-treated HEK-293 and J774A.1 cells, respectively. No cytotoxic effect was observed in any VOR-treated cell lines at any concentrations tested. With BEAS-2B and HEK-293 cells being more robust cell lines than J774A.1, we were not surprised to see the absence of toxicity in these two cell lines compared to that in J774A.1 cells, because macrophages are often short-lived and fragile

within the human body. We then assessed the toxicity of compound **2** alone as a representative of our bromperidol series derivatives (Figure 6.2B). We found no toxicity against BEAS-2B and HEK-293 cells at 64 μg/mL. Compound **2** alone exerted toxicity against J774A.1 cells and showed 72 ± 14%, 50 ± 7% and 30 ± 4% cell survival with 16, 32, and 64 μg/mL compound **2**, respectively. These findings suggested that our bromperidol series compounds had much better toxicity profiles against various mammalian cells and that the strategy of using our bromperidol series compounds in combination with azole antifungals can effectively help alleviate azole-induced toxicity by reducing the amount of azole antifungals required in treatment.

Since 8 μg/mL compound **2** was the highest concentration at which no cytotoxicity was observed with all three cell lines, we performed the cytotoxicity assay of POS and VOR against all three cell lines with 8 μg/mL compound **2** supplemented in the media (Figure 6.3C). We observed similar overall cytotoxic effect as in the azoles alone samples. The percent cell survivals were slightly lower at 8 or 16 μg/mL POS in combination compared to that of POS alone. Meanwhile, we observed no toxicity at 16 μg/mL VOR in combination with 8 μg/mL compound **2**. As J774A.1 is the most fragile cell line tested, we also tested the combination of azoles and a higher concentration of compound **2** (32 μg/mL) against the two epithelial cell lines (BEAS-2B and HEK-293 cells) (Figure 6.3D). Of the combination of POS and compound **2** against BEAS-2B cells, we observed 71 ± 11% and 38 ± 6% cell survival at 8 and 16 μg/mL POS. However, the combination toxicity of POS and 32 μg/mL compound **2** was more prominent against HEK-293 cells where we observed decreased cell survival from 80 ± 8% to 40 ± 6% as the concentration of POS increased

from 1 to 16 μg/mL. With 32 μg/mL compound **2**, we still noted no toxicity against either cell lines at any concentration of VOR, which proved the better toxicity profile of VOR compared to that of POS.

Judging from the results from cytotoxicity assays, POS seemed to be toxic to mammalian cells. Thus, developing combinational antifungal therapy that involves less POS and more of the nontoxic bromperidol (**2**) seemed to be a reasonable approach to alleviate azole-induced toxicity and other related side effects. In addition to the great potential of synergy between POS and bromperidol compounds, VOR also has great potential to be developed into combinational antifungal therapies due to its nontoxic nature.

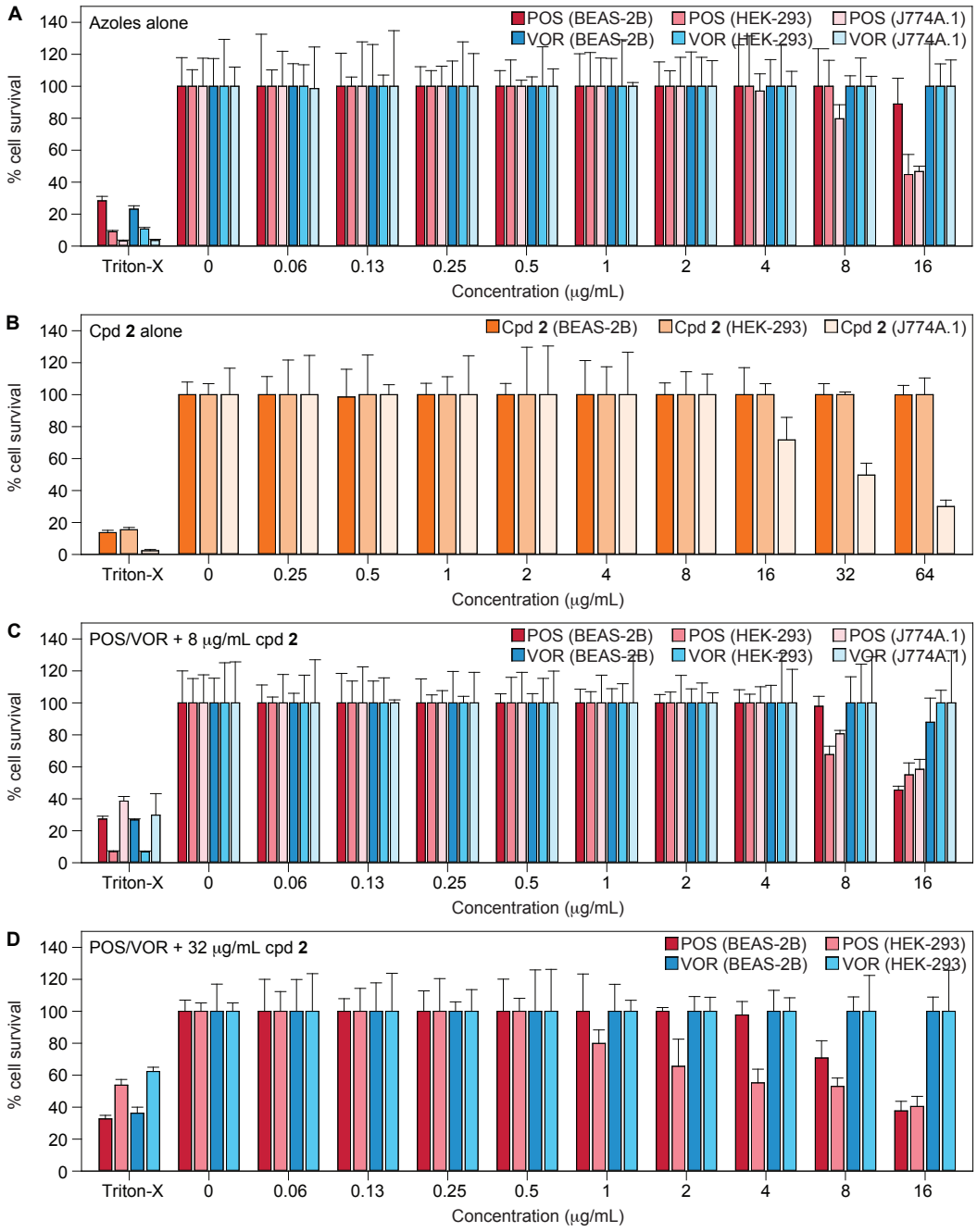

Figure 6.3. Mammalian cytotoxicity evaluation of **A.** POS and VOR alone, **B.** compound **2** alone, **C.** and **D.** representative combinations of azoles (POS or VOR) at various concentrations along with compound **2** at 8 μg/mL (panel **C**) or 32 μg/mL (panel **D**) supplemented in the media against BEAS-2B, HEK-293, and J774A.1 cells. *Note*: As at 32 μg/mL, compound **2** exerted toxicity against J774A.1 (as seen in panel **B**), this cell line was not tested in panel **D**.

Haloperidol/bromperidol, originally antipsychotic drugs, act on dopamine D2 receptors, which is a G protein-coupled receptor with P-glycoprotein properties.[40-41] However, as newly discovered antifungal candidates, their cellular target in fungal cells remained elusive. Although some reports indicated that haloperidol might target the biosynthesis and metabolism of amino acids[42] or fungal morphogenesis and hyphal formation[27, 43] in fungal pathogens, others pointed out that the multidrug-resistant transporter (MDR1), a p-glycoprotein, is more likely to be the antifungal target of this antipsychotic drug.[44] Inhibition of MDR1, an active transporter/efflux pump that contributes to efflux-related azole resistance, can further sensitize fungal pathogens to azole antifungals and prolong their antifungal effect. The bromperidol series compounds presented in this study, due to structural similarity, are also likely to exert their antifungal properties in the same way. Although determining the exact mechanism of action of bromperidol is outside of the scope of the current study, we wanted to offer a potential explanation for the synergy observed herein. This theory could also explain why the bromperidol series compounds possessed no antifungal activity by themselves but could produce great antifungal synergy in combination with various azoles. A recent study reported synergistic antifungal effect of FLC and VOR in combination with haloperidol as an MDR1 inhibitor against two *Malassezia* strains,[45] which also demonstrated the feasibility and benefits of developing new antifungal therapies with the combination of haloperidol or its derivatives and azole antifungals.

6.3. CONCLUSIONS

In this study, we evaluated the antifungal effect of bromperidol and four of its derivatives in combination with five clinically relevant azole antifungals against a wide variety of pathogenic fungi. From our extensive evaluation of the combinational antifungal effect between the two classes of compounds by checkerboard, time-kill, and biofilm disruption assays, we observed a wide range of combinational effects ranging from synergistic to weak additive effect. A considerable portion of the combinations tested in this study displayed synergy or partial synergy. We also found that POS displayed synergy in more combinations with bromperidol series compounds than VOR did. However, our cytotoxicity evaluation suggested combination therapy with VOR might have superior mammalian cytotoxicity profiles. As mentioned above, the FICI calculated in this study are likely to be higher than the true FICI values due to the unbound MIC values. Therefore, the potential synergy and the number of combinations showing synergistic effects are also likely to be underestimated. Even though the exact cellular target by which the bromperidol series compounds exert antifungal activity when combined with azole antifungals remains unclear, our results suggested that using these bromperidol derivatives in combination with clinically relevant azoles can synergistically inhibit fungal growth and effectively reduced the amount of azoles required to achieve an equivalent antifungal effect, and therefore, alleviate the toxicity and side effects resulted from administering high concentrations of azole antifungals.

6.4. MATERIALS AND METHODS

6.4.1. Chemistry Methodology

6.4.1.1. Materials and instrumentation for chemistry

All reagents were bought from commercial sources and no further purification was performed before usage. TLC analyses were performed on 0.25-mm thick silica gel plates (pre-coated on glass) with fluorescent indicator UV_{254}, and were visualized by UV or charring in a $KMnO_4$ stain. ^1H and ^{13}C NMR spectra were recorded on a 400 MHz NMR spectrometer (VARIAN INOVA) using $CDCl_3$, CD_3OD, or $(CD_3)_2SO$ as solvents. Chemical shifts were reported in parts per million (ppm) and were referenced to residual solvent peaks. All reactions were carried out under nitrogen gas with all yields reported representing isolated yields. All compounds were characterized by ^1H and ^{13}C NMR as well as mass spectrometry. Although compound **2** has been reported in the literature, its characterization has not been published in detail. NMR spectra confirm that all compounds are ≥95% pure. Further confirmation of compound purity was obtained by RP-HPLC, which was performed on an Agilent Technologies 1260 Infinity HPLC system by using the following general method 1: Flow rate = 1 mL/min; λ = 254 nm; column = Vydac 201SP^{TM} C18, 250 × 4.6 mm, 90A 5 μm; Eluents: A = H_2O + 0.1% TFA, B = MeCN; gradient profile: starting from 5% B, increasing from 5% B to 100% B over 20 min, holding at 100% B from 20-27 min, decreasing from 100% B to 5% B from 27-30 min. The HPLC column was equilibrated with 5% B for 15 min prior to each injection.

6.4.1.2. Synthesis and characterization of compounds used in this study

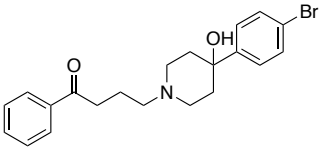

General procedure for the amination reaction (*e.g.*, synthesis of compound 1). Compound **1** was prepared following a previously published protocol for a similar molecule.[46] Sodium iodide (0.039 g, 0.260 mmol) and sodium carbonate (0.050 g, 0.472 mmol) were added to a stirred mixture of 4-chlorobutyrophenone (0.043 g, 0.236 mmol) and 4-(4-bromophenyl)-4-hydroxypiperidine (0.060 g, 0.236 mmol) in MeCN (2 mL). The reaction mixture was refluxed for 12 h. The mixture was diluted with H_2O, and extracted with CH_2Cl_2 (3×10 mL), dried over $MgSO_4$, and concentrated under reduced pressure. The residue was purified by column chromatography (SiO_2, MeOH:EtOAc/1:9, R_f 0.22), to give compound **1** (0.016 g, 17%) as a white solid: ^{1}H NMR (400 MHz, $CDCl_3$, Figure 6.4) δ 7.97 (d, J = 8.0 Hz, 2H), 7.54 (t, J = 7.2 Hz, 1H), 7.46 (d, J = 7.2 Hz, 2H), 7.42 (d, J = 8.0 Hz, 2H), 7.29 (d, J = 8.0 Hz, 2H), 3.00 (t, J = 6.8 Hz, 2H), 2.81 (m, 2H), 2.50 (t, J = 6.8 Hz, 2H), 2.44 (t, J = 12.0 Hz, 2H), 2.04-1.96 (m, 2H), 2.00 (p, J = 6.8 Hz, 2H), 1.66-1.63 (m, 3H); ^{13}C NMR (100 MHz, $CDCl_3$, Figure 6.5) δ 199.9, 147.3, 137.2, 132.9, 131.3, 128.5, 128.1, 126.4, 120.8, 71.1, 57.8, 49.2, 38.2, 36.2, 21.8; LRMS *m/z* calcd for $C_{21}H_{25}BrNO_2$ $[M+H]^+$: 402.1; found 402.7. Purity of the compound was further confirmed by RP-HPLC by using method 1: R_t = 7.75 min (97% pure; Figure 6.6).

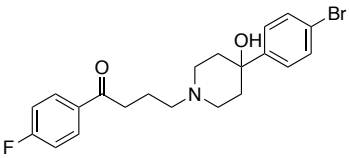

Synthesis of compound 2. Following the general procedure described for the synthesis of compound **1**, sodium iodide (0.039 g, 0.260 mmol), sodium carbonate (0.050 g, 0.472

mmol), 4'-fluoro-4-chlorobutyrophenone (0.047 g, 0.236 mmol), and 4-(4-bromophenyl)-4-hydroxypiperidine (0.060 g, 0.236 mmol) in MeCN (2 mL) were used to afford know compound **2** (also known as bromperidol)[47] (0.024 g, 24%, R_f 0.15 in MeOH:EtOAc/1:9) as a white solid: ^{1}H NMR (400 MHz, $CDCl_3$, Figure 6.7) δ 7.99 (dd, *J* = 8.4, 6.0 Hz, 2H), 7.43 (d, *J* = 8.4 Hz, 2H), 7.30 (d, *J* = 8.4 Hz, 2H), 7.11 (app. t, *J* = 8.4 Hz, 2H), 2.97 (t, *J* = 6.8 Hz, 2H), 2.79 (m, 2H), 2.48 (t, *J* = 6.8 Hz, 2H), 2.42 (t, *J* = 11.2 Hz, 2H), 2.04-1.94 (m, 2H), 1.98 (p, *J* = 6.8 Hz, 2H), 1.67-1.64 (m, 3H); ^{13}C NMR (100 MHz, $CDCl_3$, Figure 6.8) δ 198.3, 166.9, 164.3, 147.3, 133.61, 133.58, 131.3, 130.7, 130.6, 126.4, 120.9, 115.7, 115.5, 71.1, 57.8, 49.3, 38.2, 36.2, 21.8; LRMS *m/z* calcd for $C_{21}H_{24}BrFNO_2$ $[M+H]^+$: 420.1; found 420.7. Purity of the compound was further confirmed by RP-HPLC by using method 1: R_t = 7.93 min (95% pure; Figure 6.9).

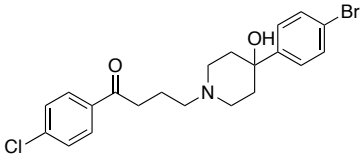

Synthesis of compound 3. Following the general procedure described for the synthesis of compound **1**, sodium iodide (0.039 g, 0.260 mmol), sodium carbonate (0.050 g, 0.472 mmol), 4'-chloro-4-chlorobutyrophenone (0.051 g, 0.236 mmol), and 4-(4-bromophenyl)-4-hydroxypiperidine (0.060 g, 0.236 mmol) in MeCN (2 mL) were used to afford compound **3** (0.024 g, 23%, R_f 0.21 in MeOH:EtOAc/1:9) as a white solid: ^{1}H NMR (400 MHz, $CDCl_3$, Figure 6.10) δ 7.89 (d, *J* = 8.4 Hz, 2H), 7.42 (d, *J* = 8.4 Hz, 4H), 7.31 (d, *J* = 8.4 Hz, 2H), 3.02 (t, *J* = 6.8 Hz, 2H), 2.97 (m, 2H), 2.77-2.68 (m, 2H), 2.66 (t, *J* = 6.8 Hz, 2H), 2.28-2.14 (m, 3H), 2.07 (p, *J* = 6.8 Hz, 2H), 1.74 (m, 2H); ^{13}C NMR (100 MHz, $CDCl_3$, Figure 6.11) δ 198.1, 146.6, 139.5, 135.1, 131.4, 129.5, 128.9, 126.4, 121.1, 70.4, 57.3, 49.1, 37.1, 36.0, 20.5; LRMS *m/z* calcd for $C_{21}H_{24}BrClNO_2$ $[M+H]^+$: 436.1; found

436.7. Purity of the compound was further confirmed by RP-HPLC by using method 1: R_t = 8.54 min (98% pure; Figure 6.12).

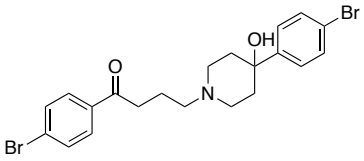

Synthesis of compound 4. Following the general procedure described for the synthesis of compound **1**, sodium iodide (0.039 g, 0.260 mmol), sodium carbonate (0.050 g, 0.472 mmol), 4'-bromo-4-chlorobutyrophenone (0.062 g, 0.236 mmol), and 4-(4-bromophenyl)-4-hydroxypiperidine (0.060 g, 0.236 mmol) in MeCN (2 mL) were used to afford compound **4** (0.034 g, 30%, R_f 0.24 in MeOH:EtOAc/1:9) as a white solid: ^{1}H NMR (400 MHz, $CDCl_3$, Figure 6.13) δ 7.81 (d, J = 8.0 Hz, 2H), 7.59 (d, J = 8.0 Hz, 2H), 7.43 (d, J = 8.8 Hz, 2H), 7.33 (d, J = 8.8 Hz, 2H), 3.14-3.07 (m, 2H), 3.06 (t, J = 6.4 Hz, 2H), 2.96-2.80 (m, 2H), 2.79-2.69 (m, 2H), 2.48-2.24 (m, 2H), 2.12 (p, J = 6.4 Hz, 2H), 1.78 (m, 2H); ^{13}C NMR (100 MHz, $(CD_3)_2SO$, Figure 6.14) δ 198.4, 135.9, 131.83, 131.77, 130.8, 130.0, 129.9, 127.1, 119.6, 68.8, 55.2, 48.5, 36.1, 35.4, 18.9; LRMS *m/z* calcd for $C_{21}H_{24}Br_2NO_2$ $[M+H]^+$: 480.0; found 480.7. Purity of the compound was further confirmed by RP-HPLC by using method 1: R_t = 8.66 min (99% pure; Figure 6.15).

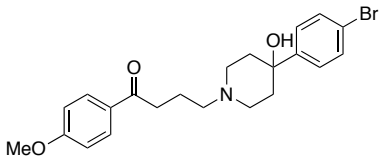

Synthesis of compound 5. Following the general procedure described for the synthesis of compound **1**, sodium iodide (0.039 g, 0.260 mmol), sodium carbonate (0.050 g, 0.472 mmol), 4'-methoxy-4-chlorobutyrophenone (0.050 g, 0.236 mmol), and 4-(4-bromophenyl)-4-hydroxypiperidine (0.060 g, 0.236 mmol) in MeCN (2 mL) were used

to afford compound **5** (0.013 g, 13%, R_f 0.20 in MeOH:EtOAc/1:9) as a white solid: ^{1}H NMR (400 MHz, $CDCl_3$, Figure 6.16) δ 7.95 (d, J = 8.4 Hz, 2H), 7.43 (d, J = 8.4 Hz, 2H), 7.32 (d, J = 8.4 Hz, 2H), 6.92 (d, J = 8.4 Hz, 2H), 3.85 (s, 3H), 2.95 (t, J = 6.8 Hz, 2H), 2.82 (m, 2H), 2.50 (t, J = 6.8 Hz, 2H), 2.45 (t, J = 11.6 Hz, 2H), 2.08-1.96 (m, 2H), 1.98 (p, J = 6.8 Hz, 2H), 1.67 (m, 2H), 1.62 (br s, 1H); ^{13}C NMR (100 MHz, CD_3OD, Figure 6.17) δ 199.5, 165.6, 148.1, 132.6, 131.7, 131.0, 128.0, 122.3, 115.1, 69.9, 56.2, 50.4, 49.6, 37.0, 36.1, 20.6; LRMS *m/z* calcd for $C_{22}H_{27}BrNO_3$ $[M+H]^+$: 432.1; found 432.7. Purity of the compound was further confirmed by RP-HPLC by using method 1: R_t = 8.22 min (95% pure; Figure 6.18).

6.4.1.3. Compound characterization

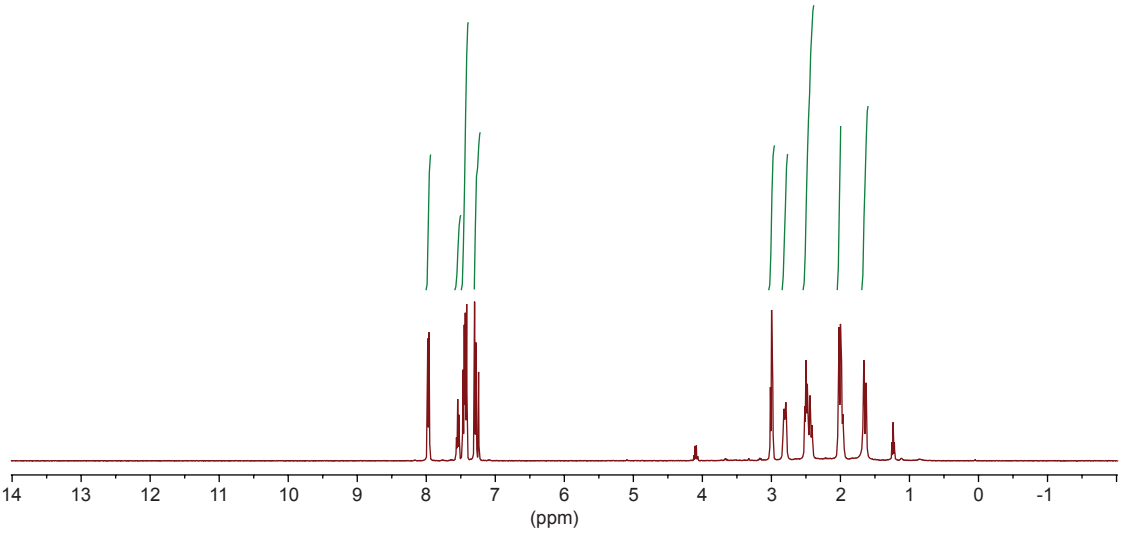

Figure 6.4. ^{1}H NMR spectrum for compound **1** in $CDCl_3$.

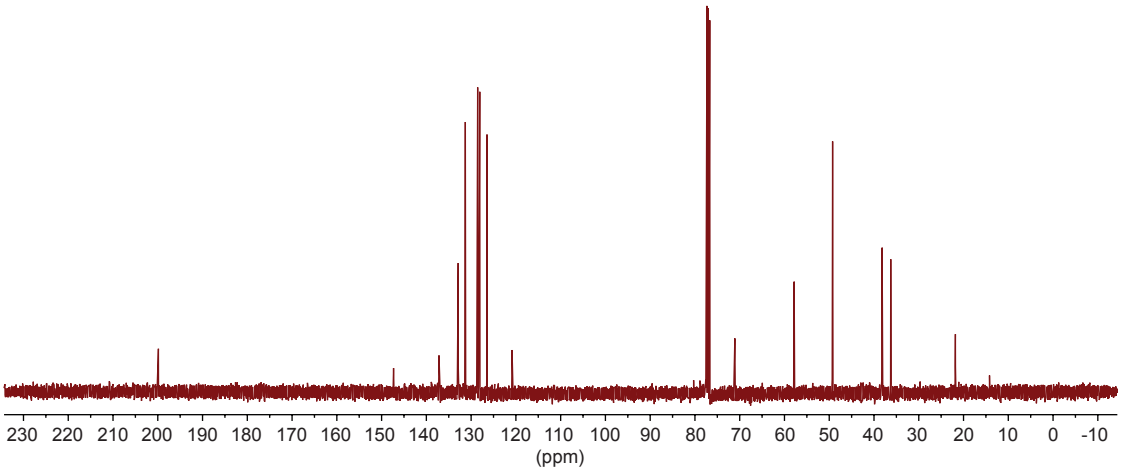

Figure 6.5. ^{13}C NMR spectrum for compound **1** in $CDCl_3$.

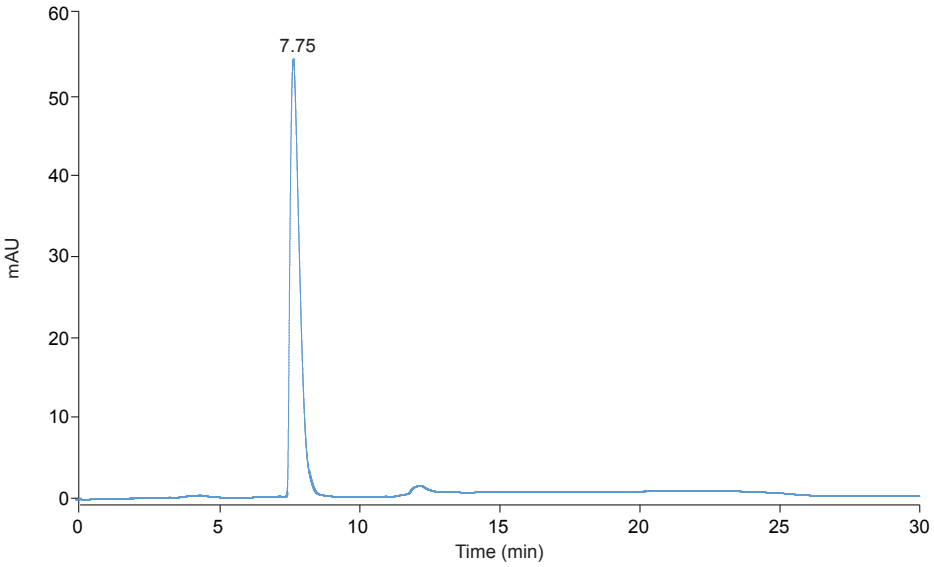

Figure 6.6. HPLC trace for compound **1**. R_t = 7.75 min.

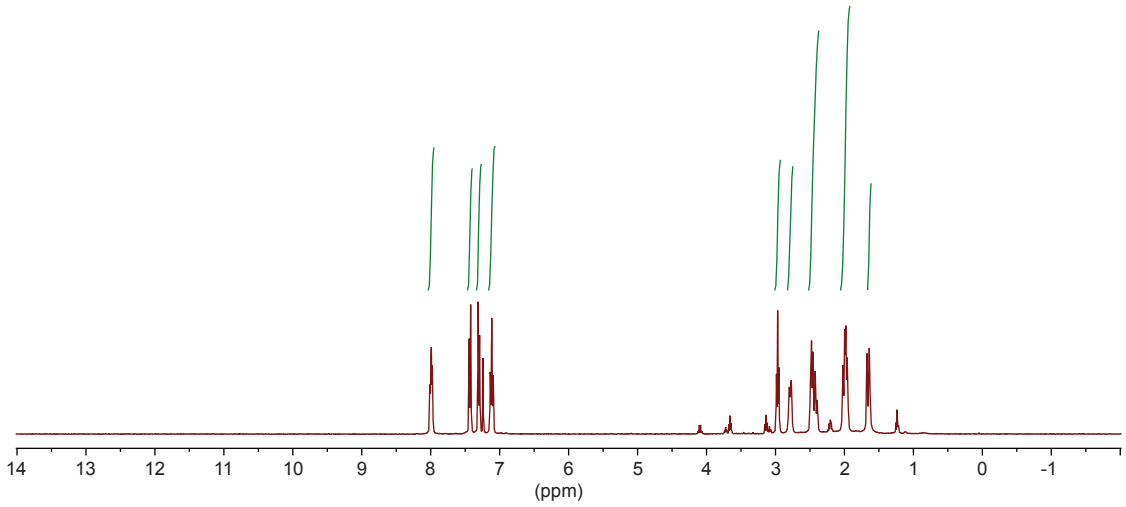

Figure 6.7. ^{1}H NMR spectrum for compound **2** in $CDCl_3$.

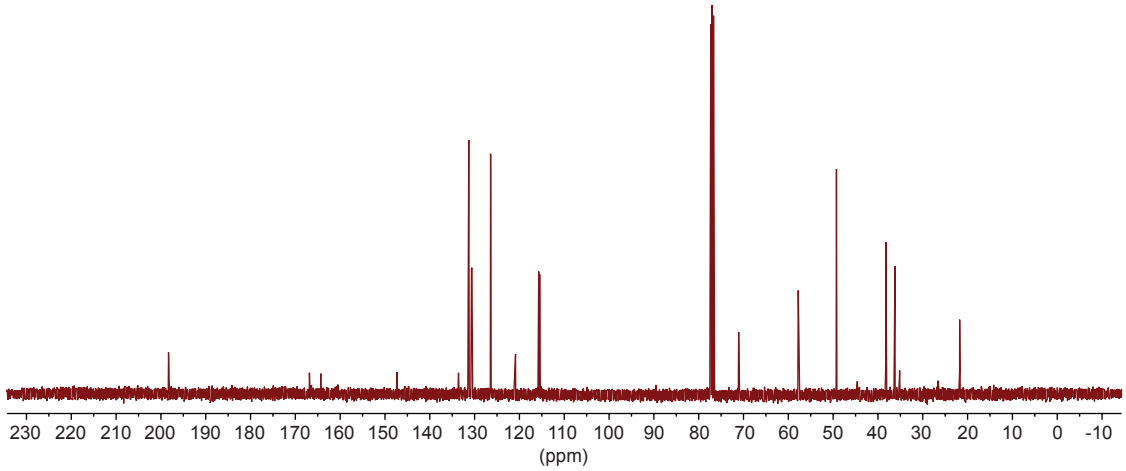

Figure 6.8. ^{13}C NMR spectrum for compound **2** in $CDCl_3$.

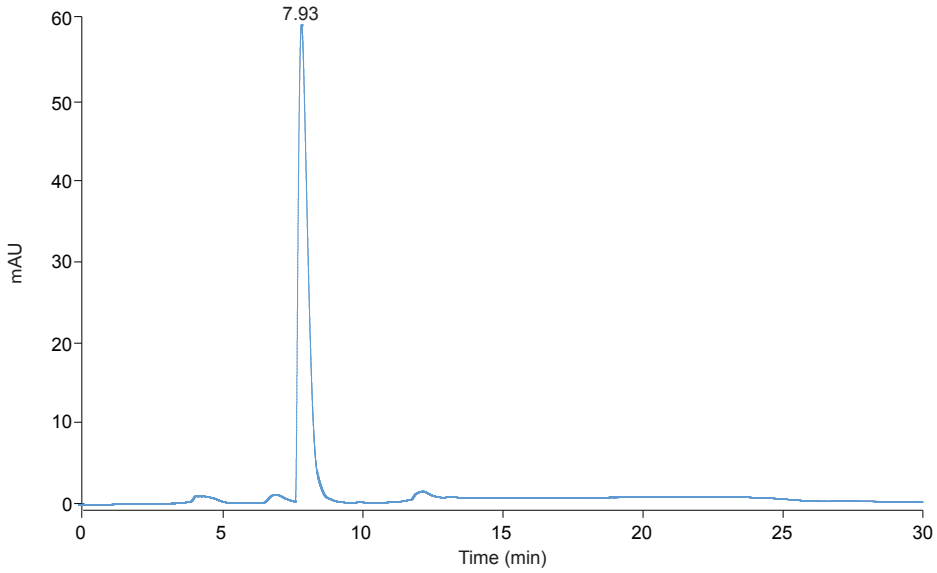

Figure 6.9. HPLC trace for compound **2**. R_t = 7.93 min.

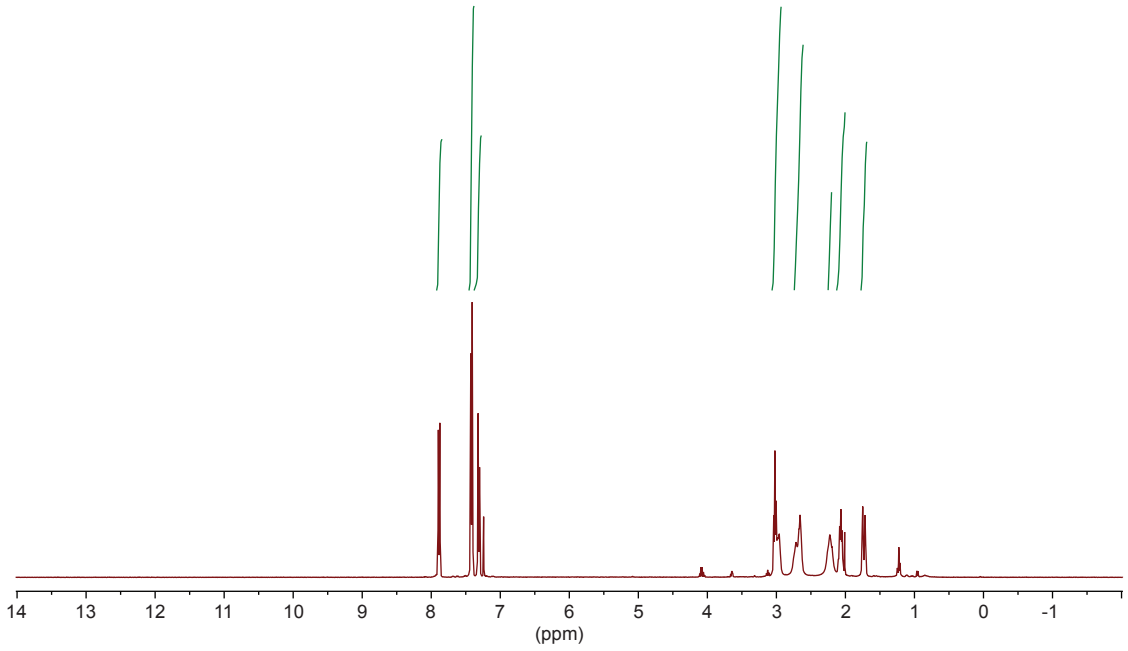

Figure 6.10. ^{1}H NMR spectrum for compound **3** in $CDCl_3$.

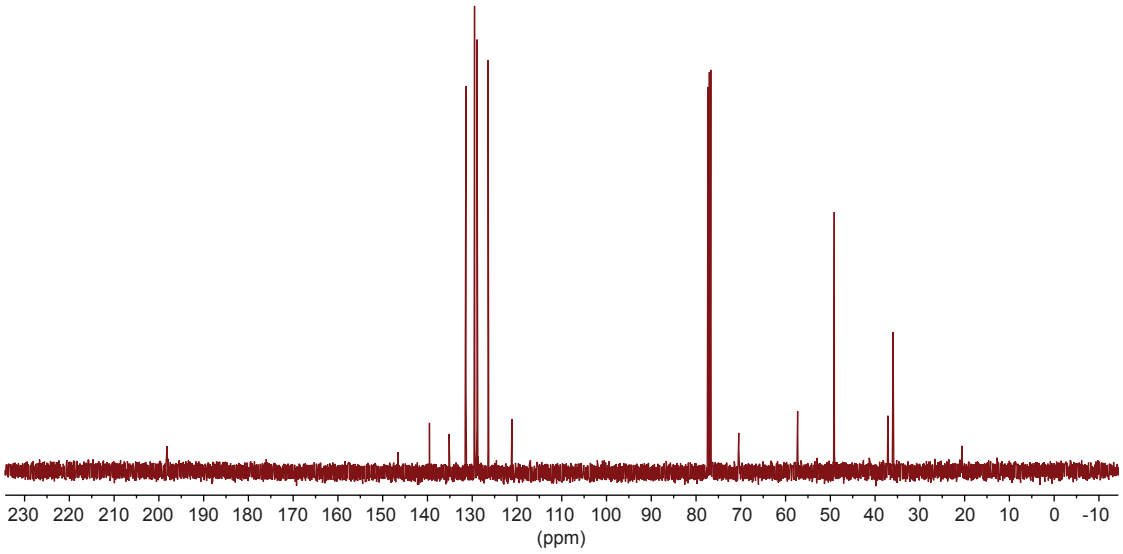

Figure 6.11. ^{13}C NMR spectrum for compound **3** in $CDCl_3$.

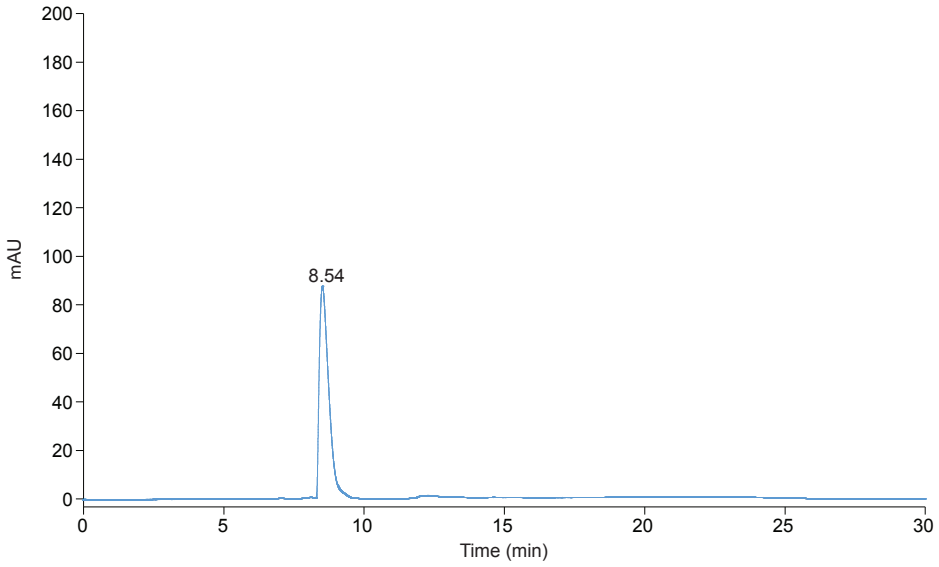

Figure 6.12. HPLC trace for compound **3**. R_t = 8.54 min.

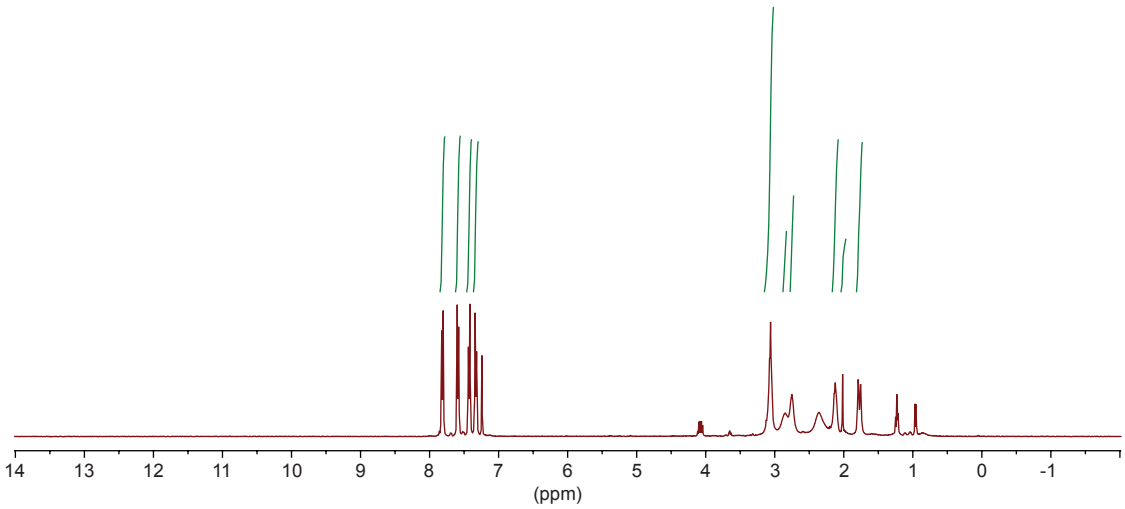

Figure 6.13. ^{1}H NMR spectrum for compound **4** in $CDCl_3$.

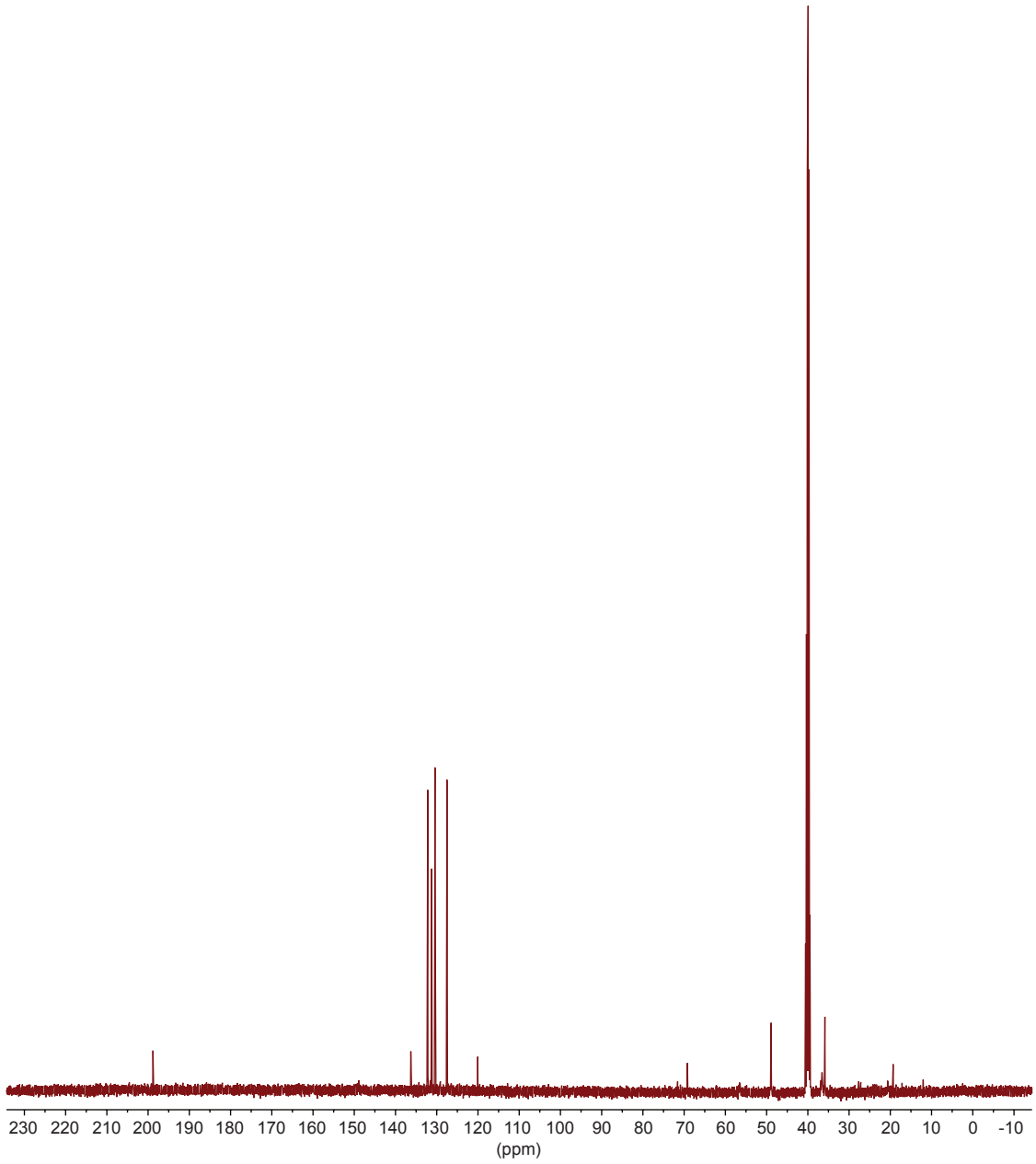

Figure 6.14. ^{13}C NMR spectrum for compound **4** in $(CD_3)_2SO$.

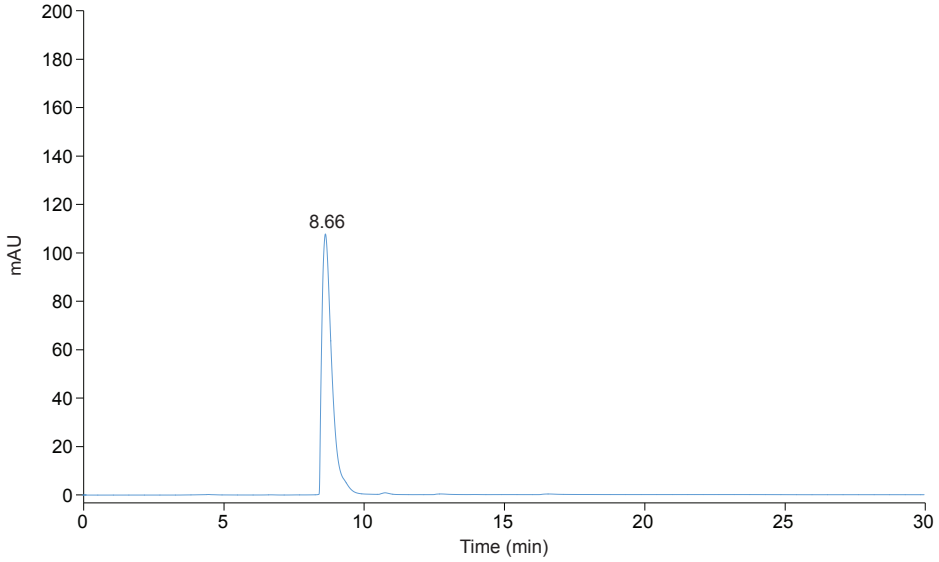

Figure 6.15. HPLC trace for compound **4**. R_t = 8.66 min.

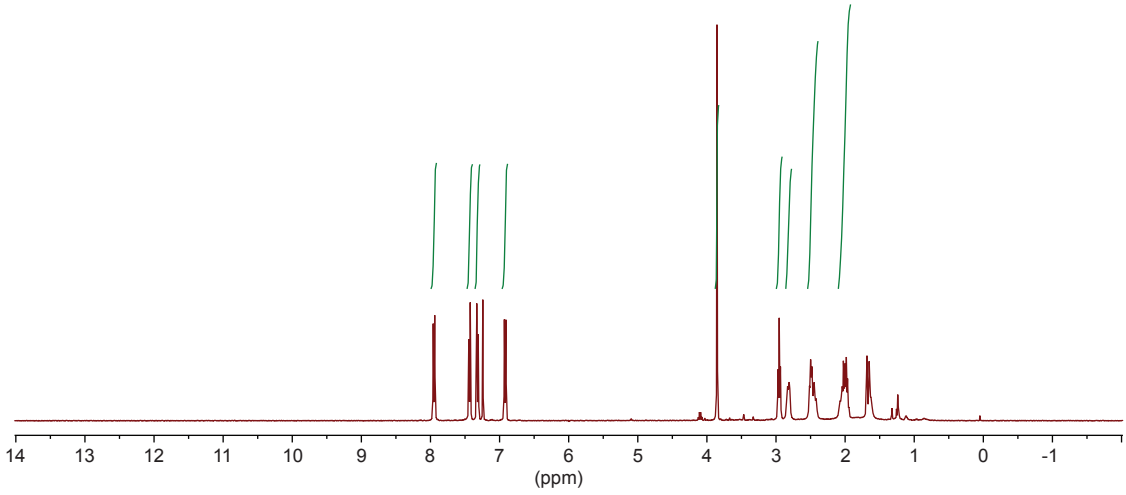

Figure 6.16. ^{1}H NMR spectrum for compound **5** in $CDCl_3$.

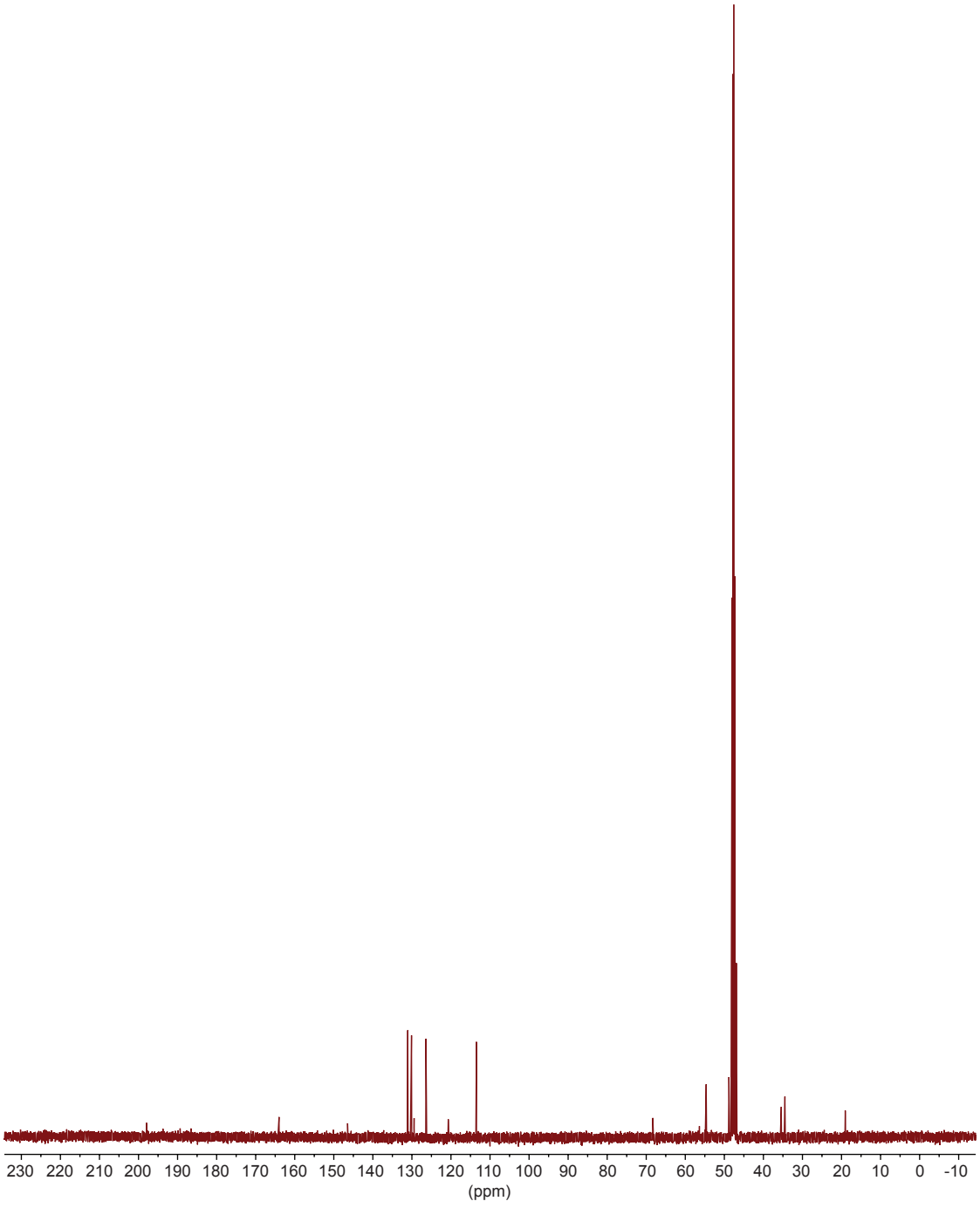

Figure 6.17. ^{13}C NMR spectrum for compound **5** in CD_3OD.

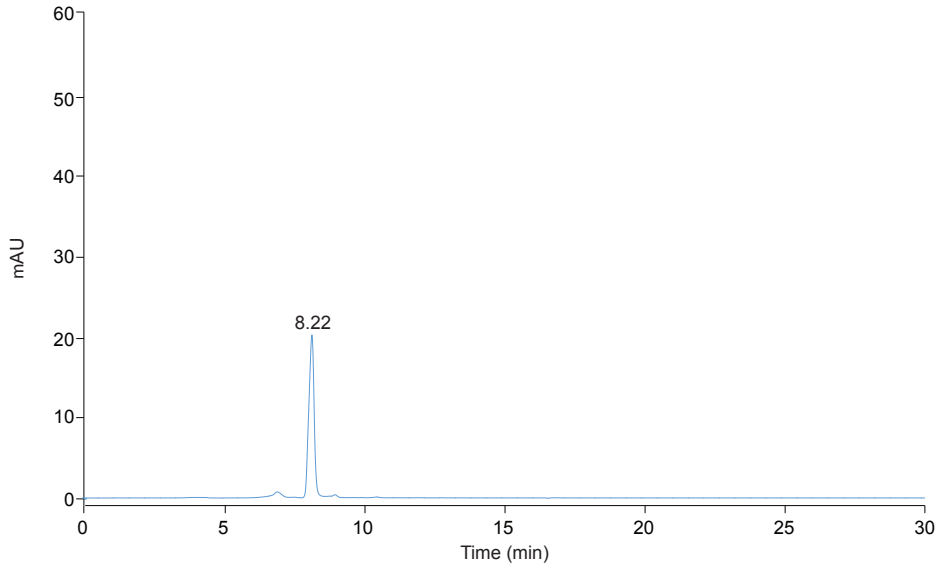

Figure 6.18. HPLC trace for compound **5**. R_t = 8.22 min.

6.4.2. Biological testing methodology

6.4.2.1. Biological reagents and instrumentation

The azole antifungal agents FLC, ITC, KCZ, POS, and VOR were purchased from AK Scientific (Union city, CA, U.S.A.). The *Candida albicans* strains, including *C. albicans* ATCC 10231 (strain *B*), *C. albicans* ATCC 64124 (strain *F*), and *C. albicans* ATCC MYA-2876 (Strain *E*) were a generous gift from Dr. Jon Y. Takemoto (Utah State University, Logan, UT, U.S.A.). The rest of the *C. albicans* strains, including *C. albicans* ATCC 90819 (strain *G*), *C. albicans* ATCC MYA-2310 (strain *D*), *C. albicans* ATCC MYA-1237 (strain *C*), and *C. albicans* ATCC MYA-1003 (strain *A*), as well as the non-*albicans Candida* fungus *C. glabrata* ATCC 2001 (strain *H*) were purchased from the American Type Culture Collection (ATCC, Manassas, VA, U.S.A.). The filamentous fungus *Aspergillus terreus* ATCC MYA-3633 (strain *I*) was also purchased from the ATCC. Yeast strains were cultured at 35 °C in yeast extract peptone dextrose (YEPD) broth. Filamentous fungi were

cultured on potato dextrose agar (PDA, catalog # 110130, EMD Millipore, Billerica, MA, U.S.A.) at 25 °C before the spores were harvested. All fungal experiments were carried out in RPMI 1640 medium (catalog # R6504, Sigma-Aldrich, St. Louis, MO, U.S.A.) buffered to pH 7.0 with 0.165 M MOPS buffer (Sigma-Aldrich, St. Louis, MO, U.S.A.). Colorimetric assessments were performed by using a SpectraMax M5 spectrometer (Molecular Devices, Sunnyvale, CA, U.S.A.).

6.4.2.2. Determination of MIC values

To assess the potential synergistic effect between various azoles and our bromperidol (**2**) as well as its derivatives **1** and **3-5**, we first needed to determine the individual minimum inhibitory concentration (MIC) values of compounds **1-5** and of the azole antifungals against each fungal strain of interest to gauge the range of concentrations to use in further assays. These MIC values were determined using the broth microdilution method in sterile 96-well plates with the highest concentrations of drugs used being 128 μg/mL for compounds **2** and **5**, 64 μg/mL for compounds **1** and **4**, and 32 μg/mL for compound **3** and for the azole antifungals. *Note*: The different starting concentrations result from the solubility limit of the compounds studied. These compounds were serially diluted (2-fold dilutions) horizontally on the plate in 100 μL of RPMI medium. A diluted yeast culture (25 μL of a fungal stock with OD_{600} of 0.125 in 10 mL of RPMI medium, which achieves a final inoculum size of around $1\text{-}5\times10^3$ CFU/mL) was plated across the plate (100 μL per well), making a final volume of 200 μL total per well. Similarly, *in vitro* MIC values for compounds **1-5** against filamentous fungi were determined as previously described in CLSI document M38-A2.[48] Briefly, 1×10^5 spores were seeded in each well in 100 μL of RPMI

medium. The MIC value of each compound was observed by visual inspection after 48 h of incubation at 35 °C for yeast or 72 h at 35 °C for the *Aspergillus* strains (Tables 6.1 and 6.3).

6.4.2.3. Combination studies of azoles and bromperidol series derivatives by checkerboard assays

To assess the potential synergistic effect between the commercially available azoles and our compounds **1-5** against various fungal strains, we employed the standard checkerboard assay as previously described[49-50] with slight variations. The commercially available azoles were serially diluted (2-fold dilutions) in the 96-well plates while the second drug, compounds **1-5**, were double-diluted in tubes outside of the 96-well plates and then later added into the plates using a multi-channel pipet. The concentration of azoles varied horizontally while that of compounds **1-5** varied vertically. The appropriate range of concentrations for each compound was determined based on their corresponding MIC values against each fungal strain. The inoculum size for yeast and filamentous fungi were the same as in the MIC experiments described in section 2.2. The 96-well plates were incubated at 35 °C for 48 h for yeasts and 72 h for the *Aspergillus* strain before visual inspection for growth. The observed MIC values of the azoles and compounds **1-5** alone as well as the MIC values for the two compounds in combo were then used to calculate the FICI using the formula below. The combinational effect of the two tested compounds were considered SYN if FICI ≤0.5, ADD if 0.5<FICI≤4, and ATG if FICI >4 (Tables 6.1-6.3).[29]

$$\text{FICI} = \frac{MIC\ of\ azole_{combo}}{MIC\ of\ azole_{alone}} + \frac{MIC\ of\ our\ compound_{combo}}{MIC\ of\ our\ compound_{alone}}$$

6.4.2.4. Time-kill assays

In order to observe the time-dependent killing effect of the combination of azoles and bromperidol (**2**) and its derivatives **1** and **3-5**, we selected two representative combinations, compound **2** with either POS or VOR, and tested the effect on *C. albicans* ATCC 64124 (strain *F*) as previously described[51] with modifications. An overnight culture of *C. albicans* ATCC 64124 (Strain *F*) in YEPD broth was inoculated at 1×10^5 CFU/mL density in liquid RPMI 1640 medium at 35 °C for each sample, including growth control, azole (POS or VOR) alone, compound **2** alone, and the combination of azole (POS or VOR) and compound **2** at 0.5× MIC, 1× MIC, 4× MIC, and 8× MIC concentrations (for the combination of VOR and compound **2**, only 1× MIC and 8× MIC combinations were performed). The concentrations of azoles or compound **2** used in the azole or compound **2** alone samples were equal to the highest concentration of that drug used in the combination samples (*e.g.*, the concentration of POS in the 8× MIC combination sample is 32 μg/mL, therefore, the concentration of POS in POS alone sample is 32 μg/mL). Each sample was incubated at 35 °C with shaking at 200 rpm. At various time points (0, 3, 6, 9, 12, and 24 h), 100 μL aliquots were taken from each sample and serially diluted (10-fold dilutions) in sterile ddH_2O. 100 μL of each dilution was spread onto PDA plates and incubated at 35 °C for 48 h before colony counts were determined (Figure 6.2). At the end of the 24 h experiment, 50 μL of 1 mM sterile resazurin solution was added to each sample for visual comparison of growth. Each experiment was performed in duplicate.

6.4.2.5. Biofilm disruption assays

In order to investigate the synergistic effect of azoles and our compounds on inhibiting biofilm formation of *C. albicans* ATCC 64124 (strain *F*), we performed a biofilm disruption assay in a checkerboard setup and used XTT reduction to examine the metabolic activity of the biofilm.[35] Briefly, *C. albicans* ATCC 64124 (strain *F*) was grown overnight in YEPD broth at 35 °C. The culture was then diluted to an OD_{600} of 0.12 (equivalent to 1×10^6 CFU/mL) and 100 μL was placed into each well of a 96-well plate. The cells were incubated at 37 °C for 24 h for growth. The following day, the spent medium containing planktonic cells was aspirated and each well was carefully washed three times with sterile phosphate buffer saline (PBS). We supplemented the washed biofilm with drug-containing RPMI 1640 medium with POS or VOR concentrations varying vertically and the concentration of compound **2** varied horizontally in a manner similar to that described above in the checkerboard assay section. The negative control (medium only) and the positive control (biofilm plus medium) wells were also included in the same 96-well plate. The plates were then incubated at 37 °C statically for additional 24 h and then washed with sterile PBS. 100 μL of a XTT (0.5 mg/mL)/menadione (1 μM) solution was added to each well, covered with aluminum foil, and incubated for 2 h at 37 °C. Then, 80 μL of the colored supernatant from each well was transferred to a new 96-well plate, and the absorption was read at OD_{490}. The percent metabolic activity of the formed biofilm at various drug concentration combinations was calculated by dividing the metabolic activity of biofilm formed for that well by that of the biofilm formed in the growth control well (in the absence of any drug). For these experiments, we determined the sessile MIC ($SMIC_{99}$), which is defined as the drug concentration required to inhibit the metabolic activity of

biofilm by 99% compared to the growth control. The $SMIC_{99}$ values were used to calculate the FICI as described above and summarized in Table 6.4. The assay for each combination was performed in duplicates.

6.4.2.6. Mammalian cytotoxicity assays

In order to evaluate the potential cytotoxic effect of the azoles and compounds **1-5** combinations against mammalian cells, we performed mammalian cytotoxicity assays as previously described with minor modifications.[52] The human embryonic kidney cell line HEK-293 was purchased from ATCC (Manassas, VA), whereas the human bronchial epithelial cells BEAS-2B and the murine macrophage cells J774A.1 were generous gifts from Prof. David K. Orren (University of Kentucky, Lexington, KY) and Prof. David J. Feola (University of Kentucky, Lexington, KY), respectively. HEK-293 and BEAS-2B cells were cultured in Dulbecco's Modified Eagle's Medium (DMEM, catalog # 11965-092, Thermo Fisher Scientific, Waltham, MA) supplemented with 10% fetal bovine serum (FBS, ATCC, Manassas, VA) and 1% penicillin/streptomycin (ATCC, Manassas, VA) at 37 °C with 5% CO_2. J774A.1 was cultured in a different DMEM (catalog # 30-2002, ATCC, Manassas, VA) with the same supplements in the medium at 37 °C with 5% CO_2. HEK-293 and BEAS-2B cells were dislodged by treating with a solution comprised of 0.05% trypsin and 0.53 mM EDTA (ATCC, Manassas, VA) when passaging, whereas J774A.1 cells were dislodged from the culture flask by mechanical scraping. All cytotoxicity assays were performed in quadruplicates in 96-well plates where both HEK-293 and J774A.1 cells were seeded at 1×10^4 cells per well and BEAS-2B cells were seeded at 3×10^3 cells per well. For the assessment of the toxicity of POS, VOR, and compound **2**

alone as well as in combination, we performed mammalian cytotoxicity assay as previously described.[52] The concentration of azoles tested in the assay ranged from 0.06 to 16 μg/mL, whereas that of compound **2** ranged from 0.25 to 64 μg/mL. When testing combination toxicity between azoles and compound **2**, we first tested the combination of various concentrations of azoles in the presence of 8 μg/mL of compound **2** for all three cell lines due to the higher toxicity that compound **2** exerted on J774A.1 cells. We additionally tested combination toxicity between either azoles and compound **2** in the presence of 32 μg/mL of compound **2** for BEAS-2B and HEK-293 cells in order to gain a better understanding of the toxicity for these two cells at higher concentrations of compound **2**. Since many xenobiotics stimulate cell growth instead of exerting toxicity at sub-IC_{50} concentrations,[23, 36-39] resulting in >100% cell survival in the treatment groups, we have considered these >100% cell survival data as no observed toxicity and expressed them as 100% cell survival (Figure 6.3).

6.5. ACKNOWLEDGEMENT

This work is supported by startup funds from the University of Kentucky (to S.G.-T.). S.Y.L.H. is supported by a University of Kentucky Presidential Fellowship.

This chapter is adapted from a published review article referenced as Holbrook, S. Y. L.; Garzan, A.; Dennis, E. K.; Shrestha, S. K.; Garneau-Tsodikova, S.. Repurposing antipsychotic drugs into antifungal agents: Synergistic combinations of azoles and bromperidol derivatives in the treatment of various fungal infections. *Eur. J med. Chem.* **2017**, *139*:12-21.

6.6. AUTHORS' CONTRIBUTIONS

S.Y.L.H. performed biological testing (including part of the checkerboard assays and all time-kill and cytotoxicity assays), wrote up the manuscript and later formatted the published manuscript into dissertation chapter. A.G. carried out the design and synthesis of compounds **1-5**. E.K.D. contributed in performing part of the checkerboard assays. S.K.S. performed biofilm disruption assays. S.G.-T. contributed in the write-up and proof-reading of the manuscript and later proof-reading the formatted dissertation chapter.

Chapter 7. Conclusions and future directions

7.1. CONCLUSIONS

In this dissertation, I have explored various strategies to discover new and effective antibacterial and antifungal therapies. First of all, my efforts to understand various aminoglycoside modifying enzymes (AMEs) have led to the engineering of the aminoglycoside *N*-acetyltransferase AAC(6')-Ie from the bifunctional AME, AAC(6')-Ie/APH(2")-Ia, by a mutation of D80G and a truncation after amino acid 240 to produce three mutant enzymes that contained mutation or truncation either alone or in combination. I found that mutation or truncation alone or in combination could cause the enzyme to expand its regiospecificity to acetylate a second amine moiety at 1-position of arbekacin and amikacin in addition to the original 6'-NH_2. This reflected the survival strategy that the bacteria might have acquired over time: possessing additional acetylating enzymes to further modify the aminoglycoside (AG) antibiotics and ensure their inactivation inside the bacteria as AGs had been shown to sometimes retain antibacterial activity after a single acetylation. In addition to this enzyme, I also presented that seven more AACs, including AAC(2')-Ic, AAC(3)-Ia, AAC(3)-Ib, AAC(3)-IV, AAC(6')-Ib', AAC(6')-IId, and the multiacetylating AAC Eis, could be inhibited by various metal salts. The organic complex zinc pyrithione further represented a good delivery strategy to increase intracellular Zn^{2+} concentration and further validated metal ions as AAC inhibitors to be used in adjunction with AG antibiotics to combat bacterial infections with AAC-associated resistance.

Furthermore, I explored another common AME, the aminoglycoside *O*-phosphotransferase APH(3')-IIa. Upon examining its substrate profiles with different NTPs, I realized that this

enzyme displayed diminishing substrate promiscuity as the cosubstrate changed from ATP to other NTPs. This revealed the dynamic interactions between the enzyme and the binding of the substrate and cosubstrate. Further kinetic analysis demonstrated that using different NTPs as cosubstrates did not universally decrease the enzyme's reactivity to all AGs but changed its substrate preference. This discovery could inspire all researchers working with AMEs that the substrate and cosubstrate share dynamic relationships with the enzyme and the three parties cannot be studied separately when investigating AMEs.

In addition to tackling the resistance problem by studying various AMEs, I also investigated the AG and carbapenem resistance in 122 *Pseudomonas aeruginosa* clinical isolates obtained from the University of Kentucky Hospital System. Upon evaluating the antibiotic resistance and the presence of various AME genes in these bacteria, we found the correlation between the resistance of two AGs and that between the resistance of AGs and carbapenems suggested a variety of antibiotic resistance mechanisms in addition to the sole presence of AME genes. We identified the lack of drug synergy between the two classes of antibiotics, which added to the existing dispute about the drastic variation of resistance epidemics based on geographical and other factors.

Lastly, my efforts in repurposing the existing antipsychotic compound, bromperidol, and its derivatives into a new combinational antifungal therapy with the azole antifungals was proven to be effective against a variety of pathogenic yeasts and filamentous fungi. In addition to displaying synergistic effects, the combination of these two classes of compounds also showed satisfying mammalian cytotoxicity. Therefore, developing these

old antipsychotic drugs as an adjuvant with the azole drugs presented promising outcomes as a new antifungal strategy.

7.2. FUTURE DIRECTIONS

In addition to the published studies, I have also investigated part of my Ph.D. in a few more projects. Some of these projects showed high potentials and should continue to be explored for future research as summarized herein.

7.2.1. Developing AGs as therapeutics for premature termination codon diseases

As introduced in Chapter 1.5, AGs along with their newly developed derivatives have displayed ability to promote read-through at premature termination codons (PTC) in some genetic disorders that are resulted from nonsense mutations. Thanks to Dr. Matthew S. Gentry and the collaboration between the two labs, I had the opportunity to explore AGs as potential therapeutic options for PTC diseases using Lafora Disease (LD) as an example.

LD is a progressive neurodegenerative disease symptomized by seizure, ataxia, myoclonus, and increasing severity of dementia.[1-5] This neurological disorder usually onsets in the early teenage years with a myoclonus epilepsy and patients survives for about ten years after onset. A hallmark of LD is the accumulation of insoluble glycogen granules known as the lafora bodies.[6] The lafora bodies are hyper-phosphorylated sparsely-branched polysaccharides that resemble amylopectin, which is insoluble, rather than the soluble glycogen. Consequently, they take up intracellular space, disturb cellular energy homeostasis, and lead to neuronal cell death as the disease progresses.

Two genes that are most frequently mutated in LD are the *EPM2A* (*epilepsy, progressive myoclonus 2A*, ~60% of the cases), which encodes for the glucanphosphatase laforin, and *EPM2B* (*epilepsy, progressive myoclonus 2B*, ~30% of the cases), which encodes for the E3 ubiquitin ligase malin.[2, 7-8] The laforin enzyme is specifically responsible for dephosphorylating phosphoglucans, which is essential for the proper branching of glycogen to maintain water solubility, while malin regulates protein turnover associated with glycogen synthesis and metabolism.

AGs' PTC suppressing efficiency is dose-, context-, and mutation-dependent.[9] Thus, PTC therapies need to be established for each unique disease and specific mutation. During my training with Dr. Vikas V. Duhkande in the Gentry lab, we used Western blot analysis testing the PTC suppression activity of various concentrations of gentamicin (GEN) in HEK-293 cells transiently transfected with *laforin wt* (negative control, no increase in the production of full-length laforin protein upon GEN treatment), *laforin Y86X*, *laforin R241X*, and *MeCP2 R294X* (positive control, a PTC mutation in Rett syndrome previously reported to produce full-length MeCP2 protein upon GEN treatments)[10-11].

Specifically, HEK-293 cells were plated in 6-well cell culture dish with 5 mL of DMEM medium supplemented with 1% Penn/Strep solution and 5% FBS at 37 °C with 5% CO_2. At 70% confluency, cells were transiently transfected with 350 ng of the above-mentioned genes constructed in a modified pcDNA3.1 with a *N*-terminal FLAG tag (for the laforin genes) or a modified pTRACER-CMV2 expression vector with an N-terminal 3x FLAG

tag (for the *MeCP2 R294* gene) with PEIMAX. At 4 h post transfection, cells were treated with various concentrations of GEN (0, 1, 1.75, and 3.5 mM) for 40 h. Whole-cell lysate were collected by lysis with 3:1 modified RIPA:RIPA buffer mixture solution. After determining the total protein concentrations using Bradford assay, SDS-PAGE samples were prepared controlling the total amount of protein in each sample and boiled for 10 min before loading onto an SDS-PAGE gel. Upon separation of proteins by electrophoresis, the proteins from the gel were transferred to a blot. Laforin protein was probed with mouse monoclonal anti-FLAG antibody coupled with HRP-conjugated goat-anti-mouse secondary antibody. β-actin was probed with a monoclonal anti-β-actin antibody coupled with HRP-conjugated goat-anti-mouse secondary antibody as a control for total protein level present on the blot for each sample. Assays were performed in triplicates.

I observed that various concentrations of GEN did not induce laforin protein over-production in the cells transfected with *laforin wt* gene but did result in upregulation of MeCP2 full-length protein production in the sample transfected with *MeCP2 R294X* gene in a dose-dependent manner. Furthermore, I observed that GEN induced the production of full-length laforin protein in the samples transfected with *laforin R241x* gene but not in the samples transfected with *laforin Y86X* (Figure 7.1).

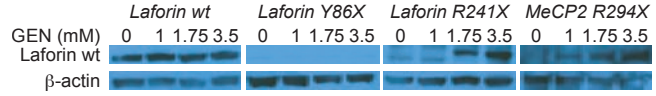

Figure 7.1. Western blot analysis of the PTC read-through induction in HEK293 cells transiently transfected with *laforin wt* (negative control), *laforin Y86X*, *laforin R241X*, and *MeCP2 R294X* (positive control) by GEN at various concentrations.

Even though Dr. Duhkande and I produced the data as shown in Figure 7.1 during the initial training, I was unable to reproduce the same results afterwards except for the controls of *laforin wt* and *MeCP2 R294X*. Even though my efforts on troubleshooting for Western blot experiments have so far been unsuccessful, AGs and their derivatives still present promising outcomes as potential therapeutic options for LD and other PTC-related disorders as shown in many other publications summarized in Chapter 1.5. Furthermore, another potential flaw in the design of the study is the mammalian expression vector used in this study. The modified pcDNA3.1 vector contains a neo^R gene in the backbone as a selection marker. However, as demonstrated in Chapter 4, the product of this neo^R gene is APH(3')-IIa enzyme that modifies a variety of AGs and their derivatives. Therefore, I have used quikchange mutagenesis to mutate the catalytic residue Asp190 into an alanine in the pcDNA3.1 *laforin wt* and *laforin R241X* with C-terminal FLAG tags. Another option would be recloning these genes into a different mammalian expression vector without any gene elements that would interfere with potential AG treatments.

7.2.2. Exploring PanD as a potential new target against *Mycobacterium tuberculosis* infections

Pyrazinamide (PZA) is a vital component of the first-line treatment regimen against *Mycobacterium tuberculosis* infections.[12-13] The use of PZA effectively allowed the treatment time for all-sensitive *Mtb* infections to reduce down to 6 months and is the only drug in the first-line treatment regimen whose mechanism of action is still in debate. In some recent studies, PanD, an aspartate decarboxylase, was proposed to be the target of pyrazinoic acid (POA), which is the active form of the prodrug PZA upon activation in

Mtb.[14-15] Some mutations in PanD were also proposed to be associated with PZA/POA resistance.[16-17] Although many details remain to be elucidated. Therefore, I would like to validate PanD as the target of PZA/POA and a new anti-tubercular target. In addition, I would also like to develop an assay for a high-throughput style screening for potential PanD inhibitors.

PanD was amplified by PCR from the *Mtb H37Rv* genomic DNA and cloned into pET22b vector for a C-terminal His_6 tag. A double point mutant H21R-I49V that was associated with PZA/POA resistance as well as both single mutants were also cloned.[17] A previous publication demonstrated the expression and purification of PanD enzyme in *E. coli*.[18] However, this manuscript reported that PanD is expressed as an π-enzyme (expected size 16.0 kDa) that undergoes self-cleavage at Ser25(expected size of 13.4 kDa after cleavage). However, as seen in Figure 7.2, the protein product after Ni^{II} affinity column purification seemed to correspond to bigger size than what was reported before. My attempts to activate/cleave the protein by incubating the protein at various concentrations (4, 20, 37, 42, 50, and 65 °C) as previously reported did not produce a shorter protein than what I originally observed in SDS-PAGE corresponding to the correct size. The expression and purification of the PanD H21R-I49V with C-His_6 tag seemed to correspond to an even bigger molecular weight on SDS-PAGE. This led me to postulate that PanD wt might be expressed in the cleaved/active form whereas the double mutant was incapable of self-cleaving due to the first H21R mutation, and they both ran slower than normal proteins of their sizes. Therefore, a future MALDI experiment may be necessary to elucidate the true state/sequence of these two proteins.

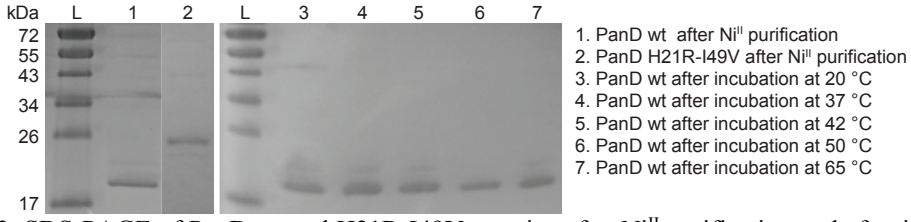

Figure 7.2. SDS-PAGE of PanD wt and H21R-I49V proteins after Ni^{II} purification and after incubation at various temperatures.

In the meanwhile, I had explored a new assay we could use to screen potential inhibitors of PanD enzyme. A previous publication suggested a high-throughput fluorescent assay to measure the activity of several amino acid decarboxylases.[19] Using *O*-diacetylbenzene (DAB) and β-mercaptoethanol (BME), this assay was reported to distinguish between a decarboxylated amine and their amino acid precursors. To test whether this assay system would work with PanD, I tested whether the assay would distinguish between various concentrations (0.1–1 mM) of L-aspartate (L-Asp) and β-alanine (β-Ala), which are the substrate and product of PanD. The assay seemed to detect low levels of product (0.1 mM), and therefore, could be used to detect PanD reactions (Figure 7.3).

Using this assay to test the activity of the protein samples with and without incubation at higher temperatures, I found that the "uncleaved" protein was indeed active and incubation at higher temperatures resulted in reduced activity over time (Figure 7.4). Therefore, the protein either was initially expressed as a cleaved protein as I have explained before or the uncleaved protein is active in its original state. Furthermore, I tested whether PZA or POA would cause inhibition of PanD wt and PanD H21R-I49V (Figure 7.5). We found neither PZA nor POA exerted inhibition on PanD wt enzyme at low concentration and POA induced ~20% inhibition in Pan Dwt activity. Additionally, the PanD H21R-I49V double

mutant was inactive. Therefore, PanD as a target of PZA/POA may require higher concentrations but still presents high potential for a new antitubercular strategy in the future.

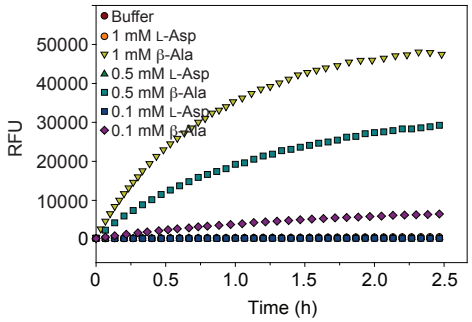

Figure 7.3. DAB and BME quenching various concentrations of L-Asp and β-Ala.

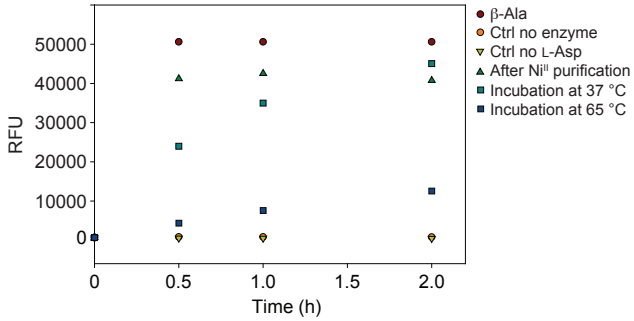

Figure 7.4. Enzymatic activity of PanD wt after Ni^{II} purification and incubation at 37 or 65 °C.

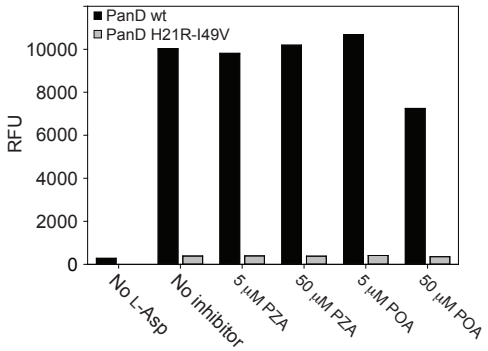

Figure 7.5. Enzymatic activity of PanD wt and H21R-I49V double mutant in the presence of 5 or 50 μM of PZA or POA as an inhibitor.

7.3. ACKNOWLEDGEMENT

I would like to thank Dr. Matthew S. Gentry and Dr. Vikas V. Dukhande (University of Kentucky, Lexington, KY, U.S.A) for the training in cell culturing and Western blot analysis. I would also like to thank Dr. Peter Huppke (Georg August University, Göttingan, Germany) the generous gift of MeCP2 R294X expression vector used in section 7.2.1.

7.4. AUTHORS' CONTRIBUTIONS

S.Y.L.H. performed all experiments presented in this chapter and wrote up the text. M.S.G and S. G.-T. both contributed in the study design of the project described in section 7.2.1 and both studies in section 7.2, respectively in this chapter.

References

Chapter 1 references

1. Houghton, J. L.; Green, K. D.; Chen, W.; Garneau-Tsodikova, S., The future of aminoglycosides: the end or renaissance? *ChemBioChem* **2010,** *11* (7), 880-902.
2. Magnet, S.; Blanchard, J. S., Molecular insights into aminoglycoside action and resistance. *Chem. Rev.* **2005,** *105* (2), 477-98.
3. Feldman, M. B.; Terry, D. S.; Altman, R. B.; Blanchard, S. C., Aminoglycoside activity observed on single pre-translocation ribosome complexes. *Nat. Chem. Biol.* **2010,** *6* (1), 54-62.
4. Borovinskaya, M. A.; Pai, R. D.; Zhang, W.; Schuwirth, B. S.; Holton, J. M.; Hirokawa, G.; Kaji, H.; Kaji, A.; Cate, J. H., Structural basis for aminoglycoside inhibition of bacterial ribosome recycling. *Nat. Struct. Mol. Biol.* **2007,** *14* (8), 727-32.
5. Park, S. R.; Park, J. W.; Ban, Y. H.; Sohng, J. K.; Yoon, Y. J., 2-Deoxystreptamine-containing aminoglycoside antibiotics: recent advances in the characterization and manipulation of their biosynthetic pathways. *Nat. Prod. Rep.* **2013,** *30* (1), 11-20.
6. Galimand, M.; Courvalin, P.; Lambert, T., Plasmid-mediated high-level resistance to aminoglycosides in Enterobacteriaceae due to 16S rRNA methylation. *Antimicrob. Agents Chemother.* **2003,** *47* (8), 2565-71.
7. Becker, B.; Cooper, M. A., Aminoglycoside antibiotics in the 21st century. *ACS Chem. Biol.* **2013,** *8* (1), 105-15.
8. Ramirez, M. S.; Tolmasky, M. E., Aminoglycoside modifying enzymes. *Drug Resist. Updat.* **2010,** *13* (6), 151-71.

9. Shi, K.; Berghuis, A. M., Structural basis for dual nucleotide selectivity of aminoglycoside 2"-phosphotransferase IVa provides insight on determinants of nucleotide specificity of aminoglycoside kinases. *J. Biol. Chem.* **2012,** *287* (16), 13094-102.

10. Shakya, T.; Wright, G. D., Nucleotide selectivity of antibiotic kinases. *Antimicrob. Agents Chemother.* **2010,** *54* (5), 1909-13.

11. Smith, C. A.; Toth, M.; Frase, H.; Byrnes, L. J.; Vakulenko, S. B., Aminoglycoside 2"-phosphotransferase IIIa (APH(2")-IIIa) prefers GTP over ATP: structural templates for nucleotide recognition in the bacterial aminoglycoside-2" kinases. *J. Biol. Chem.* **2012,** *287* (16), 12893-903.

12. Porter, V. R.; Green, K. D.; Zolova, O. E.; Houghton, J. L.; Garneau-Tsodikova, S., Dissecting the cosubstrate structure requirements of the *Staphylococcus aureus* aminoglycoside resistance enzyme ANT(4'). *Biochem. Biophys. Res. Commun.* **2010,** *403* (1), 85-90.

13. Chen, W.; Biswas, T.; Porter, V. R.; Tsodikov, O. V.; Garneau-Tsodikova, S., Unusual regioversatility of acetyltransferase Eis, a cause of drug resistance in XDR-TB. *Proc. Natl. Acad. Sci., U. S. A.* **2011,** *108* (24), 9804-8.

14. Houghton, J. L.; Green, K. D.; Pricer, R. E.; Mayhoub, A. S.; Garneau-Tsodikova, S., Unexpected *N*-acetylation of capreomycin by mycobacterial Eis enzymes. *J. Antimicrob. Chemother.* **2013,** *68* (4), 800-5.

15. Kim, K. H.; An, D. R.; Song, J.; Yoon, J. Y.; Kim, H. S.; Yoon, H. J.; Im, H. N.; Kim, J.; Kim do, J.; Lee, S. J.; Kim, K. H.; Lee, H. M.; Kim, H. J.; Jo, E. K.; Lee, J. Y.; Suh, S. W., *Mycobacterium tuberculosis* Eis protein initiates suppression of host

immune responses by acetylation of DUSP16/MKP-7. *Proc. Natl. Acad. Sci.*, *U. S. A.* **2012,** *109* (20), 7729-34.

16. Chen, W.; Green, K. D.; Tsodikov, O. V.; Garneau-Tsodikova, S., Aminoglycoside multiacetylating activity of the enhanced intracellular survival protein from *Mycobacterium smegmatis* and its inhibition. *Biochemistry* **2012,** *51* (24), 4959-67.
17. Pricer, R. E.; Houghton, J. L.; Green, K. D.; Mayhoub, A. S.; Garneau-Tsodikova, S., Biochemical and structural analysis of aminoglycoside acetyltransferase Eis from *Anabaena variabilis*. *Mol. Biosyst.* **2012,** *8* (12), 3305-13.
18. Tsodikov, O. V.; Green, K. D.; Garneau-Tsodikova, S., A Random Sequential Mechanism of Aminoglycoside Acetylation by *Mycobacterium tuberculosis* Eis Protein. *PLoS One* **2014,** *9* (4), e92370.
19. Houghton, J. L.; Biswas, T.; Chen, W.; Tsodikov, O. V.; Garneau-Tsodikova, S., Chemical and structural insights into the regioversatility of the aminoglycoside acetyltransferase Eis. *ChemBioChem* **2013,** *14* (16), 2127-35.
20. Jennings, B. C.; Labby, K. J.; Green, K. D.; Garneau-Tsodikova, S., Redesign of substrate specificity and identification of the aminoglycoside binding residues of Eis from *Mycobacterium tuberculosis*. *Biochemistry* **2013,** *52* (30), 5125-32.
21. Chen, W.; Green, K. D.; Garneau-Tsodikova, S., Cosubstrate tolerance of the aminoglycoside resistance enzyme Eis from *Mycobacterium tuberculosis*. *Antimicrob. Agents Chemother.* **2012,** *56* (11), 5831-8.
22. Green, K. D.; Chen, W.; Garneau-Tsodikova, S., Identification and characterization of inhibitors of the aminoglycoside resistance acetyltransferase Eis from *Mycobacterium tuberculosis*. *ChemMedChem* **2012,** *7* (1), 73-7.

23. Labby, K. J.; Garneau-Tsodikova, S., Strategies to overcome the action of aminoglycoside-modifying enzymes for treating resistant bacterial infections. *Future Med. Chem.* **2013,** *5* (11), 1285-309.

24. Drawz, S. M.; Bonomo, R. A., Three decades of beta-lactamase inhibitors. *Clin. Microbiol. Rev.* **2010,** *23* (1), 160-201.

25. Amstutz, P.; Binz, H. K.; Parizek, P.; Stumpp, M. T.; Kohl, A.; Grutter, M. G.; Forrer, P.; Pluckthun, A., Intracellular kinase inhibitors selected from combinatorial libraries of designed ankyrin repeat proteins. *J. Biol. Chem.* **2005,** *280* (26), 24715-22.

26. Kohl, A.; Amstutz, P.; Parizek, P.; Binz, H. K.; Briand, C.; Capitani, G.; Forrer, P.; Pluckthun, A.; Grutter, M. G., Allosteric inhibition of aminoglycoside phosphotransferase by a designed ankyrin repeat protein. *Structure* **2005,** *13* (8), 1131-41.

27. Shakya, T.; Stogios, P. J.; Waglechner, N.; Evdokimova, E.; Ejim, L.; Blanchard, J. E.; McArthur, A. G.; Savchenko, A.; Wright, G. D., A small molecule discrimination map of the antibiotic resistance kinome. *Chem. Biol.* **2011,** *18* (12), 1591-601.

28. Fong, D. H.; Xiong, B.; Hwang, J.; Berghuis, A. M., Crystal structures of two aminoglycoside kinases bound with a eukaryotic protein kinase inhibitor. *PLoS One* **2011,** *6* (5), e19589.

29. Suga, T.; Ishii, T.; Iwatsuki, M.; Yamamoto, T.; Nonaka, K.; Masuma, R.; Matsui, H.; Hanaki, H.; Omura, S.; Shiomi, K., Aranorosin circumvents arbekacin-resistance in MRSA by inhibiting the bifunctional enzyme AAC(6')/APH(2''). *J. Antibiot.* **2012,** *65* (10), 527-9.

30. Welch, K. T.; Virga, K. G.; Whittemore, N. A.; Ozen, C.; Wright, E.; Brown, C. L.; Lee, R. E.; Serpersu, E. H., Discovery of non-carbohydrate inhibitors of aminoglycoside-modifying enzymes. *Bioorg. Med. Chem.* **2005,** *13* (22), 6252-63.

31. Blount, K. F.; Zhao, F.; Hermann, T.; Tor, Y., Conformational constraint as a means for understanding RNA-aminoglycoside specificity. *J. Am. Chem. Soc.* **2005,** *127* (27), 9818-29.

32. Zhao, F.; Zhao, Q.; Blount, K. F.; Han, Q.; Tor, Y.; Hermann, T., Molecular recognition of RNA by neomycin and a restricted neomycin derivative. *Angew. Chem.* **2005,** *44* (33), 5329-34.

33. Asensio, J. L.; Hidalgo, A.; Bastida, A.; Torrado, M.; Corzana, F.; Chiara, J. L.; Garcia-Junceda, E.; Canada, J.; Jimenez-Barbero, J., A simple structural-based approach to prevent aminoglycoside inactivation by bacterial defense proteins. Conformational restriction provides effective protection against neomycin-B nucleotidylation by ANT4. *J. Am. Chem. Soc.* **2005,** *127* (23), 8278-9.

34. Bastida, A.; Hidalgo, A.; Chiara, J. L.; Torrado, M.; Corzana, F.; Perez-Canadillas, J. M.; Groves, P.; Garcia-Junceda, E.; Gonzalez, C.; Jimenez-Barbero, J.; Asensio, J. L., Exploring the use of conformationally locked aminoglycosides as a new strategy to overcome bacterial resistance. *J. Am. Chem. Soc.* **2006,** *128* (1), 100-16.

35. Kling, D.; Hesek, D.; Shi, Q.; Mobashery, S., Design and synthesis of a structurally constrained aminoglycoside. *J. Org. Chem.* **2007,** *72* (14), 5450-3.

36. Hanessian, S.; Szychowski, J.; Campos-Reales Pineda, N. B.; Furtos, A.; Keillor, J. W., 6-hydroxy to 6'''-amino tethered ring-to-ring macrocyclic aminoglycosides as probes for APH(3')-IIIa kinase. *Bioorg. Med. Chem. Lett.* **2007,** *17* (11), 3221-5.

37. Zhang, W.; Chen, Y.; Liang, Q.; Li, H.; Jin, H.; Zhang, L.; Meng, X.; Li, Z., Design, synthesis, and antibacterial activities of conformationally constrained kanamycin A derivatives. *J. Org. Chem.* **2013,** *78* (2), 400-9.

38. Michael, K.; Wang, H.; Tor, Y., Enhanced RNA binding of dimerized aminoglycosides. *Bioorg. Med. Chem.* **1999,** *7* (7), 1361-71.

39. Sucheck, S. J.; Wong, A. L.; Koeller, K. M.; Boehr, D. D.; Draker, K.-A.; Sears, P.; Wright, G. D.; Wong, C.-H., Design of bifunctional antibiotics that target bacterial rRNA and inhibit resistance-causing enzymes. *J. Am. Chem. Soc.* **2000,** *122* (21), 5230-5231.

40. Agnelli, F.; Sucheck, S. J.; Marby, K. A.; Rabuka, D.; Yao, S. L.; Sears, P. S.; Liang, F. S.; Wong, C. H., Dimeric aminoglycosides as antibiotics. *Angew. Chem.* **2004,** *43* (12), 1562-6.

41. Santana, A. G.; Batisda, A.; Del Campo, T. M.; Asensio, J. L.; Revuelta, J., An efficient and general route to the synthesis of novel aminoglycosides for RNA binding. *Synlett* **2011,** *2*, 219-222.

42. Kumar, S.; Xue, L.; Arya, D. P., Neomycin-neomycin dimer: an all-carbohydrate scaffold with high affinity for AT-rich DNA duplexes. *J. Am. Chem. Soc.* **2011,** *133* (19), 7361-75.

43. Berkov-Zrihen, Y.; Green, K. D.; Labby, K. J.; Feldman, M.; Garneau-Tsodikova, S.; Fridman, M., Synthesis and evaluation of hetero- and homodimers of ribosome-targeting antibiotics: antimicrobial activity, *in vitro* inhibition of translation, and drug resistance. *J. Med. Chem.* **2013,** *56* (13), 5613-25.

44. Thomas, J. R.; Liu, X.; Hergenrother, P. J., Size-specific ligands for RNA hairpin loops. *J. Am. Chem. Soc.* **2005,** *127* (36), 12434-5.

45. Thomas, J. R.; Liu, X.; Hergenrother, P. J., Biochemical and thermodynamic characterization of compounds that bind to RNA hairpin loops: toward an understanding of selectivity. *Biochemistry* **2006,** *45* (36), 10928-38.

46. Bodlenner, A.; Alix, A.; Weibel, J. M.; Pale, P.; Ennifar, E.; Paillart, J. C.; Walter, P.; Marquet, R.; Dumas, P., Synthesis of a neamine dimer targeting the dimerization initiation site of HIV-1 RNA. *Org. Lett.* **2007,** *9* (22), 4415-8.

47. Luedtke, N. W.; Liu, Q.; Tor, Y., RNA-ligand interactions: affinity and specificity of aminoglycoside dimers and acridine conjugates to the HIV-1 Rev response element. *Biochemistry* **2003,** *42* (39), 11391-403.

48. Riguet, E.; Desire, J.; Boden, O.; Ludwig, V.; Gobel, M.; Bailly, C.; Decout, J. L., Neamine dimers targeting the HIV-1 TAR RNA. *Bioorg. Med. Chem. Lett.* **2005,** *15* (21), 4651-5.

49. Lee, L. V.; Bower, K. E.; Liang, F. S.; Shi, J.; Wu, D.; Sucheck, S. J.; Vogt, P. K.; Wong, C. H., Inhibition of the proteolytic activity of anthrax lethal factor by aminoglycosides. *J. Am. Chem. Soc.* **2004,** *126* (15), 4774-5.

50. Fridman, M.; Belakhov, V.; Lee, L. V.; Liang, F. S.; Wong, C. H.; Baasov, T., Dual effect of synthetic aminoglycosides: antibacterial activity against *Bacillus anthracis* and inhibition of anthrax lethal factor. *Angew. Chem.* **2005,** *44* (3), 447-52.

51. Numa, M. M.; Lee, L. V.; Hsu, C. C.; Bower, K. E.; Wong, C. H., Identification of novel anthrax lethal factor inhibitors generated by combinatorial Pictet-Spengler reaction followed by screening *in situ*. *ChemBioChem* **2005,** *6* (6), 1002-6.

52. Fair, R. J.; Hensler, M. E.; Thienphrapa, W.; Dam, Q. N.; Nizet, V.; Tor, Y., Selectively guanidinylated aminoglycosides as antibiotics. *ChemMedChem* **2012,** *7* (7), 1237-44.

53. Tsai, A.; Uemura, S.; Johansson, M.; Puglisi, E. V.; Marshall, R. A.; Aitken, C. E.; Korlach, J.; Ehrenberg, M.; Puglisi, J. D., The impact of aminoglycosides on the dynamics of translation elongation. *Cell Rep.* **2013,** *3* (2), 497-508.

54. Kaul, M.; Barbieri, C. M.; Pilch, D. S., Fluorescence-based approach for detecting and characterizing antibiotic-induced conformational changes in ribosomal RNA: comparing aminoglycoside binding to prokaryotic and eukaryotic ribosomal RNA sequences. *J. Am. Chem. Soc.* **2004,** *126* (11), 3447-53.

55. Kaul, M.; Barbieri, C. M.; Pilch, D. S., Aminoglycoside-induced reduction in nucleotide mobility at the ribosomal RNA A-site as a potentially key determinant of antibacterial activity. *J. Am. Chem. Soc.* **2006,** *128* (4), 1261-71.

56. Llano-Sotelo, B.; Hickerson, R. P.; Lancaster, L.; Noller, H. F.; Mankin, A. S., Fluorescently labeled ribosomes as a tool for analyzing antibiotic binding. *RNA* **2009,** *15* (8), 1597-604.

57. Francois, B.; Szychowski, J.; Adhikari, S. S.; Pachamuthu, K.; Swayze, E. E.; Griffey, R. H.; Migawa, M. T.; Westhof, E.; Hanessian, S., Antibacterial aminoglycosides with a modified mode of binding to the ribosomal-RNA decoding site. *Angew. Chem.* **2004,** *43* (48), 6735-8.

58. Anderson, P. C.; Mecozzi, S., Minimum sequence requirements for the binding of paromomycin to the rRNA decoding site A. *Biopolymers* **2007,** *86* (2), 95-111.

59. Liang, F. S.; Greenberg, W. A.; Hammond, J. A.; Hoffmann, J.; Head, S. R.; Wong, C. H., Evaluation of RNA-binding specificity of aminoglycosides with DNA microarrays. *Proc. Natl. Acad. Sci.*, *U. S. A.* **2006,** *103* (33), 12311-6.

60. Aminova, O.; Paul, D. J.; Childs-Disney, J. L.; Disney, M. D., Two-dimensional combinatorial screening identifies specific 6'-acylated kanamycin A- and 6'-acylated neamine-RNA hairpin interactions. *Biochemistry* **2008,** *47* (48), 12670-9.

61. Paul, D. J.; Seedhouse, S. J.; Disney, M. D., Two-dimensional combinatorial screening and the RNA Privileged Space Predictor program efficiently identify aminoglycoside-RNA hairpin loop interactions. *Nucleic Acids Res.* **2009,** *37* (17), 5894-907.

62. Tran, T.; Disney, M. D., Two-dimensional combinatorial screening of a bacterial rRNA A-site-like motif library: defining privileged asymmetric internal loops that bind aminoglycosides. *Biochemistry* **2010,** *49* (9), 1833-42.

63. Tran, T.; Disney, M. D., Molecular recognition of 6'-N-5-hexynoate kanamycin A and RNA 1x1 internal loops containing CA mismatches. *Biochemistry* **2011,** *50* (6), 962-9.

64. Wang, L.; Pulk, A.; Wasserman, M. R.; Feldman, M. B.; Altman, R. B.; Cate, J. H.; Blanchard, S. C., Allosteric control of the ribosome by small-molecule antibiotics. *Nat. Struct. Mol. Biol.* **2012,** *19* (9), 957-63.

65. Francois, B.; Russell, R. J.; Murray, J. B.; Aboul-ela, F.; Masquida, B.; Vicens, Q.; Westhof, E., Crystal structures of complexes between aminoglycosides and decoding A site oligonucleotides: role of the number of rings and positive charges in the specific binding leading to miscoding. *Nucleic Acids Res.* **2005,** *33* (17), 5677-90.

66. Hobbie, S. N.; Pfister, P.; Bruell, C.; Sander, P.; Francois, B.; Westhof, E.; Bottger, E. C., Binding of neomycin-class aminoglycoside antibiotics to mutant ribosomes with alterations in the A site of 16S rRNA. *Antimicrob. Agents Chemother.* **2006,** *50* (4), 1489-96.

67. Hobbie, S. N.; Pfister, P.; Brull, C.; Westhof, E.; Bottger, E. C., Analysis of the contribution of individual substituents in 4,6-aminoglycoside-ribosome interaction. *Antimicrob. Agents Chemother.* **2005,** *49* (12), 5112-8.

68. Poehlsgaard, J.; Douthwaite, S., The bacterial ribosome as a target for antibiotics. *Nat. Rev. Microbiol.* **2005,** *3* (11), 870-81.

69. Akshay, S.; Bertea, M.; Hobbie, S. N.; Oettinghaus, B.; Shcherbakov, D.; Bottger, E. C.; Akbergenov, R., Phylogenetic sequence variations in bacterial rRNA affect species-specific susceptibility to drugs targeting protein synthesis. *Antimicrob. Agents Chemother.* **2011,** *55* (9), 4096-102.

70. Perez-Fernandez, D.; Shcherbakov, D.; Matt, T.; Leong, N. C.; Kudyba, I.; Duscha, S.; Boukari, H.; Patak, R.; Dubbaka, S. R.; Lang, K.; Meyer, M.; Akbergenov, R.; Freihofer, P.; Vaddi, S.; Thommes, P.; Ramakrishnan, V.; Vasella, A.; Bottger, E. C., 4'-*O*-substitutions determine selectivity of aminoglycoside antibiotics. *Nat. Commun.* **2014,** *5*, 3112.

71. Blount, K. F.; Tor, Y., A tale of two targets: differential RNA selectivity of nucleobase-aminoglycoside conjugates. *ChemBioChem* **2006,** *7* (10), 1612-21.

72. Scheunemann, A. E.; Graham, W. D.; Vendeix, F. A.; Agris, P. F., Binding of aminoglycoside antibiotics to helix 69 of 23S rRNA. *Nucleic Acids Res.* **2010,** *38* (9), 3094-105.

73. Trabuco, L. G.; Schreiner, E.; Eargle, J.; Cornish, P.; Ha, T.; Luthey-Schulten, Z.; Schulten, K., The role of L1 stalk-tRNA interaction in the ribosome elongation cycle. *J. Mol. Biol.* **2010,** *402* (4), 741-60.

74. Dorner, S.; Brunelle, J. L.; Sharma, D.; Green, R., The hybrid state of tRNA binding is an authentic translation elongation intermediate. *Nat. Struct. Mol. Biol.* **2006,** *13* (3), 234-41.

75. Dunkle, J. A.; Wang, L.; Feldman, M. B.; Pulk, A.; Chen, V. B.; Kapral, G. J.; Noeske, J.; Richardson, J. S.; Blanchard, S. C.; Cate, J. H., Structures of the bacterial ribosome in classical and hybrid states of tRNA binding. *Science* **2011,** *332* (6032), 981-4.

76. Munro, J. B.; Altman, R. B.; O'Connor, N.; Blanchard, S. C., Identification of two distinct hybrid state intermediates on the ribosome. *Mol. Cell* **2007,** *25* (4), 505-17.

77. Foster, C.; Champney, W. S., Characterization of a 30S ribosomal subunit assembly intermediate found in *Escherichia coli* cells growing with neomycin or paromomycin. *Arch. Microbiol.* **2008,** *189* (5), 441-9.

78. Bera, S.; Zhanel, G. G.; Schweizer, F., Design, synthesis, and antibacterial activities of neomycin-lipid conjugates: polycationic lipids with potent gram-positive activity. *J. Med. Chem.* **2008,** *51* (19), 6160-4.

79. Zhang, J.; Chiang, F. I.; Wu, L.; Czyryca, P. G.; Li, D.; Chang, C. W., Surprising alteration of antibacterial activity of 5"-modified neomycin against resistant bacteria. *J. Med. Chem.* **2008,** *51* (23), 7563-73.

80. Zhang, J.; Keller, K.; Takemoto, J. Y.; Bensaci, M.; Litke, A.; Czyryca, P. G.; Chang, C. W., Synthesis and combinational antibacterial study of 5"-modified neomycin. *J. Antibiot.* **2009,** *62* (10), 539-44.

81. Bera, S.; Dhondikubeer, R.; Findlay, B.; Zhanel, G. G.; Schweizer, F., Synthesis and antibacterial activities of amphiphilic neomycin B-based bilipid conjugates and fluorinated neomycin B-based lipids. *Molecules* **2012,** *17* (8), 9129-41.

82. Bera, S.; Zhanel, G. G.; Schweizer, F., Antibacterial activity of guanidinylated neomycin B- and kanamycin A-derived amphiphilic lipid conjugates. *J. Antimicrob. Chemother.* **2010,** *65* (6), 1224-7.

83. Herzog, I. M.; Feldman, M.; Eldar-Boock, A.; Satchi-Fainaro, R.; Fridman, M., Design of membrane targeting tobramycin-based cationic amphiphiles with reduced hemolytic activity. *MedChemComm* **2013,** *4*, 120-124.

84. Herzog, I. M.; Green, K. D.; Berkov-Zrihen, Y.; Feldman, M.; Vidavski, R. R.; Eldar-Boock, A.; Satchi-Fainaro, R.; Eldar, A.; Garneau-Tsodikova, S.; Fridman, M., *6*"-Thioether tobramycin analogues: towards selective targeting of bacterial membranes. *Angew. Chem.* **2012,** *51* (23), 5652-6.

85. Berkov-Zrihen, Y.; Herzog, I. M.; Feldman, M.; Sonn-Segev, A.; Roichman, Y.; Fridman, M., Di-alkylated paromomycin derivatives: targeting the membranes of gram positive pathogens that cause skin infections. *Bioorg. Med. Chem.* **2013,** *21* (12), 3624-31.

86. Berkov-Zrihen, Y.; Herzog, I. M.; Feldman, M.; Fridman, M., Site-selective displacement of tobramycin hydroxyls for preparation of antimicrobial cationic amphiphiles. *Org. Lett.* **2013,** *15* (24), 6144-7.

87. Bera, S.; Zhanel, G. G.; Schweizer, F., Synthesis and antibacterial activity of amphiphilic lysine-ligated neomycin B conjugates. *Carbohydr. Res.* **2011,** *346* (5), 560-8.

88. Bera, S.; Zhanel, G. G.; Schweizer, F., Evaluation of amphiphilic aminoglycoside-peptide triazole conjugates as antibacterial agents. *Bioorg. Med. Chem. Lett.* **2010,** *20* (10), 3031-5.

89. Dhondikubeer, R.; Bera, S.; Zhanel, G. G.; Schweizer, F., Antibacterial activity of amphiphilic tobramycin. *J. Antibiot.* **2012,** *65* (10), 495-8.

90. Hanessian, S.; Szychowski, J.; Adhikari, S. S.; Vasquez, G.; Kandasamy, P.; Swayze, E. E.; Migawa, M. T.; Ranken, R.; Francois, B.; Wirmer-Bartoschek, J.; Kondo, J.; Westhof, E., Structure-based design, synthesis, and A-site rRNA cocrystal complexes of functionally novel aminoglycoside antibiotics: C2" ether analogues of paromomycin. *J. Med. Chem.* **2007,** *50* (10), 2352-69.

91. Baussanne, I.; Bussiere, A.; Halder, S.; Ganem-Elbaz, C.; Ouberai, M.; Riou, M.; Paris, J. M.; Ennifar, E.; Mingeot-Leclercq, M. P.; Decout, J. L., Synthesis and antimicrobial evaluation of amphiphilic neamine derivatives. *J. Med. Chem.* **2010,** *53* (1), 119-27.

92. Bera, S.; Zhanel, G. G.; Schweizer, F., Antibacterial activities of aminoglycoside antibiotics-derived cationic amphiphiles. Polyol-modified neomycin B-, kanamycin A-, amikacin-, and neamine-based amphiphiles with potent broad spectrum antibacterial activity. *J. Med. Chem.* **2010,** *53* (9), 3626-31.

93. Zimmermann, L.; Bussiere, A.; Ouberai, M.; Baussanne, I.; Jolivalt, C.; Mingeot-Leclercq, M. P.; Decout, J. L., Tuning the antibacterial activity of amphiphilic

neamine derivatives and comparison to paromamine homologues. *J. Med. Chem.* **2013,** *56* (19), 7691-705.

94. Brogden, K. A., Antimicrobial peptides: pore formers or metabolic inhibitors in bacteria? *Nat. Rev. Microbiol.* **2005,** *3* (3), 238-50.
95. Udumula, V.; Ham, Y. W.; Fosso, M. Y.; Chan, K. Y.; Rai, R.; Zhang, J.; Li, J.; Chang, C. W., Investigation of antibacterial mode of action for traditional and amphiphilic aminoglycosides. *Bioorg. Med. Chem. Lett.* **2013,** *23* (6), 1671-5.
96. Ouberai, M.; El Garch, F.; Bussiere, A.; Riou, M.; Alsteens, D.; Lins, L.; Baussanne, I.; Dufrene, Y. F.; Brasseur, R.; Decout, J. L.; Mingeot-Leclercq, M. P., The *Pseudomonas aeruginosa* membranes: a target for a new amphiphilic aminoglycoside derivative? *Biochim. Biophys. Acta* **2011,** *1808* (6), 1716-27.
97. Lee, H. B.; Kim, Y.; Kim, J. C.; Choi, G. J.; Park, S. H.; Kim, C. J.; Jung, H. S., Activity of some aminoglycoside antibiotics against true fungi, *Phytophthora* and *Pythium* species. *J. Appl. Microbiol.* **2005,** *99* (4), 836-43.
98. Mahl, D. L.; de Jesus, F. P.; Loreto, E.; Zanette, R. A.; Ferreiro, L.; Pilotto, M. B.; Alves, S. H.; Santurio, J. M., *In vitro* susceptibility of *Pythium insidiosum* isolates to aminoglycoside antibiotics and tigecycline. *Antimicrob. Agents Chemother.* **2012,** *56* (7), 4021-3.
99. Yutani, M.; Ogita, A.; Fujita, K.-I.; Tanaka, T., Generation of novel fungicidal activity by the combined actions of hygromycin B and polymyxin B. *Int. J. Life Sci. Med. Res.* **2013,** *3* (5), 193-199.
100. Chang, C. W.; Fosso, M.; Kawasaki, Y.; Shrestha, S.; Bensaci, M. F.; Wang, J.; Evans, C. K.; Takemoto, J. Y., Antibacterial to antifungal conversion of neamine

aminoglycosides through alkyl modification. Strategy for reviving old drugs into agrofungicides. *J. Antibiot.* **2010,** *63* (11), 667-72.

101. Shrestha, S.; Grilley, M.; Fosso, M. Y.; Chang, C. W.; Takemoto, J. Y., Membrane lipid-modulated mechanism of action and non-cytotoxicity of novel fungicide aminoglycoside FG08. *PLoS One* **2013,** *8* (9), e73843.
102. Linde, L.; Kerem, B., Introducing sense into nonsense in treatments of human genetic diseases. *Trends Genet.* **2008,** *24* (11), 552-63.
103. Zingman, L. V.; Park, S.; Olson, T. M.; Alekseev, A. E.; Terzic, A., Aminoglycoside-induced translational read-through in disease: overcoming nonsense mutations by pharmacogenetic therapy. *Clin. Pharmacol. Ther.* **2007,** *81* (1), 99-103.
104. Sermet-Gaudelus, I.; Renouil, M.; Fajac, A.; Bidou, L.; Parbaille, B.; Pierrot, S.; Davy, N.; Bismuth, E.; Reinert, P.; Lenoir, G.; Lesure, J. F.; Rousset, J. P.; Edelman, A., *In vitro* prediction of stop-codon suppression by intravenous gentamicin in patients with cystic fibrosis: a pilot study. *BMC Med.* **2007,** *5*, 5.
105. Linde, L.; Boelz, S.; Nissim-Rafinia, M.; Oren, Y. S.; Wilschanski, M.; Yaacov, Y.; Virgilis, D.; Neu-Yilik, G.; Kulozik, A. E.; Kerem, E.; Kerem, B., Nonsense-mediated mRNA decay affects nonsense transcript levels and governs response of cystic fibrosis patients to gentamicin. *J. Clin. Invest.* **2007,** *117* (3), 683-92.
106. Du, M.; Keeling, K. M.; Fan, L.; Liu, X.; Kovacs, T.; Sorscher, E.; Bedwell, D. M., Clinical doses of amikacin provide more effective suppression of the human CFTR-G542X stop mutation than gentamicin in a transgenic CF mouse model. *J. Mol. Med.* **2006,** *84* (7), 573-82.

107. Du, M.; Keeling, K. M.; Fan, L.; Liu, X.; Bedwell, D. M., Poly-L-aspartic acid enhances and prolongs gentamicin-mediated suppression of the CFTR-G542X mutation in a cystic fibrosis mouse model. *J. Biol. Chem.* **2009,** *284* (11), 6885-92.

108. Rowe, S. M.; Sloane, P.; Tang, L. P.; Backer, K.; Mazur, M.; Buckley-Lanier, J.; Nudelman, I.; Belakhov, V.; Bebok, Z.; Schwiebert, E.; Baasov, T.; Bedwell, D. M., Suppression of CFTR premature termination codons and rescue of CFTR protein and function by the synthetic aminoglycoside NB54. *J. Mol. Med.* **2011,** *89* (11), 1149-61.

109. Xue, X.; Mutyam, V.; Tang, L.; Biswas, S.; Du, M.; Jackson, L. A.; Dai, Y.; Belakhov, V.; Shalev, M.; Chen, F.; Schacht, J.; Bridges, R.; Baasov, T.; Hong, J.; Bedwell, D. M.; Rowe, S. M., Synthetic Aminoglycosides Efficiently Suppress CFTR Nonsense Mutations and are Enhanced by Ivacaftor. *Am. J. Respir. Cell Mol. Biol.* **2013**.

110. Nudelman, I.; Glikin, D.; Smolkin, B.; Hainrichson, M.; Belakhov, V.; Baasov, T., Repairing faulty genes by aminoglycosides: development of new derivatives of geneticin (G418) with enhanced suppression of diseases-causing nonsense mutations. *Bioorg. Med. Chem.* **2010,** *18* (11), 3735-46.

111. Pichavant, C.; Aartsma-Rus, A.; Clemens, P. R.; Davies, K. E.; Dickson, G.; Takeda, S.; Wilton, S. D.; Wolff, J. A.; Wooddell, C. I.; Xiao, X.; Tremblay, J. P., Current status of pharmaceutical and genetic therapeutic approaches to treat DMD. *Mol. Ther.* **2011,** *19* (5), 830-40.

112. Malik, V.; Rodino-Klapac, L. R.; Viollet, L.; Mendell, J. R., Aminoglycoside-induced mutation suppression (stop codon readthrough) as a therapeutic strategy for Duchenne muscular dystrophy. *Ther. Adv. Neurol. Disord.* **2010,** *3* (6), 379-89.

113. Loufrani, L.; Dubroca, C.; You, D.; Li, Z.; Levy, B.; Paulin, D.; Henrion, D., Absence of dystrophin in mice reduces NO-dependent vascular function and vascular density: total recovery after a treatment with the aminoglycoside gentamicin. *Arterioscler. Thromb. Vasc. Biol.* **2004,** *24* (4), 671-6.

114. Malik, V.; Rodino-Klapac, L. R.; Viollet, L.; Wall, C.; King, W.; Al-Dahhak, R.; Lewis, S.; Shilling, C. J.; Kota, J.; Serrano-Munuera, C.; Hayes, J.; Mahan, J. D.; Campbell, K. J.; Banwell, B.; Dasouki, M.; Watts, V.; Sivakumar, K.; Bien-Willner, R.; Flanigan, K. M.; Sahenk, Z.; Barohn, R. J.; Walker, C. M.; Mendell, J. R., Gentamicin-induced readthrough of stop codons in Duchenne muscular dystrophy. *Ann. Neurol.* **2010,** *67* (6), 771-80.

115. Kimura, S.; Ito, K.; Miyagi, T.; Hiranuma, T.; Yoshioka, K.; Ozasa, S.; Matsukura, M.; Ikezawa, M.; Matsuo, M.; Takeshima, Y.; Miike, T., A novel approach to identify Duchenne muscular dystrophy patients for aminoglycoside antibiotics therapy. *Brain Dev.* **2005,** *27* (6), 400-5.

116. Popescu, A. C.; Sidorova, E.; Zhang, G.; Eubanks, J. H., Aminoglycoside-mediated partial suppression of MECP2 nonsense mutations responsible for Rett syndrome *in vitro*. *J. Neurosci. Res.* **2010,** *88* (11), 2316-24.

117. Brendel, C.; Klahold, E.; Gartner, J.; Huppke, P., Suppression of nonsense mutations in Rett syndrome by aminoglycoside antibiotics. *Pediatr. Res.* **2009,** *65* (5), 520-3.

118. Brendel, C.; Belakhov, V.; Werner, H.; Wegener, E.; Gartner, J.; Nudelman, I.; Baasov, T.; Huppke, P., Readthrough of nonsense mutations in Rett syndrome: evaluation of novel aminoglycosides and generation of a new mouse model. *J. Mol. Med.* **2011,** *89* (4), 389-98.

119. Vecsler, M.; Ben Zeev, B.; Nudelman, I.; Anikster, Y.; Simon, A. J.; Amariglio, N.; Rechavi, G.; Baasov, T.; Gak, E., *Ex vivo* treatment with a novel synthetic aminoglycoside NB54 in primary fibroblasts from Rett syndrome patients suppresses MECP2 nonsense mutations. *PLoS One* **2011,** *6* (6), e20733.

120. Wolstencroft, E. C.; Mattis, V.; Bajer, A. A.; Young, P. J.; Lorson, C. L., A non-sequence-specific requirement for SMN protein activity: the role of aminoglycosides in inducing elevated SMN protein levels. *Hum. Mol. Genet.* **2005,** *14* (9), 1199-210.

121. Mattis, V. B.; Rai, R.; Wang, J.; Chang, C. W.; Coady, T.; Lorson, C. L., Novel aminoglycosides increase SMN levels in spinal muscular atrophy fibroblasts. *Hum. Genet.* **2006,** *120* (4), 589-601.

122. Mattis, V. B.; Ebert, A. D.; Fosso, M. Y.; Chang, C. W.; Lorson, C. L., Delivery of a read-through inducing compound, TC007, lessens the severity of a spinal muscular atrophy animal model. *Hum. Mol. Genet.* **2009,** *18* (20), 3906-13.

123. Mattis, V. B.; Fosso, M. Y.; Chang, C. W.; Lorson, C. L., Subcutaneous administration of TC007 reduces disease severity in an animal model of SMA. *BMC Neurosci.* **2009,** *10*, 142.

124. Nudelman, I.; Rebibo-Sabbah, A.; Cherniavsky, M.; Belakhov, V.; Hainrichson, M.; Chen, F.; Schacht, J.; Pilch, D. S.; Ben-Yosef, T.; Baasov, T., Development of novel

aminoglycoside (NB54) with reduced toxicity and enhanced suppression of disease-causing premature stop mutations. *J. Med. Chem.* **2009,** *52* (9), 2836-45.

125. Rebibo-Sabbah, A.; Nudelman, I.; Ahmed, Z. M.; Baasov, T.; Ben-Yosef, T., *In vitro* and ex vivo suppression by aminoglycosides of PCDH15 nonsense mutations underlying type 1 Usher syndrome. *Hum. Genet.* **2007,** *122* (3-4), 373-81.
126. Allamand, V.; Bidou, L.; Arakawa, M.; Floquet, C.; Shiozuka, M.; Paturneau-Jouas, M.; Gartioux, C.; Butler-Browne, G. S.; Mouly, V.; Rousset, J. P.; Matsuda, R.; Ikeda, D.; Guicheney, P., Drug-induced readthrough of premature stop codons leads to the stabilization of laminin alpha2 chain mRNA in CMD myotubes. *J. Gene Med.* **2008,** *10* (2), 217-24.
127. Lai, C. H.; Chun, H. H.; Nahas, S. A.; Mitui, M.; Gamo, K. M.; Du, L.; Gatti, R. A., Correction of ATM gene function by aminoglycoside-induced read-through of premature termination codons. *Proc. Natl. Acad. Sci., U. S. A.* **2004,** *101* (44), 15676-81.
128. Pinotti, M.; Rizzotto, L.; Pinton, P.; Ferraresi, P.; Chuansumrit, A.; Charoenkwan, P.; Marchetti, G.; Rizzuto, R.; Mariani, G.; Bernardi, F.; International Factor, V. I. I. D. S. G., Intracellular readthrough of nonsense mutations by aminoglycosides in coagulation factor VII. *J. Thromb. Haemost.* **2006,** *4* (6), 1308-14.
129. Gunn, G.; Dai, Y.; Du, M.; Belakhov, V.; Kandasamy, J.; Schoeb, T. R.; Baasov, T.; Bedwell, D. M.; Keeling, K. M., Long-term nonsense suppression therapy moderates MPS I-H disease progression. *Mol. Genet. Metab.* **2013**.

130. Floquet, C.; Deforges, J.; Rousset, J. P.; Bidou, L., Rescue of non-sense mutated p53 tumor suppressor gene by aminoglycosides. *Nucleic Acids Res.* **2011,** *39* (8), 3350-62.

131. Floquet, C.; Rousset, J. P.; Bidou, L., Readthrough of premature termination codons in the adenomatous polyposis coli gene restores its biological activity in human cancer cells. *PLoS One* **2011,** *6* (8), e24125.

132. Perez, B.; Rodriguez-Pombo, P.; Ugarte, M.; Desviat, L. R., Readthrough strategies for therapeutic suppression of nonsense mutations in inherited metabolic disease. *Mol. Syndromol.* **2012,** *3* (5), 230-6.

133. Moosajee, M.; Gregory-Evans, K.; Ellis, C. D.; Seabra, M. C.; Gregory-Evans, C. Y., Translational bypass of nonsense mutations in zebrafish rep1, pax2.1 and lamb1 highlights a viable therapeutic option for untreatable genetic eye disease. *Hum. Mol. Genet.* **2008,** *17* (24), 3987-4000.

134. Shulman, E.; Belakhov, V.; Wei, G.; Kendall, A.; Meyron-Holtz, E. G.; Ben-Shachar, D.; Schacht, J.; Baasov, T., Designer Aminoglycosides That Selectively Inhibit Cytoplasmic Rather than Mitochondrial Ribosomes Show Decreased Ototoxicity: A STRATEGY FOR THE TREATMENT OF GENETIC DISEASES. *J. Biol. Chem.* **2014,** *289* (4), 2318-30.

135. Yu, H.; Liu, X.; Huang, J.; Zhang, Y.; Hu, R.; Pu, J., Comparison of read-through effects of aminoglycosides and PTC124 on rescuing nonsense mutations of *HERG* gene associated with long QT syndrome. *Int. J. Mol. Med.* **2014,** *33* (3), 729-35.

136. Goldmann, T.; Overlack, N.; Wolfrum, U.; Nagel-Wolfrum, K., PTC124-mediated translational readthrough of a nonsense mutation causing Usher syndrome type 1C. *Hum. Gene Ther.* **2011,** *22* (5), 537-47.

137. Huth, M. E.; Ricci, A. J.; Cheng, A. G., Mechanisms of aminoglycoside ototoxicity and targets of hair cell protection. *Int. J. Otolaryngol.* **2011,** *2011*, 937861.

138. Nagai, J.; Takano, M., Molecular aspects of renal handling of aminoglycosides and strategies for preventing the nephrotoxicity. *Drug Metab. Pharmacokinet.* **2004,** *19* (3), 159-70.

139. Pagkalis, S.; Mantadakis, E.; Mavros, M. N.; Ammari, C.; Falagas, M. E., Pharmacological considerations for the proper clinical use of aminoglycosides. *Drugs* **2011,** *71* (17), 2277-94.

140. Rizzi, M. D.; Hirose, K., Aminoglycoside ototoxicity. *Curr. Opin. Otolaryngol. Head Neck Surg.* **2007,** *15* (5), 352-7.

141. Guthrie, O. W., Aminoglycoside induced ototoxicity. *Toxicology* **2008,** *249* (2-3), 91-6.

142. Rybak, L. P.; Ramkumar, V., Ototoxicity. *Kidney Int.* **2007,** *72* (8), 931-5.

143. Fee, W. E., Jr., Aminoglycoside ototoxicity in the human. *The Laryngoscope* **1980,** *90* (10 Pt 2 Suppl 24), 1-19.

144. Mulheran, M.; Degg, C.; Burr, S.; Morgan, D. W.; Stableforth, D. E., Occurrence and risk of cochleotoxicity in cystic fibrosis patients receiving repeated high-dose aminoglycoside therapy. *Antimicrob. Agents Chemother.* **2001,** *45* (9), 2502-9.

145. Mingeot-Leclercq, M. P.; Tulkens, P. M., Aminoglycosides: nephrotoxicity. *Antimicrob. Agents Chemother.* **1999,** *43* (5), 1003-12.

146. Marcotti, W.; van Netten, S. M.; Kros, C. J., The aminoglycoside antibiotic dihydrostreptomycin rapidly enters mouse outer hair cells through the mechano-electrical transducer channels. *J. Physiol.* **2005,** *567* (Pt 2), 505-21.

147. Dai, C. F.; Mangiardi, D.; Cotanche, D. A.; Steyger, P. S., Uptake of fluorescent gentamicin by vertebrate sensory cells *in vivo*. *Hear Res.* **2006,** *213* (1-2), 64-78.

148. Wang, Q.; Steyger, P. S., Trafficking of systemic fluorescent gentamicin into the cochlea and hair cells. *J. Assoc. Res. Otolaryngol.* **2009,** *10* (2), 205-19.

149. Alharazneh, A.; Luk, L.; Huth, M.; Monfared, A.; Steyger, P. S.; Cheng, A. G.; Ricci, A. J., Functional hair cell mechanotransducer channels are required for aminoglycoside ototoxicity. *PLoS One* **2011,** *6* (7), e22347.

150. Lee, J. H.; Park, C.; Kim, S. J.; Kim, H. J.; Oh, G. S.; Shen, A.; So, H. S.; Park, R., Different uptake of gentamicin through TRPV1 and TRPV4 channels determines cochlear hair cell vulnerability. *Exp. Mol. Med.* **2013,** *45*, e12.

151. Warchol, M. E., Cellular mechanisms of aminoglycoside ototoxicity. *Curr. Opin. Otolaryngol. Head Neck Surg.* **2010,** *18* (5), 454-8.

152. Harvey, S. C.; Skolnick, P., Polyamine-like actions of aminoglycosides at recombinant *N*-methyl-D-aspartate receptors. *J. Pharmacol. Exp. Ther.* **1999,** *291* (1), 285-91.

153. Hong, S. H.; Park, S. K.; Cho, Y. S.; Lee, H. S.; Kim, K. R.; Kim, M. G.; Chung, W. H., Gentamicin induced nitric oxide-related oxidative damages on vestibular afferents in the guinea pig. *Hear Res.* **2006,** *211* (1-2), 46-53.

154. Liu, H. Y.; Chi, F. L.; Gao, W. Y., Taurine attenuates aminoglycoside ototoxicity by inhibiting inducible nitric oxide synthase expression in the cochlea. *Neuroreport* **2008,** *19* (1), 117-20.

155. Zhao, H.; Li, R.; Wang, Q.; Yan, Q.; Deng, J. H.; Han, D.; Bai, Y.; Young, W. Y.; Guan, M. X., Maternally inherited aminoglycoside-induced and nonsyndromic deafness is associated with the novel C1494T mutation in the mitochondrial 12S rRNA gene in a large Chinese family. *Am. J. Hum. Genet.* **2004,** *74* (1), 139-52.

156. Xing, G.; Chen, Z.; Cao, X., Mitochondrial rRNA and tRNA and hearing function. *Cell Res.* **2007,** *17* (3), 227-39.

157. Guan, M. X., Mitochondrial 12S rRNA mutations associated with aminoglycoside ototoxicity. *Mitochondrion.* **2011,** *11* (2), 237-45.

158. Wei, Q.; Xu, D.; Chen, Z.; Li, H.; Lu, Y.; Liu, C.; Bu, X.; Xing, G.; Cao, X., Maternally transmitted aminoglycoside-induced and non-syndromic hearing loss caused by the 1494C > T mutation in the mitochondrial 12S rRNA gene in two Chinese families. *Int. J. Audiol.* **2013,** *52* (2), 98-103.

159. Hobbie, S. N.; Akshay, S.; Kalapala, S. K.; Bruell, C. M.; Shcherbakov, D.; Bottger, E. C., Genetic analysis of interactions with eukaryotic rRNA identify the mitoribosome as target in aminoglycoside ototoxicity. *Proc. Natl. Acad. Sci.*, *U. S. A.* **2008,** *105* (52), 20888-93.

160. Hobbie, S. N.; Bruell, C. M.; Akshay, S.; Kalapala, S. K.; Shcherbakov, D.; Bottger, E. C., Mitochondrial deafness alleles confer misreading of the genetic code. *Proc. Natl. Acad. Sci.*, *U. S. A.* **2008,** *105* (9), 3244-9.

161. Francis, S. P.; Katz, J.; Fanning, K. D.; Harris, K. A.; Nicholas, B. D.; Lacy, M.; Pagana, J.; Agris, P. F.; Shin, J. B., A novel role of cytosolic protein synthesis inhibition in aminoglycoside ototoxicity. *J. Neurosci.* **2013,** *33* (7), 3079-93.

162. Mazurek, B.; Lou, X.; Olze, H.; Haupt, H.; Szczepek, A. J., In vitro protection of auditory hair cells by salicylate from the gentamicin-induced but not neomycin-induced cell loss. *Neuroscience letters* **2012,** *506* (1), 107-10.

163. Sha, S. H.; Qiu, J. H.; Schacht, J., Aspirin to prevent gentamicin-induced hearing loss. *N. Engl. J. Med.* **2006,** *354* (17), 1856-7.

164. Feldman, L.; Efrati, S.; Eviatar, E.; Abramsohn, R.; Yarovoy, I.; Gersch, E.; Averbukh, Z.; Weissgarten, J., Gentamicin-induced ototoxicity in hemodialysis patients is ameliorated by *N*-acetylcysteine. *Kidney Int.* **2007,** *72* (3), 359-63.

165. Tokgoz, B.; Ucar, C.; Kocyigit, I.; Somdas, M.; Unal, A.; Vural, A.; Sipahioglu, M.; Oymak, O.; Utas, C., Protective effect of *N*-acetylcysteine from drug-induced ototoxicity in uraemic patients with CAPD peritonitis. *Nephrol. Dial. Transplant.* **2011,** *26* (12), 4073-8.

166. Ojano-Dirain, C. P.; Antonelli, P. J., Prevention of gentamicin-induced apoptosis with the mitochondria-targeted antioxidant mitoquinone. *The Laryngoscope* **2012,** *122* (11), 2543-8.

167. Bas, E.; Van De Water, T. R.; Gupta, C.; Dinh, J.; Vu, L.; Martinez-Soriano, F.; Lainez, J. M.; Marco, J., Efficacy of three drugs for protecting against gentamicin-induced hair cell and hearing losses. *Br. J. Pharmacol.* **2012,** *166* (6), 1888-904.

168. Jankauskas, S. S.; Plotnikov, E. Y.; Morosanova, M. A.; Pevzner, I. B.; Zorova, L. D.; Skulachev, V. P.; Zorov, D. B., Mitochondria-targeted antioxidant SkQR1

ameliorates gentamycin-induced renal failure and hearing loss. *Biochemistry* **2012,** *77* (6), 666-70.

169. Basile, A. S.; Brichta, A. M.; Harris, B. D.; Morse, D.; Coling, D.; Skolnick, P., Dizocilpine attenuates streptomycin-induced vestibulotoxicity in rats. *Neurosci. Lett.* **1999,** *265* (2), 71-4.

170. Hainrichson, M.; Nudelman, I.; Baasov, T., Designer aminoglycosides: the race to develop improved antibiotics and compounds for the treatment of human genetic diseases. *Org. Biomol. Chem.* **2008,** *6* (2), 227-39.

171. Chen, L.; Hainrichson, M.; Bourdetsky, D.; Mor, A.; Yaron, S.; Baasov, T., Structure-toxicity relationship of aminoglycosides: correlation of 2'-amine basicity with acute toxicity in pseudo-disaccharide scaffolds. *Bioorg. Med. Chem.* **2008,** *16* (19), 8940-51.

172. O'Connor, S.; Lam, L. K.; Jones, N. D.; Chaney, M. O., Apramycin, a unique aminocyclitol antibiotic. *J. Org. Chem.* **1976,** *41* (12), 2087-92.

173. Ryden, R.; Moore, B. J., The *in vitro* activity of apramycin, a new aminocyclitol antibiotic. *J. Antimicrob. Chemother.* **1977,** *3* (6), 609-13.

174. Matt, T.; Ng, C. L.; Lang, K.; Sha, S. H.; Akbergenov, R.; Shcherbakov, D.; Meyer, M.; Duscha, S.; Xie, J.; Dubbaka, S. R.; Perez-Fernandez, D.; Vasella, A.; Ramakrishnan, V.; Schacht, J.; Bottger, E. C., Dissociation of antibacterial activity and aminoglycoside ototoxicity in the 4-monosubstituted 2-deoxystreptamine apramycin. *Proc. Natl. Acad. Sci., U. S. A.* **2012,** *109* (27), 10984-9.

175. Aggen, J. B.; Armstrong, E. S.; Goldblum, A. A.; Dozzo, P.; Linsell, M. S.; Gliedt, M. J.; Hildebrandt, D. J.; Feeney, L. A.; Kubo, A.; Matias, R. D.; Lopez, S.; Gomez,

M.; Wlasichuk, K. B.; Diokno, R.; Miller, G. H.; Moser, H. E., Synthesis and spectrum of the neoglycoside ACHN-490. *Antimicrob. Agents Chemother.* **2010,** *54* (11), 4636-42.

176. Landman, D.; Babu, E.; Shah, N.; Kelly, P.; Backer, M.; Bratu, S.; Quale, J., Activity of a novel aminoglycoside, ACHN-490, against clinical isolates of *Escherichia coli* and *Klebsiella pneumoniae* from New York City. *J. Antimicrob. Chemother.* **2010,** *65* (10), 2123-7.
177. Galani, I.; Souli, M.; Daikos, G. L.; Chrysouli, Z.; Poulakou, G.; Psichogiou, M.; Panagea, T.; Argyropoulou, A.; Stefanou, I.; Plakias, G.; Giamarellou, H.; Petrikkos, G., Activity of plazomicin (ACHN-490) against MDR clinical isolates of *Klebsiella pneumoniae*, *Escherichia coli*, and *Enterobacter* spp. from Athens, Greece. *J. Chemother.* **2012,** *24* (4), 191-4.
178. Endimiani, A.; Hujer, K. M.; Hujer, A. M.; Armstrong, E. S.; Choudhary, Y.; Aggen, J. B.; Bonomo, R. A., ACHN-490, a neoglycoside with potent *in vitro* activity against multidrug-resistant *Klebsiella pneumoniae* isolates. *Antimicrob. Agents Chemother.* **2009,** *53* (10), 4504-7.
179. Livermore, D. M.; Mushtaq, S.; Warner, M.; Zhang, J. C.; Maharjan, S.; Doumith, M.; Woodford, N., Activity of aminoglycosides, including ACHN-490, against carbapenem-resistant *Enterobacteriaceae* isolates. *J. Antimicrob. Chemother.* **2011,** *66* (1), 48-53.
180. Landman, D.; Kelly, P.; Backer, M.; Babu, E.; Shah, N.; Bratu, S.; Quale, J., Antimicrobial activity of a novel aminoglycoside, ACHN-490, against *Acinetobacter*

baumannii and *Pseudomonas aeruginosa* from New York City. *J. Antimicrob. Chemother.* **2011,** *66* (2), 332-4.

181. Reyes, N.; Aggen, J. B.; Kostrub, C. F., *In vivo* efficacy of the novel aminoglycoside ACHN-490 in murine infection models. *Antimicrob. Agents Chemother.* **2011,** *55* (4), 1728-33.

Chapter 2 references

1. Vakulenko, S. B.; Mobashery, S., Versatility of aminoglycosides and prospects for their future. *Clin. Microbiol. Rev.* **2003,** *16* (3), 430-50.
2. Magnet, S.; Blanchard, J. S., Molecular insights into aminoglycoside action and resistance. *Chem. Rev.* **2005,** *105* (2), 477-98.
3. Fosso, M. Y.; Li, Y.; Garneau-Tsodikova, S., New trends in aminoglycosides use. *MedChemComm* **2014,** *5* (8), 1075-91.
4. Houghton, J. L.; Green, K. D.; Chen, W.; Garneau-Tsodikova, S., The future of aminoglycosides: the end or renaissance? *ChemBioChem* **2010,** *11* (7), 880-902.
5. Shrestha, S.; Grilley, M.; Fosso, M. Y.; Chang, C. W.; Takemoto, J. Y., Membrane lipid-modulated mechanism of action and non-cytotoxicity of novel fungicide aminoglycoside FG08. *PLoS One* **2013,** *8* (9), e73843.
6. Chang, C. W.; Fosso, M.; Kawasaki, Y.; Shrestha, S.; Bensaci, M. F.; Wang, J.; Evans, C. K.; Takemoto, J. Y., Antibacterial to antifungal conversion of neamine aminoglycosides through alkyl modification. Strategy for reviving old drugs into agrofungicides. *J. Antibiot.* **2010,** *63* (11), 667-72.

7. Shrestha, S. K.; Fosso, M. Y.; Garneau-Tsodikova, S., A combination approach to treating fungal infections. *Sci. Rep.* **2015,** *5*, 17070.
8. Fosso, M. Y.; Shrestha, S. K.; Green, K. D.; Garneau-Tsodikova, S., Synthesis and bioactivities of kanamycin B-derived cationic amphiphiles. *J. Med. Chem.* **2015,** *58* (23), 9124-32.
9. Shrestha, S. K.; Fosso, M. Y.; Green, K. D.; Garneau-Tsodikova, S., Amphiphilic tobramycin analogues as antibacterial and antifungal agents. *Antimicrob. Agents Chemother.* **2015,** *59* (8), 4861-9.
10. Fosso, M.; AlFindee, M. N.; Zhang, Q.; Nziko Vde, P.; Kawasaki, Y.; Shrestha, S. K.; Bearss, J.; Gregory, R.; Takemoto, J. Y.; Chang, C. W., Structure-activity relationships for antibacterial to antifungal conversion of kanamycin to amphiphilic analogues. *J. Org. Chem.* **2015,** *80* (9), 4398-411.
11. Zingman, L. V.; Park, S.; Olson, T. M.; Alekseev, A. E.; Terzic, A., Aminoglycoside-induced translational read-through in disease: overcoming nonsense mutations by pharmacogenetic therapy. *Clin. Pharmacol. Ther.* **2007,** *81* (1), 99-103.
12. Linde, L.; Kerem, B., Introducing sense into nonsense in treatments of human genetic diseases. *Trends Genet.* **2008,** *24* (11), 552-63.
13. Du, M.; Keeling, K. M.; Fan, L.; Liu, X.; Kovacs, T.; Sorscher, E.; Bedwell, D. M., Clinical doses of amikacin provide more effective suppression of the human CFTR-G542X stop mutation than gentamicin in a transgenic CF mouse model. *J. Mol. Med.* **2006,** *84* (7), 573-82.
14. Xue, X.; Mutyam, V.; Tang, L.; Biswas, S.; Du, M.; Jackson, L. A.; Dai, Y.; Belakhov, V.; Shalev, M.; Chen, F.; Schacht, J.; R, J. B.; Baasov, T.; Hong, J.;

Bedwell, D. M.; Rowe, S. M., Synthetic aminoglycosides efficiently suppress cystic fibrosis transmembrane conductance regulator nonsense mutations and are enhanced by ivacaftor. *Am. J. Respir. Cell Mol. Biol.* **2014,** *50* (4), 805-16.

15. Pichavant, C.; Aartsma-Rus, A.; Clemens, P. R.; Davies, K. E.; Dickson, G.; Takeda, S.; Wilton, S. D.; Wolff, J. A.; Wooddell, C. I.; Xiao, X.; Tremblay, J. P., Current status of pharmaceutical and genetic therapeutic approaches to treat DMD. *Mol. Ther.* **2011,** *19* (5), 830-40.
16. Matsumoto, T., Arbekacin: another novel agent for treating infections due to methicillin-resistant *Staphylococcus aureus* and multidrug-resistant Gram-negative pathogens. *Clin. Pharmacol.* **2014,** *6*, 139-48.
17. Garneau-Tsodikova, S.; Labby, K. J., Mechanisms of resistance to aminoglycoside antibiotics: Overview and perspectives. *MedChemComm* **2016,** *7*, 11-27.
18. Labby, K. J.; Garneau-Tsodikova, S., Strategies to overcome the action of aminoglycoside-modifying enzymes for treating resistant bacterial infections. *Future Med. Chem.* **2013,** *5* (11), 1285-309.
19. Ramirez, M. S.; Tolmasky, M. E., Aminoglycoside modifying enzymes. *Drug Resist. Update* **2010,** *13* (6), 151-71.
20. Thompson, P. R.; Boehr, D. D.; Berghuis, A. M.; Wright, G. D., Mechanism of aminoglycoside antibiotic kinase APH(3')-IIIa: role of the nucleotide positioning loop. *Biochemistry* **2002,** *41* (22), 7001-7.
21. Burk, D. L.; Ghuman, N.; Wybenga-Groot, L. E.; Berghuis, A. M., X-ray structure of the AAC(6')-Ii antibiotic resistance enzyme at 1.8 Å resolution; examination of

oligomeric arrangements in GNAT superfamily members. *Protein Sci.* **2003,** *12* (3), 426-37.

22. Kim, C.; Hesek, D.; Zajicek, J.; Vakulenko, S. B.; Mobashery, S., Characterization of the bifunctional aminoglycoside-modifying enzyme ANT(3")-Ii/AAC(6')-IId from *Serratia marcescens*. *Biochemistry* **2006,** *45* (27), 8368-77.
23. Frase, H.; Toth, M.; Vakulenko, S. B., Revisiting the nucleotide and aminoglycoside substrate specificity of the bifunctional aminoglycoside acetyltransferase(6')-Ie/aminoglycoside phosphotransferase(2")-Ia enzyme. *J. Biol. Chem.* **2012,** *287* (52), 43262-9.
24. Houghton, J. L.; Biswas, T.; Chen, W.; Tsodikov, O. V.; Garneau-Tsodikova, S., Chemical and structural insights into the regioversatility of the aminoglycoside acetyltransferase Eis. *ChemBioChem* **2013,** *14* (16), 2127-35.
25. Chen, W.; Biswas, T.; Porter, V. R.; Tsodikov, O. V.; Garneau-Tsodikova, S., Unusual regioversatility of acetyltransferase Eis, a cause of drug resistance in XDR-TB. *Proc. Natl. Acad. Sci., U. S. A.* **2011,** *108* (24), 9804-8.
26. Tsodikov, O. V.; Green, K. D.; Garneau-Tsodikova, S., A random sequential mechanism of aminoglycoside acetylation by *Mycobacterium tuberculosis* Eis protein. *PLoS One* **2014,** *9* (4), e92370.
27. Green, K. D.; Chen, W.; Garneau-Tsodikova, S., Identification and characterization of inhibitors of the aminoglycoside resistance acetyltransferase Eis from *Mycobacterium tuberculosis*. *ChemMedChem* **2012,** *7* (1), 73-7.
28. Zaunbrecher, M. A.; Sikes, R. D., Jr.; Metchock, B.; Shinnick, T. M.; Posey, J. E., Overexpression of the chromosomally encoded aminoglycoside acetyltransferase *eis*

confers kanamycin resistance in *Mycobacterium tuberculosis*. *Proc. Natl. Acad. Sci., U. S. A.* **2009,** *106* (47), 20004-9.

29. Chen, W.; Green, K. D.; Tsodikov, O. V.; Garneau-Tsodikova, S., Aminoglycoside multiacetylating activity of the enhanced intracellular survival protein from *Mycobacterium smegmatis* and its inhibition. *Biochemistry* **2012,** *51* (24), 4959-67.
30. Pricer, R. E.; Houghton, J. L.; Green, K. D.; Mayhoub, A. S.; Garneau-Tsodikova, S., Biochemical and structural analysis of aminoglycoside acetyltransferase Eis from *Anabaena variabilis*. *Mol. BioSyst.* **2012,** *8* (12), 3305-13.
31. Jennings, B. C.; Labby, K. J.; Green, K. D.; Garneau-Tsodikova, S., Redesign of substrate specificity and identification of the aminoglycoside binding residues of Eis from *Mycobacterium tuberculosis*. *Biochemistry* **2013,** *52* (30), 5125-32.
32. Green, K. D.; Biswas, T.; Chang, C.; Wu, R.; Chen, W.; Janes, B. K.; Chalupska, D.; Gornicki, P.; Hanna, P. C.; Tsodikov, O. V.; Joachimiak, A.; Garneau-Tsodikova, S., Biochemical and structural analysis of an Eis family aminoglycoside acetyltransferase from *Bacillus anthracis*. *Biochemistry* **2015,** *54* (20), 3197-206.
33. Green, K. D.; Pricer, R. E.; Stewart, M. N.; Garneau-Tsodikova, S., Comparative study of Eis-like enzymes from pathogenic and non-pathogenic bacteria. *ACS Infect. Dis.* **2015,** *1* (6), 272-83.
34. Ishino, K.; Ishikawa, J.; Ikeda, Y.; Hotta, K., Characterization of a bifunctional aminoglycoside-modifying enzyme with novel substrate specificity and its gene from a clinical isolate of methicillin-resistant *Staphylococcus aureus* with high arbekacin resistance. *J. Antibiot.* **2004,** *57* (10), 679-86.

35. Fujimura, S.; Tokue, Y.; Takahashi, H.; Nukiwa, T.; Hisamichi, K.; Mikami, T.; Watanabe, A., A newly recognized acetylated metabolite of arbekacin in arbekacin-resistant strains of methicillin-resistant *Staphylococcus aureus*. *J. Antimicrob. Chemother.* **1998,** *41* (4), 495-7.

36. Fujimura, S.; Tokue, Y.; Takahashi, H.; Kobayashi, T.; Gomi, K.; Abe, T.; Nukiwa, T.; Watanabe, A., Novel arbekacin- and amikacin-modifying enzyme of methicillin-resistant *Staphylococcus aureus*. *FEMS Microbiol. Lett.* **2000,** *190* (2), 299-303.

37. Fujimura, S.; Tokue, Y.; Takahashi, H.; Nukiwa, T.; Watanabe, A., Specificity of 4'''-acetylation by an aminoglycoside-modifying enzyme in arbekacin-resistant strains of methicillin-resistant *Staphylococcus aureus*. *Tohoku J. Exp. Med.* **1998,** *186* (1), 67-70.

38. Green, K. D.; Chen, W.; Houghton, J. L.; Fridman, M.; Garneau-Tsodikova, S., Exploring the substrate promiscuity of drug-modifying enzymes for the chemoenzymatic generation of *N*-acylated aminoglycosides. *ChemBioChem* **2010,** *11* (1), 119-26.

39. Boehr, D. D.; Daigle, D. M.; Wright, G. D., Domain-domain interactions in the aminoglycoside antibiotic resistance enzyme AAC(6')-APH(2''). *Biochemistry* **2004,** *43* (30), 9846-55.

40. Smith, C. A.; Toth, M.; Weiss, T. M.; Frase, H.; Vakulenko, S. B., Structure of the bifunctional aminoglycoside-resistance enzyme AAC(6')-Ie-APH(2'')-Ia revealed by crystallographic and small-angle X-ray scattering analysis. *Acta Crystallogr. D* **2014,** *70* (Pt 10), 2754-64.

41. Smith, C. A.; Toth, M.; Bhattacharya, M.; Frase, H.; Vakulenko, S. B., Structure of the phosphotransferase domain of the bifunctional aminoglycoside-resistance enzyme AAC(6')-Ie-APH(2")-Ia. *Acta Crystallogr. D* **2014,** *70* (Pt 6), 1561-71.

42. Daigle, D. M.; Hughes, D. W.; Wright, G. D., Prodigious substrate specificity of AAC(6')-APH(2"), an aminoglycoside antibiotic resistance determinant in *enterococci* and *staphylococci*. *Chem. Biol.* **1999,** *6* (2), 99-110.

43. Boehr, D. D.; Jenkins, S. I.; Wright, G. D., The molecular basis of the expansive substrate specificity of the antibiotic resistance enzyme aminoglycoside acetyltransferase-6'-aminoglycoside phosphotransferase-2". The role of ASP-99 as an active site base important for acetyl transfer. *J. Biol. Chem.* **2003,** *278* (15), 12873-180.

44. Hotta, K.; Zhu, C. B.; Ogata, T.; Sunada, A.; Ishikawa, J.; Mizuno, S.; Ikeda, Y.; Kondo, S., Enzymatic 2'-*N*-acetylation of arbekacin and antibiotic activity of its product. *J. Antibiot.* **1996,** *49* (5), 458-64.

45. Hotta, K.; Sunada, A.; Ishikawa, J.; Mizuno, S.; Ikeda, Y.; Kondo, S., The novel enzymatic 3"-*N*-acetylation of arbekacin by an aminoglycoside 3-*N*-acetyltransferase of *Streptomyces* origin and the resulting activity. *J. Antibiot.* **1998,** *51* (8), 735-42.

46. Zhu, C. B.; Sunada, A.; Ishikawa, J.; Ikeda, Y.; Kondo, S.; Hotta, K., Role of aminoglycoside 6'-acetyltransferase in a novel multiple aminoglycoside resistance of an actinomycete strain #8: inactivation of aminoglycosides with 6'-amino group except arbekacin and neomycin. *J. Antibiot.* **1999,** *52* (10), 889-94.

Chapter 3 references

1. Houghton, J. L.; Green, K. D.; Chen, W.; Garneau-Tsodikova, S., The future of aminoglycosides: the end or renaissance? *ChemBioChem* **2010,** *11* (7), 880-902.
2. Fosso, M. Y.; Li, Y.; Garneau-Tsodikova, S., New trends in aminoglycosides use. *MedChemComm* **2014,** *5* (8), 1075-1091.
3. Park, S. R.; Park, J. W.; Ban, Y. H.; Sohng, J. K.; Yoon, Y. J., 2-Deoxystreptamine-containing aminoglycoside antibiotics: recent advances in the characterization and manipulation of their biosynthetic pathways. *Nat. Prod. Rep.* **2013,** *30* (1), 11-20.
4. Geller, D. E., Aerosol antibiotics in cystic fibrosis. *Respir. Care* **2009,** *54* (5), 658-70.
5. Cohen, P. R., Follicular contact dermatitis revisited: A review emphasizing neomycin-associated follicular contact dermatitis. *World J. Clin. Cases* **2014,** *2* (12), 815-21.
6. Ramirez, M. S.; Tolmasky, M. E., Aminoglycoside modifying enzymes. *Drug Resist. Updat.* **2010,** *13* (6), 151-71.
7. Labby, K. J.; Garneau-Tsodikova, S., Strategies to overcome the action of aminoglycoside-modifying enzymes for treating resistant bacterial infections. *Future Med. Chem.* **2013,** *5* (11), 1285-309.
8. Chen, W.; Biswas, T.; Porter, V. R.; Tsodikov, O. V.; Garneau-Tsodikova, S., Unusual regioversatility of acetyltransferase Eis, a cause of drug resistance in XDR-TB. *Proc. Natl. Acad. Sci., U. S. A.* **2011,** *108* (24), 9804-8.
9. Houghton, J. L.; Biswas, T.; Chen, W.; Tsodikov, O. V.; Garneau-Tsodikova, S., Chemical and structural insights into the regioversatility of the aminoglycoside acetyltransferase Eis. *ChemBioChem* **2013,** *14* (16), 2127-35.

10. Chen, W.; Green, K. D.; Tsodikov, O. V.; Garneau-Tsodikova, S., Aminoglycoside multiacetylating activity of the enhanced intracellular survival protein from *Mycobacterium smegmatis* and its inhibition. *Biochemistry* **2012,** *51* (24), 4959-67.
11. Lin, D. L.; Tran, T.; Adams, C.; Alam, J. Y.; Herron, S. R.; Tolmasky, M. E., Inhibitors of the aminoglycoside 6'-*N*-acetyltransferase type Ib [AAC(6')-Ib] identified by in silico molecular docking. *Bioorg. Med. Chem. Lett.* **2013,** *23* (20), 5694-8.
12. Green, K. D.; Chen, W.; Garneau-Tsodikova, S., Identification and characterization of inhibitors of the aminoglycoside resistance acetyltransferase Eis from *Mycobacterium tuberculosis*. *ChemMedChem* **2012,** *7* (1), 73-7.
13. Allen, N. E.; Alborn, W. E., Jr.; Hobbs, J. N., Jr.; Kirst, H. A., 7-Hydroxytropolone: an inhibitor of aminoglycoside-2"-*O*-adenylyltransferase. *Antimicrob. Agents Chemother.* **1982,** *22* (5), 824-31.
14. Welch, K. T.; Virga, K. G.; Whittemore, N. A.; Ozen, C.; Wright, E.; Brown, C. L.; Lee, R. E.; Serpersu, E. H., Discovery of non-carbohydrate inhibitors of aminoglycoside-modifying enzymes. *Bioorg. Med. Chem.* **2005,** *13* (22), 6252-63.
15. Williams, J. W.; Northrop, D. B., Synthesis of a tight-binding, multisubstrate analog inhibitor of gentamicin acetyltransferase I. *J. Antibiot.* **1979,** *32* (11), 1147-54.
16. Gao, F.; Yan, X.; Baettig, O. M.; Berghuis, A. M.; Auclair, K., Regio- and chemoselective 6'-*N*-derivatization of aminoglycosides: bisubstrate inhibitors as probes to study aminoglycoside 6'-*N*-acetyltransferases. *Angew. Chem.* **2005,** *44* (42), 6859-62.
17. Lin, D. L.; Tran, T.; Alam, J. Y.; Herron, S. R.; Ramirez, M. S.; Tolmasky, M. E., Inhibition of aminoglycoside 6'-*N*-acetyltransferase type Ib by zinc: reversal of

amikacin resistance in *Acinetobacter baumannii* and *Escherichia coli* by a zinc ionophore. *Antimicrob. Agents Chemother.* **2014,** *58* (7), 4238-41.

18. Ainsa, J. A.; Perez, E.; Pelicic, V.; Berthet, F. X.; Gicquel, B.; Martin, C., Aminoglycoside 2'-*N*-acetyltransferase genes are universally present in mycobacteria: characterization of the aac(2')-Ic gene from *Mycobacterium tuberculosis* and the aac(2')-Id gene from *Mycobacterium smegmatis*. *Mol. Microbiol.* **1997,** *24* (2), 431-41.
19. Vetting, M. W.; Hegde, S. S.; Javid-Majd, F.; Blanchard, J. S.; Roderick, S. L., Aminoglycoside 2'-*N*-acetyltransferase from *Mycobacterium tuberculosis* in complex with coenzyme A and aminoglycoside substrates. *Nat. Struct. Biol.* **2002,** *9* (9), 653-8.
20. Javier Teran, F.; Alvarez, M.; Suarez, J. E.; Mendoza, M. C., Characterization of two aminoglycoside-(3)-*N*-acetyltransferase genes and assay as epidemiological probes. *J. Antimicrob. Chemother.* **1991,** *28* (3), 333-46.
21. Dubois, V.; Poirel, L.; Marie, C.; Arpin, C.; Nordmann, P.; Quentin, C., Molecular characterization of a novel class 1 integron containing bla(GES-1) and a fused product of aac3-Ib/aac6'-Ib' gene cassettes in *Pseudomonas aeruginosa*. *Antimicrob. Agents Chemother.* **2002,** *46* (3), 638-45.
22. Kim, C.; Villegas-Estrada, A.; Hesek, D.; Mobashery, S., Mechanistic characterization of the bifunctional aminoglycoside-modifying enzyme AAC(3)-Ib/AAC(6')-Ib' from *Pseudomonas aeruginosa*. *Biochemistry* **2007,** *46* (17), 5270-82.
23. Magalhaes, M. L.; Blanchard, J. S., The kinetic mechanism of AAC3-IV aminoglycoside acetyltransferase from *Escherichia coli*. *Biochemistry* **2005,** *44* (49), 16275-83.

24. Boehr, D. D.; Daigle, D. M.; Wright, G. D., Domain-domain interactions in the aminoglycoside antibiotic resistance enzyme AAC(6')-APH(2"). *Biochemistry* **2004,** *43* (30), 9846-55.
25. Daigle, D. M.; Hughes, D. W.; Wright, G. D., Prodigious substrate specificity of AAC(6')-APH(2"), an aminoglycoside antibiotic resistance determinant in *Enterococci* and *Staphylococci*. *Chem. Biol.* **1999,** *6* (2), 99-110.
26. Caldwell, S. J.; Berghuis, A. M., Small-angle X-ray scattering analysis of the bifunctional antibiotic resistance enzyme aminoglycoside (6') acetyltransferase-ie/aminoglycoside (2") phosphotransferase-ia reveals a rigid solution structure. *Antimicrob. Agents Chemother.* **2012,** *56* (4), 1899-906.
27. Centron, D.; Roy, P. H., Presence of a group II intron in a multiresistant Serratia marcescens strain that harbors three integrons and a novel gene fusion. *Antimicrob. Agents Chemother.* **2002,** *46* (5), 1402-9.
28. Kim, C.; Hesek, D.; Zajicek, J.; Vakulenko, S. B.; Mobashery, S., Characterization of the bifunctional aminoglycoside-modifying enzyme ANT(3")-Ii/AAC(6')-IId from *Serratia marcescens*. *Biochemistry* **2006,** *45* (27), 8368-77.
29. Thumb, N., Comparison of oral and parenteral gold therapy--review of the literature. *Wien. Klin. Wochenschr. Suppl.* **1984,** *156*, 44-8.
30. Green, K. D.; Chen, W.; Garneau-Tsodikova, S., Effects of altering aminoglycoside structures on bacterial resistance enzyme activities. *Antimicrob. Agents Chemother.* **2011,** *55* (7), 3207-13.
31. Green, K. D.; Chen, W.; Houghton, J. L.; Fridman, M.; Garneau-Tsodikova, S., Exploring the substrate promiscuity of drug-modifying enzymes for the

chemoenzymatic generation of *N*-acylated aminoglycosides. *ChemBioChem* **2010,** *11* (1), 119-26.

32. Green, K. D.; Garneau-Tsodikova, S., Domain dissection and characterization of the aminoglycoside resistance enzyme ANT(3")-Ii/AAC(6')-IId from *Serratia marcescens*. *Biochimie* **2013,** *95* (6), 1319-25.
33. Almaghrabi, R.; Clancy, C. J.; Doi, Y.; Hao, B.; Chen, L.; Shields, R. K.; Press, E. G.; Iovine, N. M.; Townsend, B. M.; Wagener, M. M.; Kreiswirth, B.; Nguyen, M. H., Carbapenem-resistant *Klebsiella pneumoniae* strains exhibit diversity in aminoglycoside-modifying enzymes, which exert differing effects on plazomicin and other agents. *Antimicrob. Agents Chemother.* **2014,** *58* (8), 4443-51.

Chapter 4 references

1. Fosso, M. Y.; Li, Y.; Garneau-Tsodikova, S., New trends in aminoglycosides use. *MedChemComm* **2014,** *5* (8), 1075-91.
2. Houghton, J. L. L.; Green, K. D.; Chen, W.; Garneau-Tsodikova, S., The future of aminoglycosides: the end or renaissance? *ChemBioChem* **2010,** *11* (7), 880-902.
3. Labby, K. J.; Garneau-Tsodikova, S., Strategies to overcome the action of aminoglycoside-modifying enzymes for treating resistant bacterial infections. *Future Med. Chem.* **2013,** *5* (11), 1285-309.
4. Green, K. D.; Chen, W.; Garneau-Tsodikova, S., Identification and characterization of inhibitors of the aminoglycoside resistance acetyltransferase Eis from *Mycobacterium tuberculosis*. *ChemMedChem* **2012,** *7* (1), 73-7.

5. Holbrook, S. Y. L.; Garneau-Tsodikova, S., Expanding aminoglycoside resistance enzyme regiospecificity by mutation and truncation. *Biochemistry* **2016,** *55* (40), 5726-37.
6. Holbrook, S. Y. L.; Garneau-Tsodikova, S., Evaluation of Aminoglycoside and Carbapenem Resistance in a Collection of Drug-Resistant *Pseudomonas aeruginosa* Clinical Isolates. *Microb. Drug Resist.* **2017**, doi: 10.1089/mdr.2017.0101.
7. Li, Y.; Green, K. D.; Johnson, B. R.; Garneau-Tsodikova, S., Inhibition of aminoglycoside acetyltransferase resistance enzymes by metal salts. *Antimicrob. Agents Chemother.* **2015,** *59* (7), 4148-56.
8. Zingman, L. V.; Park, S.; Olson, T. M.; Alekseev, A. E.; Terzic, A., Aminoglycoside-induced translational read-through in disease: overcoming nonsense mutations by pharmacogenetic therapy. *Clin. Pharmacol. Ther.* **2007,** *81* (1), 99-103.
9. Linde, L.; Kerem, B., Introducing sense into nonsense in treatments of human genetic diseases. *Trends Genet.* **2008,** *24* (11), 552-63.
10. Du, M.; Keeling, K. M.; Fan, L.; Liu, X.; Kovacs, T.; Sorscher, E.; Bedwell, D. M., Clinical doses of amikacin provide more effective suppression of the human CFTR-G542X stop mutation than gentamicin in a transgenic CF mouse model. *J. Mol. Med.* **2006,** *84* (7), 573-82.
11. Xue, X.; Mutyam, V.; Tang, L.; Biswas, S.; Du, M.; Jackson, L. A.; Dai, Y.; Belakhov, V.; Shalev, M.; Chen, F.; Schacht, J.; R, J. B.; Baasov, T.; Hong, J.; Bedwell, D. M.; Rowe, S. M., Synthetic aminoglycosides efficiently suppress cystic fibrosis transmembrane conductance regulator nonsense mutations and are enhanced by ivacaftor. *Am. J. Respir. Cell Mol. Biol.* **2014,** *50* (4), 805-16.

12. Pichavant, C.; Aartsma-Rus, A.; Clemens, P. R.; Davies, K. E.; Dickson, G.; Takeda, S.; Wilton, S. D.; Wolff, J. A.; Wooddell, C. I.; Xiao, X.; Tremblay, J. P., Current status of pharmaceutical and genetic therapeutic approaches to treat DMD. *Mol. Ther.* **2011,** *19* (5), 830-40.
13. Garneau-Tsodikova, S.; Labby, K. J., Mechanisms of resistance to aminoglycoside antibiotics: Overview and perspectives. *MedChemComm* **2016,** *7* (1), 11-27.
14. Ramirez, M. S.; Tolmasky, M. E., Aminoglycoside modifying enzymes. *Drug Resist. Updat.* **2010,** *13* (6), 151-71.
15. Kim, C.; Mobashery, S., Phosphoryl transfer by aminoglycoside 3'-phosphotransferases and manifestation of antibiotic resistance. *Bioorg. Chem.* **2005,** *33* (3), 149-58.
16. Wright, G. D.; Thompson, P. R., Aminoglycoside phosphotransferases: proteins, structure, and mechanism. *Front. Biosci.* **1999,** *4*, D9-21.
17. Sanchez-Carrera, D.; Bravo-Navas, S.; Cabezon, E.; Arechaga, I.; Cabezas, M.; Yanez, L.; Pipaon, C., Fludarabine resistance mediated by aminoglycoside-3'-phosphotransferase-IIa and the structurally related eukaryotic cAMP-dependent protein kinase. *FASEB J.* **2017,** *31* (7), 3007-17.
18. Franke, C. A.; Rice, C. M.; Strauss, J. H.; Hruby, D. E., Neomycin resistance as a dominant selectable marker for selection and isolation of vaccinia virus recombinants. *Mol. Cell. Biol.* **1985,** *5* (8), 1918-24.
19. Yenofsky, R. L.; Fine, M.; Pellow, J. W., A mutant neomycin phosphotransferase II gene reduces the resistance of transformants to antibiotic selection pressure. *Proc. Natl. Acad. Sci., U. S. A.* **1990,** *87* (9), 3435-9.

20. Siregar, J. J.; Lerner, S. A.; Mobashery, S., Purification and characterization of aminoglycoside 3'-phosphotransferase type IIa and kinetic comparison with a new mutant enzyme. *Antimicrob. Agents Chemother.* **1994,** *38* (4), 641-7.
21. Kim, C.; Cha, J. Y.; Yan, H.; Vakulenko, S. B.; Mobashery, S., Hydrolysis of ATP by aminoglycoside 3'-phosphotransferases: an unexpected cost to bacteria for harboring an antibiotic resistance enzyme. *J. Biol. Chem.* **2006,** *281* (11), 6964-9.
22. Jin, Y.; Watkins, D.; Degtyareva, N. N.; Green, K. D.; Spano, M. N.; Garneau-Tsodikova, S.; Arya, D. P., Arginine-linked neomycin B dimers: synthesis, rRNA binding, and resistance enzyme activity. *MedChemComm* **2016,** *7* (1), 164-9.
23. Shakya, T.; Wright, G. D., Nucleotide selectivity of antibiotic kinases. *Antimicrob. Agents Chemother.* **2010,** *54* (5), 1909-13.
24. McKay, G. A.; Wright, G. D., Catalytic mechanism of enterococcal kanamycin kinase (APH(3')-IIIa): viscosity, thio, and solvent isotope effects support a Theorell-Chance mechanism. *Biochemistry* **1996,** *35* (26), 8680-5.
25. Nurizzo, D.; Shewry, S. C.; Perlin, M. H.; Brown, S. A.; Dholakia, J. N.; Fuchs, R. L.; Deva, T.; Baker, E. N.; Smith, C. A., The crystal structure of aminoglycoside-3'-phosphotransferase-IIa, an enzyme responsible for antibiotic resistance. *J. Mol. Biol.* **2003,** *327* (2), 491-506.
26. Thamban Chandrika, N.; Green, K. D.; Houghton, J. L.; Garneau-Tsodikova, S., Synthesis and biological activity of mono- and di-*N*-acylated aminoglycosides. *ACS Med. Chem. Lett.* **2015,** *6* (11), 1134-9.
27. Smith, C. A.; Toth, M.; Frase, H.; Byrnes, L. J.; Vakulenko, S. B., Aminoglycoside 2''-phosphotransferase IIIa (APH(2'')-IIIa) prefers GTP over ATP: structural

templates for nucleotide recognition in the bacterial aminoglycoside-2" kinases. *J. Biol. Chem.* **2012,** *287* (16), 12893-903.

28. Toth, M.; Frase, H.; Antunes, N. T.; Vakulenko, S. B., Novel aminoglycoside 2"-phosphotransferase identified in a gram-negative pathogen. *Antimicrob. Agents Chemother.* **2013,** *57* (1), 452-7.
29. Green, K. D.; Chen, W.; Houghton, J. L.; Fridman, M.; Garneau-Tsodikova, S., Exploring the substrate promiscuity of drug-modifying enzymes for the chemoenzymatic generation of *N*-acylated aminoglycosides. *ChemBiocChem* **2010,** *11* (1), 119-26.
30. Lallemand, P.; Leban, N.; Kunzelmann, S.; Chaloin, L.; Serpersu, E. H.; Webb, M. R.; Barman, T.; Lionne, C., Transient kinetics of aminoglycoside phosphotransferase(3')-IIIa reveals a potential drug target in the antibiotic resistance mechanism. *FEBS Lett.* **2012,** *586* (23), 4223-7.
31. McKay, G. A.; Wright, G. D., Kinetic mechanism of aminoglycoside phosphotransferase type IIIa. Evidence for a Theorell-Chance mechanism. *J. Biol. Chem.* **1995,** *270* (42), 24686-92.
32. Fong, D. H.; Berghuis, A. M., Substrate promiscuity of an aminoglycoside antibiotic resistance enzyme via target mimicry. *EMBO J.* **2002,** *21* (10), 2323-31.
33. McKay, G. A.; Thompson, P. R.; Wright, G. D., Broad spectrum aminoglycoside phosphotransferase type III from *Enterococcus*: overexpression, purification, and substrate specificity. *Biochemistry* **1994,** *33* (22), 6936-44.
34. Shi, K.; Berghuis, A. M., Structural basis for dual nucleotide selectivity of aminoglycoside 2"-phosphotransferase IVa provides insight on determinants of

nucleotide specificity of aminoglycoside kinases. *J. Biol. Chem.* **2012,** *287* (16), 13094-102.

Chapter 5 references

1. Boucher, H. W.; Talbot, G. H.; Bradley, J. S.; Edwards, J. E.; Gilbert, D.; Rice, L. B.; Scheld, M.; Spellberg, B.; Bartlett, J., Bad bugs, no drugs: no ESKAPE! An update from the Infectious Diseases Society of America. *Clin. Infect. Dis.* **2009,** *48* (1), 1-12.
2. Narten, M.; Rosin, N.; Schobert, M.; Tielen, P., Susceptibility of *Pseudomonas aeruginosa* urinary tract isolates and influence of urinary tract conditions on antibiotic tolerance. *Curr. Microbiol.* **2012,** *64* (1), 7-16.
3. Obritsch, M. D.; Fish, D. N.; MacLaren, R.; Jung, R., Nosocomial infections due to multidrug-resistant *Pseudomonas aeruginosa*: epidemiology and treatment options. *Pharmacotherapy* **2005,** *25* (10), 1353-64.
4. Pendleton, J. N.; Gorman, S. P.; Gilmore, B. F., Clinical relevance of the ESKAPE pathogens. *Expert Rev. Anti-Infect. Ther.* **2013,** *11* (3), 297-308.
5. Pobiega, M.; Maciag, J.; Chmielarczyk, A.; Romaniszyn, D.; Pomorska-Wesolowska, M.; Ziolkowski, G.; Heczko, P. B.; Bulanda, M.; Wojkowska-Mach, J., Molecular characterization of carbapenem-resistant *Pseudomonas aeruginosa* strains isolated from patients with urinary tract infections in Southern Poland. *Diagn. Microbiol. Infect. Dis.* **2015,** *83* (3), 295-7.
6. Qiu, X.; Kulasekara, B. R.; Lory, S., Role of horizontal gene transfer in the evolution of *Pseudomonas aeruginosa* virulence. *Genome Dyn.* **2009,** *6*, 126-39.

7. Rice, L. B., Progress and challenges in implementing the research on ESKAPE pathogens. *Infect. Control Hosp. Epidemiol.* **2010,** *31 Suppl 1*, S7-10.
8. Hirsch, E. B.; Tam, V. H., Impact of multidrug-resistant *Pseudomonas aeruginosa* infection on patient outcomes. *Expert Rev. Pharmacoecon. Outcomes Res.* **2010,** *10* (4), 441-51.
9. Fenyo, D.; Wang, Q.; DeGrasse, J. A.; Padovan, J. C.; Cadene, M.; Chait, B. T., MALDI sample preparation: the ultra thin layer method. *JoVE* **2007,** (3), 192.
10. Fujitani, S.; Moffett, K. S.; Yu, V. L., *Pseudomonas aeruginosa*. *Antimicrobe: Infectious Disease & Antimicrobial Agents http://www.antimicrobe.org/new/b112.asp* **2017**.
11. Calhoun, J. H.; Murray, C. K.; Manring, M. M., Multidrug-resistant organisms in military wounds from Iraq and Afghanistan. *Clin. Orthop. Relat. Res.* **2008,** *466* (6), 1356-62.
12. Fosso, M. Y.; Li, Y.; Garneau-Tsodikova, S., New trends in aminoglycosides use. *MedChemComm* **2014,** *5* (8), 1075-91.
13. Matt, T.; Ng, C. L.; Lang, K.; Sha, S. H.; Akbergenov, R.; Shcherbakov, D.; Meyer, M.; Duscha, S.; Xie, J.; Dubbaka, S. R.; Perez-Fernandez, D.; Vasella, A.; Ramakrishnan, V.; Schacht, J.; Bottger, E. C., Dissociation of antibacterial activity and aminoglycoside ototoxicity in the 4-monosubstituted 2-deoxystreptamine apramycin. *Proc. Natl. Acad. Sci., U. S. A.* **2012,** *109* (27), 10984-9.
14. Kang, A. D.; Smith, K. P.; Eliopoulos, G. M.; Berg, A. H.; McCoy, C.; Kirby, J. E., *In vitro* apramycin activity against multidrug-resistant *Acinetobacter baumannii* and *Pseudomonas aeruginosa*. *Diagn. Microbiol. Infect. Dis.* **2017,** *88* (2), 188-91.

15. Karlowsky, J. A.; Hoban, D. J.; Hackel, M. A.; Lob, S. H.; Sahm, D. F., Antimicrobial susceptibility of Gram-negative ESKAPE pathogens isolated from hospitalized patients with intra-abdominal and urinary tract infections in Asia-Pacific countries: SMART 2013-2015. *J. Med. Microbiol.* **2017,** *66* (1), 61-9.

16. Biedenbach, D. J.; Giao, P. T.; Hung Van, P.; Su Minh Tuyet, N.; Thi Thanh Nga, T.; Phuong, D. M.; Vu Trung, N.; Badal, R. E., Antimicrobial-resistant *Pseudomonas aeruginosa* and *Acinetobacter baumannii* from patients with hospital-acquired or ventilator-associated pneumonia in Vietnam. *Clin. Ther.* **2016,** *38* (9), 2098-105.

17. Chen, W.; Biswas, T.; Porter, V. R.; Tsodikov, O. V.; Garneau-Tsodikova, S., Unusual regioversatility of acetyltransferase Eis, a cause of drug resistance in XDR-TB. *Proc. Natl. Acad. Sci., U. S. A.* **2011,** *108* (24), 9804-8.

18. Chen, W.; Green, K. D.; Tsodikov, O. V.; Garneau-Tsodikova, S., Aminoglycoside multiacetylating activity of the enhanced intracellular survival protein from *Mycobacterium smegmatis* and its inhibition. *Biochemistry* **2012,** *51* (24), 4959-67.

19. Green, K. D.; Chen, W.; Garneau-Tsodikova, S., Identification and characterization of inhibitors of the aminoglycoside resistance acetyltransferase Eis from *Mycobacterium tuberculosis*. *ChemMedChem* **2012,** *7* (1), 73-7.

20. Houghton, J. L.; Green, K. D.; Pricer, R. E.; Mayhoub, A. S.; Garneau-Tsodikova, S., Unexpected *N*-acetylation of capreomycin by mycobacterial Eis enzymes. *J. Antimicrob. Chemother.* **2013,** *68* (4), 800-5.

21. Houghton, J. L.; Biswas, T.; Chen, W.; Tsodikov, O. V.; Garneau-Tsodikova, S., Chemical and structural insights into the regioversatility of the aminoglycoside acetyltransferase Eis. *ChemBioChem* **2013,** *14* (16), 2127-35.

22. Tsodikov, O. V.; Green, K. D.; Garneau-Tsodikova, S., A random sequential mechanism of aminoglycoside acetylation by *Mycobacterium tuberculosis* Eis protein. *PLoS One* **2014,** *9* (4), e92370.

23. Ramirez, M. S.; Tolmasky, M. E., Aminoglycoside modifying enzymes. *Drug Resist. Updat.* **2010,** *13* (6), 151-71.

24. Houghton, J. L.; Green, K. D.; Chen, W.; Garneau-Tsodikova, S., The future of aminoglycosides: the end or renaissance? *ChemBioChem* **2010,** *11* (7), 880-902.

25. Li, Y.; Green, K. D.; Johnson, B. R.; Garneau-Tsodikova, S., Inhibition of aminoglycoside acetyltransferase resistance enzymes by metal salts. *Antimicrob. Agents Chemother.* **2015,** *59* (7), 4148-56.

26. Shaul, P.; Green, K. D.; Rutenberg, R.; Kramer, M.; Berkov-Zrihen, Y.; Breiner-Goldstein, E.; Garneau-Tsodikova, S.; Fridman, M., Assessment of 6'- and 6'''-*N*-acylation of aminoglycosides as a strategy to overcome bacterial resistance. *Org. Biomol. Chem.* **2011,** *9* (11), 4057-63.

27. Green, K. D.; Chen, W.; Garneau-Tsodikova, S., Effects of altering aminoglycoside structures on bacterial resistance enzyme activities. *Antimicrob. Agents Chemother.* **2011,** *55* (7), 3207-13.

28. Thamban Chandrika, N.; Green, K. D.; Houghton, J. L.; Garneau-Tsodikova, S., Synthesis and biological activity of mono- and di-*N*-acylated aminoglycosides. *ACS Med. Chem. Lett.* **2015,** *6* (11), 1134-9.

29. Fong, D. H.; Xiong, B.; Hwang, J.; Berghuis, A. M., Crystal structures of two aminoglycoside kinases bound with a eukaryotic protein kinase inhibitor. *PLoS One* **2011,** *6* (5), e19589.

30. Lopez, C.; Arivett, B. A.; Actis, L. A.; Tolmasky, M. E., Inhibition of AAC(6')-Ib-mediated resistance to amikacin in *Acinetobacter baumannii* by an antisense peptide-conjugated 2',4'-bridged nucleic acid-NC-DNA hybrid oligomer. *Antimicrob. Agents Chemother.* **2015,** *59* (9), 5798-803.

31. Shakya, T.; Stogios, P. J.; Waglechner, N.; Evdokimova, E.; Ejim, L.; Blanchard, J. E.; McArthur, A. G.; Savchenko, A.; Wright, G. D., A small molecule discrimination map of the antibiotic resistance kinome. *Chem. Biol.* **2011,** *18* (12), 1591-601.

32. Welch, K. T.; Virga, K. G.; Whittemore, N. A.; Ozen, C.; Wright, E.; Brown, C. L.; Lee, R. E.; Serpersu, E. H., Discovery of non-carbohydrate inhibitors of aminoglycoside-modifying enzymes. *Bioorg. Med. Chem.* **2005,** *13* (22), 6252-63.

33. Zhang, W.; Chen, Y.; Liang, Q.; Li, H.; Jin, H.; Zhang, L.; Meng, X.; Li, Z., Design, synthesis, and antibacterial activities of conformationally constrained kanamycin A derivatives. *J. Org. Chem.* **2013,** *78* (2), 400-9.

34. Fair, R. J.; Hensler, M. E.; Thienphrapa, W.; Dam, Q. N.; Nizet, V.; Tor, Y., Selectively guanidinylated aminoglycosides as antibiotics. *ChemMedChem* **2012,** *7* (7), 1237-44.

35. Tsai, A.; Uemura, S.; Johansson, M.; Puglisi, E. V.; Marshall, R. A.; Aitken, C. E.; Korlach, J.; Ehrenberg, M.; Puglisi, J. D., The impact of aminoglycosides on the dynamics of translation elongation. *Cell Rep.* **2013,** *3* (2), 497-508.

36. Llano-Sotelo, B.; Hickerson, R. P.; Lancaster, L.; Noller, H. F.; Mankin, A. S., Fluorescently labeled ribosomes as a tool for analyzing antibiotic binding. *RNA* **2009,** *15* (8), 1597-604.

37. Chang, C. W.; Fosso, M.; Kawasaki, Y.; Shrestha, S.; Bensaci, M. F.; Wang, J.; Evans, C. K.; Takemoto, J. Y., Antibacterial to antifungal conversion of neamine aminoglycosides through alkyl modification. Strategy for reviving old drugs into agrofungicides. *J. Antibiot.* **2010,** *63* (11), 667-72.

38. Maianti, J. P.; Kanazawa, H.; Dozzo, P.; Matias, R. D.; Feeney, L. A.; Armstrong, E. S.; Hildebrandt, D. J.; Kane, T. R.; Gliedt, M. J.; Goldblum, A. A.; Linsell, M. S.; Aggen, J. B.; Kondo, J.; Hanessian, S., Toxicity modulation, resistance enzyme evasion, and A-site X-ray structure of broad-spectrum antibacterial neomycin analogs. *ACS Chem. Biol.* **2014,** *9* (9), 2067-73.

39. Duscha, S.; Boukari, H.; Shcherbakov, D.; Salian, S.; Silva, S.; Kendall, A.; Kato, T.; Akbergenov, R.; Perez-Fernandez, D.; Bernet, B.; Vaddi, S.; Thommes, P.; Schacht, J.; Crich, D.; Vasella, A.; Bottger, E. C., Identification and evaluation of improved 4'-*O*-(alkyl) 4,5-disubstituted 2-deoxystreptamines as next-generation aminoglycoside antibiotics. *mBio* **2014,** *5* (5), e01827-14.

40. Nakamura, A.; Hosoda, M.; Kato, T.; Yamada, Y.; Itoh, M.; Kanazawa, K.; Nouda, H., Combined effects of meropenem and aminoglycosides on *Pseudomonas aeruginosa in vitro*. *J. Antimicrob. Chemother.* **2000,** *46* (6), 901-4.

41. Ferrara, A.; Grassi, G.; Grassi, F. A.; Piccioni, P. D.; Gialdroni Grassi, G., Bactericidal activity of meropenem and interactions with other antibiotics. *J. Antimicrob. Chemother.* **1989,** *24 Suppl A*, 239-50.

42. Kropec, A.; Lemmen, S.; Wursthorn, M.; Daschner, F. D., Combination effect of meropenem with aminoglycosides and teicoplanin on *Pseudomonas* and *enterococci*. *Infection* **1994,** *22* (4), 306-8.

43. Oie, S.; Sawa, A.; Kamiya, A.; Mizuno, H., *In-vitro* effects of a combination of antipseudomonal antibiotics against multi-drug resistant *Pseudomonas aeruginosa*. *J. Antimicrob. Chemother.* **1999,** *44* (5), 689-91.

44. Clinical and Laboratory Standards Institute, *Performance Standards for antimicrobial susceptibility testing; twenty-fourth informational supplement, CLSI document M100-S24. Wayne, PA.* 2014.

45. Barry, A. L.; Miller, G. H.; Hare, R. S.; Jones, R. N.; Thornsberry, C., Modification of interpretive breakpoints for netilmicin disk susceptibility tests with *Pseudomonas aeruginosa*. *J. Clin. Microbiol.* **1984,** *19* (3), 311-4.

46. Barry, A. L.; Miller, G. H.; Hare, R. S.; Jones, R. N.; Thornsberry, C., Modification of interpretive breakpoints for netilmicin disk susceptibility tests with *Pseudomonas aeruginosa*. *J. Clin. Microbiol.* **1984,** *19* (3), 311-4.

47. Hawkey, P. M.; Jones, A. M., The changing epidemiology of resistance. *J. Antimicrob. Chemother.* **2009,** *64 Suppl 1*, i3-10.

48. Grall, N.; Lazarevic, V.; Gaia, N.; Couffignal, C.; Laouenan, C.; Ilic-Habensus, E.; Wieder, I.; Plesiat, P.; Angebault, C.; Bougnoux, M. E.; Armand-Lefevre, L.; Andremont, A.; Duval, X.; Schrenzel, J., Unexpected persistence of extended-spectrum beta-lactamase-producing *Enterobacteriaceae* in the faecal microbiota of hospitalised patients treated with imipenem. *Int. J. Antimicrob. Agents* **2017,** *50* (1), 81-7.

49. Hansen, K. C. M.; Schwensen, S. A. F.; Henriksen, D. P.; Justesen, U. S.; Sydenham, T. V., Antimicrobial resistance in the *Bacteroides fragilis* group in faecal samples from patients receiving broad-spectrum antibiotics. *Anaerobe* **2017,** *47*, 79-85.

50. Chuanchuen, R.; Beinlich, K.; Hoang, T. T.; Becher, A.; Karkhoff-Schweizer, R. R.; Schweizer, H. P., Cross-resistance between triclosan and antibiotics in *Pseudomonas aeruginosa* is mediated by multidrug efflux pumps: exposure of a susceptible mutant strain to triclosan selects nfxB mutants overexpressing MexCD-OprJ. *Antimicrob. Agents Chemother.* **2001,** *45* (2), 428-32.
51. Almaghrabi, R.; Clancy, C. J.; Doi, Y.; Hao, B.; Chen, L.; Shields, R. K.; Press, E. G.; Iovine, N. M.; Townsend, B. M.; Wagener, M. M.; Kreiswirth, B.; Nguyen, M. H., Carbapenem-resistant *Klebsiella pneumoniae* strains exhibit diversity in aminoglycoside-modifying enzymes, which exert differing effects on plazomicin and other agents. *Antimicrob. Agents Chemother.* **2014,** *58* (8), 4443-51.
52. Yadav, R.; Landersdorfer, C. B.; Nation, R. L.; Boyce, J. D.; Bulitta, J. B., Novel approach to optimize synergistic carbapenem-aminoglycoside combinations against carbapenem-resistant *Acinetobacter baumannii*. *Antimicrob. Agents Chemother.* **2015,** *59* (4), 2286-98.
53. Clock, S. A.; Tabibi, S.; Alba, L.; Kubin, C. J.; Whittier, S.; Saiman, L., *In vitro* activity of doripenem alone and in multi-agent combinations against extensively drug-resistant *Acinetobacter baumannii* and *Klebsiella pneumoniae*. *Diagn. Microbiol. Infect. Dis.* **2013,** *76* (3), 343-6.
54. Principe, L.; Capone, A.; Mazzarelli, A.; D'Arezzo, S.; Bordi, E.; Di Caro, A.; Petrosillo, N., *In vitro* activity of doripenem in combination with various antimicrobials against multidrug-resistant *Acinetobacter baumannii*: possible options for the treatment of complicated infection. *Microb. Drug Resist.* **2013,** *19* (5), 407-14.

55. Clinical and Laboratory Standard Institute, *Methods for dilution antimicrobial susceptibility tests for bacteria that grow aerobically - Approved standard, 9th edition. CLSI document M07-A9. Wayne, PA.* 2012.

56. Barry, A. L.; Thornsberry, C.; Jones, R. N.; Gerlach, E. H., Gentamicin, tobramycin, and sisomicin disc susceptibility tests. Revised zone standards for interpretation. *Am. J. Clin. Pathol.* **1981,** *75* (4), 524-31.

57. Watkins, D.; Kumar, S.; Green, K. D.; Arya, D. P.; Garneau-Tsodikova, S., Influence of linker length and composition on enzymatic activity and ribosomal binding of neomycin dimers. *Antimicrob. Agents Chemother.* **2015,** *59* (7), 3899-905.

58. Meletiadis, J.; Mouton, J. W.; Meis, J. F.; Verweij, P. E., *In vitro* drug interaction modeling of combinations of azoles with terbinafine against clinical *Scedosporium prolificans* isolates. *Antimicrob. Agents Chemother.* **2003,** *47* (1), 106-17.

Chapter 6 references

1. Ngo, H. X.; Garneau-Tsodikova, S.; Green, K. D., A complex game of hide and seek: the search for new antifungals. *MedChemComm* **2016,** *7* (7), 1285-306.

2. Arendrup, M. C., Epidemiology of invasive candidiasis. *Curr. Opin. Crit. Care* **2010,** *16* (5), 445-52.

3. Vandeputte, P.; Ferrari, S.; Coste, A. T., Antifungal resistance and new strategies to control fungal infections. *Int. J. Microbiol.* **2012,** *2012*, 713687.

4. Pfaller, M. A.; Diekema, D. J., The Epidemiology of invasive candidiasis. In *Candida and candidiasis*, 2nd edition ed.; Calderone, R. A.; Clancy, C. J., Eds. ASM Press: Washington, DC, 2012; pp 449-50.

5. Denning, D. W.; Pleuvry, A.; Cole, D. C., Global burden of allergic bronchopulmonary aspergillosis with asthma and its complication chronic pulmonary aspergillosis in adults. *Med. Mycol.* **2013,** *51* (4), 361-70.
6. Russell, P. E., A century of fungicide evolution. *J. Agr. Sci.* **2005,** *143*, 11-25.
7. Yoshida, K.; Schuenemann, V. J.; Cano, L. M.; Pais, M.; Mishra, B.; Sharma, R.; Lanz, C.; Martin, F. N.; Kamoun, S.; Krause, J.; Thines, M.; Weigel, D.; Burbano, H. A., The rise and fall of the *Phytophthora infestans* lineage that triggered the Irish potato famine. *Elife* **2013,** *2*, e00731.
8. Singh, R. P.; Hodson, D. P.; Huerta-Espino, J.; Jin, Y.; Bhavani, S.; Njau, P.; Herrera-Foessel, S.; Singh, P. K.; Singh, S.; Govindan, V., The emergence of Ug99 races of the stem rust fungus is a threat to world wheat production. *Annu. Rev. Phytopathol.* **2011,** *49*, 465-81.
9. Pappas, P. G.; Kauffman, C. A.; Andes, D. R.; Clancy, C. J.; Marr, K. A.; Ostrosky-Zeichner, L.; Reboli, A. C.; Schuster, M. G.; Vazquez, J. A.; Walsh, T. J.; Zaoutis, T. E.; Sobel, J. D., Clinical practice guideline for the management of candidiasis: 2016 update by the infectious diseases society of America. *Clin. Infect. Dis.* **2016,** *62* (4), e1-e50.
10. Laniado-Laborin, R.; Cabrales-Vargas, M. N., Amphotericin B: side effects and toxicity. *Rev. Iberoam. Micol.* **2009,** *26* (4), 223-7.
11. Rex, J. H.; Bennett, J. E.; Sugar, A. M.; Pappas, P. G.; van der Horst, C. M.; Edwards, J. E.; Washburn, R. G.; Scheld, W. M.; Karchmer, A. W.; Dine, A. P.; et al., A randomized trial comparing fluconazole with amphotericin B for the treatment

of candidemia in patients without neutropenia. Candidemia Study Group and the National Institute. *N. Engl. J. Med.* **1994,** *331* (20), 1325-30.

12. Charlier, C.; Hart, E.; Lefort, A.; Ribaud, P.; Dromer, F.; Denning, D. W.; Lortholary, O., Fluconazole for the management of invasive candidiasis: where do we stand after 15 years? *J. Antimicrob. Chemother.* **2006,** *57* (3), 384-410.
13. Ghannoum, M. A.; Rice, L. B., Antifungal agents: mode of action, mechanisms of resistance, and correlation of these mechanisms with bacterial resistance. *Clin. Microbiol. Rev.* **1999,** *12* (4), 501-17.
14. Sheehan, D. J.; Hitchcock, C. A.; Sibley, C. M., Current and emerging azole antifungal agents. *Clin. Microbiol. Rev.* **1999,** *12* (1), 40-79.
15. Lempers, V. J.; Martial, L. C.; Schreuder, M. F.; Blijlevens, N. M.; Burger, D. M.; Aarnoutse, R. E.; Bruggemann, R. J., Drug-interactions of azole antifungals with selected immunosuppressants in transplant patients: strategies for optimal management in clinical practice. *Curr. Opin. Pharmacol.* **2015,** *24*, 38-44.
16. Prasad, R.; Shah, A. H.; Rawal, M. K., Antifungals: Mechanism of Action and Drug Resistance. *Adv. Exp. Med. Biol.* **2016,** *892*, 327-49.
17. Shrestha, S. K.; Garzan, A.; Garneau-Tsodikova, S., Novel alkylated azoles as potent antifungals. *Eur. J. Med. Chem.* **2017,** *133*, 309-18.
18. Nagappan, V.; Deresinski, S., Reviews of anti-infective agents: posaconazole: a broad-spectrum triazole antifungal agent. *Clin. Infect. Dis.* **2007,** *45* (12), 1610-7.
19. Xiao, L.; Madison, V.; Chau, A. S.; Loebenberg, D.; Palermo, R. E.; McNicholas, P. M., Three-dimensional models of wild-type and mutated forms of cytochrome P450 14alpha-sterol demethylases from *Aspergillus fumigatus* and *Candida albicans*

provide insights into posaconazole binding. *Antimicrob. Agents Chemother.* **2004,** *48* (2), 568-74.

20. Cowen, L. E.; Singh, S. D.; Kohler, J. R.; Collins, C.; Zaas, A. K.; Schell, W. A.; Aziz, H.; Mylonakis, E.; Perfect, J. R.; Whitesell, L.; Lindquist, S., Harnessing Hsp90 function as a powerful, broadly effective therapeutic strategy for fungal infectious disease. *Proc. Natl. Acad. Sci., U. S. A.* **2009,** *106* (8), 2818-23.
21. Mangoyi, R.; Midiwo, J.; Mukanganyama, S., Isolation and characterization of an antifungal compound 5-hydroxy-7,4'-dimethoxyflavone from *Combretum zeyheri*. *BMC Complement Altern. Med.* **2015,** *15*, 405.
22. Niimi, K.; Harding, D. R.; Parshot, R.; King, A.; Lun, D. J.; Decottignies, A.; Niimi, M.; Lin, S.; Cannon, R. D.; Goffeau, A.; Monk, B. C., Chemosensitization of fluconazole resistance in Saccharomyces cerevisiae and pathogenic fungi by a D-octapeptide derivative. *Antimicrob. Agents Chemother.* **2004,** *48* (4), 1256-71.
23. Shrestha, S. K.; Fosso, M. Y.; Green, K. D.; Garneau-Tsodikova, S., Amphiphilic tobramycin analogues as antibacterial and antifungal agents. *Antimicrob. Agents Chemother.* **2015,** *59* (8), 4861-9.
24. Shrestha, S. K.; Fosso, M. Y.; Garneau-Tsodikova, S., A combination approach to treating fungal infections. *Sci. Rep.* **2015,** *5*, 17070.
25. Zhai, B.; Wu, C.; Wang, L.; Sachs, M. S.; Lin, X., The antidepressant sertraline provides a promising therapeutic option for neurotropic cryptococcal infections. *Antimicrob. Agents Chemother.* **2012,** *56* (7), 3758-66.
26. Afeltra, J.; Verweij, P. E., Antifungal activity of nonantifungal drugs. *Eur. J. Clin. Microbiol. Infect. Dis.* **2003,** *22* (7), 397-407.

27. Stylianou, M.; Kulesskiy, E.; Lopes, J. P.; Granlund, M.; Wennerberg, K.; Urban, C. F., Antifungal application of nonantifungal drugs. *Antimicrob. Agents Chemother.* **2014,** *58* (2), 1055-62.

28. Ramon-Garcia, S.; Ng, C.; Anderson, H.; Chao, J. D.; Zheng, X.; Pfeifer, T.; Av-Gay, Y.; Roberge, M.; Thompson, C. J., Synergistic drug combinations for tuberculosis therapy identified by a novel high-throughput screen. *Antimicrob. Agents Chemother.* **2011,** *55* (8), 3861-9.

29. Meletiadis, J.; Mouton, J. W.; Meis, J. F.; Verweij, P. E., *In vitro* drug interaction modeling of combinations of azoles with terbinafine against clinical *Scedosporium prolificans* isolates. *Antimicrob. Agents Chemother.* **2003,** *47* (1), 106-17.

30. Donlan, R. M., Biofilms: microbial life on surfaces. *Emerg. Infect. Dis.* **2002,** *8* (9), 881-90.

31. Costerton, J. W.; Stewart, P. S.; Greenberg, E. P., Bacterial biofilms: a common cause of persistent infections. *Science* **1999,** *284* (5418), 1318-22.

32. Ramage, G.; Saville, S. P.; Thomas, D. P.; Lopez-Ribot, J. L., *Candida* biofilms: an update. *Eukaryot. Cell* **2005,** *4* (4), 633-8.

33. Bachmann, S. P.; VandeWalle, K.; Ramage, G.; Patterson, T. F.; Wickes, B. L.; Graybill, J. R.; Lopez-Ribot, J. L., *In vitro* activity of caspofungin against *Candida albicans* biofilms. *Antimicrob. Agents Chemother.* **2002,** *46* (11), 3591-6.

34. Al-Fattani, M. A.; Douglas, L. J., Biofilm matrix of *Candida albicans* and *Candida tropicalis*: chemical composition and role in drug resistance. *J. Med. Microbiol.* **2006,** *55* (Pt 8), 999-1008.

35. Pierce, C. G.; Uppuluri, P.; Tristan, A. R.; Wormley, F. L., Jr.; Mowat, E.; Ramage, G.; Lopez-Ribot, J. L., A simple and reproducible 96-well plate-based method for the formation of fungal biofilms and its application to antifungal susceptibility testing. *Nat. Protoc.* **2008,** *3* (9), 1494-500.

36. Quave, C. L.; Estevez-Carmona, M.; Compadre, C. M.; Hobby, G.; Hendrickson, H.; Beenken, K. E.; Smeltzer, M. S., Ellagic acid derivatives from *Rubus ulmifolius* inhibit *Staphylococcus aureus* biofilm formation and improve response to antibiotics. *PLoS One* **2012,** *7* (1), e28737.

37. Hall, B. S.; Bot, C.; Wilkinson, S. R., Nifurtimox activation by trypanosomal type I nitroreductases generates cytotoxic nitrile metabolites. *J. Biol. Chem.* **2011,** *286* (15), 13088-95.

38. Xu, W.; Zhu, X.; Tan, T.; Li, W.; Shan, A., Design of embedded-hybrid antimicrobial peptides with enhanced cell selectivity and anti-biofilm activity. *PLoS One* **2014,** *9* (6), e98935.

39. Fosso, M. Y.; Shrestha, S. K.; Green, K. D.; Garneau-Tsodikova, S., Synthesis and bioactivities of kanamycin B-derived cationic amphiphiles. *J. Med. Chem.* **2015,** *58* (23), 9124-32.

40. Seeman, P., Atypical antipsychotics: mechanism of action. *Can. J. Psychiatry* **2002,** *47* (1), 29-40.

41. Grigoriadis, D. E.; Niznik, H. B.; Jarvie, K. R.; Seeman, P., Glycoprotein nature of D2 dopamine receptors. *FEBS Lett.* **1988,** *227* (2), 220-4.

42. Ericson, E.; Gebbia, M.; Heisler, L. E.; Wildenhain, J.; Tyers, M.; Giaever, G.; Nislow, C., Off-target effects of psychoactive drugs revealed by genome-wide assays in yeast. *PLoS Genet.* **2008,** *4* (8), e1000151.

43. Miwa, T.; Takagi, Y.; Shinozaki, M.; Yun, C. W.; Schell, W. A.; Perfect, J. R.; Kumagai, H.; Tamaki, H., Gpr1, a putative G-protein-coupled receptor, regulates morphogenesis and hypha formation in the pathogenic fungus *Candida albicans*. *Eukaryot. Cell* **2004,** *3* (4), 919-31.

44. Iwaki, K.; Sakaeda, T.; Kakumoto, M.; Nakamura, T.; Komoto, C.; Okamura, N.; Nishiguchi, K.; Shiraki, T.; Horinouchi, M.; Okumura, K., Haloperidol is an inhibitor but not substrate for MDR1/P-glycoprotein. *J. Pharm. Pharmacol.* **2006,** *58* (12), 1617-22.

45. Iatta, R.; Puttilli, M. R.; Immediato, D.; Otranto, D.; Cafarchia, C., The role of drug efflux pumps in Malassezia pachydermatis and *Malassezia furfur* defence against azoles. *Mycoses* **2017,** *60* (3), 178-82.

46. Hulshof, J. W.; Casarosa, P.; Menge, W. M.; Kuusisto, L. M.; van der Goot, H.; Smit, M. J.; de Esch, I. J.; Leurs, R., Synthesis and structure-activity relationship of the first nonpeptidergic inverse agonists for the human cytomegalovirus encoded chemokine receptor US28. *J. Med. Chem.* **2005,** *48* (20), 6461-71.

47. Suehiro, M.; Yokoi, F.; Nozaki, T.; Iwamoto, M., No-carrier-added radiobromination *via* the Gattermann reaction. Synthesis of bromine-75 and bromine-77 bromperidol. *J. Labelled Comp. Radiopharm.* **1987,** *24* (10), 1143-57.

48. Clinical and Laboratory Standard Institute, *Reference method for broth dilution antifungal susceptibility testing of filamentous fungi - 2nd Edition: CLSI document M38-A2. Wayne, PA.* 2008.
49. Clinical and Laboratory Standard Institute, *Reference method for broth dilution antifungal susceptibility testing of yeasts - Approved standard. CLSI document M27-A3. Wayne, PA.* 2008.
50. Garcia, L. S., Synergism testing: broth microdilution checkerboard and broth madrodilution methods. In *Clinical microbiology procedures handbook*, 3rd edition ed.; ASM Press: Washington, DC, 2010; pp 140-62.
51. Klepser, M. E.; Malone, D.; Lewis, R. E.; Ernst, E. J.; Pfaller, M. A., Evaluation of voriconazole pharmacodynamics using time-kill methodology. *Antimicrob. Agents Chemother.* **2000,** *44* (7), 1917-20.
52. Garzan, A.; Willby, M. J.; Ngo, H. X.; Gajadeera, C. S.; Green, K. D.; Holbrook, S. Y.; Hou, C.; Posey, J. E.; Tsodikov, O. V.; Garneau-Tsodikova, S., Combating enhanced intracellular survival (Eis)-mediated kanamycin resistance of *Mycobacterium tuberculosis* by novel pyrrolo[1,5-a]pyrazine-based Eis inhibitors. *ACS Infect. Dis.* **2017,** *3* (4), 302-9.

Chapter 7 references

1. Sherwood, A. R.; Johnson, M. B.; Delgado-Escueta, A. V.; Gentry, M. S., A bioassay for Lafora disease and laforin glucan phosphatase activity. *Clin. Biochem.* **2013,** *46* (18), 1869-76.

2. Roma-Mateo, C.; Sanz, P.; Gentry, M. S., Deciphering the role of malin in the lafora progressive myoclonus epilepsy. *IUBMB life* **2012,** *64* (10), 801-8.
3. Gentry, M. S.; Roma-Mateo, C.; Sanz, P., Laforin, a protein with many faces: glucan phosphatase, adapter protein, et alii. *FEBS J.* **2013,** *280* (2), 525-37.
4. Tagliabracci, V. S.; Girard, J. M.; Segvich, D.; Meyer, C.; Turnbull, J.; Zhao, X.; Minassian, B. A.; Depaoli-Roach, A. A.; Roach, P. J., Abnormal metabolism of glycogen phosphate as a cause for Lafora disease. *J. Biol. Chem.* **2008,** *283* (49), 33816-25.
5. Gentry, M. S.; Worby, C. A.; Dixon, J. E., Insights into Lafora disease: malin is an E3 ubiquitin ligase that ubiquitinates and promotes the degradation of laforin. *Proc. Natl. Acad. Sci.*, *U. S. A.* **2005,** *102* (24), 8501-6.
6. Sullivan, M. A.; Nitschke, S.; Steup, M.; Minassian, B. A.; Nitschke, F., Pathogenesis of Lafora Disease: Transition of Soluble Glycogen to Insoluble Polyglucosan. *Int. J. Mol. Sci.* **2017,** *18* (8).
7. Turnbull, J.; Tiberia, E.; Striano, P.; Genton, P.; Carpenter, S.; Ackerley, C. A.; Minassian, B. A., Lafora disease. *Epileptic Disord* **2016,** *18* (S2), 38-62.
8. Jansen, A. C.; Andermann, E., Progressive Myoclonus Epilepsy, Lafora Type. In *GeneReviews((R))*, Adam, M. P.; Ardinger, H. H.; Pagon, R. A.; Wallace, S. E.; Bean, L. J. H.; Stephens, K.; Amemiya, A., Eds. Seattle (WA), 1993.
9. Cogan, J.; Weinstein, J.; Wang, X.; Hou, Y.; Martin, S.; South, A. P.; Woodley, D. T.; Chen, M., Aminoglycosides restore full-length type VII collagen by overcoming premature termination codons: therapeutic implications for dystrophic epidermolysis bullosa. *Mol. Ther.* **2014,** *22* (10), 1741-52.

10. Popescu, A. C.; Sidorova, E.; Zhang, G.; Eubanks, J. H., Aminoglycoside-mediated partial suppression of MECP2 nonsense mutations responsible for Rett syndrome in vitro. *J. Neurosci. Res.* **2010,** *88* (11), 2316-24.
11. Vecsler, M.; Ben Zeev, B.; Nudelman, I.; Anikster, Y.; Simon, A. J.; Amariglio, N.; Rechavi, G.; Baasov, T.; Gak, E., Ex vivo treatment with a novel synthetic aminoglycoside NB54 in primary fibroblasts from Rett syndrome patients suppresses MECP2 nonsense mutations. *PLoS One* **2011,** *6* (6), e20733.
12. Njire, M.; Tan, Y.; Mugweru, J.; Wang, C.; Guo, J.; Yew, W.; Tan, S.; Zhang, T., Pyrazinamide resistance in *Mycobacterium tuberculosis*: Review and update. *Adv. Med. Sci.* **2016,** *61* (1), 63-71.
13. Nusrath Unissa, A.; Hanna, L. E.; Swaminathan, S., A Note on Derivatives of Isoniazid, Rifampicin, and Pyrazinamide Showing Activity Against Resistant *Mycobacterium tuberculosis*. *Chem. Biol. Drug Des.* **2016,** *87* (4), 537-50.
14. Gopal, P.; Nartey, W.; Ragunathan, P.; Sarathy, J.; Kaya, F.; Yee, M.; Setzer, C.; Manimekalai, M. S. S.; Dartois, V.; Gruber, G.; Dick, T., Pyrazinoic Acid Inhibits Mycobacterial Coenzyme A Biosynthesis by Binding to Aspartate Decarboxylase PanD. *ACS Infect. Dis.* **2017,** *3* (11), 807-819.
15. Anthony, R. M.; den Hertog, A. L.; van Soolingen, D., 'Happy the man, who, studying nature's laws, Thro' known effects can trace the secret cause.' Do we have enough pieces to solve the pyrazinamide puzzle? *J. Antimicrob. Chemother.* **2018**.
16. Gopal, P.; Tasneen, R.; Yee, M.; Lanoix, J. P.; Sarathy, J.; Rasic, G.; Li, L.; Dartois, V.; Nuermberger, E.; Dick, T., *In Vivo*-Selected Pyrazinoic Acid-Resistant

Mycobacterium tuberculosis Strains Harbor Missense Mutations in the Aspartate Decarboxylase PanD and the Unfoldase ClpC1. *ACS Infect. Dis.* **2017,** *3* (7), 492-501.

17. Zhang, S.; Chen, J.; Shi, W.; Liu, W.; Zhang, W.; Zhang, Y., Mutations in panD encoding aspartate decarboxylase are associated with pyrazinamide resistance in *Mycobacterium tuberculosis*. *Emerg. Microbes Infect.* **2013,** *2* (6), e34.
18. Chopra, S.; Pai, H.; Ranganathan, A., Expression, purification, and biochemical characterization of *Mycobacterium tuberculosis* aspartate decarboxylase, PanD. *Protein Expr. Purif.* **2002,** *25* (3), 533-40.
19. Médici, R.; de María, P. D.; Otten, L. G.; Straathof, A. J., A High-Throughput Screening Assay for Amino Acid Decarboxylase Activity. *Adv. Synth. Catal.* **2011,** *353*, 2369-76.

Selina Yijia Li Holbrook

(Previously Yijia Li)

EDUCATION

2009 – 2013 **B.S. in Biochemistry & Molecular Biology and Financial Economics**, Center College, Danville, KY, U.S.A.

POSITIONS HELD

Winter 2013 **International Settlement Intern**, Department of International Settlement, Bank of China, Hebei Branch, Hebei Province, China.

Summer 2012 **Summer Researcher**, Department of Pharmaceutical Sciences, College of Pharmacy, University of Kentucky, Lexington, Kentucky, U.S.A.

Fall 2011 **Research student,** Department of Chemistry, Centre College, Danville, Kentucky.

Summer 2011 **Research Assistant,** Department of Toxicology Safety Assessment, National Institute of Nutrition and Food Safety, China, Beijing, China.

HONORS AND AWARDS

Jun. 2017 Second place in poster presentation in the graduate student group at the 3rd Annual Society of Postdoctoral Scholars Research Symposium

Mar. 2017 First place in poster presentation in the graduate student group at the Annual Rho Chi Research Day

2016 – 2017 University of Kentucky Presidential Fellowship

Mar. 2016 Second place in poster presentation in the graduate student group at the Annual Rho Chi Research Day

Sep. 2015 Second place in Elevator Speech Competition at the Annual Symposium on Drug Discovery & Development

PUBLICATIONS

1. **Holbrook, S. Y. L.**; Gentry, M. S., Tsodikov, O. V., Garneau-Tsodikova, S., Nucleoside triphosphate cosubstrates control and substrate profile and efficiency of aminoglycoside 3'-*O*-phosphotransferase type IIa. *MedChemComm* **2018,** Epub ahead of print.
2. Ngo, H. X.; Green, K. D.; Gajadeera, C. S.; Willby, M. J.; **Holbrook, S. Y. L.**; Hou, C.; Garzan, A.; Mayhoub, A.; Posey, J. E.; Tsodikov, O. V.; Garneau-Tsodikova, S. Potent 1,2,4-triazino[5,6b]indole-3-thioether inhibitors of the kanamycin resistance enzyme Eis from *Mycobacterium tuberculosis*. *ACS Infect. Dis.* **2018,** Epub ahead of print.
3. **Holbrook, S. Y. L.**; Garneau-Tsodikova, S., What is medicinal chemistry?–Demystifying a rapidly evolving discipline! *MedChemComm* **2017**, *8*(9), 1739-41.
4. **Holbrook, S. Y. L.**; Garneau-Tsodikova, S., Evaluation of aminoglycoside and carbapenem resistance in a collection of drug-resistant *Pseudomonas aeruginosa* clinical isolates. *Microb. Drug Resist.* **2017**, doi: 10.1089/mdr.2017.0101.
5. **Holbrook, S. Y. L.**; Garzan, A.; Dennis, E. K.; Shrestha, S. K.; Garneau-Tsodikova, S., Repurposing antipsychotic drugs into antifungal agents: Synergistic combinations

of azoles and bromperidol derivatives in the treatment of various fungal infections. *Eur. J. Med. Chem.* **2017**, *139*, 12-21.

6. Garzan, A.; Willby, M. J.; Ngo, H. X.; Gajadeera, C. S.; Green, K. D.; **Holbrook, S. Y.L.**; Hou, C.; Posey, J., E.; Tsodikov, O., V.; Garneau-Tsodikova, S., Combating enhanced intracellular survival (Eis)-mediated kanamycin resistance of *Mycobacterium tuberculosis* by novel pyrrolo [1, 5-a] pyrazine-based Eis inhibitors. *ACS Infect. Dis.* **2017**, *3*(4), 302-9.
7. Green, K. D.; **Holbrook, S. Y. L.**; Ngo, H. X.; Garneau-Tsodikova, S., Emerging targets in anti-tubercular drug design. In *Antibiotic Drug Discovery* **2017**, 141-203.
8. **Holbrook, S. Y. L.**; Garneau-Tsodikova, S., Expanding aminoglycoside resistance enzyme regiospecificity by mutation and truncation. *Biochemistry* **2016**, *55*(40), 5726-37.
9. **Li, Y.**; Green, K. D.; Johnson, B. R.; Garneau-Tsodikova, S., Inhibition of aminoglycoside acetyltransferase resistance enzymes by metal salts. *Antimicrob. Agents Chemother.* **2015**, *59*(7), 4148-56.
10. Fosso, M. Y.; **Li, Y.**; Garneau-Tsodikova, S., New trends in the use of aminoglycosides. *MedChemComm* **2014**, *5*(8), 1075-91.